THE
PHYSICAL REVIEW
A Journal of Experimental and Theoretical Physics Established by E. L. Nichols in 1893
VOL. 55, NO. 12 JUNE 15, 1939 SECOND SERIES

Further Study of Cosmic Rays on the Pacific Ocean

PIARA S. GILL
The University of Chicago, Chicago, Illinois
(Received April 24, 1939)

Records of cosmic-ray intensity obtained on the *R. M. S. Aorangi* during 15 new voyages between Vancouver, Canada, and Sydney, Australia, from July 28, 1937, to September 23, 1938, with a Carnegie model C cosmic-ray meter, are discussed and compared with records taken during 11 voyages on the same route previously reported by Compton and Turner. The observed minimum of cosmic-ray intensity near the equator averages 10.3 percent less than the intensity at Vancouver, in good agreement with the value given by Compton and Turner. The correlation between the cosmic-ray intensity and the atmospheric temperature is confirmed. An atmospheric temperature coefficient is found to be a function of latitude, with its highest numerical value of -0.25 percent per °C for latitudes higher than 40° (N and S). With this variable temperature coefficient a latitude effect (about 8.5 percent) of magnetic origin alone is found. The mean latitude effect curve for 25 trips, corrected for external temperature, is flat beyond the critical latitudes (about 40°N and 38°S). The difference in cosmic-ray intensity between the Northern and Southern Hemispheres beyond the critical latitudes after this temperature correction is found to be 0 ± 0.1 percent (probable error). This is inconsistent with a galactic rotation effect as great as the 0.5 percent predicted by Compton and Getting, but does not definitely rule out a more recent modification of their calculation. The origin of the latitude effect knee is ascribed to the minimum energy required for a primary electron to produce mesotrons capable of traversing the atmosphere. The small magnitude of the latitude effect is shown to supply strong evidence of the secondary nature of mesotrons.

A. H. COMPTON and R. N. Turner have recently described and discussed the records of cosmic-ray intensity obtained on the *R. M. S. Aorangi* during eleven voyages between Vancouver, Canada, and Sydney, Australia, from March 17, 1936, to January 18, 1937, with a Carnegie Model C cosmic-ray meter.[1] The present paper describes the cosmic-ray records obtained on the *R. M. S. Aorangi* during fifteen additional voyages over the same route from July 28, 1937, to September 23, 1938, with the same meter. From January 29, 1937, to July 13, 1937, the meter was on the *S. S. Talune*, traveling between Newcastle (New South Wales) and Hobart (Tasmania). The method of collection and reduction of the data has already been explained.[1]

ANALYSIS OF THE DATA

In analyzing the data, the procedure of Compton and Turner was followed. The barometer effect was determined by correlating the daily mean values of the ionization I_0 with the daily mean values of barometer B in inches of Hg. For 1936–37 a barometer effect of -10.9 millivolts per hour per atmosphere of argon per inch of mercury was determined, which value was used throughout. This corresponds to -1.74 percent per cm of mercury. Compton and Turner used the value -10 millivolts per hour per atmosphere of argon per inch of mercury, or -1.6 percent per cm of mercury for the barometer effect. The

[1] A. H. Compton and R. N. Turner, Phys. Rev. **52**, 799 (1937).

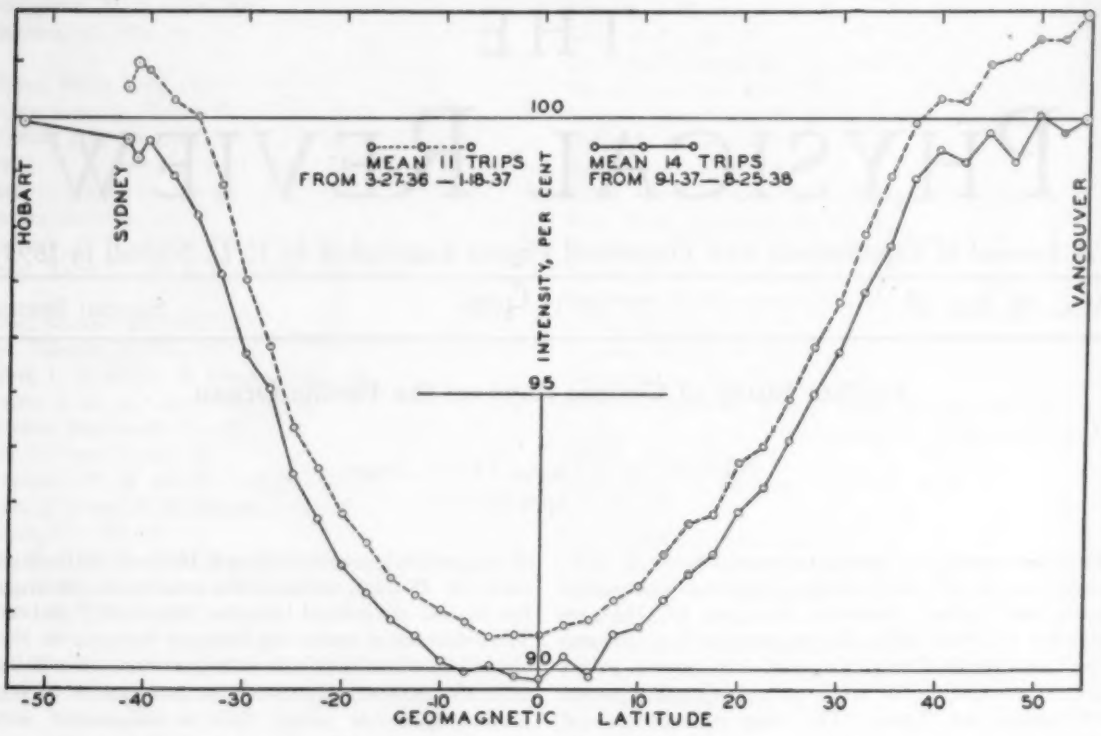

FIG. 1. Cosmic rays on the Pacific Ocean.

daily mean values of the barometric pressure for 1936–37 were obtained from a barograph calibration not significantly different from that found for the new series of data used in this paper. The absolute ionization at the latitude of Chicago is given by Compton and Turner as 249 millivolts per hour per atmosphere of argon, which corresponds to 84 ions per cm^3 per sec. in 50 atmospheres of argon, or 1.22 ions per cm^3 per sec. in standard air. The final observed intensities, after applying the barometric correction, are expressed in percentages of this normal ionization.

It has not been considered necessary to give all fifteen curves, each representing one trip, while the ship was at sea. All the data have been grouped, however, into two seasons, colder months (November 6–May 7) and warmer months (May 8–November 5), in order to discuss the dependence of cosmic-ray intensity on seasonal temperature. It has been previously shown by Compton and Turner[1] and Forbush[2] that the temperature coefficient of the meter is insignificant.

[2] S. E. Forbush, Terr. Mag. **42**, 1 (1937); Phys. Rev. **54**, 975 (1938).

ANNUAL MEAN AND SEASONAL DIFFERENCES

The solid curve in Fig. 1 shows the 12-month mean of all the observations taken between Auckland and Vancouver, while the broken curve shows the corresponding data (Fig. 6) of Compton and Turner. Each point represents the arithmetic average of the values observed at the corresponding 2.5° interval. The total change between Vancouver and the equator is 10.3 percent, which is the average of seasonal means that vary from 9.8 percent in the warmer months to 10.9 percent in the colder months.

This value of 10.3 percent is identical with that reported by Compton and Turner. Previous measurements over the same route include the value of 13 percent given by Compton,[3] as based on measurements with a shield equivalent to 6.5 cm of lead, and the value of 11 percent given by Millikan and Neher,[4] who used a shield equivalent to 12 cm of lead, the same as that for measurements here reported.

Minor differences between the present and the

[3] A. H. Compton, Rev. Sci. Inst. **7**, 71 (1936), Fig. 1.
[4] R. A. Millikan and H. V. Neher, Phys. Rev. **50**, 15 (1936), Fig. 14.

earlier data of Compton and Turner are that the knee in the Southern Hemisphere comes at a higher latitude than in their curve, and that at latitudes higher than the knee the increase in intensity with latitude is smaller than theirs in both hemispheres. The intensity at Sydney is 0.4 percent higher than the intensity at Auckland, while Fig. 6 of Compton and Turner shows 0.2 percent higher intensity at Auckland than at Sydney.

The latitude curve of Fig. 1 is extended farther south from Sydney (42.2°S)* to Hobart (Tasmania) (51.6°S) by adding the data collected on *S. S. Talune*. Because the meter on *S. S. Talune* was placed under deck, the mean value of I_0 at Sydney was 3.88 percent lower than the mean value of I_0 at the same place while the meter was on *R. M. S. Aorangi*. Since no essential changes in the meter were made when it was transferred from *R. M. S. Aorangi* to *S. S. Talune*, it was assumed that the daily mean values of I_0 at Sydney were unchanged. As the ship traveling between Newcastle (NSW) and Hobart (Tasmania) was seldom in port at Sydney over five hours, the mean I_0 at the port was obtained from daily means of I_0 for the days when the ship was between Newcastle (41.2°S) and 43.5°S.

Figure 1 now shows the knees more distinctly.

* Geomagnetic latitudes are used throughout.

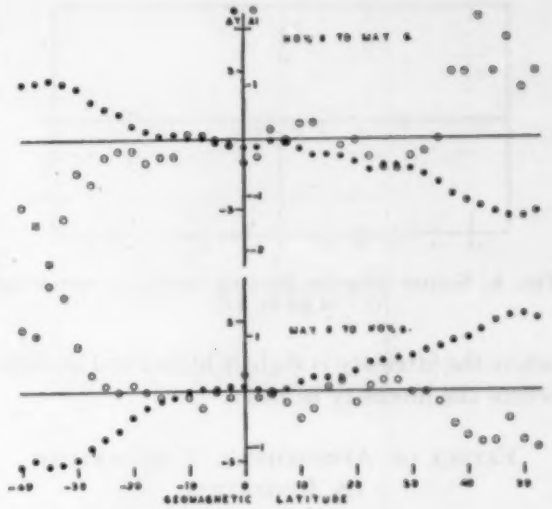

FIG. 3. Departures for colder and for warmer months from annual mean of ionization (ΔI) and shade temperature of the outside air (ΔT), plotted for the various latitudes.

They lie at about 40° in the Northern Hemisphere and at about 38° in the Southern Hemisphere. The increase in ionization beyond the knees is, within experimental error, the same in both hemispheres.

The fluctuations of I_0 from 40°N to 52.5°N and from 10°N to 7.5°S are not ascribable to experimental error, but are due to diurnal changes in cosmic-ray intensity. For most of the trips the ship crossed at about noon the latitudes

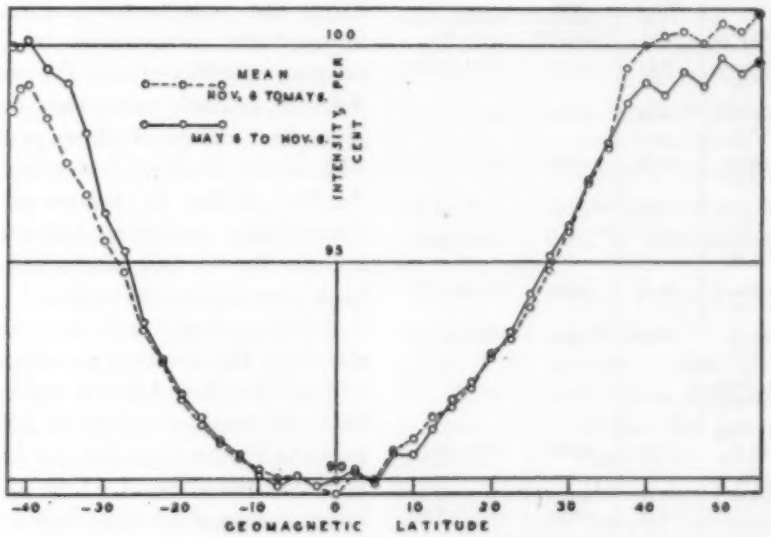

FIG. 2. Latitude effect curves for colder months (Nov. 6 to May 6) and for warmer months (May 7 to Nov. 5) for 1937–38 data.

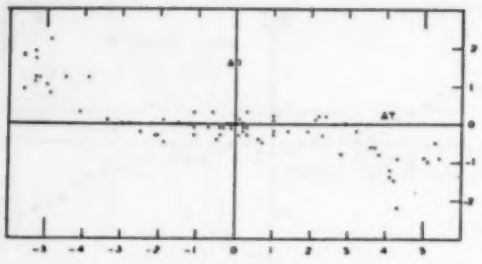

FIG. 4. Scatter diagram showing nonlinear correlation of ΔI *vs.* ΔT.

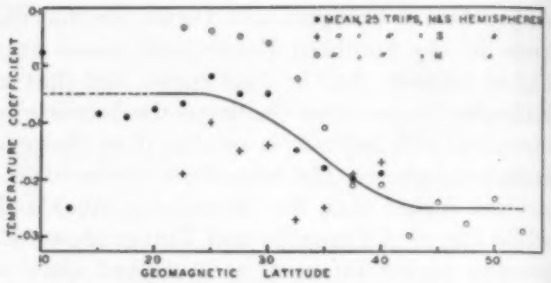

FIG. 5. Atmospheric temperature coefficient as a function of geomagnetic latitude.

where the intensity is slightly higher and at night where the intensity is lower.

EFFECT OF ATMOSPHERIC TEMPERATURE ON IONIZATION

Figure 2 shows that, in both the Northern and Southern Hemispheres, the intensity is greater during the cold months, as was likewise evident from Fig. 7 of Compton and Turner. They ascribed this variation to atmospheric rather than astronomical changes, a conclusion which was confirmed by the writer[5] from data obtained at four widely separated stations, which showed no significant correlation with various astronomical variables.

For each of the two curves of Fig. 2, the departure of the ionization from the annual mean was noted for each 2.5° interval of latitude. These departures in the ionization were compared (Fig. 3) with the departure in the outside shade temperature from its annual mean at the same latitude. This analysis shows a definite correlation of opposite sign between the external shade temperature and the observed ionization only in regions outside an equatorial belt extending approximately 10° either side of the magnetic equator. In Fig. 3 are shown at each latitude the departures from the annual mean values of the external temperatures for cold and hot months of the year. Outside of the equatorial belt, the opposing trends of this temperature and ionization are evident in both curves. The opposing trends of temperature and ionization in the equatorial belt for summer and winter are not evident in Fig. 8 of Compton and Turner,[1] but do appear in their curves for spring and autumn. From the data in the scatter-diagrams of the atmospheric temperature *vs.* ionization, temperature coefficients of the ionization for two different latitude zones were computed. Table I gives the values of these coefficients together with those obtained last year by Compton and Turner[1] (Table I). Values of the atmospheric temperature coefficient calculated in a similar manner for various land stations have recently been reported by the writer.[5]

TABLE I. *Atmospheric temperature coefficient of cosmic-ray ionization (reduced to standard barometer).*

AUTHORITY	YEAR	LOCATION	COEFFICIENT PERCENT	PROBABLE ERROR PERCENT	CORRELATION FACTOR
Compton and Turner	Mar. 17, 1936, to Jan. 18, 1937	Vancouver (54.8)	−0.22	±0.02	−0.85 ±0.04
		Auckland (41.1)	−0.16	±0.04	−0.47 ±0.15
		Sydney (42.2)	−0.10	±0.02	−0.67 ±0.10
		At Sea	−0.18	±0.01	−0.68 ±0.03
This Paper	July 28, 1937, to Sept. 23, 1938	Vancouver (54.8)	−0.13	±0.02	−0.62 ±0.07
		Auckland (41.1)	−0.12	±0.04	−0.50 ±0.12
		Sydney (42.2)	−0.085	±0.03	−0.36 ±0.12
		At Sea between:			
		λ = 15 S & 15 N	−0.05	±0.04	−0.17 ±0.13
		λ = 17½ & 40 N & S	−0.31 −0.29	±0.03 ±0.04	−0.87 ±0.04 −0.72 ±0.07

A scatter diagram of ΔI *vs.* ΔT for all the data shown in Fig. 3 indicates (Fig. 4) that ΔI is not a linear function of ΔT. It will be noted, however, that the smaller values of ΔT are obtained at lower latitudes than are the higher values. The fact that the slope of ΔI *vs.* ΔT is steeper at the larger values of ΔT thus means that at the higher latitudes the atmospheric temperature coefficient is greater.

[5] P. S. Gill, Phys. Rev. **55**, 429 (1939).

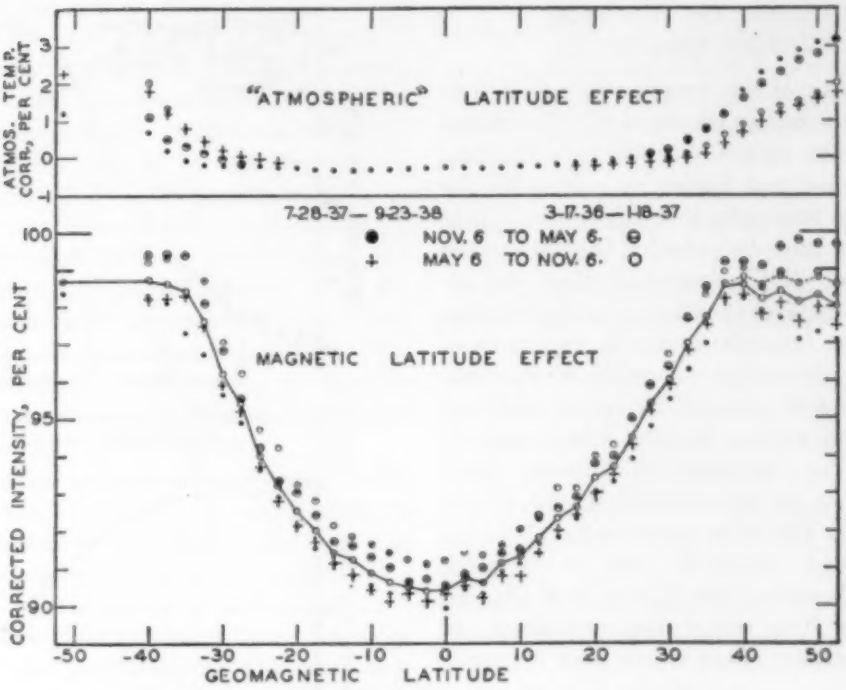

FIG. 6. Magnetic and atmospheric latitude effect for twenty-five trips.

The values of α, the atmospheric temperature coefficient of the ionization, at intervals of 2.5° geomagnetic latitude can be found as follows: By definition $\alpha=(1/I_a)(\Delta I/\Delta T)$, where I_a is the absolute ionization due to cosmic rays and ΔI and ΔT are the mean ranges between summer and winter deviations from the annual mean at the latitude for which α is evaluated. The value of α was calculated separately from the data for 10 trips reported by Compton and Turner and for the 15 trips analyzed in the present paper, and the mean was weighted accordingly. The results for latitudes greater than 10°N and S are shown in Fig. 5. At lower latitudes, because of the smallness of ΔT, the values of α become experimentally indeterminate.

The open circles represent the coefficients thus calculated for the Northern Hemisphere, the crosses for the Southern Hemisphere, and the solid circles the mean between the two values. One of the most important sources of error is the occurrence of world wide changes in cosmic-ray intensity.[5] When such a change persists for a prolonged period, it increases the apparent temperature coefficient in one hemisphere and decreases it in the other. For this reason the value of the mean between the two hemispheres is much more reliable than either individual value. Thus the atmospheric temperature coefficients beyond 40°, being based on measurements in the Northern Hemisphere alone, cannot be relied upon with the confidence that we have in the data between 30° and 40°. It is evident, however, that beyond 42.5°α appears to stay constant, and has its greatest numerical value. On the other hand, α decreases rapidly from 42.5° to 25° where it again appears to approach a constant minimum numerical value. This is in accord with Blackett's[6] view, in which he points out that the temperature coefficient at the equator should be lower than at bordering latitude zones.

It will be noted in Table I that the value of the temperature coefficient at Vancouver for this paper is 60 percent of that given by Compton and Turner, while those at Auckland and Sydney are the same within the probable error. The difference at Vancouver may be caused by sudden changes in ionization due to magnetic storms or other causes independent of the temperature of the atmosphere.

[6] P. M. S. Blackett, Phys. Rev. **54**, 973 (1938).

Atmospheric and Magnetic Latitude Effects

The upper part of Fig. 6 shows the corrections to be applied to the two curves of Fig. 2, and also to the two similar curves obtained from the data used by Compton and Turner, to correct for the changes in the atmospheric temperature. These corrections are made by reducing the data to the mean value of 21°C, supposing that the atmospheric temperature coefficient is the function of geomagnetic latitude shown in the curve of Fig. 5. These correction curves thus represent a latitude effect of atmospheric origin, differing with colder and warmer months, which must be subtracted from the observed latitude effect curves to obtain the effect caused by the earth's magnetic field. The solid curve of Fig. 6 is the mean (weighted, ratio 10 : 15) of 10 trips reported by Compton and Turner and 15 trips analyzed here. This curve thus represents the part of the latitude effect which is of magnetic origin.

The lower (solid) curve beyond 35°N is obtained by applying the temperature coefficient as given in Fig. 5. This curve shows a slight decrease for latitudes higher than the knee (40°N). Since from theoretical reasons it is very improbable that the corrected cosmic-ray intensity should thus diminish with increasing latitude, the decrease shown by the solid curve presumably indicates that an over-correction has been made for the atmospheric temperature coefficient. By the method of trial and error, it is found that if for these latitudes the value of α is taken as -0.19 percent per degree C, instead of -0.25 as given in Fig. 5, the magnetic latitude

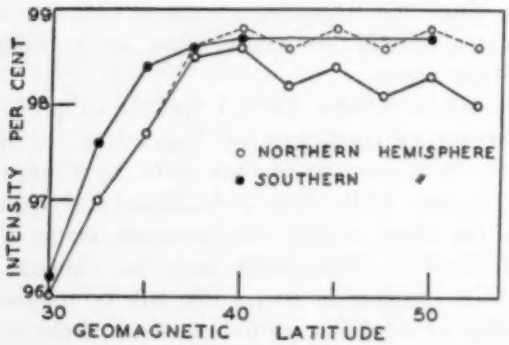

Fig. 7. Comparison of corrected latitude effect for Northern and Southern Hemispheres.

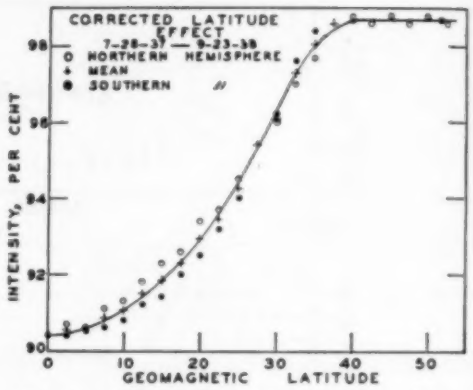

Fig. 8. Magnetic latitude effect averaged for both hemispheres.

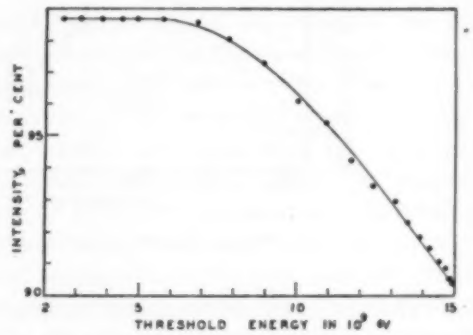

Fig. 9. Cosmic-ray ionization as a function of geomagnetic energy threshold.

effect curve becomes horizontal. It is thus that the broken curve of Fig. 6 is calculated. The assumption of a flat geomagnetic latitude effect curve beyond the knee thus affords an independent method of determining the atmospheric temperature coefficient. Since the result does not differ too greatly from that obtained directly,* we may conclude that the assumption of flatness is consistent with the experimental data. That is, there is no evidence of a geomagnetic latitude effect beyond the knee.

Comparison of Intensity in the Northern and Southern Hemispheres

Compton and Getting[7] predicted an excess of cosmic-ray intensity of about 0.5 percent in the

* It may be noted that the temperature correction applied in Fig. 6 should be correct only if, for a sea-level temperature of 21°C, the temperature at every altitude is the same at all latitudes. It is clear that this is not in general true. The method of correction can thus be expected to remove differences of only the first order.

[7] A. H. Compton and I. A. Getting, Phys. Rev. **47**, 817 (1935).

north, due to the motion of the earth with the rotation of the galaxy. The comparison of intensity in the Northern and Southern Hemispheres should be significant only for latitudes where the influence of the earth's magnetic field becomes negligible, that is, beyond the latitude knees (40°N and 38°S). This portion is shown in Fig. 7, where the corrected intensity curves for latitudes higher than 30°N and S are given. The question arises, which of the two curves in the north (broken or solid, as explained in the last section) is to be taken as the more reliable. Supposing that the curve which shows a flat plateau is the better measure, we find an exact equality of intensity in the two hemispheres.

A rough estimate of the probable error of this equality gives ± 0.1 percent, in which estimate the largest factor is that introduced by the uncertainty in the temperature correction.

This result indicates that a difference of 0.5 percent between the Northern and Southern Hemispheres are predicted by Compton and Getting is very improbable. It should be noted, however, that if the sun's motion with the rotation of the galaxy is, as indicated by the recent study by Camm,[8] only 200 instead of 300 km per sec., as assumed in the earlier calculations, the precision of the present measurements is inadequate definitely to rule out the possibility of the predicted effect.

Discussion of Latitude Curve

In Fig. 8 is shown the mean cosmic-ray intensity I for 25 trips, corrected for external temperature, as a function of λ. This curve, based upon the broken curve of Fig. 6, shows no increase in intensity for latitudes higher than 40°. That is, at sea level, beyond Compton's latitude knee, no detectable latitude effect of geomagnetic origin exists. Lemaitre and Vallarta[9] have given the threshold energy E_0 as a function of λ for vertically incident electrically charged primaries (electrons). Thus at a certain latitude only those electrons can enter the earth's atmosphere which have energies greater than E_0. From this relation between E_0 and λ, the curve of Fig. 9 shows the cosmic-ray intensity *vs.* threshold energy E_0. As this curve is obtained at sea level with a lead shield around the ionization chamber of 12 cm, the curve represents the latitude sensitive part of the penetrating radiation, presumably mesotrons, as a function of the threshold energy E_0 of the primary electrons.

One can compare the mesotron intensity at different latitudes corresponding to certain threshold energies E_0 as given in Fig. 9 with the energy distribution curve of mesotrons obtained by the Wilson chamber method[10] and as calculated by Euler and Heisenberg.[11] In order to calculate the energy spectrum at sea level Euler and Heisenberg assumed that all of the mesotrons are produced as secondaries by the soft component at the same altitude (about 16.6 km) in the atmosphere. For the spectrum of the primary electrons they consider a distribution function of the following kind: $F(E) = I_0 \times E^{-\gamma}$ where $F(E)$ represents the number of the vertically incident electrons having energies greater than E, I_0 and

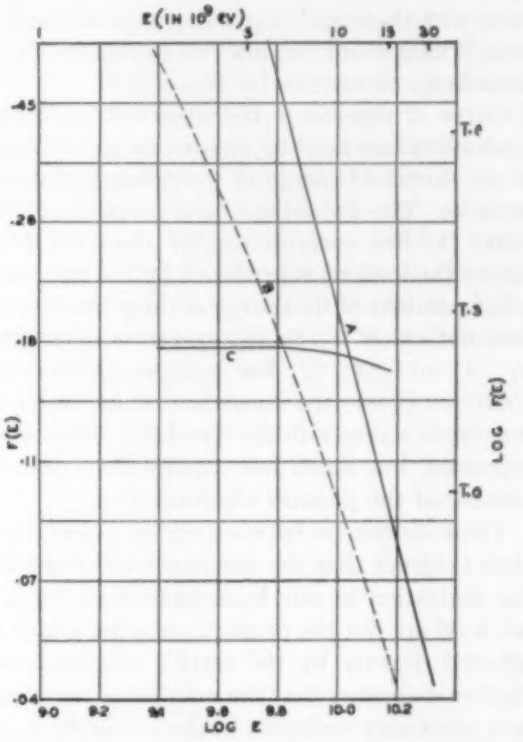

FIG. 10. Energy distribution curves: (*A*) for electrons at the top of the atmosphere; (*B*) mesotrons at sea level; (*C*) latitude *vs.* threshold energy.

[8] G. L. Camm, Roy. Astr. Soc. **99**, 71 (1938).

[9] G. Lemaitre and M. S. Vallarta, Phys. Rev. **50**, 493 (1936).

[10] P. M. S. Blackett, Proc. Roy. Soc. **A159**, 1 (1937).

[11] H. Euler and W. Heisenberg, Ergeb. Exakt. Naturwiss. **17**, 1–70 (1938).

γ are empirical constants. On the further assumption that the created mesotrons have the same energy distribution as the primaries, Euler and Heisenberg calculate the variation of the energy spectrum as the mesotrons travel through the earth's atmosphere losing energy by ionization[12] and by spontaneous decay.[13] Thus at sea level they obtain an energy distribution of mesotrons given by the broken line B of Fig. 10. This curve is represented in a double logarithmic diagram where log $F(E)$ (number of vertically incident mesotrons per minute per cm^2) is ordinate and log E is abscissa. The curvature in the energy spectrum of the mesotrons at sea level compared with the straight line distribution at the top of the atmosphere is caused by the spontaneous decay of mesotrons in air which increases with decreasing energy of the particles. The straight line A in Fig. 10 represents the corresponding energy distribution of electrons at the top of the atmosphere when γ is given the value 1.8.[14] The broken curve is in good agreement with the energy distribution curve obtained from Wilson cloud-chamber measurements in the same range of energies by Blackett.[10]

Curve C represents the observed ionization, produced at sea level by mesotrons, as a function of the threshold energy of the primary electrical particles. The following characteristics are evident: (1) For energies smaller than 6×10^9 ev (knee) the ionization produced by the mesotrons is independent of the energy of the primaries, and does not follow the energy spectrum determined by (A) and (B). (2) For energies greater than 6×10^9 ev (knee) the ionization produced by the mesotrons varies with the threshold energy of the primaries, but much less rapidly than does the number of the primary electrons (A).

These differences between curves C and A give clear evidence that the mesotrons which produce the ionization in our lead-shielded chamber at sea level are not the primary particles which are affected directly by the earth's magnetic field. Rather it appears that the mesotrons are created as a secondary radiation in the atmosphere, and hence reflect only that dependence on the earth's magnetic field to which the much higher energy primaries that excite them are subject. This evidence for the secondary nature of the mesotrons from a consideration of the latitude effect has been discussed by Euler and Heisenberg.[11]

Professor Compton has suggested that the knee of the latitude curve should occur for that minimum energy of the secondary mesotrons which enables them to penetrate the barrier of the earth's atmosphere. This hypothesis is based on the now evident fact that neither electrons nor photons of any reasonable energy are able to penetrate the atmosphere, and that the predominant ionization at sea level seems to be caused by mesotrons and their secondaries. If we make the reasonable assumption that some of these mesotrons traverse the atmosphere with no energy loss other than that caused by ionization, various calculations[15] give for the minimum required energy about 2.5×10^9 ev. It may be noted that the mean decay constant for mesotrons is taken as $t_0=2\times10^{-6}$ sec., and their effective height of production as 25 km, considering merely the decay, there should remain at sea level about 30 percent of the initial mesotrons of this threshold energy. Thus the sharply limiting factor is not the decay rate, but the ionization.

The minimum energy of the primary particle required to excite such secondary mesotrons will depend upon the nature of the exciting process. Perhaps as probable a mechanism as any is that the primary cosmic ray is an electron, positive or negative, which on collision with an atomic nucleus in the atmosphere produces a photon (x-ray) whose energy will be of the order of, but less than, that of the primary electron. As in electron pair production, we may suppose that if the resulting photon generates a mesotron, a pair of positive and negative mesotrons is produced, between which the energy is approximately equally divided. Thus if E_e is the energy of the primary electron, E_p that of the photon, and E_m that of each of the mesotrons,

$$E_e \geqslant E_p = 2E_m.$$

From $E_m=2.5\times10^9$ ev, we thus find for the

[12] H. A. Bethe and W. Heitler, Proc. Roy. Soc. **A146**, 83 (1934).
[13] Yukawa and M. Taketani, Proc. Phys. Math. Soc. Jap. **20**, 720 (1938).
[14] L. W. Nordheim, Phys. Rev. **53**, 694 (1938); W. Heitler, Proc. Roy. Soc. **A161**, 261 (1937).
[15] H. J. Bhabha, Proc. Roy. Soc. **A164**, 257 (1938).

threshold energy of the primary electrons,

$$E_e \geqslant 5\times 10^9 \text{ ev}.$$

This is in satisfactory agreement with the threshold energy of the latitude effect, which according to Fig. 9 occurs at about 6×10^9 ev.

Primary particles with energies less than 5×10^9 ev should thus not produce any ionization at sea level, which would account for the absence of any latitude effect beyond 40 degrees. At higher altitudes, since the minimum energy required to penetrate the atmosphere is less, one should expect a shift of the knee to higher latitudes. This is in qualitative agreement with the recent experimental results.

On the other hand, mesotrons of energies less than 2×10^9 ev, which constitute the more abundant part of those observed at sea level, have too little energy to penetrate the atmosphere. These must therefore have been produced far below the height (about 25 km) at which the first production occurs, and hence must be the result of several stages of energy transfer. That such production of mesotrons at relatively low altitudes does indeed occur is demonstrated by the recent airplane experiments of Schein and Wilson.[16] It follows that the energies of the primaries producing them must have been manyfold greater than the mesotron energies. It is thus not to be expected that they would be influenced by the earth's magnetic field. In this manner we can account for the small magnitude of the observed latitude effect, and the difference between curves *B* and *C* of Fig. 10.

For threshold energies higher than 6×10^9 ev (knee) a certain number of the primary electrons, producing those mesotrons which are capable of penetrating the barrier of the earth's atmosphere, is cut off at certain latitudes by the earth's magnetic field. Therefore a definite latitude effect of the penetrating radiation at sea level is present for energies between $E=6\times 10^9$ ev and $E=15\times 10^9$ ev, beyond which energy the earth's field, even at the equator, ceases to act as a barrier.

The author wishes to express his sincere appreciation to Professor A. H. Compton for assigning the problem and for his inspiring guidance throughout the investigation. It is a pleasure to thank Mr. R. N. Turner for his careful and remarkable work in taking care of the meter. Thanks are due likewise to the Canadian Australasian Steamship Company for permission to build the cosmic-ray observatory on the *R. M. S. Aorangi*, to the Union Carbide and Carbon Corporation for supplying the batteries required for operating the meter, and to the Carnegie Institution of Washington for the use of the cosmic-ray meter. The author also wishes to thank Mrs. Ardis T. Monk for help in calculations, and Dr. M. Schein for valuable discussions. Professor P. W. Burbidge of Auckland University College and Mr. F. L. Code of Vancouver have given valued help in the adjustments of the meter.

[16] M. Schein and V. C. Wilson, Phys. Rev. **54**, 304 (1938).

A Compact Pressure-Insulated Electrostatic X-Ray Generator

JOHN G. TRUMP AND R. J. VAN DE GRAAFF
Massachusetts Institute of Technology, Cambridge, Massachusetts

(Received April 11, 1939)

A compact, pressure-insulated, electrostatic x-ray generator has been developed for scientific and medical purposes. A major object of the work was the investigation, with a small and thus flexible machine, of the principles and design factors involved in pressure-insulated electrostatic generators with a view to the subsequent development of higher voltages in compact apparatus. The generator is housed in a steel tank 34 in. in diameter and 100 in. high. At air pressures of 11 atmospheres absolute, 1250-kv x-rays are obtained with target currents of over one milliampere supplied by the single 14-in. belt. With Freon gas the same voltages and currents can be obtained at one-third the pressure required with air. The problem of belt charge is analyzed and a method is described for controlling the electrostatic fields within the column in order to realize the high charge densities possible at high pressure. The construction of a supporting column of high breakdown strength, and other features of the design are described. At 1250 kv the x-ray intensity per milliampere of target current is about 340 roentgens per minute at 50 cm from the target in the direction of the electron beam with five mm of lead equivalent filtration.

A 1.25-MEGAVOLT x-ray generator using compressed-gas insulation has been developed at the Massachusetts Institute of Technology for scientific and medical purposes. This is a continuation of the Institute's program of developing penetrating x-ray sources, using electrostatic generators. A previous 1.0-megavolt air-insulated x-ray generator[1] has been in use at the Huntington Memorial Hospital in Boston since March 1, 1937, during which period about 700 complete treatment series totaling about 10,000 individual treatments have been given. The clinical results obtained with the Huntington generator have indicated, in a preliminary way at least, the advantage of very high voltage x-rays for certain types of malignancy.[2, 3] The present development was undertaken with the object of producing a more simple and compact source of such radiation. A further object was to investigate the design factors involved in the application of pressure insulation to electrostatic generators and acceleration tubes, with a view to later developing very compact generators capable of many megavolts.

HIGH VOLTAGE SOURCE

Figure 1 shows a sectional view of the apparatus. The generator and acceleration tube are contained within a vertical steel tank 34 in. in inside diameter and 100 in. in length. The tank is divided into three sections, the upper two being completely removable for accessibility to the apparatus within. The high voltage source is an electrostatic generator of the belt type,[4] in which electric charge is continuously transferred between a high voltage terminal and ground by a rapidly moving belt of insulating material. The terminal consists of a brass spinning set on a brass casting, and is 24 inches in diameter and 19 inches in over-all height. The gap from terminal to tank is 5 inches at the sides of the terminal and about 7 inches at the top.

GENERATOR COLUMN

The high voltage terminal is supported on three Textolite pillars built up of a series of corrugated Textolite disks 3 inches in diameter with laminations horizontal. These disks are separated by thin brass sheets which extend across the column so as to define a succession of flat conducting surfaces between the high voltage terminal and the ground plane. These transverse sheets each support a brass hoop made of $\frac{3}{4}$-inch tubing so as to present a smooth exterior column surface.[5] The total potential on the terminal is divided equally between these transverse conducting members by connecting a spiral-type high voltage resistance of 400 megohms across

[1] J. G. Trump and R. J. Van de Graaff, J. App. Phys. **8**, 602 (1937).
[2] R. Dresser and J. Spenser, New England J. Med. **218**, 415 (1938).
[3] R. Dresser and J. Rude, J. Am. Med. Assoc. **111**, 1834 (1938).
[4] R. J. Van de Graaff, Phys. Rev. **38**, 1919 (1931).
[5] R. G. Herb, D. B. Parkinson and D. W. Kerst, Phys. Rev. **51**, 75–83 (1937).

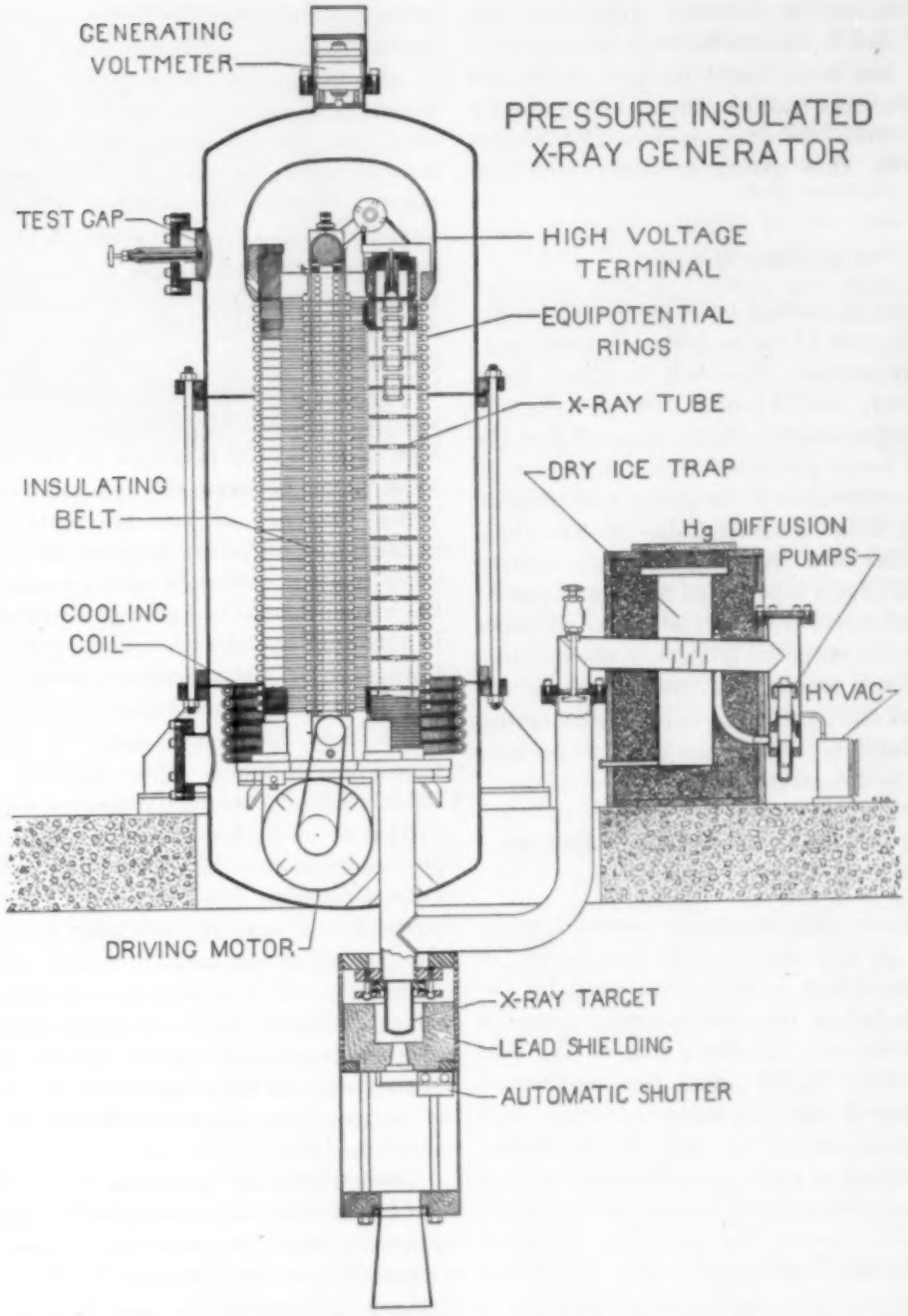

FIG. 1. Sectional view of pressure-insulated x-ray generator.

each gap, following a previously described principle.[6] The length of the column is about 50 inches. There are a total of 40 insulating sections in this distance, and the lowest of the transverse conducting members establishes the ground plane. The use of solid insulation with the laminations flatwise so as to present the direction of greatest dielectric strength to the voltage was found necessary to insulate the generator voltage in the short column length. At 11 atmospheres

[6] R. J. Van de Graaff, K. T. Compton and L. C. Van Atta, Phys. Rev. **43**, 149 (1933).

pressure absolute the flashover strength of the corrugated disk insulators between the conducting planes has been found by test to be 220 kilovolts whereas when the generator is operating at 1000 kilovolts the stress is only 25 kilovolts per insulator, thus giving a safety factor of about nine.

Charging System

The charge is carried on a single, three-ply, rubber-fabric belt 14 inches wide and running at 5000 ft. per minute. This belt is driven by a 10-horsepower, 3450-r.p.m., 3-phase induction motor. Negative electric charge is sprayed on the belt at the lower grounded end from a row of corona points directed at the pulley and supplied with power from a controllable 40-kv transformer-rectifier set. Within the high voltage terminal this charge is collected by a corona-point collector and serves to bring the insulated upper pulley to such a potential relative to the terminal that a second corona rod connected to the terminal and directed at the upper pulley sprays an approximately equal amount of positive charge on the downward run of belt.

Control of the Electric Field Due to Belt Charge

If the charge distribution is assumed to be uniform on all belt surfaces, the current of 370 microamperes which is now transferred by the 14-inch wide belt at one atmosphere pressure of air corresponds to a gradient due to the belt charge of about 12,000 volts per centimeter. This gradient is directed outward from each surface of each run of the belt. At the higher currents obtained at higher pressures this surface gradient is proportionately higher; for example, at 1.85 milliamperes, the gradient is about 60,000 volts per centimeter. The transverse gradient due to belt charge, though rarely a source of difficulty at atmospheric pressure, may cause serious sparking difficulties at higher pressure unless the problem is recognized and suitable control of the fields due to belt charge established.

In the usual arrangement[4, 6] employed in pressure-insulated electrostatic generators the electric field due to the belt charge extends the entire distance from the belt surface to the equipotential rings, and hence causes the potential of the belt to be greatly different from the potential of the ring at that same level. Moreover, since the belt looks out upon a ring which is at a varying distance due to its curvature, the potential across the width of the belt is also varying at any transverse level. On the inner surfaces of the belt, the field due to belt charge usually extends across the distance between belt runs, the lines of force from a negatively charged belt terminating on the positive charges carried by the adjacent run. Here the relatively large spacing between belt runs again results in a high difference of potential in the same transverse plane between the two runs of the belt. When the runs of belt are carrying unequal currents the variation of potential in the transverse plane is evidently even greater than with the assumed balanced charge distribution. Thus in the usual construction large potential variations exist in the transverse plane due to the charge carried by the belt, potential variations which may be of the order of hundreds of thousands of volts. This situation has been found to limit the steady current which can be carried under high pressure to a value not much greater than can be carried by a belt under normal pressure. It is evidenced by great current unsteadiness and by sparking or gliding discharges along the belt even with the terminal grounded, and it results in a limitation of the steady voltages which can be insulated by the pressure generator when an increase in current is attempted; this limitation is due to the condition of ionization and local breakdown which sets in along the belt.

These difficulties due to the charge on the belts can be substantially eliminated by localizing the resultant field by means of conducting tubes connected to the column hoops and closely spaced and parallel to each face of each belt. These tubes which are shown endwise in Fig. 1, and again in the partially assembled column in Fig. 2, evidently reduce to a relatively small value the variation in potential in the transverse plane due to the belt charge. While these parallel tubes have an important corrective effect even when spaced several inches from the belt, it has been found best to place them almost in contact

FIG. 2. View of partially assembled generator column.

with the belt surface. In this generator the spacing is one-quarter inch from the belt surface to control tube. If a surface gradient of 60,000 volts per centimeter is assumed, the potential difference between the charged belt and the column in any transverse plane is only about 40,000 volts. Without such control, the expected increase in the charge densities and current output of the belt with pressure could not be obtained.

This arrangement of field-control tubes closely spaced to each side of each run of the belt at the same time effectively divides the belt lengthwise into a series of short sections with a controlled potential applied to each, and thereby increases the breakdown strength along the belt. Since the length of the column is governed primarily by the length of belt required to insulate the desired terminal voltage, this increase in the dielectric strength along the belt is significant. Moreover, the requirement of equal charge on each run of belt, which is difficult to realize for all currents and all pressures, particularly when a self-inducing charging arrangement is used in the high voltage terminal, is eliminated by the shielding effect of the conducting tubes which pass between the two runs of the belt. The acceleration tube is likewise shielded from the electrostatic field due to the belt charge.

With this method of belt charge control the expected steady increase with pressure of the charge-carrying capacity can be obtained. This is shown in Fig. 3 for the case of air and Freon. All currents are measured with the terminal approximately at ground potential. The increase in current is nearly linear with pressure, steady currents of almost two milliamperes being obtained at 11 atmospheres of air absolute. Freon is seen to give the same currents at one-third the pressure required in the case of air. The above principle of controlling and limiting the electric field due to the belt charge appears to be fundamental to the realization of the full current-carrying capacity and full compactness of pressure-insulated electrostatic belt generators.

EFFECT OF PRESSURE AND GAS ON VOLTAGE

Figure 4 shows the variation of maximum voltage with pressure for air and Freon. In all cases the voltage limitation, as was desired in the design, was due to sparking from the high voltage terminal to the side of the tank. With air at 165 lb. per square inch absolute, maximum voltages of 1.4 megavolts can be obtained. With pure Freon at 50 lb. per square inch absolute, voltages up to 1.5 megavolts are obtained. The voltage rises nearly linearly, and insulation for a million volts is obtained at 30 lb. per square inch absolute. It is seen that with this gas the same voltage is insulated at somewhat less than one-third the pressure required with air. The use of Freon (dichlorodifluoromethane) for the time involved in these tests did not produce any injurious effect on the material, although considerable sparking and hence decomposition of the

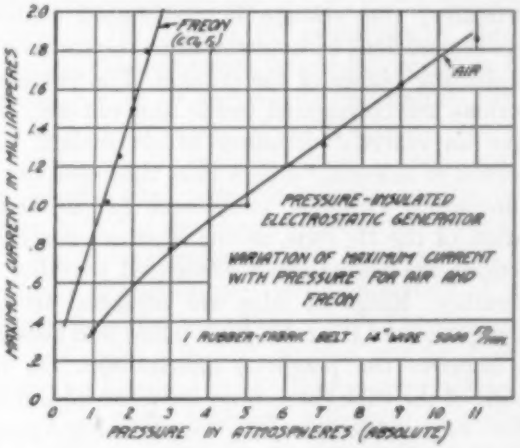

FIG. 3. Increase of generator current with pressure for air and Freon.

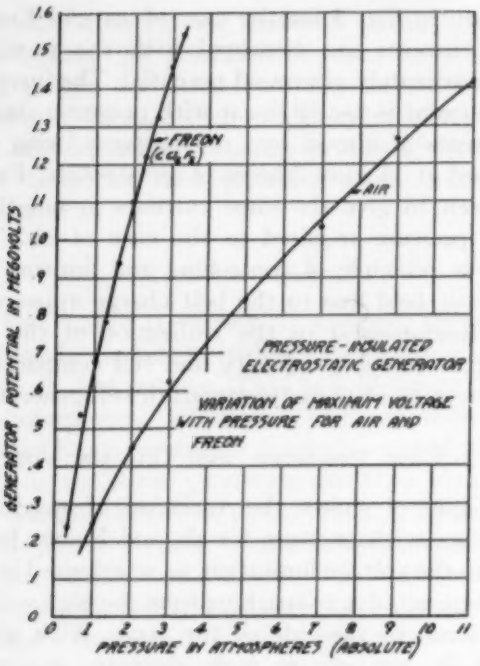

FIG. 4. Increase of generator voltage with pressure for air and Freon.

gas was permitted in order to determine the maximum voltage. The study of this and other gaseous compounds for use as the insulating medium in pressure-insulated electrostatic generators is being carried on as a separate research.

X-RAY ACCELERATION TUBE

The x-ray tube is of the cascade type and consists of sixteen porcelain sections mounted vertically; the voltage is distributed equally between sections by connection to the transverse conducting planes of the column. The porcelain sections are corrugated inside and outside, and have an external diameter of six inches. The method of assembly differs from that used in the Huntington Hospital x-ray tube in the elimination of the tie rods, as the separate porcelain sections are permanently cemented together at assembly. Rings of wire are attached to the corrugations of the tube, both inside and outside, to improve the potential distribution. On the inside of the tube these rings have the additional effect of preventing axially unsymmetrical space charges on the tube walls, which would have a deflecting effect on the cathode stream.

Electrons are emitted from a 10-mil flat spiral filament in a hemispherical cup at the upper end of the tube, and directed in a parallel beam by electrostatic lenses which acquire their potential from the column. At the cathode end of the tube a series of annular rings are mounted on rods fixed to each of the transverse conducting planes as shown in Fig. 1. Except for these first few acceleration stages, the accelerating electrodes each consists merely of a flat metal disk with a large central hole. This general construction is simple, permits higher pumping speed due to elimination of the usual tubular electrodes, and allows excellent focusing. The electron source is mounted with a metal bellows to permit the centering of the focal spot on the target. The position of the focal spot does not shift over the entire range of voltage; the size of the spot diminishes from approximately three-quarters of an inch in diameter at 200 kv to three-eighths of an inch in diameter at 1.25 megavolts. No magnetic focusing is used. The x-ray target consists of a double copper cup between which water is circulating, the inside of which is coated with a 10-mil thickness of gold. The target is insulated from the tube extension so that the current to the target can be read on a milliammeter at the control panel. The x-rays are defined to a beam by a four-inch lead sheath with a bottom portal so that the rays utilized in treatment are those transmitted in the downward direction through the target and water-cooling jacket.

OPERATION

Instruments for reading the current arriving at the target, the accelerating voltage, and the x-ray intensity, are mounted on a remotely located control panel. The controls may be left at a predetermined voltage and current setting, and full voltage and current applied in about a second without injury to the tube. The generator remains stable at the same voltage and current values over long periods of time and requires only occasional adjustment to prevent slow drifting. The voltage is read with an accuracy of about one percent by means of a generating voltmeter of special design, mounted on the top of the tank.

X-Ray Output

The generator can be operated at all voltages from 200 kv to 1250 kv with a current on the target of well over one milliampere. At 1250 kv with about 5 mm of lead equivalent filtration, the x-ray intensity per milliampere in the downward direction 50 centimeters from the target is about 340 roentgens per minute. Various measurements of the physical properties of the radiation produced are now being made.

Acknowledgments

We are glad to take this opportunity of acknowledging the very able assistance in this development of Mr. Robert W. Cloud and Mr. Augustus T. Norton, Jr., as well as the help of Mr. Francis J. Safford during the summer of 1938.

In conclusion we gratefully acknowledge the generous grant of the Godfrey M. Hyams Trust which made possible the work described in this paper.

JUNE 15, 1939 PHYSICAL REVIEW VOLUME 55

Dipole-Dipole Resonance Forces

G. W. King,* *Sterling Chemistry Laboratory, Yale University, New Haven, Connecticut*

AND

J. H. Van Vleck, *Harvard University, Cambridge, Massachusetts*

(Received April 12, 1939)

London has shown that at fairly large interatomic distances r, the polarization energy of a molecule composed of two identical atoms varies not as the customary r^{-6}, but rather as r^{-3} in case one atom is in the ground state, and the other is in an excited state which can combine by dipole transitions with the ground level. The present paper is concerned with the size and sign of this dipole-dipole resonance energy obeying the inverse cube law. The sign has no immediate relation to the sign of the exchange and penetration forces which predominate at closer approach. This possibility of a change from repulsion to attraction results in one of the stable levels of the group of first excited states (derived from separate atom configuration $S+P$ for example) having a lip of activation energy before decomposition into atoms. There will also be a "repulsive" state having a shallow minimum at large separations. Molecules of the heavy atoms have an activation lip so large that the whole stable region is above the dissociation energy. Potential curves of this type have previously been derived empirically from spectroscopic analysis in the case of Hg_2 and Cd_2. The lip is less pronounced in lighter atoms but is none the less real, and has experimental confirmation in the Na_2 spectrum.

Introduction

IT IS well known that the polarization of van der Waals energy of a molecule composed of two unexcited atoms varies as the inverse sixth power of the interatomic distance r. The inverse third power, however, occurs for a molecule composed of two identical atoms when one of them is in the ground state, and the other is in an excited state which can "combine," in the spectroscopic sense, with the normal state. The mathematical origin of this anomalous inverse cube energy is quite clear. In the energy matrix the elements connecting the different approximate states are, at large distances, dipole-dipole interactions proportional to $1/r^3$. In the diagonalization of the matrix by perturbation theory such nondiagonal terms in general occur as the square, $\sim 1/r^6$, in the energy expression, corresponding to the potential of the familiar van der Waals forces. If, however, there is degeneracy, the nondiagonal elements appear to the first power, $\sim 1/r^3$ in the energy expression. Physically this kind of coupling could be described as exchange of excitation—the de-excitation of one atom with excitation of the other. The existence of a $1/r^3$ term was first pointed out by Eisenschitz and London[1] in the first excited states of H_2. Such a term, however, will occur in certain

* This work was done as a National Research Fellow, 1937.

[1] R. Eisenschitz and F. London, Zeits. f. Physik **60**, 491 (1930). See also H. Margenau and W. W. Watson, Rev. Mod. Phys. **8**, 33 (1936).

levels of any molecule formed of like atoms, and often is of considerable magnitude and long range. It is the purpose of the present paper to examine it somewhat more thoroughly than previously.

Calculation of the Interaction

The only molecular states in which such forces occur are those composed of atoms in states between which there is a dipole moment, e.g., $S+P$, $P+D$, etc. The most important cases are the states arising from the configuration $S+P$.

At distances where electronic exchange integrals are small, molecular binding is Hund's case b; single electronic eigenfunctions need be used no longer, but simply functions of the atom as a whole, say S and P. That is, the approximate molecular functions may be taken as SP and PS, the notation PS indicating interchange of the whole atoms. We must make a definite convention once and for all about this operation of "interchange of atoms," say

$$x_i,\ y_i,\ z_i \text{ (atom 1)} \rightarrow x_i,\ y_i,\ z_i \text{ (atom 2)}, \quad (1)$$

where the x, y, z, coordinates of each atom are parallel. In what follows, we shall take the z axes to be parallel to the internuclear axis. This definition of "interchange" means simple translation, with no reflection in center of gravity. The latter definition, of course, would be just as good.

The mathematics of finding the energy levels and the wave functions is the same as in the Heitler-London treatment of the hydrogen molecule. The energy matrix (Slater's notation) is, allowing for nonorthogonality

$$\begin{pmatrix} (SP, H\,SP) & (SP, H\,PS) \\ (PS, H\,SP) & (PS, H\,PS) \end{pmatrix} \times \begin{pmatrix} 1 & (SP, PS) \\ (PS, SP) & 1 \end{pmatrix}^{-1} \quad (2)$$

with energy levels

$$W=[(SP, H\,SP)\pm(SP, H\,PS)]/[1\pm(SP, PS)^2] \quad (3)$$

for eigenfunctions symmetric S^4 and antisymmetric A^4 with respect to interchange of the atoms. The corresponding wave functions are

$$\psi=(SP\pm PS)/[2\pm 2(SP, PS)^2]^{\frac{1}{2}}. \quad (4)$$

We shall henceforth disregard the small nonorthogonality corrections and so treat the denominator of (3) as unity.

Perturbation energy

In the general case of n electrons in each atom the perturbing part of the Hamiltonian is

$$H'=\sum_{i,j}\left[-\frac{eE_A}{r_{iB\,A}}-\frac{eE_B}{r_{iA\,B}}+\frac{e^2}{r_{ij}}+\frac{E_AE_B}{r}\right], \quad (5)$$

that is, the potential of the electrons of one atom in the field of the other nucleus, and the mutual repulsions of all the electrons and of the two nuclei.

Whatever the value of n this potential function may be expanded in a Taylor series to give, in terms of the Cartesian coordinates of the electrons,

$$r^3e^{-2}H'=(\sum_i^n x_{iA})(\sum_i^n x_{iB})+(\sum_i^n y_{iA})(\sum_i^n y_{iB})-2(\sum_i^n z_{iA})(\sum_i^n z_{iB}) \quad (6)$$

plus higher terms. The terms written are dipole-dipole interactions.

Thus the matrix element $(SP, H'\,SP)$ is zero, while the atom exchange element $(SP, H'\,PS)$ becomes

$$e^2r^{-3}\left[\left(\int S\sum x_i P\,d\tau\right)^2+\left(\int S\sum y_i P\,d\tau\right)^2-2\left(\int S\sum z_i P\,d\tau\right)^2\right]. \quad (7)$$

Now in the spherical symmetry of the atomic field the dipole moment induced in any *one* of the Zeeman components of the atomic transition $S\longleftrightarrow P$ is (x, y, z, being equivalent)

$$\mu_m=e\int S\sum q_i P\,d\tau \quad (q=x, y, z). \quad (8)$$

Thus the difficult part of the molecular calculation is referred back to the theory of atomic

structure. The dipole moment μ_m may be obtained either from theory (as in the case of H or Na) or from experimentally determined values of the number of dispersion electrons,

$$\mu_m^2 = f_{ij} R / \nu_{ij} g_j, \tag{9}$$

where g_j is the weight factor of the lower state, and ν_{ij}/R is the energy of the transition in atomic units (R being the Rydberg constant). Note that the square of the dipole moment associated with a normal atomic transition is three times this expression (9), as one sums over the three Zeeman components, i.e., over m. There are then no undetermined constants in our calculations, as μ_m can thus be regarded as known.

The energy of interaction is then proportional to μ^2_m/r^3, the proportionality factor depending on the orientation of the P state to the molecular axis. In the language of resonance phenomena, as an S and a P atom approach, each atom resonates between its S and its P state. The coupling energy is due to the interaction of the two dipoles induced by this resonance, or *atom*-exchange, the magnitude and sign depending on the orientation of the dipoles with respect to the internuclear axis.

Our molecular states $SP \pm PS$ have a threefold orbital degeneracy at infinite internuclear distance because of the three possible orientations of the orbital angular momentum. At closer approach, however, the energy is different for the Σ and Π levels, which have, respectively, $\Lambda = 0$ and $\Lambda^2 = 1$, where Λ is the component of orbital angular momentum parallel to the figure axis, measured in multiples of $h/2\pi$. The Π levels are, of course, doubly degenerate because of the two sign possibilities for Λ. Now the matrix elements of z vanish unless $\Delta\Lambda = 0$, while those of x, y obey the selection rule $\Delta\Lambda = \pm 1$. Hence for Σ states, the expression (7) becomes $-2\mu_m^2/r^3$, because the integrals (8) over x and y are zero. For Π states, on the other hand, (7) gives μ_m^2/r^3 since here the integral[2] over z and over x *or* y disappears.

TABLE I. *Coupling energies of the four distinct states.*

STATE	WAVE FUNCTION	COUPLING ENERGY
Σ_u	$SP+PS$	-2
Π_u		$+1$
Σ_g	$SP-PS$	$+2$
Π_g		-1

It is customary to classify molecular states as g or u according as they are even or odd under reflection in the center of symmetry, midway between the nuclei, defined by the operation

$$x_i, y_i, z_i \text{ (atom 1)} \rightarrow -x_i, -y_i, -z_i \text{ (atom 2)}. \tag{10}$$

Now the reflection (10) can be interpreted as a translation (1) followed by a reflection in a nucleus. Furthermore the atomic wave functions S and P must have opposite symmetries or Laporte parities as regards nuclear reflection because otherwise the S and P states could not combine in dipole transitions, as we have supposed. It therefore follows that the substitution (10) takes the wave function SP into $-SP$, and that the upper and lower sign choices in (3) or (4) correspond to u and g states, respectively. Taking into account the results of the preceding paragraph, we thus find that the inverse cube term in the energy has the values given in Table I. The coefficients for the Π but not the Σ states were also previously calculated by Eisenschitz and London. Table I is applicable regardless of the multiplicity, i.e., whether the state is a singlet, triplet, etc., since the symmetry as regards electron in distinction from atom exchange has not entered into our calculations in any way. It is also to be noted that our computations are independent of the number of electrons in the system: the energetics of a diatomic molecule, at fairly large distances, has been reduced to a two-body problem, although the two bodies individually may be very complex, the only requirement for our calculations being that the transition probabilities between their states are available.

Since electron-exchange integrals die out ex-

[2] Each Π level is twofold except insofar as the degeneracy is lifted by molecular rotation giving the phenomenon of "Λ-type doubling" which we neglect. We need not enter into the question of the precise linear combinations of wave functions appropriate to the two components of the Λ-doublet, and instead for our purposes the Π levels may be supposed to have a cosine or sine azimuthal factor, so that either the x or y component drops out. With exponential azimuthal functions, there are both x and y contributions, but then there is an additional factor $\frac{1}{2}$, so that in any case the absolute value of the coefficient of our $1/r^3$ term is half as large for the Π as the Σ states. That $\mu_x^2+\mu_y^2$ gives no bigger effect than μ_z^2 is essentially a reflection of the fact that the x, y intensity must be apportioned between the two practically coincident Π states.

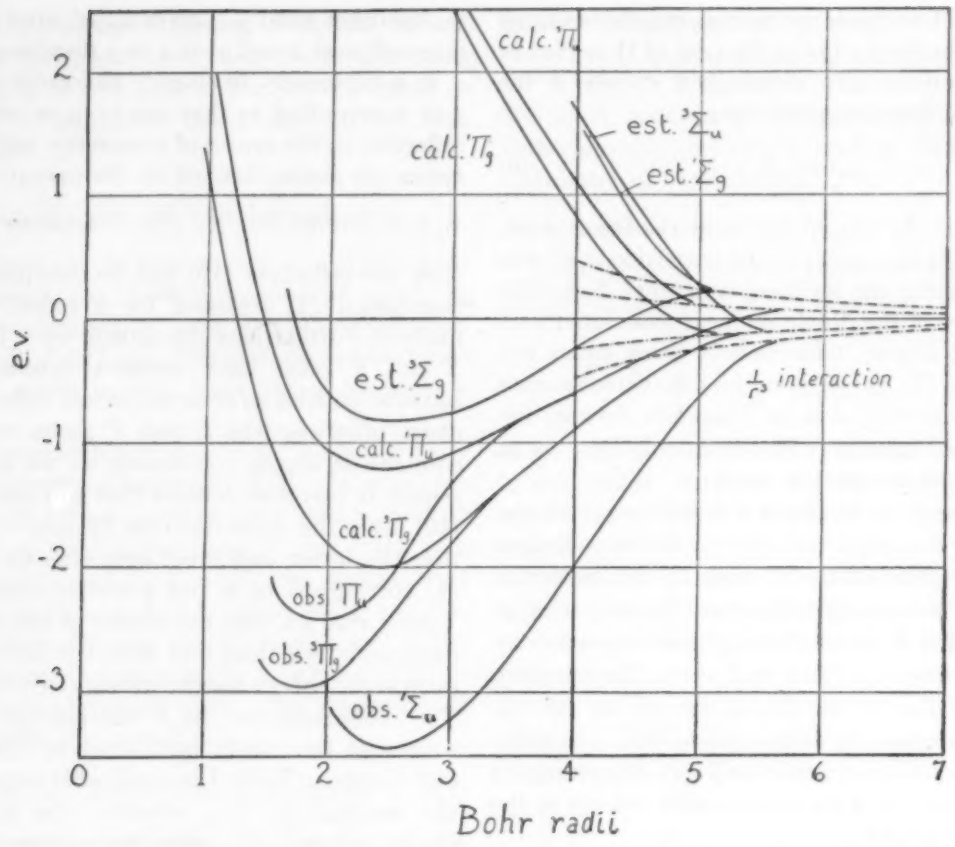

FIG. 1. First excited states of H_3. The curves $C\,^1\Pi_u$, $B\,^1\Sigma_u$, $^3\Sigma_g$ are known experimentally in the neighborhood of their minima. The course of the Π states have been calculated theoretically as far as $4a_0$ by Kemble and Zener (reference 4). The Σ states have been sketched in by analogy, the $-\cdot-\cdot-$ curves at the asymptotic μ^2/r^3 curves.

ponentially the above calculations will give the correct interaction at large distances. At shorter distances, exchange becomes predominant, but the *sign of the total exchange terms has no relation to the sign of the* $1/r^3$ *term*. Some states then may be repulsive at large distances, but attractive and stable closer in, and vice versa. For atoms with one valence electron, each one of the states listed in Table I corresponds to a singlet and a triplet, and in general one of these multiplets will change the sign of its interaction as the atoms approach to distances where electron exchange predominates.

Thus it is possible to have an activation energy of dissociation, the $1/r^3$ force causing a peak or lip in the potential curve, above the limit of dissociation energy (see figures).

Similarly, the $1/r^3$ term may be attractive reverting to a repulsive electronic exchange term, thus giving rise to a stable molecule only at fairly large distances.

The actual magnitude of the activation lip, or the small dissociation energy just mentioned, is very sensitive to the balance of the exchange and $1/r^3$ terms at moderate distances. All molecules in the states discussed, i.e., those formed from $S+P$ atom states, will have the μ^2/r^3 energy at some separation r. In some molecules we believe this activation energy is detectable.

In other cases the effect of this term is detected only in the anharmonicity in the upper slopes of the potential curve, showing up as a change in the course of the Birge-Sponer extrapolation of the vibrational levels.[3]

[3] W. Jevons, *Band Spectra of Diatomic Molecules* (Cambridge Univ. Press, 1932), p. 194.

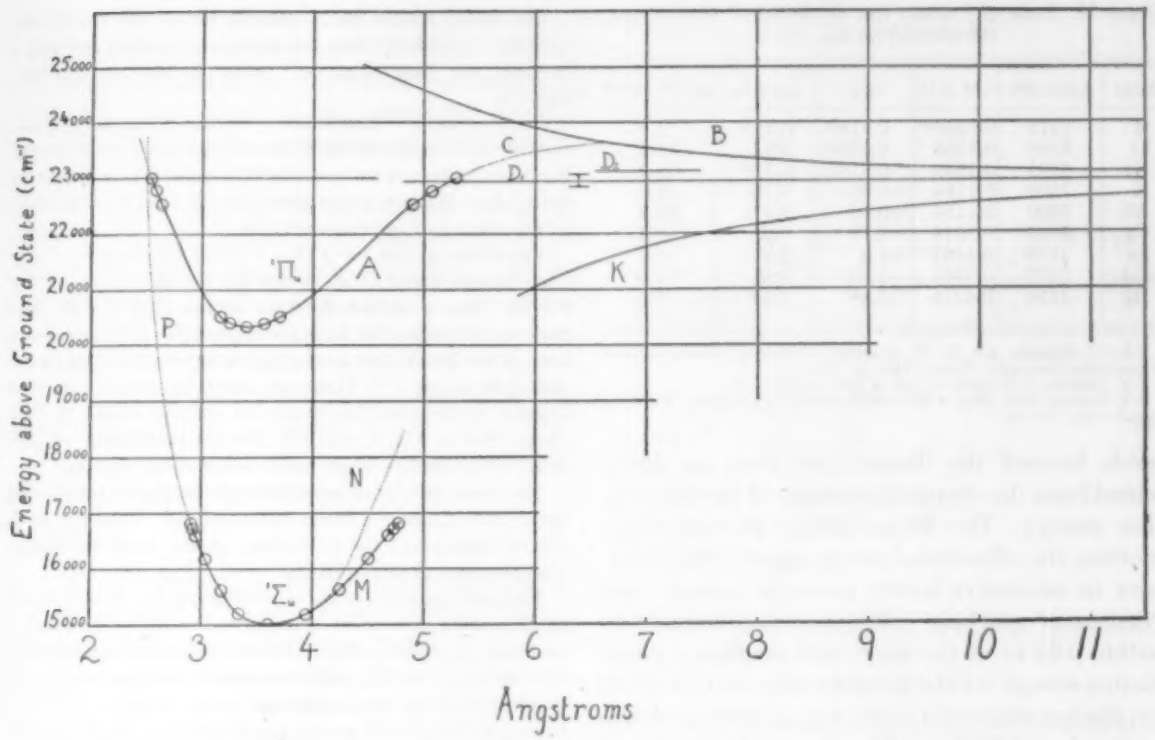

FIG. 2. First excited states of Na_2. The circles represent points calculated from the experimental data.

APPLICATIONS

Hydrogen

The asymptotic interaction energies calculated for H_2 and Na_2 are plotted in Figs. 1 and 2. The dipole moment μ for these atoms can be obtained from theory. For the $1s-2p$ transition of hydrogen, $\mu=0.745$ atomic unit, so the interaction energy of H(S) and H(P) becomes 15 ev/r^3, with r measured in atomic units (Bohr radii). The potential curves of all the states arising from this configuration are drawn in Fig. 1.

The effect of the $-2\mu^2/r^3$ term is definitely detected in the shallow experimentally determined curve of $B^1\Sigma_u$. The curve of $C^1\Pi_u$ has not been followed experimentally close enough to the dissociation limit to make connection with the predicted $+\mu^2/r^3$ lip, but its sharp rise and low anharmonicity relative to B indicates the course may be as in Fig. 1.

The electronic exchange energy in the Π states has been calculated by Kemble and Zener,[4] and the courses of the $^{1,3}\Sigma$ states have been sketched in by analogy. Both $^1\Pi_g$ and $^3\Sigma_u$ are repulsive except for shallow minima at $4a_0$ but as far as we know these stable levels have never been observed.

Since the basis functions ($1s$ and $2p$) used by Kemble and Zener, are the true atomic function in this case of hydrogen, namely our S and P, the curves calculated for the Π states should agree exactly with our dipole-dipole calculation at larger distances of separation.

Alkali molecules

The potential curves[5] of the $^1\Sigma_u$ and $^1\Pi_u$ states of Li_2, Na_2 and K_2 very definitely show the effect of the $1/r^3$ term, the $^1\Pi_u$ potential curve rising sharply and the $^1\Sigma_u$ curve being very shallow. The vibrational levels have been measured to very high quantum numbers permitting the construction of the potential curves almost to the dissociation limit.

In the case of Na_2 there is a possibility of an actual activation lip, i.e., there are vibrational

[4] E. Kemble and C. Zener, Phys. Rev. **33**, 512 (1929).

[5] See, for example, H. Sponer, *Molekulspektren II* (Julius Springer, Berlin, 1935), p. 155, Fig. 53.

TABLE II. *Table of f values and dipole-dipole interactions, calculated from Eq. (9).*

ATOM	$\lambda A(S\to P)$	ν/R at.u.	$fS-P$	μ_m^2 at.u.	μ_m^2/r^3 EV/A^3
H	1215	0.7500[18]	0.416[19]	0.555	2.2
Li	6708	0.1358	0.7500	5.52	22.0
Na	5893	0.1546	0.9755	6.31[20]	25.2
K	7699	0.1184	~0.98	8.28	33.0
Rb	7900	0.1154	~0.98	8.47	33.8
Cs	8943	0.1019	0.98	9.62	38.4
Zn	2139	0.4261	~1.2	2.82	11.2
Cd	2289	0.3981	1.20	3.01	12.0
Hg	1850	0.4926	1.19	2.42	9.6

[18] E. U. Condon and G. H. Shortley, *Theory of Atomic Spectra* (Cambridge University Press, 1935), p. 133.
[19] Y. Sugiura, J. de phys. et rad. **8**, 133 (1927).
[20] Y. Sugiura, Phil. Mag. **4** 502 (1927) calculates a value of 18.89 for $\Sigma_m\mu_m^2=3\mu_m^2$ for Na.

levels beyond the dissociation limit as determined from the chemical estimate of the dissociation energy. The Birge-Sponer extrapolation, plotting the vibrational energy against the difference in successive levels, given by Loomis and Nusbaum,[6] has been followed experimentally to within 0.02 ev of the limit, and predicts a dissociation energy (of the ground state) of 0.76 ± 0.02 ev, the last measured point, Fig. 2, corresponding to a value of 0.74 ev. The chemical evidence of Lewis[7] gives 0.728 ± 0.013 ev. The sharp break in the extrapolation curve,[6] marks the onset of the $1/r^3$ law.

In Fig. 2, curve A is the potential curve of the $^1\Pi_u$ state of Na_2 constructed from the experimental data[6] by O. Klein's[8] formulation of Rydberg's method, $\int p\,dr=(v+\frac{1}{2})h$, etc. That is, curve A can be considered as having been determined experimentally. The width of each level, $r_{max}-r_{min}$, is accurately known from the vibrational energy. The positions of the walls of the potential curve are fixed by $1/r_{max}-1/r_{min}$, determined from B_v. Since the latter are not known at the higher levels except by extrapolation of $B_v-\alpha(v+\frac{1}{2})$ the curve as drawn may not be pushed sufficiently far out. However, even in the most extreme case[9] the upper slopes of $^1\Pi_u$ show that it will be difficult to extrapolate to the dissociation energy calculated as 22,952 cm^{-1} from the chemical determination of the ground state dissociation energy,[7] 5900 ± 100 cm^{-1} plus atomic activation 16,966, (represented by D_1 on the diagram).

On the contrary the curve definitely tends to the limiting $+\mu^2/r^3$ law (curve B) plotted upwards from 22,952 cm^{-1}.

The upper slopes of A can be fitted by $E=23{,}840-3520/r^6$, which function was used to interpolate (curve C) between the "experimental" curve A and the limiting curve B.

Predissociation.—Examination of the observed intensities[6] of the v'-progressions leads one to expect some $v'=27$ bands to appear with considerable intensity, whereas in actual fact there is a complete cut-off after $v'=26$, indicating some sort of predissociation.

The value of $2\frac{1}{2}\pi h^{-1}m^{\frac{1}{2}}\int(E-V(r))^{\frac{1}{2}}dr$ obtained from our combination curve C, B, is 300 for $v'=26$, and is 40 for $v'=29$. Thus a sudden decrease occurs after $v'=26$, but these estimates are too large for appreciable predissociation even in the latter case, as the significant exponential factor would be about e^{-80}. However, these values are for zero angular momentum; the curves for nonzero values of J lie above that of Fig. 2, and the average probability of predissociation for the whole band is somewhat greater.

The error in the construction of the curve mentioned above would favor a lower potential hill. However, it is the thickness, i.e., the $1/r^3$ effect, rather than the height that prevents predissociation.

The other possible cause of predissociation, proximity of another state into which a radiationless transition can occur, may be effective here. The only permissible perturbing state of Na_2 is the $^1\Sigma_u$, which conceivably might cross $^1\Pi_u$ at a radius less than the equilibrium value, near r_{min}, and not having the lip, could permit predissociation. If so, the $^1\Sigma_u$ state would have to be sharply repulsive at small distances, as shown by the dotted line in Fig. 2. The $^1\Sigma_u$ and $^1\Pi_u$ levels can interact when rotational distortion terms in the Hamiltonian function are included.[10] The possibility that at small distances the $^1\Sigma_u$ curve actually crosses above the $^1\Pi_u$ is not merely an *ad hoc* suggestion, for it is indicated by two lines of evidence, *viz.* by the higher vibration frequency for $^1\Sigma_u$ than for $^1\Pi_u$ and also by the fact that $^1\Pi_u$ coalesces[11] into a state of lower energy for the united atom than does $^1\Sigma_u$.

The experimental data for the $^1\Sigma_u$ state have not been extended to high enough v's to make the connection with $-2\mu^2/r^3$. Curve M is constructed by the Klein-Rydberg method, curve N by Condon's formulae[12] as given by Loomis and Nile.[13]

In Li_2 too, the vibrational levels have been observed[14] to within a few hundredths of a volt of the dissociation limit. The value calculated for the dissociation energy of the ground state is 1.14 ev, considerably higher than the value of 1.02 ev obtained by other means.[7]

[6] F. W. Loomis and R. E. Nusbaum, Phys. Rev. **40**, 384 (1932). The convergence limit thus calculated is marked as D_2 in Fig. 2.
[7] C. Lewis, Zeits. f. Physik **69**, 786 (1931).
[8] O. Klein, Zeits. f. Physik **76**, 226 (1932).
[9] The fact that the inner wall cannot have an overhang, i.e., r_{min} undoubtedly decreases as the energy increases, affords a limit to the possible displacement of the (known) width $r_{max}-r_{min}$.

[10] R. de L. Kronig, *Band Spectra and Molecular Structure* (Cambridge University Press, 1930), Chap. II.
[11] R. S. Mulliken, Rev. Mod. Phys. **4**, 1 (1932), especially Fig. 43.
[12] E. U. Condon, Phys. Rev. **28**, 1182–1201 (1926).
[13] F. W. Loomis and S. W. Nile, Phys. Rev. **32**, 873 (1928).
[14] F. W. Loomis and R. E. Nusbaum, Phys. Rev. **38**, 1447 (1938).

The chemical dissociation energy[15] of K_2 is within the experimental error the value obtained by extrapolation of the vibrational levels. The lip must be very small in the case—the negative exchange integrals extending a little further out than in Na_2.

In Rb_2 the value of the dissociation energy obtained by extrapolation of the levels of $^1\Pi_u$ state,[16] is very high, showing the steep rise due to the positive $+\mu^2/r^3$ term.

In these alkali molecules the dipole moment produced in the atomic transition is extremely large, making the $1/r^3$ interaction unusually large and of long range, as shown in Fig. 2 and Table II. This effect will then cause considerable self-broadening in the atomic lines of the alkalis.

Cadmium

The calculation of the $1/r^3$ interaction energy is independent of the number of electrons. Consequently the same formulas (Table I) apply to the first excited states of He_2, Hg_2, Cd_2, Zn_2, even though there are now two valence electrons per atom, so that the coupling is of the type s^2-sp rather than $s-p$. There is experimental evidence on the importance of this type of interaction in the spectra of Hg_2 and Cd_2.

Cram[17] has analyzed the bands of Cd_2 lying on either side of the $^1S_0-^1P_1$ atomic line and can only account for the spectra by assuming a curve of the type drawn in Fig. 3 for the state $\Lambda=1[^1\Pi_u]$ arising from the configuration $5S+5P$.

The dipole moment of the atomic transition $S\leftrightarrow P$ of Cd can be calculated from the experimentally determined f values (see Table II). In Fig. 3, the course of the molecular energy of Cd_2 at large distances is drawn, B, from the state having the asymptotic energy $+\mu^2/r^3$. The curve A is the experimentally determined potential curve for the state $\Lambda=1$ which differs from $+\mu^2/r^3$ by the predominance of stabilizing exchange, etc. energy at closer approach. Thus the difference of A and B, represented by C, is an empirical determination of exchange and penetration energies. This curve compares favorably with that for the binding energy in normal molecular states—where the asymptotic expression is of the van

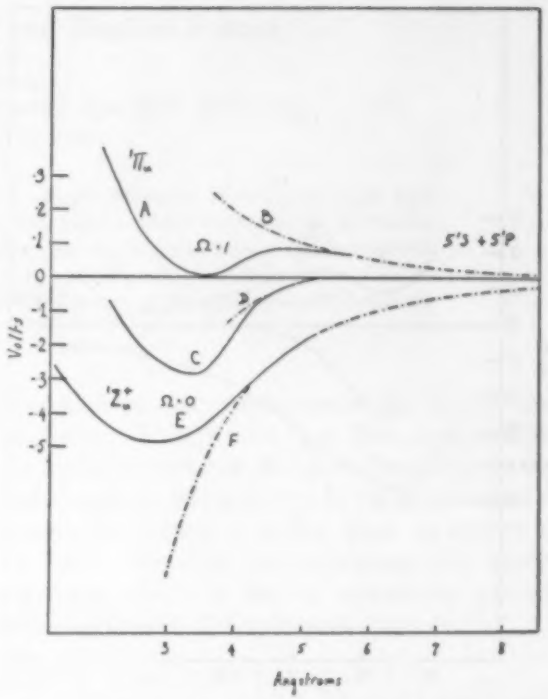

FIG. 3. First excited states of Cd_2, bordering the atomic line $5S_0-5P_1$. Curve A was determined by Cram (reference 17). B and F are the μ^2/r^3 limiting laws.

der Waals $1/r^6$ type. Curve D is an example of the latter as obtained from the calculated $1/r^6$ curve for normal Hg_2 (see below) modified for the larger dipole of Cd. Comparison of D with B or F shows the essential difference between $1/r^3$ and $1/r^6$ forces, i.e., between resonating and induced dipole-dipole interactions.

Curve F is the $-2\mu^2/r^3$ energy of another stable state of Cd_2, $\Lambda=0$, sketched as E.

Mercury

This same type of potential curve, with a minimum above the dissociation limit has been deduced[21] from the spectrum analysis of Hg_2 for the state $\Lambda=1$ arising from the configuration $6S_0+6P_1$, and is likewise predicted by theory. The curves of Fig. 4 show the experimental, calculated, μ^2/r^3 exchange and van der Waals energies, as described under "Cadmium." The μ of the calculated curves of Hg (B and F) were obtained from the f values of the $^1S_0\leftrightarrow{}^1P_1$ transition of atom Hg (Table II). The van der Waals

[15] C. Lewis, reference 7, corrected by F. W. Loomis and R. E. Nusbaum, Phys. Rev. **39**, 89 (1932).
[16] P. Kusch, Phys. Rev. **49**, 218 (1936).
[17] Winston Cram, Phys. Rev. **46**, 205 (1934).

[21] W. Finkelnburg, *Kontinuierliche Spektren* (Julius Springer, Berlin, 1938), p. 204.

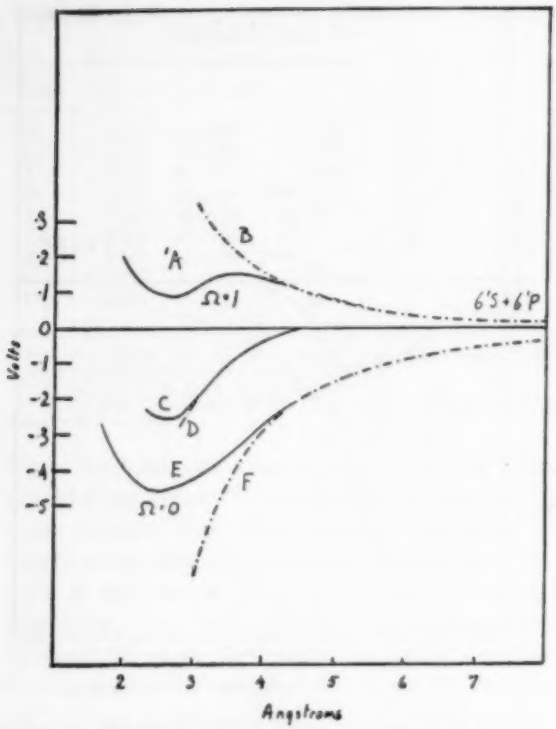

FIG. 4. First excited states of Hg_2, bordering the atomic line $6S_0-6P_1$. The course of the level $\Lambda=0$ was predicted by spectroscopic analysis by various observers (reference 21).

expression for normal Hg_2, curve D has been calculated as -159 ev$/r^6$ (r in A) by F. London.[22]

SUMMARY

One level of the group of first excited states of all identical molecules has an asymptotic coupling energy $+\mu^2/r^3$ *above* the dissociation limit. In molecules composed of atoms of low atomic number, the stabilizing energy (exchange, etc.) has fairly long range and quenches the $1/r^3$ term to an almost insignificant lip (that is, the negative energy does not change over to $+\mu^2/r^3$ until r is very large). However, in heavy atoms, the $1/r^3$ term is powerful enough to keep the whole stable region above the dissociation limit. There levels may lose much of their sharpness due to penetration of the potential barrier.

This type of curve should be found in excited states of Zn_2 and molecules of other heavy atoms and also in polyatomic molecules composed of two like radicals such as C_2H_2, C_2H_4, C_2H_6, N_2O_4.

Information of a more general nature can be deduced from the above discussion. The existence of the positive, hence repulsive, limiting law even in stable states, and the large negative energy in the other cases, affords a means of discerning the London-van der Waals type of force, and distinguishing it from exchange and penetration, whereas in normal states, in particular the most important ground state, the transition of the limiting $1/r^6$ interaction into the short range interactions cannot be detected from the nature of the potential curve. Since the course of our curves, especially those of Na_2, are fixed fairly accurately by experiment and by theory, we can make a definite observation as to the importance and extent of the London-van der Waals forces. In the cases of Cd_2 and Hg_2 the $1/r^3$ law predominates even at the equilibrium distance; in Na_2 it accounts for about 0.1 ev, but in H_2 it represents only a small fraction of the total binding energy.

In closing, we may suggest the possibility that the repulsive $1/r^3$ type of van der Waals force furnish the activation hill in, perhaps, e.g., the dimerization of NO_2.

Acknowledgment.—The authors express their appreciation of the hospitality of the Physics Department of Princeton University, where this work was done.

[22] F. London, Zeits. f. physik. Chemie **B11**, 222 (1930).

Binding Energy of He^6 and Nuclear Forces

H. MARGENAU
Sloane Physics Laboratory, Yale University, New Haven, Connecticut
(Received April 14, 1939)

A second-order perturbation calculation of the energy difference He^6-Li^6 is made with inclusion of all doubly excited oscillator states. The result, which improves the first-order energy by about 100 percent, alters this difference only slightly and leaves agreement with experiment, already found in first order by Feenberg and Wigner, practically intact. Certain conclusions which may be drawn concerning the detailed nature of the spin forces are discussed.

THE spin dependent constituents of the nuclear forces affect the binding energies of the lightest nuclei (up to He^4) only in an unimportant way, so that their study cannot lead to detailed information regarding the spin parts of the nuclear Hamiltonian operator. The simplest instance which may illuminate these matters is afforded by the pair of nuclei He^6 and Li^6. It is therefore of interest to calculate the energy difference between the normal states of He^6 and Li^6 on the basis of an assumed Hamiltonian and to see what restrictions must be imposed upon the spin parts of the latter. Although it is now fairly certain that a symmetrical Hamiltonian with central pair forces does not afford an entirely adequate description of the nuclear situation, its use in this work was dictated by the complex nature of the calculations involved in dealing with the six-body problem. The conclusions, however, are probably of significance for other forms of interaction.

If the energy difference in question is calculated by means of the Hartree method as was done by Feenberg and Wigner,[1] it turns out to be proportional to the *total* spin force, i.e., to the sum of the parameters measuring the Heisenberg and Bartlett parts. It is only by going to higher approximations that terms proportional to the *difference* of these parameters are introduced, and since our interest is focused upon them, we must take the trouble to compute the second-order Schrödinger perturbation upon the Hartree energy of He^6 in a manner similar to that explained in a previous paper on Li^6.[2]

The difference in energy of the two nuclei is known from the experiments of Bjerge and Broström.[3] They found that He^6, produced by the bombardment of Be^9 with neutrons, is unstable and transforms into Li^6 with emission of β-rays, the fastest of which have an energy of 3.7 Mev. We thus conclude that the energy difference which is due to specifically nuclear forces, exclusive of Coulomb energy, is

$$E(He^6)-E(Li^6)=(4n+2p)-(3n+3p)-\Delta E_c+3.7\text{ Mev}+mc^2.$$

The difference in Coulomb energies, ΔE_c, may be estimated in first order to be 1.1 Mev; $(n-p)$, the mass difference between a neutron and a proton, corresponds to 0.7 Mev; mc^2 is the mass energy of the emitted electron, 0.5 Mev. Hence $E(He^6)-E(Li^6)=3.8\pm0.6$ Mev, the indicated error allowing for uncertainties in the experimental data and (±0.1 Mev) in ΔE_c.

Li^6, having two unlike particles outside the α-particle configuration, has a ^3S state as its lowest state. He^6, however, having two protons in the p shell, is forced by the exclusion principle to assume a ^1S state which has a higher energy. 3.8 Mev must, therefore, represent the difference in the binding energies of the ^3S and the ^1S states of the nuclear six-body problem.

All calculations here discussed are based upon the work on Li^6.[2] Reference is made to that paper for more specific explanation of terminology and symbolism here employed. The Hamiltonian is written in the form

$$H=E_{\text{kin}}-A\sum_{i>j}(w+mP_{ij}+bQ_{ij}+hP_{ij}Q_{ij})\times\exp(-r_{ij}^2/a^2). \quad (1)$$

A and a are again given the values 35.6 Mev and

[1] E. Feenberg and E. Wigner, Phys. Rev. **51**, 95 (1937).
[2] H. Margenau and K. G. Carroll, Phys. Rev. **54**, 705 (1938).
[3] T. Bjerge and K. J. Broström, Nature **138**, 400 (1936).

2.25×10^{-13} cm. The ground state function having the correct symmetry for the ^1S state is

$$\psi(^1S)=(1/6!)^{\frac{1}{2}}(1/3)^{\frac{1}{2}}\times\{|s\eta_1\cdot s\eta_2\cdot s\eta_3\cdot s\eta_4\cdot p_1\eta_3\cdot p_{-1}\eta_4|+|s\eta_1\cdots s\eta_4\cdot p_{-1}\eta_3\cdot p_1\eta_4|+|s\eta_1\cdots s\eta_4\cdot p_0\eta_3\cdot p_0\eta_4|\}. \quad (2)$$

s and $p_{\pm1,\,0}$ denote the $1s$ and $2p$ functions describing the motion of a single particle in the field of an isotropic oscillator, the potential being $\frac{1}{2}(\hbar^2\sigma^2/Ma^2)(r/a)^2$. The parameter σ is adjusted for minimum energy.

$\psi(^3S)$ differs from (2) only by having η_2 in place of η_3 associated with the orbital of the fifth particle. This means that there are exactly as many functions combining perturbationally with $\psi(^1S)$ as with $\psi(^3S)$, and these functions may be obtained by simple changes from the list of functions tabulated for Li^6. Their contributions, of course, are different. With the use of (1) and (2) we find

$$(^1S|H|^1S)=E_{\text{kin}}-\{5+10w-2b-10h+[8-20w-14b+2h]u+[5-10(b+h)]u^2\}(\sigma u)^1A, \quad (3)$$

where u has been written for $(\sigma+2)^{-1}$. With the parameters labeled choice (a) in reference 2, this expression has a minimum of -8 Mev, occurring at $\sigma\approx1.3$, which of course is a very poor approach to the experimental binding energy of 29 Mev. Eq. (3) differs from $(^3S|H|^3S)$ by

$$\Delta_1E=2(b+h)(1-2u+5u^2)(\sigma u)^1A. \quad (4)$$

E_{kin} is equal in the two cases. Feenberg and Wigner have pointed out that $E(He^6)-E(Li^6)$, if computed from (4), agrees quite well with the experimental value. Indeed for $\sigma=1.3$, this expression takes on the value $15.2(b+h)$, so that we are led to conclude $0.21<(b+h)<0.29$. This is about the range in which the parameter $b+h$ (usually denoted by g) is known to lie from other considerations. Thus far, nothing can be said about b and h separately.

In the further pursuit of the problem it is necessary to calculate the matrix elements H_{0i} where the index 0 refers to the ^1S state (2) and i to any function which combines with it. The H_{0i} are then to be substituted into the second-order perturbation formula in order to find the effect on the energy. It is impossible to include all excited states. From the Li^6-problem, however, it is apparent that the doubly excited states make the largest contribution, and that the labor of going beyond them would be quite considerable. Furthermore, it was shown that higher *orders* of the perturbation calculus reduce the contribution of the second, which means that the inclusion of all excited states in the second order would give too low an energy. In the present work, therefore, only doubly excited states will be considered.

In finding the matrix elements use is made of a simple parallelism between the perturbation scheme for Li^6 and for He^6. The functions pertaining to excited configurations may be arranged and numbered in such a way that every H_{0i} for He^6 is identical with that for Li^6, except for the substitution of $-h$ for b, and of $-b$ for h. The reason for this is that the same operation which converts $\psi(^3S)$ into $\psi(^1S)$ changes $bQ+hPQ$ into $-bPQ-hQ$.

Every H_{0i} for Li^6 may be written in the form

$$H_{0i}=(wS_w+mS_m+bS_b+hS_h)(\sigma u)^1A+S_TT\sigma,$$

where the various S are polynomials in $u=(\sigma-2)^{-1}$, and $T=\hbar^2/Ma^2$. The last term represents the kinetic energy. Hence we have in view of the foregoing remarks:

$$(H_{0i}^2)_{\text{Li}}-(H_{0i}^2)_{\text{He}}=2(S_b+S_h)\times[(wS_w+mS_m)(\sigma u)^1A+S_TT\sigma](b+h)(\sigma u)^1A+(S_b^2-S_h^2)(b+h)(b-h)(\sigma u)^3A^2. \quad (5)$$

The first term on the right is proportional to $(b+h)$ and produces in general only a slight modification of the Hartree result. The second, however, depends besides on $b-h$; it may become appreciable unless b and h are nearly equal.

The second-order energy difference is given by

$$\Delta_2E=(2T\sigma)^{-1}\sum_i[(H_{0i}^2)_{\text{He}}-(H_{0i}^2)_{\text{Li}}], \quad (6)$$

where the divisor $2T\sigma$ represents the difference between the unperturbed energy of the doubly excited states and the ground state of the assemblage of oscillators. There are 152 terms in the summation indicated in (6), but many of

TABLE I. *Constituents of* $E(He^6)-E(Li^6)$ *for different values of the variation parameter* σ. *Energies are in Mev.*

σ	Δ_1E	Δ_2E'	Δ_2E''
1	12.2g	$(10.6w+7.8m-4.9)g$	$2.92(h-b)g$
1.2	14.3g	$(11.1w+8.3m-5.4)g$	$2.87(h-b)g$
1.4	15.9g	$(11.1w+8.0m-5.6)g$	$2.66(h-b)g$

them are equal. We split Δ_2E into two parts, in which Δ_2E' is the sum of all the terms proportional to $g=b+h$, and Δ_2E'' is proportional to $g(b-h)$. One then obtains

$$\Delta_2E'=(2T\sigma)^{-1}g(\sigma u)^{\frac{1}{2}}A[(114.8C_1w+34.8C_2m)\times(\sigma u)^{\frac{1}{2}}u^2A-9.62C_3T\sigma u].$$

The coefficients C are the following functions of u:

$$C_1=1-5.82u+16.2u^2-19.2u^3+11.5u^4,$$
$$C_2=1-3.07u+10.3u^2-23.2u^3+37.9u^4,$$
$$C_3=1-3.96u+6.93u^2.$$

The energy minimum for Li^6 lies in the range $1<\sigma<1.4$. For the purposes of the present investigation it is permissible to assume that the minimum for He^6 occurs at the same value of σ as for Li^6; the minimum is very shallow. Now in the above range of σ, C_1 varies from 0.289 to 0.287, C_2 from 0.732 to 0.686, C_3 from 0.45 to 0.42; while u goes from 0.333 to 0.294. Insertion of these values leads to the entries in Table I. Δ_2E' adds but little to Δ_1E as calculated from Eq. (4). For whatever the magnitude of w and m, their sum must be g and hence in the neighborhood of 0.25. But as long as this is true the kinetic energy term in Δ_2E' (last one written) nearly cancels the contributions of the Wigner and the Majorana forces. Δ_1E' is approximately 0.1 Mev for the three values of σ listed; it is the same for both choices of nuclear constants considered.[2] (Cf. caption of Table II.)

We turn next to the calculation of Δ_2E''. On summing over all the states in (6) there results

$$\Delta_2E''=(2T\sigma)^{-1}\cdot 25\sigma^3u^5\times(1-9.6u+24u^2-22.4u^3)g(b-h)A^2.$$

The polynomial in parenthesis is negative for values of u which are here of interest. Δ_2E'' is entered in the last column of Table I. It has the value -0.4 Mev. for the three values of σ and is also the same for both choices of constants.[2] Choice (b), which gives the poorer result for the binding energy of Li^6, yields better values for the energy difference of the singlet and triplet states.

TABLE II. $E(He)-E(Li)$ *for two typical choices of force constants: (a)* $w=-2/15$, $m=14/15$, $b=7/15$, $h=-4/15$; *(b)* $w=-1/12$, $m=10/12$, $b=5/12$, $h=-2/12$,

	$E(He^6)-E(Li^6)$		Feenberg-Wigner approximation (Δ_1E)	
σ	(a)	(b)	(a)	(b)
1	2.2	2.8	2.4	3.1
1.2	2.6	3.3	2.9	3.6
1.4	2.9	3.6	3.2	4.0

It is to be noted that the higher approximations here computed have only a small effect on this difference, although they improve the total binding energy by 100 percent. The contrary was found to be true in connection with the spacing between the ^3S and the ^3D states of Li^6, two states of different orbital symmetry.[2] Agreement with experiment is in the present instance made slightly poorer by the inclusion of higher approximations, but is not destroyed.[4]

If the energy difference in question were known with greater experimental precision, the present calculation would permit the determination of the quantity $(h-b)$ as a function of $(h+b)$. Thus, let us suppose it to be 3.8 Mev exactly. Taking the best value of σ to be 1.3 (maximum binding for Li^6) and determining the coefficients of the force constant by interpolation from Table I, we find that the following correlation must hold between $(h+b)$ and $(h-b)$:

$(h+b)$	$(h-b)$
0.20	1.1
0.25	−0.1
0.30	−0.9

To derive it, it is only necessary to replace $w+m$ by its equivalent $1-h-b$, and to use an approximate value (-0.1) for w in the small term which contains this coefficient. Unfortunately, with an experimental error of ± 0.6 in ΔE, the uncertainty in $(h-b)$ is of the order ± 1. Reduction of this uncertainty by further experiments would seem desirable because of the information which it can furnish regarding spin forces.

[4] Contradictory results stated in Abstract 31 at the New York meeting were based upon an unsatisfactory choice of force constants and are herewith corrected.

The Nuclear Magnetic Moments of N^{14}, Na^{23}, K^{39} and Cs^{133} *

P. KUSCH, S. MILLMAN AND I. I. RABI
Columbia University, New York, New York

(Received May 1, 1939)

The nuclear gyromagnetic ratios of N^{14}, Na^{23}, K^{39} and Cs^{133} have been measured by the molecular beam magnetic resonance method. The values of the nuclear magnetic moments, obtained from these measurements and the known spins, are 0.402, 2.216, 0.391 and 2.572 nuclear magnetons for N^{14}, Na^{23}, K^{39} and Cs^{133}, respectively. The shape of the resonance curves in some cases indicates a type of interaction of the nucleus with the rest of the molecule which may arise from the nuclear electric quadrupole moment. It is of interest to note that for the case of the alkali nuclei the magnetic moments calculated from the observed hyperfine splitting of atomic energy states by use of the Goudsmit, Fermi-Segrè formula agree fairly well with the results here given.

INTRODUCTION

BRIEF preliminary reports on the application of the molecular beam magnetic resonance method to the determination of the nuclear magnetic moments of N^{14}, Na^{23}, K^{39} and Cs^{133} have already been published.[1] In the present paper we will give a more complete report of the work on these nuclei.

The method, which has been described in a recent paper,[2] measures the Larmor precession frequency, ν, in a known magnetic field, H, of a nucleus which possesses spin, I, (in units of $h/2\pi$) and magnetic moment, μ. These quantities are related by the formula, $\nu=\mu H/hI$. A knowledge of the precession frequency and the magnetic field permits an immediate evaluation of the ratio of nuclear magnetic moment to nuclear spin. The determination of the magnetic moment is then possible for all cases for which the spin is known.

Apart from the high precision of which it is capable, a most important advantage of this method lies in the fact that the moment is obtained from experimental data directly by means of the simplest physical concepts. The values of the nuclear moments which we obtain are interesting not only for nuclear physics but also for a discussion of the large body of experimental and theoretical work which concerns the measurement and evaluation of the hyperfine structure of atomic energy levels.

In a recent paper Millman[3] has pointed out that it is possible to determine the sign of nuclear moments by taking advantage of certain asymmetries in the resonance curves introduced by the end effects of currents in the wires which produce the oscillating magnetic field.

The N^{14} nucleus belongs to the group of stable nuclei characterized by an odd atomic number and even mass number, and whose other members are the nuclei ${}_1D^2$, ${}_3Li^6$ and ${}_5B^{10}$. These nuclei should, on the basis of simple models,[4] have the same spin and the same magnetic moment. In fact ${}_1D^2$ and ${}_3Li^6$, both of which have a spin of 1, have moments of 0.853 and 0.820 nuclear magneton, respectively,[2, 5] in first-order agreement with these predictions. The nuclear spin of N^{14} is known[6] to be 1 from observations on the alternation of intensities in the band spectrum of the N_2 molecule but Bacher[7] who attempted to observe the h.f.s. of N^{14} concluded from its nonappearance that the moment is less than 0.2 nuclear magneton.

The hyperfine splitting of the atomic energy states of Na^{23}, K^{39} and Cs^{133} has been studied extensively[8] both by spectroscopic means and by the use of atomic beam methods, from which the spins are known to be 3/2, 3/2 and 7/2, respectively.[9] The h.f.s. of the ground states of these

* Publication assisted by the Ernest Kempton Adams Fund for Physical Research of Columbia University.

[1] S. Millman, P. Kusch and I. I. Rabi, Phys. Rev. **54**, 968 (1938); P. Kusch and S. Millman, Phys. Rev. **55**, 596 (1939).

[2] I. I. Rabi, S. Millman, P. Kusch and J. R. Zacharias, Phys. Rev. **55**, 526 (1939).

[3] S. Millman, Phys. Rev. **55**, 628 (1939).

[4] M. E. Rose and H. A. Bethe, Phys. Rev. **51**, 205 (1937).

[5] J. M. B. Kellogg, I. I. Rabi, N. F. Ramsey, Jr. and J. R. Zacharias, Phys. Rev. **55**, 595 (1939).

[6] L. S. Ornstein and W. R. Van Wijk, Zeits. f. Physik **49**, 315 (1928).

[7] R. F. Bacher, Phys. Rev. **43**, 1001 (1933).

[8] References to the work on these nuclei are given in the article on nuclear moments by H. A. Bethe and R. F. Bacher, Rev. Mod. Phys, **8**, 82 (1936).

[9] I. I. Rabi and V. W. Cohen, Phys. Rev. **46**, 707 (1934); S. Millman, Phys. Rev. **47**, 739 (1935); V. W. Cohen, Phys. Rev. **46**, 713 (1934).

TABLE I. *The values of g here given are defined by the ratio of the magnetic moment, μ, of the nucleus in units of $eh/4\pi M_p c$ to the nuclear spin, I, in units of $h/2\pi$, or by μ/I. The diamagnetic correction A is calculated from a simple electron precession model using appropriate screening constants. The correction B is calculated from the Fermi-Thomas model. The values for the magnetic moments from h.f.s. data have been calculated from the ground state with the formula of Fermi and Segrè.*

NUCLEUS	I	g OBS.	μ OBS.	DIAMAGNETIC CORRECTION A (%)	DIAMAGNETIC CORRECTION B (%)	CORRECTED μ	MOMENTS FROM H.F.S.
N^{14}	1	0.402	0.402	0.03	0.04	0.402	$\mu<0.2$*
Na^{23}	3/2	1.476	2.214	0.08	0.08	2.216	2.01
K^{39}	3/2	0.260	0.390	0.13	0.16	0.391	0.374
Cs^{133}	7/2	0.730	2.555	0.57	0.67	2.572	2,53

* Absence of h.f.s.

alkali atoms as determined by the two methods are in excellent agreement. Data for the splitting of excited energy levels are available only from spectroscopic investigations. Our results indicate, as seen from Table I, that with the exception of N^{14} the nuclear moments which were obtained from h.f.s. with the use of the Goudsmit, Fermi-Segrè formula[10] were accurate to within a few percent. The values of nuclear magnetic moments as obtained from the h.f.s. of different levels and as obtained by different methods of calculation applied to a single level disagree between themselves far beyond the limits of error of the experimental data.[8] The results of the present method furnish a criterion by means of which the validity of various methods of analysis of h.f.s. data may be tested and can thus lead to a deeper insight into the nature of atomic energy levels.

EXPERIMENTAL

The apparatus and experimental procedure used in this work have been described elsewhere.[2] We shall merely discuss the molecular compounds used in these determinations. A nucleus whose magnetic moment is to be determined by means of the present apparatus must occur in a molecule having several special properties. The molecule must contain an alkali atom, since the detector is of the surface ionization type and can detect only substances whose ionization potential is less than the work function of the tungsten filament. The molecule must be sufficiently stable so that it will not decompose to any large degree at temperatures at which its vapor pressure is sufficiently high (about 1 mm of Hg) to produce an intense beam. Finally the molecule must be in such a state that no appreciable magnetic moment is contributed by the electronic structure of the molecule, in order that the deflections in the inhomogeneous magnetic fields arise chiefly from the nuclear moments. In practice the last requirement introduces no difficulty since the ground states of most molecules are characterized by the absence of resultant electronic moment.

The molecules NaCN, KCN and RbCN were used for the work on N^{14}. At temperatures of about 1000°K, to which these compounds had to be raised in order to obtain a sufficiently intense beam, considerable dissociation occurred. In the absence of any fields the alkali atoms constituted about 50 percent of the beam intensity. However, when the inhomogeneous fields were turned on, the atomic portion of the beam, possessing large extranuclear moment, was deflected onto the pole faces of the magnets producing the fields and was thus lost. The free atoms, then, interfered in no way with a study of the nuclear moments of the atoms in the molecule. An attempt was made to observe the N^{14} resonance minimum in molecules other than the cyanides. The two compounds, $NaNO_3$ and $NaNH_2$, decomposed to such a degree that the observed molecular beam was of insufficient intensity and altogether too unsteady to permit of the observation of resonance curves.

Na_2, K_2 and Cs_2 were the simplest molecules used in the study of the nuclear moments of Na^{23}, K^{39} and Cs^{133}. These molecules were produced by heating the metallic element in an oven. The beam observed in the absence of magnetic field consisted for the most part of atoms. The molecular content was less than 1 percent of the total beam for K_2 and Cs_2 and about 1.5 percent

[10] S. Goudsmit, Phys. Rev. **43**, 636 (1933); E. Fermi and E. Segrè, Zeits. f. Physik **82**, 729 (1933).

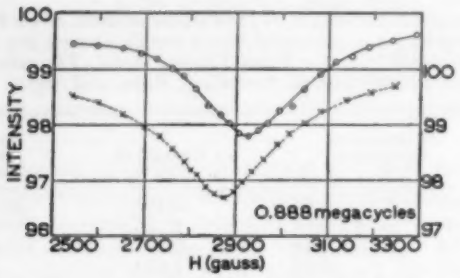

FIG. 1. Resonance curves for N^{14} observed in NaCN. An oscillating current of about 40 amperes produced a field of amplitude of the order of 100 gauss. The length of the oscillating field was about 7 cm.

for Na_2. It depended upon a number of factors such as the slit width of the oven and the temperature. When the inhomogeneous magnetic fields were turned on, the atomic content, as in the case of the cyanides, was removed from the beam. In spite of the low molecular content of the original beam the molecular beam so obtained was very steady and could be maintained at sufficient intensity to study the resonance minima. Other sources yielding resonance curves were: for Na^{23}, the molecules NaF, $Na_2B_4O_7$ and NaCN; for K^{39}, the molecule KCN; and for Cs^{133}, the molecules CsF and CsCl.

Resonance curves for each nucleus were observed for a wide range of values of the homogeneous magnetic field for each of the molecules used. The resonance curves were taken alternately with the homogeneous field in one direction and with the field direction reversed. This procedure permits the determination of the signs of the nuclear moments and leads to more accurate measurements of magnetic moments than would otherwise be possible.[3]

RESULTS

Resonance curves in which the beam intensity is plotted as a function of the magnetic field for a fixed frequency of the oscillating field are shown in Figs. 1, 2, 3 and 4 for the nuclei N^{14}, Na^{23}, K^{39} and Cs^{133}, respectively. The two curves in Fig. 1 were observed for N^{14} in NaCN under identical conditions except that the homogeneous field in one curve was opposite in direction to that for the other curve. The shift in the apparent minimum is due to end effects in the oscillating field and a determination of the sign of the nuclear moment may be made from an observation of the direction of shift on reversal of field.[3] Figs. 2 and 3 show the resonance curves of Na^{23} and K^{39} observed for the molecules Na_2 and K_2. The central minimum in each curve corresponds to the resonance minimum due to the nuclear magnetic moment as can be determined by comparison with the resonance minima observed for other molecules. Additional evidence on this point is the fact that the central minimum is the only one for which the ratio of the frequency to

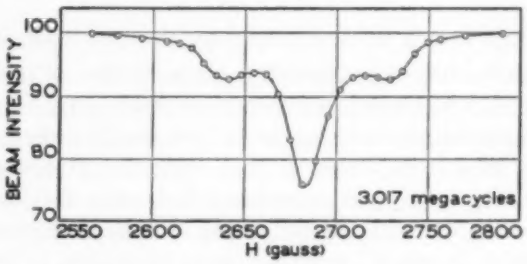

FIG. 2. Resonance curve for Na^{23} observed in Na_2 with an oscillating current of about 3 amperes.

the applied magnetic field, f/H, is independent of field. The structure observed on both sides of these minima will be discussed in a following section. No appreciable shift of the minima occurred due to field reversal in the resonance curves for Na^{23} and Cs^{133} shown in Figs. 2 and 4, because of the small amplitude of the oscillating magnetic field. The observation of the shift of the minimum for the determination of the sign of the moment was made when larger amplitudes of oscillating field were used. A small shift was observed for the case of K^{39} shown in Fig. 3.

The assignment of an observed resonance minimum to a nuclear moment may be made unambiguously in the case of each of the three alkali atoms, since only one common resonance minimum occurs for a wide variety of molecular compounds. The case of the nitrogen moment presents a somewhat more difficult problem because of the similarity of all the molecules for which the resonance minimum was observed. A resonance minimum characterized by a constant f/H was observed for the molecules NaCN and KCN. The same resonance minimum was observed for RbCN although in this case the insufficient beam intensity prevented an accurate test of the constancy of f/H. The question occurs as to whether this observed resonance minimum

is due to N^{14} or to some other moment common to the molecules. The minimum cannot be due to C^{12} since the nucleus possesses no magnetic moment. The observed effect is much too large to be due to C^{13} which has an abundance of only about 1 percent. It seems unlikely that the observed moment is due to a rotation of the molecule as a whole because of the fact that the three cyanide molecules will have different moments of inertia and hence probably different gyromagnetic ratios. The assumption that the rotation of the CN group, as such, which might be common to the three molecules studied, has a moment which is the cause of the observed resonance, is ruled out by the fact that f/H is constant. This means complete decoupling of the hypothetical rotation from the rotation of the molecule as a whole which seems absurd at the low magnetic fields used in this work. (H varied from 1000 to 5000 gauss.)

An approximate estimate of the over-all magnetic moment of a molecule may be made by observing the deflection of a molecular beam in a single inhomogeneous magnetic field. In this way the average over-all magnetic moment of the KCN molecule was found to be about one nuclear magneton. The smallest moment of inertia which the cyanides may have is that of the CN group about its center of gravity. The separation of the carbon and nitrogen atom is known[11] to be 1.15×10^{-8} cm in the HCN molecule and this value probably is not very different from that of

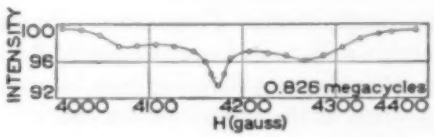

FIG. 3. Resonance curve for K^{39} observed in K_2 with an oscillating current of about 30 amperes.

the corresponding value in KCN. With this value the moment of inertia of the CN group becomes $I=14.2\times10^{-40}$ g cm². The most probable rotational angular momentum at the temperature of the oven (about 1000°K) can be found from $Jh/2\pi=(2IkT)^{\frac{1}{2}}$ and is about $19h/2\pi$. Since the observed g is 0.402, this would result in a magnetic moment of $19\times0.4\sim8$ nuclear magnetons. Any larger moment of inertia, such as that of the molecule rotating as a whole, would give rise to a still larger magnetic moment. These magnetic moments do not occur and the observed gyromagnetic ratio cannot, therefore, be assigned to the rotation of the molecule or any part of it. It seems certain that the common minimum observed for the cyanides can only be due to the nuclear magnetic moment of nitrogen.

No resonance minimum was observed which could be attributed to K^{41}. The low abundance of this isotope is not the only reason why it is unobserved in our apparatus. A nucleus with a small g value is subject to a small deflecting force in the inhomogeneous magnetic fields. If the deflection is small compared with the width of the beam, the change in orientation, which occurs in the homogeneous field, produces only a small change in the beam intensity at the detector.

It is noteworthy that the depths of the resonance minima vary widely for the same nucleus in different molecules. For example, the maximum observed drop in intensity at the minimum of Na^{23} was 4 percent in NaF, 9 percent in NaCN and 50 percent in Na_2. Similar effects are observed in the other cases. The specific nature of this effect, which probably depends on the interaction of the nuclear spin with the molecule, is not yet understood. Fortunately this effect does not interfere with the measurement of nuclear magnetic moment, because the results for the same nucleus in different molecules, yielding resonance curves of widely varying depths and widths, are in excellent agreement.

The observed values of the gyromagnetic ratio, the known spins and the resultant magnetic moments are listed in Table I. The values given refer to the value of the nuclear moment of Li^7 ($\mu_{Li^7}=3.250$). The corrections listed in columns 5 and 6 arise from the diamagnetism of the

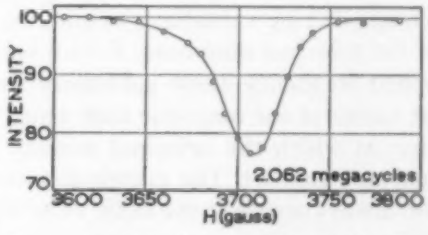

FIG. 4. Resonance curve for Cs^{133} observed in Cs_2 with an oscillating current of about 2 amperes.

[11] H. Sponer, *Molekulspektren* (J. Springer, 1935).

atoms and tend to raise the value of the nuclear moment. The evaluation of these corrections is discussed in a later section. The corrected values of the nuclear moments are given in column 7. As was pointed out in an earlier paper, all magnetic moment measurements on the present apparatus are in doubt by about 0.5 percent because of an uncertainty in the calibration of the magnetic fields. From the point of view of the internal consistency of the data alone the relative values of the nuclear moments of N^{14}, Na^{23}, K^{39} and Cs^{133} referred to that of Li^7 have a precision of about 0.4, 0.1, 0.3 and 0.2 percent, respectively. Since the curves for the three alkali atoms are very narrow (in all cases the half-width is of the order of 1 percent), it seems unlikely that any interaction not contemplated by the simple theory could shift the minimum from its ideal position by an amount great enough to affect seriously these precision values. In the case of the N^{14} nucleus, however, the resonance curves were obtained for large amplitudes of oscillating field in order to give an observable effect. The observed resonance curves were broad (the half-widths were of the order of 5 to 10 percent) and it is possible that asymmetries in the structure of the curve, not corrected for, may shift the minimum in some systematic way so as to introduce an additional error. It is to be expected that this error will be no greater than 0.5 percent.

The signs of all nuclear moments here reported were found to be positive. No previous determinations are available for the sign of the moment of N^{14}. The results for the alkali nuclei are in agreement with those obtained from h.f.s. and atomic beam methods.[8, 12]

Discussion

It will be observed (Figs. 2 and 3) that the resonance minima for both sodium and potassium are accompanied by subsidiary minima on both sides of the principal minimum. For all values of the applied frequency these subsidiary minima occur at values of the magnetic field which differ from that at which the principal minima occur by a constant amount. The principal minimum, however, always occurs at the same value of f/H. These facts imply the existence of some form of interaction between the nuclear spin and the rest of the molecular structure. Such an interaction, in sufficiently high external magnetic fields, will no longer depend on the applied field but will be given by some terms such as Am_Im_J as in the Paschen-Back effect. There may possibly be a nuclear quadrupole interaction with the rest of the molecule which will also give a term independent of field. It is evident that such an interaction will give a group of lines rather than a single line because of the many values which may be assumed by the rotational quantum numbers J and m_J. Such a group of lines, probably overlapping, when combined with the appropriate statistical weights, may result in a simple broadening of the resonance minimum or even the appearance of wings. However, these perturbation effects must be symmetrical about the principal energy value which corresponds to the precession of the nucleus in the external field and the central minimum is, therefore, the appropriate point from which to evaluate the nuclear moment. This is confirmed by the fact that only the central minimum has the constant value of f/H.

The observed field difference between the central minimum and either of the satellites in Na_2 is 47 gauss and in the case of K_2 is about 100 gauss. These results may be expressed in wave numbers by the use of the expression, $\Delta\nu(\text{cm}^{-1}) = 2.54\times10^{-8}g\Delta H$. The separations are 1.76×10^{-6} cm^{-1} and 0.66×10^{-6} cm^{-1} for Na_2 and K_2, respectively. These intervals, though apparently small, are, from the point of view of our experiments, very large as may be seen from an inspection of the resonance curves.

As a model, merely to fix orders of magnitude, consider the field due to a unit charge rotating about the nucleus in question at a distance equal to the internuclear distance. This distance is 3.07×10^{-8} cm for Na_2 and 3.91×10^{-8} cm for K_2. A simple calculation shows that this extra field, in gauss, is $J/33$ for Na_2 and $J/117$ for K_2, where J is the rotational angular momentum quantum number. At the oven temperatures we use, the most probable value of J is about 55 for Na_2 and about 80 for K_2. The field at the nucleus due to the rotation is of the order of 1 gauss. The magnetic dipole interaction of the two nuclei

[12] H. C. Torrey, Phys. Rev. **51**, 501 (1937); S. Millman and J. R. Zacharias, Phys. Rev. **51**, 1049 (1937).

gives a field of the order of μ/r^3 where μ is the nuclear moment and r the internuclear distance. The fields due to the dipole interaction are 0.4 and 0.03 gauss for Na_2 and K_2, respectively. It is apparent that we have to deal with effects of a much higher order of magnitude to account for the observed separations of 47 gauss for Na_2 and 100 gauss for K_2.

It appears likely to us that these large effects may be due, in part, to the presence of a quadrupole electrical moment in the nucleus which interacts electrostatically with the rest of the molecule. Our knowledge of the molecules concerned is, at present, too meager to test this hypothesis.

Finally we must consider an effect arising from the diamagnetic susceptibility of the atom which introduces a small correction in the evaluation of the magnetic moment of the heavier nuclei with the molecular beam magnetic resonance method. The Larmor rotation of the electrons in the molecule produces a magnetic field at the nucleus which opposes the external field. The real field acting on the nucleus is less than the applied field, so that the value of f/H which we take from the observed resonance minima is too small. The correction serves to increase the value of the moment. For the purposes of this evaluation we may neglect the influence of the molecular forces on the atom of the nucleus in question since the contribution to the local field by an inner electron is greater than that by an outer electron, in contradistinction to their contributions to the diamagnetic moment. Consider the field produced by the Larmor rotation of a ring-shaped element of charge rotating about the z axis, which coincides with the direction of the applied field. Every point of this element has polar coordinates r and θ. The field $d\bar{H}$ in the z direction at the origin due to this element of charge is $2\pi\rho\omega r\sin^3\theta dr d\theta$ where ρ is the charge density and ω is the Larmor frequency $eH/2mc$. For a single electron the integral of the charge density over an infinite volume is e/c. The value of the integral $\bar{H}$ for a single electron then becomes $e^2H/3mc^2\bar{r}$. If the electron has a quantum number n, $1/\bar{r}=Z/a_0n^2$ where Z is the atomic number and a_0 the Bohr radius. Since there are $2n^2$ electrons for each quantum number n, the contribution to the field at the nucleus by the electrons is $2Ze^2H/3mc^2a_0\times$(number of electron shells), if penetration and screening are neglected. The correction to the field is therefore $\bar{H}/H=2Ze^2/3mc^2a_0$ for each electron shell. The inclusion of screening constants lowers this value. The corrections obtained from this formula by the use of screening constants given by Slater[13] are tabulated in column 5 of Table I. A calculation by Dr. W. E. Lamb, Jr. of the Columbia University Physics Department with the use of the Fermi-Thomas atom model yields the more convenient expression, $\bar{H}/H=CZ^{4/3}$, where $C=0.320\times10^{-4}$. The corrections obtained from this formula are listed in column 6 of Table I. It is seen that they are in substantial agreement with the corrections obtained from the simple electron precession model. It is evident that the correction is of importance only for atoms of high atomic number; the corrections may almost be neglected for K and Na.

This research has been aided by a grant from the Research Corporation.

[13] J. C. Slater, Phys. Rev. **36**, 57 (1930).

Coulomb Energies and Nuclear Models

HARRISON BROWN AND D. R. INGLIS
Remsen Chemical Laboratory and Rowland Physical Laboratory, The Johns Hopkins University, Baltimore, Maryland

(Received April 22, 1939)

Electrostatic energy differences of isobaric light nuclei, estimated by use of the alpha-model, do not agree with experiment as well as those given by Bethe for the central model. The comparison with experiment of the binding energies of alphas in the light $4n$-particle nuclei, given by Hafstad and Teller for the alpha-model, is improved by inclusion of the Coulomb energy.

IN THE face of the intricacy of nuclear structure, attempts have been made to correlate certain properties by means of simplifying models. In particular, two models have been useful: the central model in which the particles (protons and neutrons) are initially considered as moving independently in a central field;[1] and the alpha-model in which the particles are pictured as clustered into alpha-particles as far as possible.[2] In the $(4n+1)$-particle nuclei, the alpha-model has one particle moving in the field of the alphas. In the $(4n-1)$-particle nuclei, one of the alphas lacks a particle; the deficit is exchanged rapidly between the alphas. Geometrically the two models are opposite extremes, although they exhibit striking similarity where angular momenta are concerned.[2(g)]

The Coulomb energy of nuclei should depend principally on the geometrical properties of the nuclei and not directly on the nature of the binding forces, of which we must still profess ignorance. It is therefore of interest to determine whether calculation of this energy can furnish a criterion of the relative value of the two extreme models. The electrostatic energy differences of isobaric pairs of light nuclei according to the central model have been compared with experimental values by Bethe.[3] He considered two approximations to the central model, (I) one in which the particle density is constant throughout a sphere, and (II) one in which the most loosely bound proton has a preferentially large radius. Using only one value (marked with an asterisk) to determine parameters, he was able to reproduce the other experimental values rather well, as indicated in columns I and II of Table I. In the alpha-model the geometrical environment of the "most loosely bound" particle is quite different in the $(4n-1)$- and $(4n+1)$-particle nuclei, so that comparison of nuclei in different groups involves unjustifiably detailed assumptions about the model. Comparison of the few nuclei within one group, however, involves only the more immediate features of the model.

For the purpose of estimating the Coulomb energy (neglecting exchange, as done in reference 3), a $(4n-1)$-particle nucleus is pictured as $n-1=0$, 1, 2, or 3 alpha-particles and a triton (or He^3); the alpha-alpha distances all have the same value $r_{\alpha\alpha}$ and the triton-alpha distances all

TABLE I. *Coulomb energies involved in isobaric transitions (in mMU).*

	n	Isobaric Pair	Central Model[3] I	Central Model[3] II	Alpha-model	Observed[3]
$(4n-1)$	1	H^3-He^3	0.87	0.84	0.74*	0.74
	2	Li^7-Be^7	2.0	1.99	1.92	<1.94
	3	$B^{11}-C^{11}$	2.7	3.0	3.1*	3.1
	4	$N^{15}-O^{15}$	3.5	3.8	4.28	3.7
$(4n+1)$	3	$C^{13}-N^{13}$	3.21*	3.21*	(3.54)	3.21
	4	$O^{17}-F^{17}$	3.9	3.9	(4.26)	3.9

[1] (a) W. Heisenberg, Zeits. f. Physik **96**, 473 (1935); (b) E. Feenberg and E. Wigner, Phys. Rev. **51**, 95 (1937); (c) M. E. Rose and H. A. Bethe, Phys. Rev. **51**, 205 (1937); (d) D. R. Inglis, Phys. Rev. **55**, 329 (1939), (erratum: 13 and 14 lines from the end of p. 335, and in the third line of p. 336, the words "positive" and "negative" should be exchanged); (e) H. Margenau and K. G. Carrol, Phys. Rev. **54**, 705 (1938); (f) W. J. Kroeger, Phys. Rev. **54**, 1048 (1938).

[2] (a) J. H. Bartlett, Jr., Nature **130**, 165 (1932); (b) E. Teller and J. A. Wheeler, Phys. Rev. **53**, 778 (1938); (c) L. R. Hafstad and E. Teller, Phys. Rev. **54**, 681 (1938); (d) W. Wefelmeier, Zeits. f. Physik **107**, 332 (1937); (e) H. A. Bethe, Phys. Rev. **53**, 843 (1938); (f) B. O. Grönblom and R. E. Marshak, Phys. Rev. **55**, 229 (1939); (g) R. G. Sachs, Phys. Rev. **55**, 825 (1939).

[3] H. A. Bethe, Phys. Rev. **54**, 436 (1938). *Note added in proof* (suggested by Professor Teller):—The central-model calculation of Coulomb energies, taking into account the concentration in angle of the p-protons, was carried out earlier by Feenberg and Wigner, Phys. Rev. **51**, 95 (1937). Their values, in the order of listing in Table I, are 0.74, (1.4), 2.2, 3.0, 2.5, 3.1. These are consistently small, parameters having been determined by other data. They would be increased (the first less than the others) if the better inverse-square-range parameter $\alpha=22$ were used. Simple multiplication of each value but the first by 1.28 gives about as good agreement as does column II.

have the value r_{ta}. In this model, the transition from one isobar to the other involves the transition $H^3 \rightarrow He^3$, the energy of which is taken from experiment to be 0.74 mMU. In the field of $n-1$ alphas at a distance r_{ta}, the Coulomb energy due to each of the alphas is $D=2e^2/r_{ta}$. The Coulomb energy C involved in an isobaric transition is then

$$C=(n-1)D+0.74 \text{ mMU}.$$

From the experimental difference $B^{11} \rightarrow C^{11}$ $(n=3)$, we determine $D=1.18$ mMU. The consequent values for $n=2$ and 4 are listed in Table I.

The lack of agreement for $N^{15} \rightarrow O^{15}$ is rather striking. It might be associated with the low stability of Be^8 thus: the three alphas in N^{15} may be closer together than the two alphas in B^{11}, and the more crowded alphas might hold the triton further off by the exclusion principle, and thus reduce C for the case $n=4$. However, this is hardly compatable with a rapid exchange of alpha and triton, and such an artificial modification of the model practically destroys its utility.

The case $(4n+1)$ is less definitely determined by the alpha-model, since the extra particle is not pictured as having a definite position in the framework, but merely as having nodes at the alphas.[2(c)] Furthermore, the data on this type are rather sparse. The particle taken to be situated just where a triton would be in the previous case (and taking $r_{aa}=r_{ta}$) gives the values listed in parentheses in Table I, but this has relatively little meaning. It is qualitatively understandable that the values so obtained are too high; the superfluous triton binding has drawn the particle inward unduly.

Such comparison of the ground states of isobaric pairs is not possible for the $4n$ nuclei. The binding energies of the $4n$ nuclei have been correlated by Hafstad and Teller,[2(c)] with the alpha-model. In their interesting considerations, the Coulomb energy was neglected. Although the Coulomb energy is very small compared with the total binding energy in light nuclei, it is actually not so very small compared with the binding between alphas which one treats by the alpha-model. It has therefore some interest to modify their correlation by taking into account the Coulomb energy. In so doing we take $r_{aa}=r_{ta}$ in the $4n-1$ case (as is reasonable because of the exchange), and take for D the average value $D=1.1$ mMU (or $r_{aa}=2.8\times10^{-13}$ cm) determined by both $n=3$ and $n=4$ of the $4n-1$ nuclei. This is probably an underestimate of the Coulomb energy of the $4n$ nuclei; alphas are somewhat smaller and more closely packed than tritons. The geometrical configurations are taken from

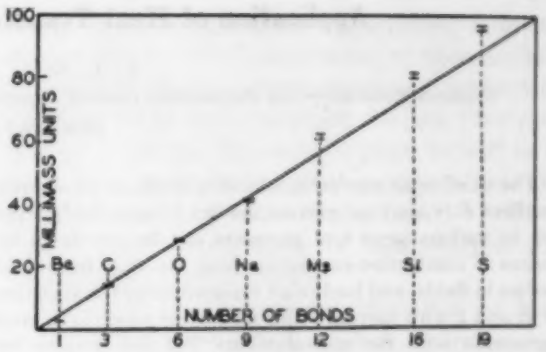

FIG. 1. Bond energy of the $4n$ nuclei (mass defect relative to alphas, plus Coulomb energy).

reference 2(c). The results are plotted in Fig. 1, which is to be compared[4] with Fig. 2 of reference 2(c). In Fig. 1 the experimental values represent the magnitude of the energy due to the binding forces between alphas (mass defect relative to alphas, plus estimated Coulomb energy), which should be proportional to the number of bonds. (The pairs of limiting values indicate the experimental uncertainty only.) The Coulomb energy alone is also proportional to the number of bonds up to O^{16}, after which it increases more rapidly than the number of bonds and raises the experimental lines. The discrepancy for Be^8 is thus not affected in magnitude by these considerations, that for Ne^{20} is removed, and instead one has discrepancies for the heavier elements, for which the use of the model is more questionable. The Be^8 discrepancy is less striking in Fig. 1 than in Fig. 2 of reference 2(c), mostly because of inclusion of the Coulomb energy and consequent change of scale, but also to a slight extent because of more recent experimental data.[5]

The application of the alpha-model to the light $4n$ nuclei is thus rather satisfactory, due probably to the great stability of the alphas. The less satisfactory result for the $(4n-1)$ nuclei may be ascribed to the fact that the internal binding of the triton is small compared to several triton-alpha bonds, insufficient to retain the identity of the triton in N^{15}, for example. It is not small compared to one bond, so this view is compatible with the relative success of the alpha-model in regard to the Li^7 magnetic moment.[2(c), 1(d)]

[4] Note change of scale by a factor 2, due to Coulomb energy.

[5] Allison, Graves, Skaggs and Smith, Phys. Rev. 55, 107 (1939).

Application of Heat Transfer Data to Arc Characteristics

C. G. SUITS AND H. PORITSKY
Research Laboratory and Engineering General Department, General Electric Company, Schenectady, New York

(Received April 27, 1939)

The chief experimental results of a study of the electric gradient E (v/cm) and current density I (amp./cm^2) in the arc in various gases and pressures can be correlated by means of conduction-convection heat loss data from solid bodies in fluids, and lead to an explanation of the variation of E and I with current i and pressure p which is in good agreement with the measurements. For this purpose we neglect radiation and use an equation of the Nusselt type

$$(W/k\Delta T\pi)=f(D^3\rho^2g\Delta T\beta_0/\eta^2)=f(x),$$

where W=watts per unit length of arc column; k=conductivity; D=diameter; ρ=density; β_0=expansion coefficient; and η=viscosity. In the range of interest in arcs $f(x)=x^\alpha$, where $\alpha=0.1$ is a satisfactory approximation. On the assumption that (1) the heat loss from the arc column is given by an equation of the Nusselt type and (2) the variation of arc temperature with i is a small effect, the $E-i$ relation at constant p is found to be $E=$const. i^{-n} where $n=(2-3\alpha)/(2+3\alpha)$. The exponent n_{exp} for nitrogen $=0.6$, while the $n_{\text{calc}}=0.74$. When p varies, the arc temperature variation becomes important and the effect is included implicitly in the theory, leading to $E=$const. p^m, and $D=$const. $p^{-\gamma}$. From heat transfer data and N_2 arc experiments we find that $m_{\text{exp}}=0.32$, $m_{\text{calc}}=0.31$, $\gamma_{\text{exp}}=0.38$, and $\gamma_{\text{calc}}=0.28$. For cases of forced convection we apply correlation data for forced convection cooling in the form $W/\Delta Tk\pi=f(DV\rho/\eta)=(DV\rho/\eta)^\varphi$, where V is the fluid velocity. As above, this leads to the $E-i$ expression for an arc in forced convection $E=$const. $i^{-n'}$ where $n'=(2-\varphi)/(2+\varphi)$. The exponent $n'_{\text{calc}}=0.54$, while n'_{exp} is not known. For arcs in a variable gravity field g (as in the experiments of Steenbeck), we find $E=$const. g^q where $q=2\alpha/(2+3\alpha)$. The $q_{\text{calc}}=0.087$, while q_{exp} is not known.

1. INTRODUCTION

ANY comprehensive theory of the electric arc must be consistent with the general character of the experimental results on the electrical properties of arcs in various gases.[1] In broad terms, the fundamental observations are (1) the gradient-current relationship* of the form $i=a_1E^{-n}$ where the exponent is always negative and lies in the numerical range $0.25<n<0.70$, (2) the gradient-pressure variation of the form $E=a_2p^m$ where the exponent is always positive and numerically of magnitude $0.15<m<0.32$, and (3) the gradient-gas dependence which shows an increasing gradient through the series Hg, A, N_2, He and H_2.

An arc may be considered as a mechanism of energy transfer. First the electrical energy input is used to dissociate and ionize the gas molecules and atoms and to raise the arc temperature to a high value. The second stage of the energy transfer consists in the dissipation of the thermal energy by radiation, conduction and convection. We consider radiation to be a negligibly small factor in the energy balance. From the low luminous efficiency of these arcs in the visible radiation, and from the total radiation measurements[2] which have been taken on a relatively efficient radiator, the Hg arc, it seems to be a reasonable assumption. Only for very high pressure mercury arcs does the radiation amount to an appreciable fraction of the energy input.[3]

In considering conduction and convection heat loss we are immediately confronted with the question of deciding whether convection can be neglected in the treatment. Elenbaas has shown in an interesting series of papers[4] that the important quantitatives of the high pressure mercury arc can be accounted for satisfactorily on the assumption that the chief energy loss takes place by a process of pure conduction. These mercury arcs are confined to tubes which for stabilizing purposes must necessarily interfere with free convection, so that this result is not evidence that convection heat loss can be neglected as a factor in the treatment of arcs in other media, as for example under conditions of free convection in air. An excellent direct means of investigating the importance of convection effects is to measure the electric gradient E in a

[1] C. G. Suits, Phys. Rev. **55**, 561 (1939).
* A nomenclature table appears at the end of the paper.

[2] W. Elenbaas, Physica **4**, 413 (1937).
[3] W. Elenbaas and W. deGroot, Physica **2**, 807 (1935).
[4] W. Elenbaas, Physica (a) **1**, 211 (1933–34); (b) **1**, 675 (1933–34); (c) **2**, 169 (1935); (d) **2**, 757 (1935); (e) **2**, 787 (1935); (f) **4**, 279 (1937); (g) **4**, 747 (1937); (h) **4**, 761 (1937),

gravity-free chamber, as in the ingenious experiment of Steenbeck.[5] Steenbeck found that for arcs in air (in the four-ampere range) the total voltage e decreased by a factor of two to three times; while the current density I decreased from two to five times in the gravity-free chamber. This is very important direct evidence that convection plays an important role in the energy balance. Steenbeck measured total arc voltage e; if the measurements had been made only on the positive column, a larger reduction of gradient might have been found. When this experiment is performed[6] with the atmospheric pressure mercury arc, the reduction of arc voltage in the gravity-free chamber is only one percent, which justifies the neglect of the convection factor in calculations involving these lamps.

The available evidence indicates quite conclusively the necessity for considering both conduction and convection in the energy balance. For this purpose we shall apply the methods which have been developed in the solution of a similar problem—the conduction and convection heat loss from solid bodies.

2. Convection Heat Loss

The general character of conduction-convection heat loss from solid bodies has been studied by numerous investigators.[7] It is found that the convection currents, which are zero at the surface of the hot body and at a distance of several centimeters, rise to a maximum at a distance of several millimeters from the surface. The full drop in temperature takes place in this region of a few centimeters, with the steepest temperature gradients being directly at the surface of the hot body.

For small temperature differences, approximate solutions of the equations of viscous fluid flow and of the heat conduction and convection equation have been obtained for the free convection problems of a vertical plate as well as of around a horizontal cylinder, based on the Prandtl boundary layer equations.[7(i),8] They explain the general form of temperature and velocity distribution curves.

The most comprehensive correlation of heat transfer measurements from hot cylinders has been carried out by means of dimensional analysis. By expressing the heat dissipation in terms of dimensionless units, there results, as shown by Nusselt,[7(g)]

$$\left(\frac{hD}{k}\right)=f\left[\left(\frac{D^3\beta_0\rho^2g\Delta T}{\eta^2}\right),\left(\frac{c_p\eta}{k}\right)\right], \qquad (1)$$

where h = coefficient of heat transfer (heat dissipation per unit area per unit time, per unit temperature difference), D = diameter, k = thermal conductivity, ρ = density, β_0 = temperature coefficient of volume expansion, g = gravity acceleration, η = viscosity, c_p = specific heat, and ΔT = temperature difference between body and ambient fluid. The three dimensionless constants (the terms in parentheses) occurring in (1) are sometimes referred to as the "Nusselt," the "Grashoff," and the "Prandtl" numbers, respectively. The experimental results for liquids and gases prove further that the "Nusselt" number hD/k depends only on the *product* of the Grashoff and Prandtl numbers:

$$\frac{hD}{k}=f\left[\left(\frac{D^3\beta_0\rho^2g\Delta T}{\eta^2}\right)\left(\frac{c_p\eta}{k}\right)\right]. \qquad (2)$$

A survey of all available data on free heat convection from solids (vertical cylinders and planes, horizontal cylinders) confirms this equation with an average scattering of not more than 10 percent in the heat transferred; the data covers a density range of $1:10^4$, a pressure range of $1:10^3$, and a range of the product of the Grashoff and Prandtl of $1:10^{17}$. The form of the curve (2) can be found in McAdams' textbook.[9] Because of the large range of variables, the

[5] M. Steenbeck, Zeits. f. tech. Physik **18**, 593 (1937). In this experiment the arc chamber is allowed to fall freely over a vertical path of 7 meters. The measurements are made during the free fall or gravity-free period.

[6] By private communication from Dr. Carl Kenty, of the General Electric Vapor Lamp Co.

[7] (a) L. Lorenz, Wied. Ann. **13**, 582 (1881); (b) W. Nusselt, Gesundh.-Ing. **38**, 477 (1915); (c) I. Langmuir, Phys. Rev. **34**, 401 (1912); (d) C. W. Rice, J. A.I.E.E. **42**, 1288 (1923); (e) E. Griffiths and A. H. Davis, Report 9, Food Invest. Bd., H. M. Stationery Off., London (1922); (f) E. Schmidt, Zeits. f. Gesamte Kalt-Ind. **35**, 213 (1928); Forschung **3**, 181 (1932); (g) W. Nusselt and W. Jürges, Zeits. V.D.I. **72**, 597 (1928); (h) E. Schmidt and W. Beckmann, Tech. Mech. and Thermo. **1**, 341 (1930); **1**, 391 (1930); (i) R. H. Heilman, Trans. Am. Soc. Mech. Eng. **51**, 257 (1929); (j) K. Jodlbauer, Zeits. V.D.I. **76**, 1031 (1932); (k) R. B. Kennard, Nat. Bur. Stand. J. Research **8**, 787 (1932).

[8] (a) K. Jodlbauer, Forschung **4**, 168 (1933); (b) R. Hermann, Physik. Zeits. **34**, 211 (1933).

[9] W. H. McAdams, *Heat Transmission* (McGraw-Hill, 1933), p. 248.

curve (2) is commonly plotted on log-log scales. The resulting slope α is found to vary from 0.04 to 0.25. Hence, over several ranges (2) can be given the form

$$\frac{hD}{k}=\text{const.}\left[\left(\frac{D^3\beta_0\rho^2g\Delta T}{\eta^2}\right)\left(\frac{c_p\eta}{k}\right)\right]^{\alpha}, \quad (3)$$

where α varies from 0.04 to 0.25; the multiplicative constant also varies.

The product $c_p\eta/k$ is constant for gases; it is 0.73 for diatomic gases and 0.67 for monatomic gases, and can be absorbed into the constant. Also, for perfect gases, $\beta_0=1/T$, $\rho=Mp/RT$. Hence

$$\frac{hD}{k}=\text{const.}\left[\frac{D^3M^2p^2g\Delta T}{T\eta^2R^2T^2}\right]^{\alpha}. \quad (4)$$

3. Application to Arcs

In applying the above formula to arcs[10] we are faced with several difficulties. The relation (2) is based on free convection around solids; at the boundary of the latter there is no flow; near an arc, however, the convection velocity is nearly a maximum. Thus the relative heat transfer by convection and conduction from an arc must differ from the transfer around a solid cylinder. Direct measurement of the convection velocities around arcs in air[11] have shown that the actual heat convected upward within the luminous core may be as small as seven percent of the total energy loss. No gross error will be involved if we neglect this portion of the convection loss, for which there is no analog in the heat loss from a solid cylinder.

Another difficulty is due to the large temperature variation within the film; this causes both β_0 and ρ to vary considerably, as well as η, k and c_p, with a resulting uncertainty in the dimensionless constants. While no difficulty arises in the product $c_p\eta/k$, which remains constant in spite of the variation of its components, large variations do occur in hD/k and in $D^3\beta_0\rho^2/\eta^2$. In plotting the available data on heat transfer for purposes of deriving (2), it is customary to evaluate the gas constants at the mean film temperature T_f:

$$T_f=T_{\text{ambient}}+\Delta T/2.$$

It must be kept in mind, however, that the extension of (2) to arc temperatures constitutes a distinct extrapolation.

By replacing h by $W/\pi D\Delta T$, where W is the loss in calories per unit length of arc, and converting to watts, we have $h=Ei/4.18\Delta T\pi D$, and (4) takes the form

$$Ei=(\pi k_f\Delta T)\,\text{const.}\left(\frac{D^3M^2p^2g\Delta T}{T\eta^2R^2T^2}\right)^{\alpha}. \quad (5)$$

4. $E-i$ Relations

The uncertainties regarding the mean temperature and the proper values for β_0, k, η, ρ disappear if we assume the arc temperature T to be constant and vary only the remaining quantities E, i, R, p (provided it is assumed that the mean values are not affected by these variations). Holding p constant, we have $Ei=\text{const. } D^{3\alpha}$. From the Saha equation, n_0, the number of electrons per unit volume, is a function of temperature T only.* The arc current is given by

$$i=(\pi D^2/4)n_0e\mu E, \quad (6)$$

where n_0 is the number of electrons per unit volume, e the electron charge and μ the electron mobility. Since n_0 depends on the temperature only, $i=\text{const. } D^2E$; eliminating D, we get

$$i/E=\text{const. } (Ei)^{1-\alpha}, \quad (7)$$

and solving for E, we have

$$E=\text{const. } i^{-n}, \text{ where } n=(2-3\alpha)/(2+3\alpha). \quad (8)$$

Thus, on the assumptions (1) that the heat loss from the arc column is chiefly by conduction and convection, (2) that the relationship of the physical factors is the same as for heat loss from solid bodies, and (3) that the variation of temperature with i at constant pressure is a negligible factor, we obtain an expression for the gradient E as a function of i.

[10] The first attempts in this direction were made by one of us late in 1934. A summary of results was published in 1937 (Phys. Rev. 52, 136 (1937)). Publication of the complete paper was delayed for more accurate experimental data.

[11] C. G. Suits, Phys. Rev. 55, 198 (1939).

* The arguments which lead us to apply the Saha equation appear in much recent arc literature and will not be reiterated here.

From experimental data on arcs the exponent of i in (8) lies in the range $0.54<n<0.73$ for common gases, being 0.6 for N_2, CO_2 and air. For n to be negative, in agreement with experiment, α must be less than 0.66. Now, the extreme range of α is $0.04<\alpha<0.25$, while for the portion of the heat transfer curve of interest for arcs ($\log hD/k$ near 0), α has the range $0.09<\alpha<0.2$. For the entire range of fluid properties represented by (2) the exponent n of the gradient Eq. (8) would thus be negative, in agreement with experimental data on arcs. For the range of $0.04<\alpha<0.25$, corresponding to the fluid properties and temperatures found in high pressure arcs, the calculated exponent n varies from 0.54 to 0.76, which can be compared to the measured values between 0.54 and 0.73. These values include all of the gases for which free convection arc gradient measurements exist, except Hg vapor. The n for Hg has the value 0.26; in the tubes for which these measurements apply, conditions of free convection are only partially satisfied, as noted previously, which may be to some extent accountable for this result. For air at arc temperatures the heat transfer curve has a slope $\alpha=0.1$; the corresponding value of n is thus -0.74, which can be compared to the experimental value of $n=-0.60$. In summary, it can be said that the fundamental property of a negative $E-i$ arc characteristic at constant pressure can be derived from an application of the conduction-convection heat transfer laws of solid bodies to the arc column if its temperature variation is neglected; and that the exponent of the gradient characteristic is correctly predicted.

5. Variation of D and E with Pressure

In a similar way the $E-p$ and $D-p$ relations can be obtained. The current density I is, of course, given by (6). Pressure p as a variable is included as follows: From the Saha equation,

$$\log_{10}\left(\frac{n_0^2}{N}\right)=-\frac{5040\,V_e}{T}+1.5\log_{10}T+15.38. \quad (9)$$

At constant temperature, $n_0\sim p^{\frac{1}{2}}$; however, the increase in arc temperature with pressure is not a negligible effect in this instance, since n_0 depends upon both p and T. From experimental data on the variation of T with p, we can calculate from (9) the electron density n_0 as a function of p. This has been done for the nitrogen arc $T-p$ data at $i=10$ amperes,[1] as shown in Fig. 1. In general we can put

$$n_0=\text{const. } p^{\beta}, \quad (10)$$

where $\beta=1.44$ from Fig. 1.

The dotted curve of this figure expresses the variation of electron density n_0 with pressure as calculated from the ionization equation on the assumption that the arc temperature is constant, while for the upper (solid) curve this variation of n_0 with pressure is calculated from the same equation, but we use at each pressure the corresponding arc temperature from arc data. The importance of taking the temperature change into account is illustrated by the following calculations. If we neglect the temperature change, the electron density (compared to one atmosphere) will increase 3.16 times at 10 atmospheres. But as a result of the increase of arc temperature with pressure, the actual increase of n_0 with p is 27.5 times at 10 atmospheres. The discrepancy is thus 8.7 times for this pressure interval.

Since arc temperature does not enter explicitly as a variable, the pressure variation of temperature appears as a possible error at other points in the treatment. A detailed investigation shows, however, that it is only in the calculation of n from the ionization equation as described above that this factor need be considered. For example, in the mobility equation

$$\mu=\text{const.}\frac{e}{m_0}\frac{\lambda}{c}, \quad (11)$$

we assume that at constant temperature $\mu\sim 1/p$, and we neglect the small dependence of μ on arc temperature T which enters in the terms λ and c. Similarly, in the heat transfer equation, (5), we neglect the dependence of the right-hand member on temperature which appears chiefly in the terms $k_f(\sim T^{3/4})$ and $\Delta T(\sim T)$ in comparison to the much larger effect of the temperature variation in (9).

Including these factors, we find that

$$i=\text{const. } D^2Ep^{\beta-1}. \quad (12)$$

From $W=Ei$ we obtain

$$\frac{dW}{W}=\frac{dE}{E}+\frac{di}{i}. \quad (13)$$

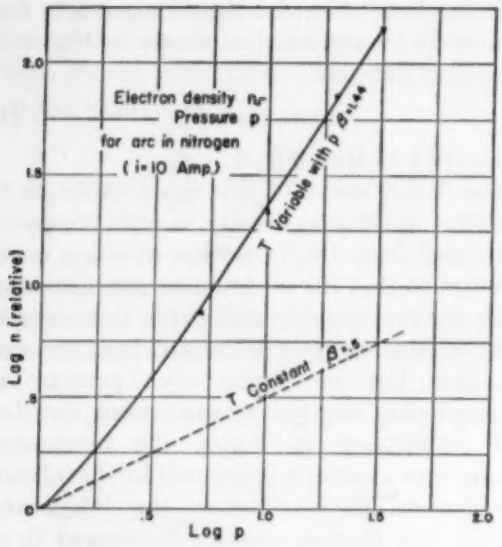

FIG. 1. Electron density as a function of pressure.

Taking logarithmic differentials of (12), we have

$$\frac{di}{i}=\frac{2dD}{D}+\frac{dE}{E}+(\beta-1)\frac{dp}{p}. \tag{14}$$

Similarly, for the heat transfer equation, (5),

$$\frac{dW}{W}=2\alpha\frac{dp}{p}+3\alpha\frac{dD}{D}. \tag{15}$$

Case I

If p is constant, as in the simpler derivation,

$$E=\text{const.}\ i^{-(2-3\alpha)/(2+3\alpha)} \tag{16}$$

as above.

Case II. i constant, D as $f(p)$

We have, from (13), (14) and (15)

$$2\frac{dD}{D}+\frac{dE}{E}+(\beta-1)\frac{dp}{p}=0, \tag{17}$$

$$3\alpha\frac{dD}{D}-\frac{dE}{E}+2\alpha\frac{dp}{p}=0. \tag{18}$$

Eliminating dE/E and combining terms we obtain

$$\frac{dD}{D}+\frac{dp}{p}\left(\frac{\beta+2\alpha-1}{2-3\alpha}\right)=0. \tag{19}$$

Finally,

$$D=\text{const.}\ p^{-(\beta+2\alpha-1)/(2-3\alpha)}=\text{const.}\ p^{-\gamma}, \tag{20}$$

which expresses the dependence of the arc diameter D on pressure p in terms of the exponent α of the heat transfer equation and the experimental constant β for the variation of electron density with pressure and temperature.

Case III. i constant, E as $f(p)$

Eliminating dD/D in (17) and (18)

$$\frac{dE}{E}\left(\frac{1}{2}-\frac{1}{3\alpha}\right)+\frac{dp}{p}\left[\left(\frac{\beta-1}{2}\right)+\frac{2}{3}\right]=0. \tag{21}$$

Finally, we have

$$E=\text{const.}\ p^{-\alpha[3(\beta-1)+4]/(3\alpha-2)}=\text{const.}\ p^{m}. \tag{22}$$

Eq. (22) expresses the pressure variation of the arc gradient in terms of the exponents β and α.

For nitrogen and air $\beta=1.44$ and $\alpha=0.1$. The calculated values of γ and m are compared in Table I. The experimental values for γ and m show a dependence on current which is not predicted by the theory. This effect arises from the small arc current-arc temperature variation which could be taken into account by evaluating β for different values of current.

The calculated values of m and γ lie in the correct range and, in view of the assumptions, show a satisfactory agreement with the measured values. The lack of comprehensive pressure-temperature data for other gases prevents a calculation of m and γ for these cases at present.

6. Arcs in Forced Convection

It is of some interest to examine the case of arcs in fluids under conditions of forced convection, since in this case the arc temperature T does not appear explicitly in the right-hand member of the heat transfer expression, which has the form

$$\frac{hD}{k}=\frac{W}{\Delta T k\pi}=f\left(\frac{DV\rho}{\eta}\right)=\text{const.}\left(\frac{DV\rho}{\eta}\right)^{\varphi}, \tag{23}$$

where all the quantities are defined above, except V, which is the fluid velocity. Considering first the case of constant temperature with variable

current and pressure, we have from (31)

$$\frac{dW}{W}=\varphi\left(\frac{dD}{D}+\frac{dp}{p}\right). \tag{24}$$

Combining (23) with the previously determined relations above, we obtain, at constant pressure

$$E=\text{const. } i^{-(2-\varphi)/(2+\varphi)}=\text{const. } i^{-n'}. \tag{25}$$

Thus under conditions of forced convection the exponent n' of the current in the $E-i$ relation has the form $(2-\varphi/2+\varphi)$, which can be compared to the same quantity for free convection where $n=(2-3\alpha/2+3\alpha)$. The $E-i$ characteristic will be negative for forced convection cooling of the arc when $\varphi<2$. A probable value of φ estimated from known correlation data is $\varphi=0.6$, for which $-n'=-0.54$. When careful measurements of arc gradient for forced convection conditions are available, it will become of interest to examine them from the viewpoint of the above calculation.

7. Arcs in a Variable Gravity Field

In view of the experiments of Steenbeck[5] and some unpublished experiments of our own in which an arc is subjected to a centrifugal field, it is of interest to calculate the variation of E with g on the basis of the relationships used above. To include g, we write

$$Ei=\text{const. } D^{3\alpha}g^{\alpha}, \tag{26}$$

which may be combined with $i=\text{const. } D^2E$ to obtain

$$E=\text{const. } g^{2\alpha/(2+3\alpha)}=\text{const. } g^{q}. \tag{27}$$

With $\alpha=0.1$ as used previously, this expression becomes

$$E=\text{const. } g^{0.087}. \tag{28}$$

This relationship (27) expresses the dependence of arc gradient E upon the gravity field g. Applying (27) to Steenbeck's experiments shows that E and g both go to zero together. If g is sufficiently small, the arc voltage observed in the gravity-free chamber should be the sum of the anode drop e_A and cathode drop e_c, since the positive column drop will become zero. This could be checked by actually measuring the positive column gradient in the gravity-free chamber by the vibrating electrode method. An alternative check would be a separate measurement of e_A+e_c as, for example, by shorting electrodes. This latter method is somewhat indirect and involves additional postulates.

We have some incomplete data on the variation of E with g where g is increased by centrifuging the arc. The dependence of E on g is so small, however, that very large values of g must be used to obtain accuracy. In the measurements we have available the accuracy is not satisfactory, but it can be said for certain that the coefficient q of the gravity effect is much smaller than the coefficient m of the pressure effect.

8. Discussion

The method of treatment yields expressions for the chief electrical measurables of the high pressure* arc in terms of heat transfer quantities and one experimental constant depending upon the pressure variation of arc temperature. The important assumption is that the heat loss from the arc column is given by a relationship of the form known to apply to convection loss from solid bodies. The general agreement between the measured and calculated quantities is evidence that for the experimental conditions considered no prominent variables have been omitted. Since all of the quantities involved in convection heat loss as expressed by (5) are not varied explicitly in the experiment, we cannot conclude in general that the heat loss from the

Table I. *Values of γ and m for nitrogen.*

$\gamma_{CALC}=0.28$ $(i=10)$	$m_{CALC}=0.31$ $(i=10)$
$\gamma_{exp}=0.30$ for $i=1$	$m_{exp}=0.29$ for $i=1$
$=0.30$ for $i=2$	$=0.31$ for $i=5$
$=0.35$ for $i=5$	$=0.32$ for $i=10$
$=0.38$ for $i=10$	

* "High pressure," in this sense, refers to the range around and above atmospheric pressure. More fundamentally, the thermal equilibrium considerations apply to discharges in which the energy acquired by the electron per mean free path is small compared to its thermal energy. This criterion is best satisfied at high pressure and high current. From the fact that there is direct evidence from spectroscopic studies that thermal equilibrium is established in the current range of our experiments at one atmosphere pressure in air, it can be inferred that the same is true at higher pressures and currents.

arc column involves all of these quantities in this particular relationship. That p and D enter in the form D^2p^2 is, however, a proper deduction. It is evident that some of the other quantities in (5) could be varied experimentally and some evidence of the result is already known. In the experiments of Steenbeck, for example, g has been reduced to practically zero with the result that could be predicted from (27). More experiments with a gravity-free chamber or an arc centrifuge would be interesting, particularly if E were measured instead of e. The other quantity which could be varied in (5) is the ambient temperature, and so far as is known no data exist on the effect on arc gradient E.

These conclusions apply, of course, to arcs under conditions of free convection (except Section 6). One would expect the effect of pressure on arc gradient to be different if free convection is not possible in the experiment. However, since the convection force increases linearly with pressure for the same temperature difference, an arc space which would be totally inadequate for convection at one atmosphere may permit prominent convection effects at higher pressure. Similarly, in the case of transient arcs, a time interval which would at one atmosphere be short in terms of the thermal processes in the arc may be relatively very long at higher pressure. In other words, the "thermal time constant," which involves the rate of convection heat flow, must be much shorter at higher pressures.

It would be better in general if the theory included the arc temperature T as an explicit variable, but some new relationship not known at present will be required for that purpose. In the case of constant pressure, the inclusion of T is not of great importance since temperature measurements show a small dependence on current. When pressure varies, however, the temperature change is important because a rather large variation of pressure is required to measure gradient changes with accuracy, and for this case a means of including T explicitly would improve the treatment.

In the analysis given, a relationship between D and p of the form (5) results in a satisfactory agreement with experiment. It is important to note that this is not equivalent to saying that (5) can be used to calculate the heat loss from the arc column; that is a relevant but different question which involves the constant of proportionality of (5). An investigation of this subject will be reported in a separate paper. The results show that (5) can be applied to arcs with a suitable interpretation of the constants. The method of interpretation is determined from a study of the data on heat loss from wires at high temperatures, which show systematic deviations from the Nusselt correlative curve at the highest temperatures.

It is clear that the conduction-convection heat loss in a series of gases increases in the same order as the gradient,[1] although the detailed analysis of this question is not given here. Some uncertainty exists in the relative order of He and N_2 in regard to heat transfer. Experimentally E is slightly greater in He than in N_2 for steady-state arcs. For some transient arcs He and N_2 appear to be identical within the errors of measurement. Although the low temperature heat transfer in N_2 is much lower than He, it appears that at high temperature the contribution of nitrogen dissociation to heat transfer balances the more favorable kinetic factors of He.

We may presume that the correlation of heat transfer data and the electrical properties of arcs is a matter of considerable generality and is not limited to the case of free convection. It would be of interest to examine cases of forced convection with that in mind. There seems little doubt that the arc gradient in a forced convection air stream of 1 meter sec.$^{-1}$ velocity would be the same as in an arc in air under free convection velocities[11] which are known to be of this same magnitude.

Nomenclature
(in order of appearance)

E—Electric gradient along the axis of the positive column of the arc (volts cm^{-1})
e—Total voltage drop between the electrodes (volts)
i—Current (amp.)
I—Current density (amp. cm^{-2})
h—Surface coefficient of heat transfer (cal. sec.$^{-1}$ cm^{-2} deg.$^{-1}$)
D—Diameter of cylinder
k—Thermal conductivity (cal. sec.$^{-1}$ cm^{-1} deg.$^{-1}$)
β_0—Temperature coefficient of volume expansion (deg.$^{-1}$)
ρ—Density (g cm^{-3})

g—Acceleration of gravity (cm sec.$^{-2}$)
η—Viscosity (g sec.$^{-1}$ cm^{-1})
c_p—Specific heat at constant pressure (cal. g^{-1} deg.$^{-1}$)
ΔT—Temperature difference (max.) between hot surface and surrounding fluid (deg.)
a—Exponent of the "Grashoff" term in the approximate expression for convection heat transfer.
M—Molecular weight
p—Pressure (g cm^{-2})
T—Temperature absolute (deg.)
R—Gas constant (cm deg.$^{-1}$)
π—3.1416
W—Heat loss per unit length of arc column (cal. cm^{-1})
$-n$—Exponent of the current in the $E-i$ relation
n_0—Number of electrons per unit volume (cm^{-3})
μ—Mobility of the electron (cm^2 sec.$^{-1}$ volt^{-1})
e—Electronic charge (coulombs)
N—Molecules per unit volume (cm^{-3}) (Loschmidt number)
V_0—Effective ionization potential (volts)
β—Exponent of p in the n_0-p relation
m_0—Mass of the electron (g)
λ—Mean free path (cm)
c—Average velocity (cm sec.$^{-1}$)
$-\gamma$—Exponent of p in the $D-p$ relation
m—Exponent of p in the $E-p$ relation
V—Fluid velocity (cm sec.$^{-1}$)
φ—Exponent of the term $(DV\rho/\eta)$ for forced convection heat transfer
$-n'$—Exponent of i in $E-i$ expression for forced convection cooling
q—Exponent of g in the $E-g$ relation
e_A—Anode drop (volts)
e_c—Cathode drop (volts)

JUNE 15, 1939 PHYSICAL REVIEW VOLUME 55

Electron Scattering and Plasma Oscillations*

HARRISON J. MERRILL AND HAROLD W. WEBB
Columbia University, New York, New York

(Received April 26, 1939)

The dependence of electron scattering upon plasma oscillations was studied in a mercury arc discharge tube containing a movable probe. The best conditions for studying these relations were found when the vapor pressures and arc currents were small. Probe volt-ampere characteristics showed the presence of ultimate electrons with a Maxwell-Boltzmann distribution corresponding to about 30,000°K and a superposed stream of fast electrons emitted from the cathode. These fast electrons were scattered without appreciable change in direction in well-defined, approximately plane regions only a few tenths of a millimeter wide. The plasma oscillations were studied with a crystal detector in the probe circuit supplemented by a Lecher wire system. In addition to "turbulent" disturbances with no measurable frequencies found throughout the tube, narrow regions were found in which stable periodic oscillations of considerable magnitude were detected. These regions and the scattering regions were, in general, equal in number and coincided except for a small shift of the former in the direction of the anode. The observed frequencies agreed well with the formula derived by Tonks and Langmuir. The scattering regions and the regions in which periodic oscillations were observed became less marked and moved toward the cathode as either the vapor pressure or arc current were increased. The periodic oscillations were found only in regions traversed by the fast electrons. The results are interpreted as showing that scattering is due to plasma oscillations which receive their energy from the fast electrons. The process by which the oscillations were detected by the probe is discussed to account for the shift of the regions in which oscillations were observed with respect to the scattering regions.

INTRODUCTION

IN 1924 Langmuir and Mott-Smith[1] showed that in an electric discharge in a gas or vapor the primary electrons emitted by the cathode suffer scattering, resulting in a redistribution of velocities. Starting with a homogeneous primary beam of electrons, they found scattered electrons with velocities considerably in excess of the original value as well as those with much less velocity, although the mean energy in the beam was not much changed. Dittmer[2] has shown that the region of scattering approaches the cathode as the discharge current is increased. Penning[3] found oscillations of frequencies from 3×10^8 to

* Publication assisted by the Ernest Kempton Adams Fund for Physical Research of Columbia University.

[1] I. Langmuir and H. Mott-Smith, Gen. Elec. Rev. **27**, 449, 538, 616, 762, 810 (1924).

[2] A. F. Dittmer, Phys. Rev. **28**, 507 (1926); I. Langmuir, Phys. Rev. **26**, 585 (1925).

[3] F. M. Penning, Physica **6**, 241 (1926); Nature **118**, 301 (1926).

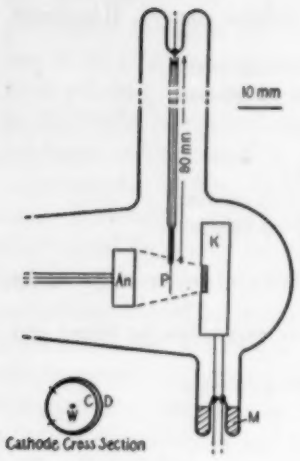

FIG. 1. Experimental tube.

6×10^8 and observed that electron scattering was accompanied by oscillations. Druyvesteyn and Warmoltz[4] observed that the changes in velocity distribution, space potential and electron concentration occur in distinct narrow regions. The phenomenon is especially interesting in its relation to arc discharges with a hot cathode, particularly as it effects the distribution of excitation and ionization.

The most satisfactory explanation, suggested by Dittmer, for the scattering is that it is caused by rapidly varying potential gradients in the discharge due to oscillations of the plasma electrons. Tonks and Langmuir[5] have developed a theory for these oscillations and have shown that, if the reaction of the tube walls and electrodes be negligible, the frequency of oscillation is given by the simple relation $\nu=(ne^2/\pi m_e)^{\frac{1}{2}}$ where e and m_e are the electronic charge and mass, respectively, and n is the concentration of the plasma electrons. Such oscillations may produce alternating potential gradients of many volts per cm, and a stream of primary electrons traversing these regions would be scattered accordingly.

In the investigation described in this paper the relation between the plasma oscillations and the scattering of the primary beam was further studied. With a probe which could be moved by very small steps to any part of the discharge and selecting those low pressures and small currents which gave most clearly defined effects, it was possible to study the process in greater detail than has been possible in earlier investigations.

EXPERIMENTAL

The experimental tube is shown in Fig. 1. The indirectly heated oxide-coated cathode K had an active emitting surface, 4×6 mm. A piece of fine nickel mesh of these dimensions was welded to the convex surface of a nickel cylinder C, 6 mm in diameter, inside of which was a tungsten heater W. The mesh was coated with oxide, and care was taken to avoid spreading of the coating on neighboring parts of the cylinder. To further insure a sharp limitation of the emitting surface, a second cylinder D slightly larger in diameter was placed outside the first and in contact with it along the front. The second cylinder had a window, also 4×6 mm, opposite the oxide-covered mesh. Since it was cooler than the inner cylinder, there was no stray emission from it due to sputtered oxide coating. The anode An was a hollow nickel cylinder 12 mm in diameter and 6 mm deep.

A small pool of mercury M in an arm below the cathode supplied the vapor for the arc. This was kept at the temperature corresponding to the desired pressure by immersing it in an oil bath. To prevent condensation, the tube was enclosed in a superheating oven, into which it was rigidly clamped.

The probe P was a tungsten wire, 0.05 mm in diameter and 6 mm long, projecting out of a quartz tube, the lower 1.5 cm of which had a diameter of 0.6 mm. This was supported at the top by what was equivalent to a universal joint, by hanging it on a short section of fine tungsten wire with small clearance between it and the glass wall. To move the probe relatively to the discharge, the oven was tilted either about a horizontal axis parallel to the anode-cathode axis or about one perpendicular thereto. As the probe was easily disturbed by jars and was little damped, the oven was placed on a heavy platform hung from the ceiling. Since changes as small as 0.1 mm in the position of the probe along the anode-cathode axis resulted in marked changes in the observed results, this motion was

[4] M. J. Druyvesteyn and N. Warmoltz, Physica **4**, 51 (1937).

[5] L. Tonks and I. Langmuir, Phys. Rev. **33**, 195 (1929); **33**, 990 (1929); I. Langmuir, Proc. Nat. Acad. Sci. **14**, 627 (1928); L. Tonks, Phys. Rev. **38**, 1219 (1931); L. Tonks, Phys. Rev. **37**, 1458 (1931); M. Steenbeck, Zeits. f. Physik **76**, 260 (1932).

controlled by hinging one end of the oven and supporting the other end on a long wire hung from a post on the platform. The thermal expansion of this wire was large, so that by varying its temperature by passing a current through it the probe could be moved in this direction without jarring by steps as small as 0.1 mm. Scales were provided so that the position of the probe in the discharge could be read off directly.

The probe circuit, which was usually completed through the anode, included circuits for detecting and measuring high frequency currents picked up by the probe. Several types of vacuum tubes were tried, but most satisfactory results were obtained with a galena crystal detector, with a circuit similar to that used by Tonks and Langmuir. A Lecher wire was connected in parallel with the detector circuit so that periodic oscillations could be observed and their wavelengths determined. The crystal was calibrated for every set of observations to eliminate errors caused by variations in the sensitivity of the crystal. Tests were made to make certain that these oscillations were independent of the properties of the external circuit.

Before making measurements, the arc was run until it had come to an equilibrium temperature and pressure. When measuring the voltage-current characteristics, it was found that under some conditions the probe disturbed the discharge so that the arc voltage changed by as much as five percent as the probe voltage was varied: in such cases the current controlling rheostats were varied to maintain the arc current constant.

After correcting in the usual manner for the positive ion current to the probe, the resulting electron current-probe voltage curves were analyzed to find the velocity distribution of the electrons. Typical characteristic curves are shown in Fig. 2(A). The curves in this and subsequent figures are numbered in the order in which they were determined in the investigation. In Fig. 2(A), the ordinates are the probe currents plotted to a logarithmic scale and the abscissas the voltages on the probe, with the space potential taken as zero. The arrows marked A and K indicate the potentials of the anode and cathode, respectively. In all of the curves the analysis showed that two groups of electrons were present. For voltages greater than -5 volts the predominate group was the "ultimate" electrons (plasma electrons with random velocity corresponding to a Maxwell-Boltzmann distribution). For voltages less than -5 volts the "primary" and "secondary" electrons became important. The former are the electrons emitted by the cathode which have suffered no scattering, the latter those primary electrons which have been scattered but not sufficiently to have the same distribution as the ultimate electrons. Both primary and secondary electrons will be referred to as "fast" electrons in the remainder of this paper. The ultimate electrons alone give for negative voltages a straight line relation between the log of the probe electron current and the probe voltage, from which the electron temperature is calculated. For positive voltages a straight line relation between current squared and voltage is found,[1] from which the electron concentration and space potential are calculated. The current to a cylindrical electrode in a homogeneous stream of fast electrons of energy V_0 is given by,

$$i = 2rlI(1+V/V_0)^{\frac{1}{2}}; \qquad V > -V_0,$$
$$i = 0; \qquad V < -V_0,$$

where $2rl$ is the projected area of the probe, I the current density, and i the fast electron current to the probe when at the potential V. By the use

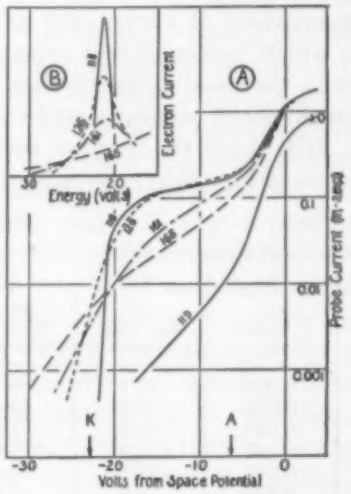

FIG. 2. (A) Typical probe characteristic curves in defined regions of a test mercury discharge: arc vapor pressure, three microns; arc current, 0.042 ampere. (B) Volt-energy distribution of electrons as a function of current in the discharge.

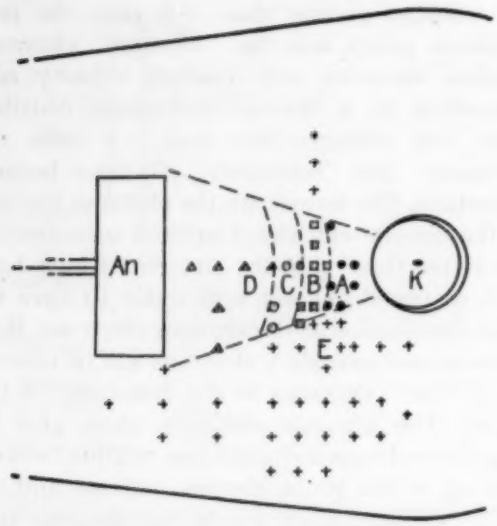

FIG. 3. Probe positions for determining the probe characteristic curves of the test discharge. The discharge is divided into regions, each of which, has a typical probe characteristic current,

of this formula that part of the probe current characteristic caused primarily by fast electrons was analyzed to find their velocity distribution. This was done by dividing them up into a large number of approximately homogeneous groups and building up a synthetic curve, which when added to the curve due to the ultimate electrons, fitted well the experimental results over the whole range of voltages. The precision with which this analysis could be made may be seen from a comparison of curves 423 and 427, in Fig. 5(A), which, although they represent small differences in the electron distribution, were derived from distinctly different probe characteristics. Fig. 2(B) shows the result of such analysis for the curves of Fig. 2(A); the ordinates are the relative number of fast electrons having the energies given in electron-volts by the abscissas. In computing the curves of 2(B), as well as in all similar curves described in this paper, a correction has been made to allow for the increase of the cross section of the arc discharge as the anode is approached. The ordinates in the corrected curves are therefore proportional to the total current of fast electrons rather than their current density.

RESULTS

The temperature and concentration of the ultimate electrons, the velocity distribution of the fast electrons and the space charge oscillations were determined for a large number of points in the axial plane for pressures varying from three to seven microns and for currents between 0.020 and 0.100 amp. Over six hundred complete probe characteristic curves were made in the course of the investigation, and the results were found to be generally reproducible. The results for a number of typical cases are given in Table I. In column (*a*) the pressures of the vapor are given in microns, in (*b*) the arc current in amperes, in (*c*) the arc drop in volts, and in (*d*) the space potential in volts with respect to the anode. Column (*e*) shows the voltage difference between the cathode and space, (*f*) the velocity acquired by electrons falling through this potential difference, and (*g*) lists the observed electron concentrations.

The discharges were all of the well-known type, with cathode drop between 16 to 21 volts and a nearly constant space potential extending almost to the anode, where there was a negative anode

TABLE I. *Data on mercury arc.*

(*a*) Arc Pressure (Microns)	(*b*) Arc Current (amp.)	(*c*) Arc Drop (volts)	(*d*) Space Potential (volts)*	(*e*) Energy Primary Beam (volts)	(*f*) Electron Velocity (cm/sec.)	(*g*) Electron Concentration (No./cc)	(*h*) Oscillation Frequency $8980\sigma\sqrt{\frac{}{}}$	(*i*) Oscillation Frequency Lecher
3	0.020	11.7	8.1	19.8	2.65×10^{8}	1.77×10^{10}	1.20×10^{9}	1.18×10^{9}
	0.030	12.4	8.4	20.8	2.72	2.56	1.44	1.44
	0.040	13.5	7.3	20.8	2.72	3.33	1.64	1.50
	0.045	14.0	7.0	21.0	2.73	3.72	1.73	—
	0.050	14.7	7.2	21.9	2.78	3.94	1.79	—
7	0.020	9.4	7.5	16.9	2.45×10^{8}	1.93×10^{10}	1.25×10^{9}	1.17
	0.030	9.8	7.0	16.8	2.42	3.09	1.58	1.34
	0.040	10.4	6.5	16.9	2.45	3.85	1.76	—
	0.050	11.3	4.8	16.1	2.39	5.65	2.14	—

* Measured from the anode.

drop of from five to eight volts. The part of the discharge in which there were not a negligible number of fast electrons will be referred to as the "arc discharge," and was practically included in a region defined by the active part of the cathode and the periphery of the anode, as shown in Fig. 3. Within this region the paths of nearly all the fast electrons made angles with the cathode-anode axis not greater than 10°.

In Fig. 3 the positions at which probe characteristics were taken are shown for a typical test by the sets of dots, squares, circles, triangles and crosses. The pressure was three microns, the arc current 0.042 amp. and the arc drop 17 volts. Five of the probe current-voltage curves are shown in Fig. 2(A), and are typical of all of the fifty-eight characteristic curves determined for these conditions. The discharge was divided into five regions, marked *A–E* in Fig. 3, in each of which characteristics of one type only were found, 118 in *A* (dots), 126 in *B* (squares), 161 in *C* (cricles), 165 in *D* (triangles), and 119 in *E* (crosses). The first four regions lay entirely in the arc discharge and were separated from one another by surfaces symmetrical to the axis and slightly convex to the cathode. Region *E* included all parts of the tube outside the arc discharge. The boundary of the arc discharge was so sharp that curves such as 118, 126, 161 and 165

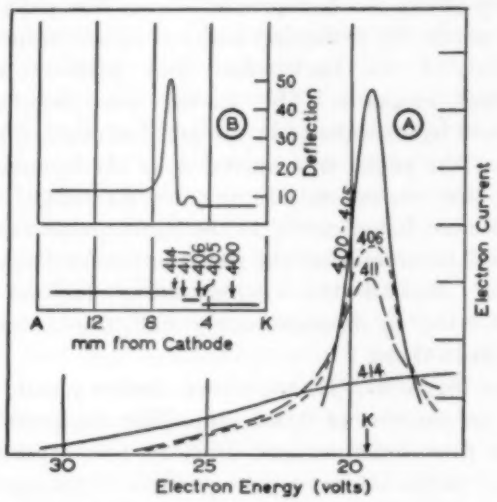

FIG. 4. (A) Volt-energy distribution of electrons to show positions of the regions of scattering: arc vapor pressure, three microns; arc current, 0.020 ampere. (B) The rectified current of the crystal detector circuit as a function of the position of the probe along the axis.

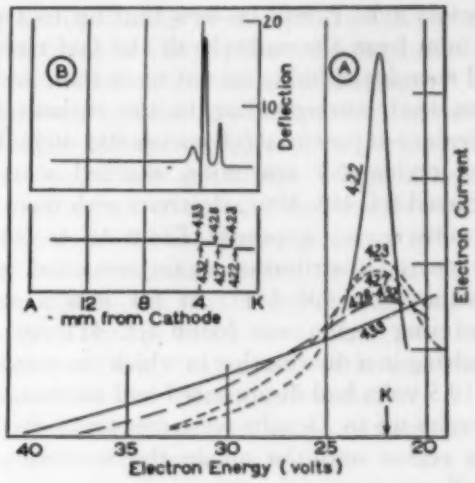

FIG. 5. (A) Volt-energy distribution of electrons to show positions of the regions of scattering: arc vapor pressure, three microns; arc current, 0.045 ampere, (B) The rectified current of the crystal detector circuit as a function of the position of the probe along the axis.

were obtained only 0.5 mm distant from points in *E* for which curves such as 119 were recorded.

Analysis of the ultimate electrons, as discussed above, showed that in every part of the arc discharge and in its immediate environment there was a nearly uniform concentration of the order of 3×10^{10} per cc. The electron temperatures for all points in a given arc discharge and in the neighboring parts of region *E* were practically the same, about 30,000°K.

In Figs. 4 and 5 the results of two more detailed studies of the scattering process as well as the simultaneous measurements of the plasma oscillations are shown. The probe was moved along the axis of the discharge in steps of 0.2 mm, and particular attention was given to the narrow regions in which scattering was observed. The results shown in Fig. 4 were obtained at three microns pressure, with arc current 0.020 amp., arc drop 11.7 volts and space potential 8.1 volts with respect to the anode. In Fig. 4(A) are given a few of the numerous curves obtained, showing the velocity distribution of the fast electrons at critical points. The position of the probe corresponding to each of these is indicated by arrows on the broken line in the lower part of Fig. 4(B), in which the abscissas are distances from the cathode. In Fig. 4(A), the potential of the cathode relative to space potential is indicated by the arrow *K*, at 19.5 volts on the

abscissa axis. It will be seen that up to a point 4.3 mm from the cathode all the fast electrons had energies differing by not more than one volt from that corresponding to the cathode-space difference of potential (cf. curves 400–405). Then, in a region 0.2 mm wide, marked scattering occurred (cf. 405–406); electrons with more than 26 volts energy appeared. From 4.5 to 6.1 mm the energy distribution again remained nearly constant (cf. 406–411). At 6.1 mm a second scattering region was found (cf. 411 and 414) resulting in a distribution in which the maximum at 19.5 volts had disappeared and electrons with energies up to 33 volts were measured. Between this region and the anode the scattering was small.

The boundary between the region by the cathode and the adjoining region in the arc discharge was clearly defined visually, by differences in intensity and color. The boundary between the arc discharge and the region outside was also sharply defined by intensity differences.

In Fig. 4(B) the results of the measurements of oscillations as picked up by the probe circuit are shown. The galvanometer deflections due to the current rectified by the crystal are plotted as a function of the distance of the probe from the cathode. At points between the cathode and a point 5 mm distant there was a constant deflection, corresponding to five millivolts across the crystal. No change in this deflection was observed as the Lecher bridge was moved, so that no frequency can be assigned to these disturbances. Furthermore, as the same deflection was observed for all positions of the probe outside the arc discharge, even near the walls, whether the probe circuit was completed to the anode, the cathode or to an electrode pasted on the outside of the tube, it was concluded that this background disturbance was picked up indirectly and could be neglected in studying the variation in the oscillations with position.

At 5.3 mm from the cathode a small peak in the deflection was observed, and the Lecher system gave measurable response throughout this region with nodes spaced 12.7 cm apart. At 6 mm the deflection was again approximately that of the background and there was no response on the Lecher system. At 6.8 mm a larger peak was observed; periodic oscillations of the same frequency as found in the first peak, 1.18×10^9 cycles, were observed for all currents substantially above the background. From this peak to the anode the deflection had a constant value in excess of the background but without any Lecher response. The excess was definitely caused by turbulence in the arc discharge, since, when the probe was moved over the boundary into the region outside the arc discharge, the deflection fell abruptly to the background value. It will be noted that the peaks in the oscillations occur beyond the corresponding regions of scattering by approximately half the distance between them.

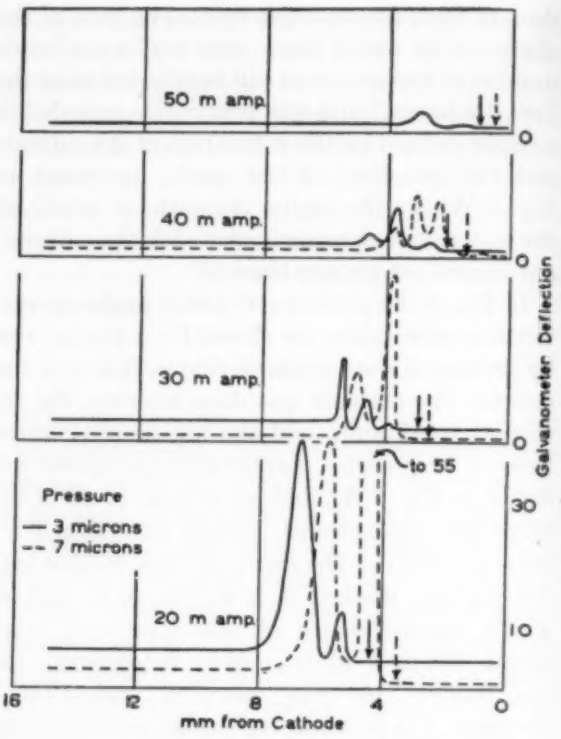

FIG. 6. The rectified current of the crystal detector circuit as a function of the position of the probe along the axis. The arrows show the position of the first region of scattering as found in a family of curves such as shown in Figs. 4 and 5.

In Fig. 5(A), (B) are shown similar results for an arc current of 0.045 amp. The arc pressure was three microns, arc drop 14 volts and the space potential seven volts positive to the anode. With this higher current the regions of scattering were closer to the cathode, the first being only 1.6 mm distant. Three distinct regions of scattering were observed in place of two, and corre-

sponding to these were three oscillation peaks, throughout which the Lecher system showed a definite frequency. The background again gave about 5 mv across the crystal, with no measurable frequency. Between the third peak and the anode the deflection was slightly in excess of the background without any indication of periodicity.

Column (h) of Table I gives the frequencies calculated by the Tonks and Langmuir formula for a number of typical cases and (i) the corresponding frequencies observed with the Lecher wires. These usually agreed to better than ten percent; the difficulties involved in measuring the concentrations were responsible for much of the lack of precision. For currents greater than 0.040 amp. no frequency is recorded as the response to the tuning on the Lecher wires was so unstable that the frequency could not be determined precisely.

In general, increase of either current or pressure moves the singular regions toward the cathode. In Fig. 6 the observed oscillations are plotted for two pressures, three and seven microns, at four currents, 0.020, 0.030, 0.040 and 0.050 amp. It will be seen that for a given current the curve taken at seven microns pressure has its peaks nearer the cathode than that for the lower pressure and that the effect of increasing the current is also to move the peaks toward the cathode as well as to make them less pronounced. For 0.020 amp. the peaks are exceptionally large; the one nearest the cathode extends to the ordinate value 55, while for 0.050 amp. the peak is very small in the three-micron curve and was unobservable at the seven-micron pressure. The positions of the scattering region nearest the cathode are indicated by solid arrows on the three-micron curve and by broken arrows on the seven-micron curves. It will be noted that these behave in the same way as the oscillation peaks, and that they again occur nearer the cathode.

No measurements of either scattering or oscillation were made at lower arc currents and pressures since the discharges became too unsteady for analysis.

Discussion

The close correlation between the scattering phenomena and the oscillations strongly confirms the conclusion of earlier investigators that the scattering is due to plasma oscillations of the type described by Tonks and Langmuir.[5] The agreement between the frequencies observed and those calculated from their formula (1), $\nu=(ne^2/\pi m_e)^{\frac{1}{2}}$, is of particular interest. The fact that oscillations of definite frequencies are observed only in the arc discharge where fast electrons are undergoing scattering leads to the further conclusion that these electrons furnish the energy for the oscillations. There are, however, several important points to be considered in connection with these conclusions.

The scattering regions were observed to be quite narrow, of the order of a few tenths of a millimeter. On the other hand, a single scattering process results in increases in energy of the order of five electron volts. This requires a large electric intensity in the scattering region. Let us assume that a single oscillation region is confined to the space between two parallel infinite planes at $x=o$ and $x=b$, respectively, and that the oscillations are due to motions of the plasma electrons parallel to the X axis. Let the electron concentration at any point be $n=n_0[1+\varphi(t)f(x)]$, where n_0 is the mean electron concentration, $\varphi(t)$ a periodic function of the time, and $f(x)$ some function of x which is zero except in the oscillation region and is such that its instantaneous mean value from o to b is zero. The number of electrons in excess of the mean in the region o to x is

$$S=\int_0^x n_0\varphi(t)f(x)dx$$

and the electric field strength at x resulting from this electron distribution is $4\pi\epsilon S$. Now if ξ is the displacement from its mean position of an electron when it is at x, and if we assume for simplicity that all electrons in a plane perpendicular to the X axis have the same velocity, we have $S=-n_0\xi$. The potential difference across the region is then

$$4\pi\epsilon\int_0^b(-n_0\xi)dx.$$

If this is put equal to five volts = 0.017 e.s.u. and if typical values, $b=0.03$ cm and $n_0=3\times10^{10}$ are

used, the mean value of ξ is approximately 0.003 cm. We see then that n in these experiments probably varied throughout the scattering region by as much as ten percent. The precision of measuring the concentration of the plasma electrons was, however, not sufficient to necessitate taking this variation in n into account, and in calculating the values in Table I the mean concentration was used.

It has been pointed out that the peaks in the oscillation curves occurred from one-half to one millimeter beyond the corresponding scattering regions, and that when the probe was in these latter regions no definite frequency could be detected. The actual plasma oscillations have, however, been assumed to be in the scattering region. To explain the shift it is necessary to consider how the alternating potential is impressed on the probe. Only a negligible part of the periodic current picked up by the probe was caused by the ultimate electrons. That this was principally caused by the fast electrons was shown by a study of the oscillation curves taken with different potential impressed on the probe. Only small changes were noted as this potential was decreased from a value slightly positive to the space potential to a value negative to the space potential by an amount equal to the cathode-space difference of potential. For more negative potentials the peaks decreased in height and finally disappeared, leaving only turbulent disturbances such as were always observed outside these regions. From this we conclude that the periodic fluctuation in the current density of the fast electrons accounted for the alternating potential picked up by the probe. Since a scattering region was narrow and the current density before scattering was practically constant, these periodic fluctuations became appreciable only at some distance beyond the region, where the fast electrons had to some extent overtaken those of mean velocity and the slower ones had dropped back. It is interesting to note the result of a calculation of the magnitude of the fluctuations in the current of fast electrons at the probe, for a simple case in which all of the electrons have the velocity v_0 before entering a narrow scattering region at $x=0$, while those emerging have the velocity, $v=v_0-A\cos 2\pi\nu t$. We find that the amplitude of the current density at any point x is equal to $(a_1^2+b_1^2)^{\frac{1}{2}}$ where,

$$a_1=2(2\nu C_0)\int_0^{\frac{1}{2}\nu}\cos(2\pi\nu x/v)\cos 2\pi\nu t\,dt$$

and

$$b_1=2(2\nu C_0)\int_0^{\frac{1}{2}\nu}\sin(2\pi\nu x/v)\cos 2\pi\nu t\,dt;$$

C_0 is the initial current density. Now since A is, in general, small with respect to v_0, it can be shown that $(a_1^2+b_1^2)^{\frac{1}{2}}=2C_0J_1(2\pi\nu xA/v_0^2)$. This expression has a maximum for the argument equal to 1.84. For $A=0.1v_0$, the value of x for maximum amplitude is approximately equal to 6 mm for typical values of ν and v_0. This is much larger than the observed distances between the oscillation peaks and the corresponding scattering regions. This is probably because we have assumed too simple conditions.

One of the assumptions which is most probably in error is that at any point at a given time all the fast electrons had the same velocity. A study of the velocity distribution of these electrons after scattering shows that there were fewer electrons in the faster and slower groups in comparison with those which retained their original velocity than would be expected on this assumption. It is probable, therefore, that there were always present mixtures of fast electrons of different velocities.

While results seem to point to the fast electrons as the source of the energy necessary to maintain the oscillations, attempts to calculate the energy transfer have not been successful.

For larger currents and pressures than those reported here, the electrons emerge from the immediate vicinity of the cathode already scattered, but no measurements could be made to study the details of the process. The above results suggest that a very violent oscillatory disturbance must exist in a very narrow layer close to the cathode.

The Variation with the Density of Mercury Vapor of the Intensity of the Spectral Lines of Mercury Excited by Electron Impact

O. S. DUFFENDACK AND O. G. KOPPIUS*
University of Michigan, Ann Arbor, Michigan

(Received May 1, 1939)

The variation in the intensities of mercury lines with the abundance of mercury present was investigated experimentally both for mercury alone and for mercury vapor in a mixture with another gas. The source consisted of a normal low voltage arc and this source was used because it closely approximates the simple ideal source desired; namely, one in which electrons of definite and controlled energy are projected through a space containing mercury and possibly other atoms so that an electron may not make more than one exciting or ionizing collision in its passage through the gas. Tests indicated that the ideal conditions were closely approximated. Theoretical formulae were developed for the relationship between the intensities of the mercury lines and the density of the mercury vapor (abundance of mercury). The measured values were found to be in good agreement with those given by the formulae. The relation of this investigation to the practices of quantitative spectrochemical analysis is pointed out. An analytical curve for the determination of mercury in such mixtures as were employed can be gotten from the data and the equation of the curve can be derived from the formulae derived from the theory given.

A. INTRODUCTION

EXPERIMENTS have brought to light many methods for the production of spectra. In former years the analysis and classification of spectra were some of the most important problems. The type of discharge which would produce the spectra was of secondary importance. The knowledge gained about the spectra and the extensive development of spectral theory now make it possible to use spectroscopic methods for the investigation of phenomena in the discharge of electricity through gases.

In this investigation one would, ideally, like to project into an extended region containing gas atoms a large number of electrons of definitely controlled energy. Within this region the electrons should be free and gain no more energy. Their energy should be such that upon an occasional exciting collision, the electron would lose most of its energy and could not excite any other atom upon which it might make an impact.

The low voltage arc[1] was chosen as a discharge source because it offers the simplest means of excitation by electron impacts. The reasons are as follows: (1) In the normal low voltage arc, after the discharge has reached a steady state, the whole fall in potential between the filament and the anode is concentrated in a thin sheath close to the cathode. The rest of the space is field free and is known as the plasma. (2) The current through the tube and the potential difference applied to the electrodes can be changed independently. This mode of discharge permits the mechanism for excitation to be adjusted so that the primary electrons have only one exciting collision. Further, this method facilitates an exact control of a given excitation condition.

Any investigation of a discharge as a source of light must involve radiation processes and the mechanism of the discharge. In fact, as C. G. Found[2] has stated, "Any discussion of the production of light in a gaseous discharge must involve a consideration of such a discharge as a conductor of electricity, since the fundamental function of the applied voltage is to establish a passage of current. Any light produced is merely incidental to and a by-product of the processes which render the tube conducting."

Although the production of light does not constitute a major role of a gaseous discharge, nevertheless, the mode in which light is produced is utilized in the field of quantitative spectrochemical analysis. This field of investigation presents numerous problems in which the conduction of electricity through gases plays a major role. Besides the more obvious value, the field of quantitative spectrochemical analysis affords, and is affording, an accurate quantitative

* Now at the Mathieson Alkali Works, Inc., Niagara Falls, New York.

[1] O. S. Duffendack, Phys. Rev. **20**, 665 (1922); K. T. Compton, Phys. Rev. **15**, 30 (1920).

[2] C. G. Found, Gen. Elec. Rev. **37**, 269 (1934).

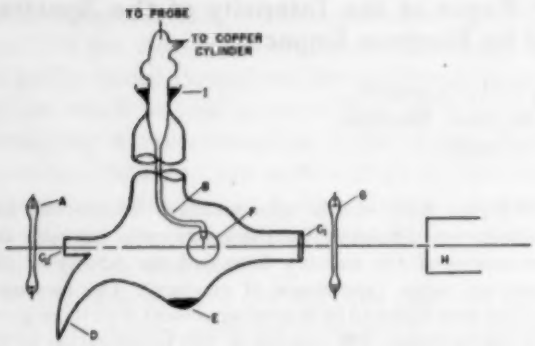

FIG. 1. Diagram of apparatus. *A*, mercury glow tube. *B*, probe. C_1, C_2, quartz windows. *E*, mercury reservoir. *F*, plate (anode). *G*, helium glow tube. *H*, spectrograph. *I*, mercury seal.

check of some phases of the extensive spectral theory and a correlation of this theory with discharge phenomena. Through extensive developments in quantitative spectrochemical analysis and in other fields by many investigators, the technique of spectral photometry has been improved to a high degree of reliability so that repeat measurements of a single plate agree within ± one percent. The principal problem in the development of the technique of spectrochemical analysis lies in a better understanding of the mechanism occurring in a gaseous discharge and its relation to spectral theory.

B. Purpose of Investigation

The purpose of the investigation was threefold: First, to make a quantitative study of the variation of intensity of the spectral lines of an element present alone in the discharge as a function of the amount. Second, to make a quantitative study of the variation of intensity of the spectral lines of one element, in the presence of definite amounts of foreign gas, as a function of the amount of the element present. Third, to tie up the general problem stated above to the more practical problem of quantitative spectrochemical analysis.

C. Experimental Procedure

Figure 1 gives a detailed view of the Pyrex experimental tube, also a schematic arrangement of the experimental tube, two auxiliary tubes *G* and *A*, and the spectrograph, *H*.

The experimental tube was constructed so as to carry out several different types of measurements without disturbing the discharge. The electrons from the hot tungsten filament were accelerated toward the nickel plate, *F*, a distance, $d=3$ cm, from the filament. The radiation from the discharge could be studied by allowing it to pass through a quartz window, C_1, and thence finally to a medium quartz spectrograph, *H*. A movable probe, *B*, was provided to determine the discharge conditions electrically. It could be set at any point within the discharge by turning the probe through the mercury seal, *I*. The light trap, *D*, served to eliminate reflections of the radiation from the back wall. In direct line with the main quartz window, C_1, but on the opposite side of the experimental tube was another quartz window, C_2. *E* is a reservoir containing the excess mercury.

Two magnetically controlled traps were provided to insure that whatever gas was admitted to the tube would remain at constant density as the temperature was changed. Both traps could be lifted by means of solenoids placed around the side tubes. The discharge tube was connected to a high vacuum system. A second mercury diffusion pump permitted the gases to be circulated through a charcoal trap, a hot copper oxide trap, a liquid-air trap, and through the experimental tube. Since there are no wax joints on this tube, contamination from this source was avoided.

The auxiliary tubes, *A* and *G*, were constructed similarly; both have fused quartz center sections. The electrodes were made of nickel. After the tubes were well outgassed, *G* was filled with pure helium to a pressure of 5 mm and *A* with pure argon to a pressure of 3 mm and an excess of redistilled mercury. Both tubes were then sealed off from the vacuum system.

The probe design has been described before by Sloane and Emeleus.[3] The probe wire was tungsten, five mm in length and three mm in diameter.

The electrical connections for the experimental tube were arranged so that the plate voltage and filament current could be changed independently. An adequate power source insured a plate current

[3] R. H. Sloane and K. G. Emeleus, Phys. Rev. **44**, 333 (1933).

which did not fluctuate more than ± one percent.

The method of measuring relative intensities of spectral lines was that given by Thomson and Duffendack.[4] Eastman Polychrome plates were used throughout this investigation.

The gases used in this investigation were helium, argon and mercury vapor. No impurities were found in any of these gases when spectroscopically examined.

The auxiliary helium discharge tube, *G*, served as a standard reference of intensity for the investigation of the test element, mercury. The constancy of the auxiliary discharge tubes was tested as will be described later. As shown in Fig. 1, the standard helium tube was placed in direct line with the spectrograph. Thus one could photograph simultaneously the radiation emitted by inelastic impacts of the electrons within the experimental tube and the radiation emitted by the standard helium lamp. This procedure permitted a study to be made of the dependence of relative intensities of mercury transitions to that of a particular helium transition = 2945.11A. This dependence was studied under constant excitation conditions as the density of mercury was changed.

The density of the mercury in the discharge was changed by simply varying the temperature of the water bath. In this investigation the temperature was changed from 0°C to 40°C; this corresponds to a change in pressure (reduced to 0°C) from 1.8×10^{-4} mm to 53×10^{-4} mm of mercury.

A medium quartz spectrograph, Hilger E2, was used throughout this investigation. It was adjusted so that the contribution from every portion of the discharge was always taken into consideration.

Argon in definite amounts was admitted to the discharge tube in order to investigate the variation of intensity of the line spectra of mercury in the presence of a foreign gas, as a function of the amount of mercury present. Finally, as a check, the argon was removed and helium introduced.

A probe was used to determine the electrical conditions within the discharge. The theory and analysis by probe methods have been described before.[5]

The constancy of the auxiliary discharge tubes was tested photographically. A series of timed exposures were taken on one plate for the same setting of the auxiliary tube and spectrograph. The values of the blackening produced were then compared and were found to be constant to within ±3 percent. The helium lamp was tested over a 40-hour period; whereas the mercury lamp was tested over a 6-hour period.

D. Experimental Results

Transitions from both the singlet and triplet states to the 6^3P_2, 6^3P_1, 6^3P_0 states of mercury were investigated. Resonance radiation was not considered.

Two striking phenomena were observed: (1) All curves of intensity *versus* abundance of mercury (pressure) show saturation. That is, after a certain pressure of mercury in the discharge tube the intensity no longer increases when additional amounts of the element are added. This is true for both mercury alone and for mixtures. (2) All curves of intensity *versus* abundance of mercury (pressure) behave similarly but not identically. That is, the series $6^3P_2-n^3D_2$ behaves similarly to $6^3P_2-n^1D_2$.

Two different explanations for the observed phenomena suggested themselves and were critically checked. The first one, which proved false, was as follows: At low concentration of mercury in the discharge, the number of atoms in the metastable states (6^3P_2 and 6^3P_0) is small and thus the radiation passes directly out of the discharge. At higher densities of mercury vapor, the concentration of atoms in 6^3P_2 and 6^3P_0 states is large and the radiation does not immediately pass from the bulb. The radiation from the entire volume of the discharge passes through the quartz window at low pressures of mercury and the intensity *versus* abundance plot varies linearly with the pressure. Because of the scattering of radiation at the higher pressures of mercury, the radiation no longer comes from the entire volume, but from the outer layer of excited gas near the tube wall. Some of the radiation emitted within the center of the dis-

[4] K. T. Thomson and O. S. Duffendack, J. Opt. Soc. Am. **23**, 101 (1933).

[5] I. Langmuir and H. M. Mott-Smith, Gen. Elec. Rev. **27**, 732–770 (1924).

charge is trapped and lost. The mechanism in this case could be a collision of the second kind between an excited mercury atom and an electron. Depending on the energy of the electron, the excited atom could either be ionized or lowered to a metastable state. The energy of the metastable atoms and ions could then be dissipated in the form of heat at the walls of the discharge tube. Since, in the case of a high concentration of mercury within the discharge, the radiation comes only from the outer layer of excited gas near the tube wall, any further increase of pressure does not increase the area of excited vapor since the area is bounded by the tube container. Thus the intensity *versus* abundance plot shows saturation.

The following experiment was performed to test this hypothesis. Radiation from a constant auxiliary mercury tube was passed directly through the discharge of the experimental tube and the absorption determined for transitions of mercury ending in the metastable states. Table I shows the method of procedure and the results. These data were taken at a pressure of 30×10^{-4} mm at which, as the curves show, the intensity has reached nearly its maximum value.

The results of this experiment show that the saturation of the intensity versus abundance plots are not due to absorption and re-emission, and thus the hypothesis is false. Cumulative excitation and ionization is consequently very improbable due to the small concentration of atoms in the lower states (6^3P_2 and 6^3P_0).

The second explanation assumes that the excitation of the mercury lines is due solely to inelastic collisions between mercury atoms and primary electrons. It will be shown that upon this basis formulae can be deduced such that the experimental data fit the curves representing the formulae.

The proof of the second explanation comes from probe analysis. To establish the mechanism of the saturation effect observed, the solution of the following problems must be known. Do the primary electrons coming from the filament have enough energy left after exciting once to again excite? After exciting once, can the resulting secondary electrons gain enough energy from the field in the discharge to again excite? Consideration will now be given to data that answer these questions.

From the straightness of the lower end of the semi-logarithm probe characteristic plots one can conclude that one and only one Maxwellian distribution of electrons was found. Thus, only two groups of electrons need be considered; namely, the primary electrons and the Maxwellian group given by these data.

The variation of electron temperature as a function of the abundance of mercury for the probe fixed at the center of the tube shows that the inelastic impacts made by the ultimate electrons can be neglected. The highest electron temperature observed was 11,000°K in mercury alone. The electron temperature drops quickly as the pressure of mercury is increased until at 20×10^{-4} mm it is 4000°K. For the mixtures of mercury and foreign gas the curves are similar to those for mercury alone. In this case the curves start initially at a much lower value of the electron temperature, and decrease rapidly to about 4000°K as the pressure of mercury is increased. A change of 7000°K in electron temperature corresponds approximately to a decrease of 10^5 in the number of electrons available for excitation. In contrast one observes a maximum value of the intensity in the region where the electron temperature is the lowest. Hence, only an extremely small fraction of this group of Maxwellian electrons have enough energy to again excite. A special tube was constructed to lend experimental proof to this fact. A cold cathode discharge tube was made containing a mixture of argon and excess mercury. The electron temperature was measured in the region of the Faraday dark space. In this region, prac-

TABLE I. *Measurements to detect absorption. For no absorption $a=b+c$ and this is found to be true.*

Experimental Arrangement	Intensity 2697A $6^1P_0-7^1D_1$	Intensity 3341A $6^1P_2-7^1S_1$
	Units	*Units*
(a) Radiation from the experimental tube plus radiation of standard mercury lamp	3.01	3.67
(b) Radiation from standard mercury lamp alone	1.65	2.65
(c) Radiation from experimental tube alone	1.49	1.11

tically no excitation takes place yet electron temperatures of the order of 8000 to 9000°K were observed.

The electron temperature was approximately a constant throughout the plasma for any given pressure of mercury in the discharge tube. A sharp increase in temperature was observed in the vicinity of the filament. This was due to the fact that the probe was collecting some primary electrons. The maximum drop in potential observed within the plasma was less than one volt. Thus the electrons after exciting once cannot gain enough energy from the field within the plasma to excite again.

The results of this experiment show that the primary electrons either have no inelastic impacts, or one and only one inelastic impact while going from the cathode to the anode. The radiation is produced solely by the inelastic impacts of primary electrons with mercury atoms.

Formulae accounting for the variation of the intensities of the spectral lines can be deduced in the following way. When the discharge is in a steady state, the intensity of a spectral line due to the transition from state j to state k of the atom will be proportional to the concentration N_j, of atoms in the state j, the probability of transition A_{jk}, and the magnitude of the light quantum, $h\nu$, that is $I_{\nu j} \alpha N_j \cdot A_{jk} \cdot h\nu$. For one type of atom and for one transition N_j is the only parameter. Since it was shown that no cumulative impacts occur, N_j is proportional to the number of inelastic impacts made by the primary electrons. Formulae determining N_j can be derived in the following manner. Let n_0 = total number of electrons per square centimeter per second which are accelerated across the cathode fall in potential; p = pressure of mercury vapor (corrected to 0°C); λ_E = average mean free path of an electron in mercury vapor for the excitation of any level in the mercury atom; λ_{1E} = average mean free path for the excitation of the mercury atom at unit pressure (0°C and 1 mm pressure), (thus $1/\lambda_E = p/\lambda_{1E}$); P_j = probability that an electron upon exciting the mercury atom will excite the particular state j; d = distance from cathode to anode and x = distance of any electron from the cathode. Hence, dx/λ_E = probability that an electron will have an inelastic collision within the interval dx. $-dn = ndx/\lambda_E$ is the number of ultimate electrons formed by inelastic impacts of high energy electrons with mercury atoms per unit area per element of distance in the direction of motion.

Integrating this expression from $x=0$ to $x=d$ we have the total number of electrons which suffer no inelastic impacts.

$$n' = n_0 e^{-d/\lambda_E}.$$

Consequently the number having inelastic collisions is simply $n = n_0(1-e^{-d/\lambda_E})$. Upon multiplying this expression by P_j we have the number of these excited atoms, N_j, which are in state j. In terms of pressure of mercury vapor and the current, i, passing through the discharge tube, the equation can be written

$$I_{\nu j} = A \cdot i(1-e^{-dp/\lambda_{1E}})P_j. \qquad (1)$$

Where A is a multiplicative constant, i is the tube current in milliamperes, p is the pressure of mercury in millimeters, P_j is a constant for any one particular state j.

The following consideration needs to be taken into account when the discharge tube contains a mixture of mercury and helium or argon. The electrons that excite atoms other than mercury are no longer available to excite mercury. The fraction of electrons that hit mercury atoms in a mixture of gases will be the ratio of the excitation cross section for collision with mercury atoms to the total excitation cross section. Thus, the intensity of a particular mercury transition in a mixture of mercury and argon or helium will be

$$I_{\nu j} = Ai\frac{1/\lambda_E}{1/\lambda_E + 1/\lambda_A}(1-e^{-dp/\lambda_m})P_j. \qquad (2)$$

λ_A is the average mean free path of an electron for excitation of a foreign atom. λ_m is the average mean free path of an electron for excitation of either a mercury or a foreign atom. All the other symbols have the same meaning as defined before. In this investigation the quantity measured was J = log (ratio of intensity of a Hg line to the intensity of a He line). Hence, calling

$$B = (A/I_{\mathrm{Hg}})P_j, \quad a = d/\lambda_{1E}, \quad b = (p_A/\lambda_{1A})\lambda_{1E},$$

Eqs. (1) and (2) become

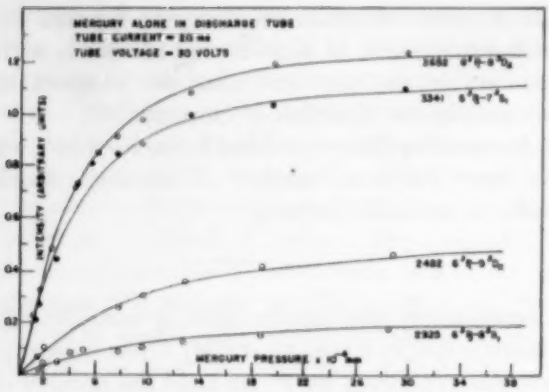
MERCURY ALONE IN DISCHARGE TUBE
TUBE CURRENT = 20 ma
TUBE VOLTAGE = 30 VOLTS
INTENSITY (ARBITRARY UNITS)
MERCURY PRESSURE x 10⁻³ mm

FIG. 2. Variation of intensity with abundance. Mercury alone.

$$e^J = Bi(1-e^{-ap_{Hg}}), \tag{3}$$

$$e^J = Bi\frac{1}{1+(b/p_{Hg})}(1-e^{-dp_{Hg}/\lambda_m}). \tag{4}$$

In all figures e^J was designated as "Intensity (Arbitrary units)" and is spoken of hereafter as intensity.

Equation (3) is valid for one element alone in the discharge tube; whereas Eq. (4) applies for the mixtures. B is a multiplicative constant which depends upon the geometry of the experimental tube, arrangement of spectrograph, position of helium lamp, the amount of absorption in the quartz and air of the particular wave-length of light under investigation, the probability of transition A_{jk}, and the magnitude of the light quantum $h\nu$. The constant, a, depends only upon the distance, d, and upon the probability of exciting the mercury atom. It should change only slightly for the various mercury transitions. By a suitable choice of constants the data for all the spectral lines, both when excited in mercury alone and when excited in mixtures, can be made to fit the curves representing Eqs. (3) and (4).

In the discussion that follows only typical sets of data will be considered. The experimental points and the theoretical curve are given in each case.

E. Discussion and Interpretation of Results for Mercury Alone

Equation (3) gives the relation between the intensity (e^J) of any particular transition of mercury, the current through the tube, and the abundance of mercury (pressure). For large values of the pressure, the intensity approaches a constant value. Fig. 2 shows this to be correct for transitions considered.

Table II gives a typical set of constants for eight different transitions. The classification includes transitions from both singlet and triplet states of mercury. Thus, in general, all transitions behave similarly, but not identically. The constant, a, is approximately a constant for all term values. This follows naturally due to the fact that, a, is proportional to the probability of exciting the mercury atom by electrons of a definite energy.

The value of λ_{1E} is of the same order of magnitude as the kinetic theory values. The value of d is uncertain due to the fact the trajectory of the electrons is altered by the many elastic collisions. Due to the zigzag motion of the electrons, the effective distance traversed is actually greater than the distance from cathode to anode. An increase in the value of d would cause the experimental value of λ_{1E} given in Table II to approach more nearly kinetic theory values. Exact agreement cannot be expected. The kinetic theory values were computed upon the false assumption that the cross section of the atom was the same for both high and low energy electrons.

For large values of the pressure Eq. (1) reduces to $I_{\nu j}=A\cdot i\cdot P_j$.

The difference in intensity of two mercury transitions should be a constant in the region where the above-made assumption is valid, for $I_{\nu j_1}-I_{\nu j_2}=Ai(P_{j_1}-P_{j_2})=\text{const}$. The exact difference in the P_j's cannot be determined since nothing is known of the magnitude of the constant, A. The differences in intensities should

TABLE II. *Mercury alone in the discharge tube. Kinetic theory value for* $\lambda_{1E}=9\times10^{-3}$ *centimeter. Tube voltage = 30 volts. Tube current = 20 ma.*

WAVE-LENGTH	CLASSIFICATION	B	a	λ_{1E} CM
3021A	$6^3P_2-8^3D_3$	1.045	0.20×10^4	1.5×10^{-3}
2803A	$6^3P_2-9^3D_3$	0.368	0.12×10^4	2.5×10^{-3}
2652A	$6^3P_1-8^3D_2$	1.20	0.20×10^4	1.5×10^{-3}
2482A	$6^3P_1-9^3D_2$	0.475	0.10×10^4	3.0×10^{-3}
3341A	$6^3P_2-7^3S_1$	1.09	0.18×10^4	1.66×10^{-3}
2925A	$6^3P_2-8^3S_1$	0.368	0.16×10^4	1.88×10^{-3}
2655A	$6^3P_1-8^1D_2$	1.15	0.24×10^4	1.25×10^{-3}
2483A	$6^3P_1-9^1D_2$	0.348	0.18×10^4	1.66×10^{-3}

TABLE III. *Intensities of mercury transitions for various pressures of mercury in the discharge. Tube voltage = 30 volts. Tube current = 20 ma.*

Mercury Pressure $\times 10^{-4}$ mm	Intensity (Arbitrary Units)														
	2652A		3341A		2482A		2925A		2655A		3021A		2803A		2483A
6	0.84	0.08	0.76	0.53	0.23	0.14	0.09	0.79	0.88	0.16	0.72	0.49	0.23	0.03	0.20
10	1.05	.14	.91	.60	.31	.185	.125	.905	1.03	.13	.90	.61	.29	.01	.28
14	1.13	.15	.98	.62	.36	.22	.14	.95	1.09	.11	.98	.67	.31	.01	.30
18	1.16	.14	1.02	.63	.39	.23	.16	.96	1.12	.11	1.01	.68	.33	.01	.32
22	1.19	.15	1.04	.62	.42	.225	.165	.965	1.13	.11	1.02	.68	.34	.01	.33
26	1.21	.15	1.06	.62	.44	.27	.17	.97	1.14	.11	1.03	.69	.34	.00	.34
30	1.22	.14	1.08	.63	.45	.27	.18	.97	1.15	.11	1.04	.69	.35	.00	.35
34	1.22	.13	1.09	.62	.47	.29	.18	.98	1.16	.12	1.04	.69	.35	.01	.36

approximately be zero for transitions starting on levels having approximately the same energy value and ending on the same state. Several examples are 2483A *vs.* 2482A, 2655A *vs.* 2652A, 3341A *vs.* 3021A etc.

Table III shows a typical set of data illustrating these points. For the various transitions indicated the intensity is given for several pressures of mercury in the discharge tube.

In order to illustrate the first point, consider the difference of intensities for 2652A and 3341A. This gives 0.08, 0.14, 0.15, 0.15, 0.14 and 0.13 intensity units. This relationship holds generally for the differences of any two transitions. The differences between the intensities of the lines in adjacent columns in Table III are given by the numbers between the columns.

At the lowest pressures the above simplified equation is no longer valid, and the values of the differences are no longer constant. The numbers in the table for the lowest pressures indicate that such a condition was being approached. The second point becomes obvious upon examining the intensity values in the table for the examples given.

F. Discussion and Interpretation of Results for Typical Cases for Mercury Mixed with Helium or Argon

Equation (4) was found to be applicable to all cases investigated. It was found that d/λ_m was of the order of magnitude of 8×10^4 to 10^5 for all transitions and for the different pressures of argon and helium. For example, at the lowest pressure of mercury investigated, the value of the exponential term was found to be 3×10^{-4} which is negligible compared with unity. Eq. (4) can now be simplified to

$$e^J = Bi\frac{1}{1+(b/p_{He})}. \tag{5}$$

This equation fits the experimental points exceedingly well for all mercury transitions, and for the various pressures of argon or helium in the experimental discharge tube. Fig. 3 shows the experimental points and theoretical curves for typical transitions. Similar results were obtained for mixtures of helium and mercury vapor.

Tables IV and V give a typical set of values for the constants B, b, λ_{1A} and λ_{1He}. From the constant, b, the value of λ_{1A} or λ_{1He} may be computed from the known value of the pressure of argon or helium in the tube, and the value or λ_{1E} given in Table II. λ_{1A} and λ_{1He} are the probabilities of an electron exciting the argon or the helium atom and their values should be approximately constant. Data given in Tables IV and V show this to be true. The values of λ_{1A} and λ_{1He} agree within the right order of magnitude with kinetic theory values. The discrepancy may again be attributed, as before, to the fact that the value of d is not known accurately. The constant, b, should increase proportionally with the pressure of argon or helium in the discharge tube. This has been only qualitatively verified.

For large values of the mercury pressure, the discharge equation (2), which is valid for the gas mixtures, reduces to the same form as Eq. (1). A mixture of mercury and a foreign gas should exhibit accordingly the same characteristics as found for mercury alone in the discharge tube. In Table VI is given a set of data similar to Table III for the case of mercury admixed with argon. The difference in intensities for any two transi-

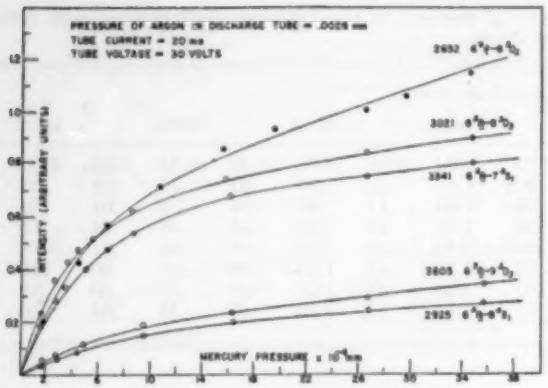

FIG. 3. Variation of intensity with abundance. Mercury vapor and argon.

tions gives approximately a constant as was found for mercury alone in the discharge. Likewise any two transitions starting from quantum levels having approximately the same energy value and ending on the same level have roughly the same intensity. A similar table for mixtures of mercury vapor and helium would show analogous results.

A direct comparison of the constant differences of intensities of various mercury transitions for mercury alone and for mercury admixed with a foreign gas can be made.

According to the simplified equation $I_{ij}=AiP_j$ the same constant difference in intensities taken for two different transitions at the same pressure of mercury should occur regardless of the amount and type of foreign gas contained in the discharge tube. Unfortunately, as was mentioned before, a direct comparison in this manner is not altogether valid. The position of the spectrograph and of the helium lamp was changed for each set of measurements. Their positions were approximately the same, however, and a rough check on the constancy of the intensity differences should be permissible.

Table VII gives a set of data taken for one pressure (34×10^{-4} mm) of mercury in the discharge tube. The intensities of various mercury transitions are given for mercury alone, mercury admixed with argon, and mercury admixed with helium. For example 3021A–2803A gives 0.68, 0.55, 0.41, and 0.46; also 2655A–3341A gives 0.13, 0.32, 0.13, 0.29, and 0.18. The transition 2655A seems to be in error in all cases. It is believed that the discrepancies are due mainly to the change in the positions of the apparatus.

Equation (5) represents a family of hyperbolae considering b as a parameter. The larger the value of b, the more quickly this curve approaches a straight line. The value of the multiplicative constant, B, was different for various pressures of argon and helium. Consequently, a family of hyperbolae for different values of b cannot be shown. Fig. 4 represents an experiment in which the constant $B\cdot i$ was identical for two cases; Eq. (3) is applicable to the curves marked "mercury," whereas Eq. (5) is applicable to the curves marked "mercury-helium." From the Eqs. (3) and (5) both curves should approach the same value of intensity asymptotically for large values of the pressure. At the origin the slope of Eq. (3) should be greater than the slope of Eq. (5). At very large values of the pressure, Eq. (3) should approach the asymptotic value sooner than Eq. (5). Hence, if the two curves cross at all after leaving the origin, they must do so an even number of times.

Experimentally, the curves show; first, that the slope of Eq. (3) is greater than the slope of Eq. (5) at the origin; second, the curves may or

TABLE IV. *A mixture of argon and mercury in the discharge tube. Kinetic theory value for* λ_1 *argon* $=29.3\times10^{-8}$ *centimeter. Pressure of argon* $=0.0028$ *mm. Tube voltage* $=30$ *volts. Tube current* $=20$ *ma.*

WAVE-LENGTH	CLASSIFICATION	B	b	$\lambda_{1,4}$ (CM)
3021A	$6^1P_2-8^1D_3$	0.98	4.3×10^{-4}	8.8×10^{-8}
2803A	$6^1P_2-9^1D_3$	0.39	12.9×10^{-4}	5.43×10^{-8}
2652A	$6^1P_2-8^1D_2$	1.47	12.2×10^{-4}	3.44×10^{-8}
2482A	$6^1P_2-9^1D_2$	0.54	15.5×10^{-4}	5.1×10^{-8}
3341A	$6^1P_2-7^1S_1$	0.93	5.9×10^{-4}	7.9×10^{-8}
2925A	$6^1P_2-8^1S_1$	0.37	15.8×10^{-4}	3.4×10^{-8}
2655A	$6^1P_2-8^1D_2$	1.20	8.0×10^{-4}	4.4×10^{-8}
2483A	$6^1P_2-9^1D_2$	0.27	5.9×10^{-4}	7.9×10^{-8}

TABLE V. *A mixture of helium and mercury in the discharge tube. Kinetic theory value for helium* $=77\times10^{-8}$ *centimeter. Pressure of helium* $=0.025$ *mm. Tube voltage* $=30$ *volts. Tube current* $=20$ *ma.*

WAVE-LENGTH	CLASSIFICATION	B	b	λ_1He
3021A	$6^1P_2-8^1D_3$	0.99	10.4×10^{-4}	36×10^{-8}
2803A	$6^1P_2-9^1D_3$	0.48	22.4×10^{-4}	28.0×10^{-8}
2652A	$6^1P_2-8^1D_2$	1.41	20.2×10^{-4}	18.6×10^{-8}
2482A	$6^1P_2-9^1D_2$	0.33	12.65×10^{-4}	59.0×10^{-8}
3341A	$6^1P_2-7^1S_1$	0.79	9.77×10^{-4}	42.5×10^{-8}
2655A	$6^1P_2-8^1D_2$	0.96	12.0×10^{-4}	26.0×10^{-8}
2483A	$6^1P_2-9^1D_2$	0.22	10.7×10^{-4}	38.8×10^{-8}

TABLE VI. *Intensity of mercury transitions for various pressures of mercury in a discharge containing argon. Pressure of argon = 0.0028 mm. Tube voltage = 30 volts. Tube current = 20 ma. Differences of intensities are also shown.*

Mercury Pressure × 10^{-4} mm	Intensity															
	2652A		3341A		2482A		2925A		2655A		3021A		2803A		2483A	
6	0.49	0.05	0.44	0.29	0.15	0.05	0.10	0.44	0.54	−0.01	0.55	0.41	0.13	0.01	0.12	
10	.67	.10	.57	.36	.21	.07	.14	.54	.68	.02	.66	.48	.18	.01	.17	
14	.74	.12	.66	.42	.24	.06	.18	.58	.76	.04	.72	.51	.21	.02	.19	
18	.87	.17	.70	.42	.28	.08	.20	.63	.83	.06	.77	.54	.23	.01	.22	
22	.94	.21	.73	.42	.31	.09	.22	.66	.88	.08	.80	.54	.26	.03	.23	
26	1.0	.24	.76	.43	.33	.09	.24	.69	.93	.10	.83	.55	.28	.05	.23	
30	1.06	.24	.78	.43	.35	.10	.25	.74	.99	.14	.85	.55	.30	.06	.24	
34	1.12	.28	.80	.42	.38	.11	.27	.77	1.04	.16	.88	.55	.33	.09	.24	

may not cross; third, the curves begin to approach approximately the same saturation value. The latter point could not be further investigated due to the fact that cumulative ionization sets in at higher pressures. In the case of cumulative ionization, the abundance *versus* intensity plot does not remain constant as the pressure is increased, but shows a break in the curve at a definite value of the pressure. For higher pressures than this critical value, the intensity *versus* abundance plots increase again with approximately the same slope as for very low values of the pressure. That is, the curve seems to be starting to duplicate itself.

Equation (4) was verified for different current values. Two intensity curves were taken for tube currents of 40 and 60 ma, respectively. The plots of log (ratio of intensity of Hg line to the intensity of a He line) *versus* log (pressure of mercury) differed by exactly one logarithm unit (base 1.5). Thus,

$$e^{-0.810}/e^{-0.405}=0.67.$$

No experimental verification of Eq. (3) was carried out. However, since, as shown, the intensity varies accurately with the current as predicted by Eq. (4), one would expect Eq. (3) to hold likewise.

G. A Brief Statement of the Physical Meaning of the Phenomena Observed

Mercury alone in the discharge tube

The intensity of any particular transition of an atom is proportional to the number of inelastic impacts that occur. When the gas pressure is low, the number of elastic collisions and likewise the number of inelastic collisions is small, and the observed intensity of the transition is weak. As the pressure increases, more and more inelastic impacts occur due to the greater number of times the electron comes in contact with the atoms. Correspondingly, the observed intensity of the transition increases. This continues until finally practically all of the electrons have an inelastic impact before reaching the anode, and any further increase in pressure does not yield any more inelastic impacts. In this state, the intensity of the different lines *versus* abundance plot shows saturation.

Mercury in a mixture of gases

Each high velocity electron can have one and only one inelastic impact and this may be with a

TABLE VII. *Intensity of various mercury transitions at a pressure of mercury equal to 34×10^{-4} mm in discharge tube. Tube voltage = 30 volts. Tube current = 20 ma.*

Wave-length	Hg Alone	P_A = 0.0028 mm	P_A = 0.0038 mm	P_{He} = 0.025 mm	P_{He} = 0.046 mm
2655A	1.16	1.04	0.82	0.68	0.59
3021A	1.04	0.88	0.77	0.72	0.80
2803A	0.36	0.33		0.32	0.34
2483A	0.35	0.24	0.21	0.71	0.13
2655A	1.22	1.12	0.91	0.88	0.68
3341A	1.09	0.80	0.78	0.59	0.50
2482A	0.47	0.37		0.24	0.24
2925A	0.18	0.27			

foreign or a mercury atom. The fraction of high energy electrons having exciting collisions with mercury will be the ratio of the excitation cross section of the mercury atoms to the total excitation cross section. As the pressure of the mercury is increased the fraction slowly approaches a constant value. The rate of approach depends upon the amount of foreign gas present. Thus, the intensity *versus* abundance plots show saturation.

H. Results of This Investigation as Applied to Practical Quantitative Spectrochemical Analysis

A plot of J, $\log (I_{\mathrm{Hg}}/I_{\mathrm{He}})$, *versus* $\log X$, (log percent Hg) is a straight line. The straight lines are the standard analytical curves used in practice.

When the concentration of the test element, i.e. mercury, is high Eq. (5) is no longer valid. In this case the exact Eq. (4) applies. For high concentrations of the test element, $b \ll p$, the multiplicative factor simply reduces to $B \cdot i$. The plot of the resulting equation shows saturation for large values of the pressure. Under these conditions the spectral line is said to be insensitive.

This insensitiveness is the reason why quantitative spectrographic analysis fails for high percentages of the test element.

The answer to more practical and important problems can now be given; namely, what can be done if one desires to analyze a substance containing a high percentage of the test element and what spectral lines are most suitable? From Eq. (4) the spectral lines of an element become insensitive when $b \ll p$ and p itself becomes large.

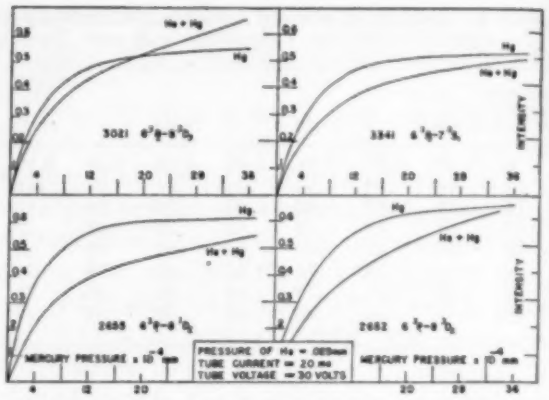

FIG. 4. Comparison of variations of intensity of mercury lines with abundance in mercury alone and mercury-helium mixtures.

To regain sensitivity the specimen must be diluted with foreign atoms, i.e., make b greater. Higher term members will be more sensitive than lower term members because b is proportional to the average mean free path of the electron for excitation of the test element. As may be seen from Table II, λ_{1E} is greater for higher term members.

In this discussion it has been tacitly assumed that the mechanism for excitation in practice is the same as the excitation condition of this investigation. Actually the mechanism is far more complicated as the sources used in spectrochemical analysis do not provide such simple excitation conditions as the sources used in this investigation. Nevertheless, the analytical curves for most sources used in practice are straight lines for a given range of abundance and the departures from these straight lines are as one would expect from the reasoning given above.

New Terms in Fe I, II, and III and Additional Far Ultraviolet Standards*

LOUIS C. GREEN
*Princeton University Observatory, Princeton, New Jersey***

(Received January 7, 1939)

The iron spectrum excited in the Schüler discharge in He and Ne and the iron arc and spark in nitrogen have been studied in the ultraviolet from λ2300 to λ600. New terms have been identified in Fe I, II, and III and in addition a number of unclassified levels have been found in Fe II. Lists of all the lines identified from new or previously known levels are given. These lists include a number of lines in the region λ2225 to λ1550 whose wave-length can be accurately calculated by the combination principle from levels whose positions are determined by measures at longer wave-lengths. These lines will be useful as standards.

THE iron spectrum has been investigated in the far ultraviolet from λ2300 to λ600. Plates have been taken, on the Princeton two-meter vacuum spectrograph, of the iron spectrum excited in the Schüler discharge in He and Ne and of the iron arc and spark in nitrogen. A large amount of laboratory work, which will be described elsewhere, has been devoted to the development of the Schüler tube technique to the point where the discharge becomes an effective source for the iron spectrum.

Fe I

Three new terms forming a $^5(PDF)$ triad, a separate ^5P,† and one new unidentified level have been found in Fe I; they are listed in Table I. The electron configuration is given in the first column, the term designation in the second, the J value in the third, the height of the level above a^5D_4 in the fourth, the interval in the fifth, and the number of combinations which the level makes in the sixth. An intensity diagram is given, Table II. The intensities of the lines arising from transitions down to a^5D are taken from the author's lists of the arc in nitrogen; the rest are from Burns and Walters[1] with the exception of those followed by B, Burns;[2] S, Schumacher;[3] K, Kayser.[4] The $v^5D_1{}^0$ level is not well established but nothing else in the region can be made to serve any better. An unusual distribution of intensity analogous to that in the $a^5D-v^5D^0$ multiplet has been found by Findlay[5] in the $d^74s\ ^5F-d^74p\ ^5F^0$ of Co II.

The question arises whether the new triad is in series with the upper or lower of the two known $^5(PDF)$ triads. The lower triad is usually attributed to $3d^64s(^6D)4p$ and the upper to $3d^64s(^4D)4p$. There is no proof that this is correct and the reverse assignment seems equally probable. However if for the moment we assume the first assignment, we can predict the position of the second triad in each series. The results are rough since series involving a running p electron are very rarely regular in many-electron spectra.

TABLE I. *New terms in* Fe I.

CONFIGURATION	TERM DESIG.	J	LEVEL	INTERVAL	NO. OF COMB.
	58^0	1	48350.65		9
$3d^64s(^6D)5p$	v^5F^0	5	51016.71	−364.80	3
$3d^64s(^6D)5p$	v^5F^0	4	51381.51	−237.63	5
$3d^64s(^6D)5p$	v^5F^0	3	51619.14	−208.48	7
$3d^64s(^6D)5p$	v^5F^0	2	51827.62	−118.24	7
$3d^64s(^6D)5p$	v^5F^0	1	51945.86		5
$3d^64s(^6D)5p$	v^5D^0	4	51076.67	−284.79	6
$3d^64s(^6D)5p$	v^5D^0	3	51361.46	−268.60	8
$3d^64s(^6D)5p$	v^5D^0	2	51630.06	−206.7	8
$3d^64s(^6D)5p$	v^5D^0	1	51836.8	−105.0	2
$3d^64s(^6D)5p$	v^5D^0	0	51941.76		3
$3d^64s(^6D)5p$	u^5P^0	3	51692.2	−252.9	5
$3d^64s(^6D)5p$	u^5P^0	2	51945.1	−165.5	4
$3d^64s(^6D)5p$	u^5P^0	1	52110.6		6
	t^5P^0	3	53388.68	−723.60	4
	t^5P^0	2	54112.28	−158.84	7
	t^5P^0	1	54271.12		9

* Submitted to the Faculty of Princeton University in partial fulfillment of the requirements for the degree of Doctor of Philosophy.

** Now at Allegheny College, Meadville, Pennsylvania.

† These three levels were identified as ^5P by Professor H. N. Russell.

[1] K. Burns and F. M. Walters, Publication of the Allegheny Observatory **8**, No. 4.

[2] K. Burns, Lick Obs. Bull., No. 247 (1913).

[3] Schumacher, Zeits. f. Wiss. Photogr. **19**, 149 (1919).

[4] Kayser, *Handbuch der Spectroscopie* **6**, 892 and **7**, 405.

[5] J. H. Findlay, Phys. Rev. **36**, 5 (1930).

TABLE II. *Intensities of lines in* Fe *arc.*

		a^5D					a^5F					a^5P		
		4	3	2	1	0	5	4	3	2	1	3	2	1
z^5P^0	1			2	5	2							3*B*	1*K*
	2		5	8	1				1*uS*			4	2	3
	3	8	15						1*uS*			2		
u^5P^0	1			20	25	20*				1*S*			5	1*aK*
	2		25	25*	30*				12					
	3	25	25	25				45				2*K*		
v^5D^0	0				15						9			1
	1			20*	0									
	2		25	10	0				9	9	1*S*		2*K*	2*K*
	3	30	20	1				8	15*	5		1*K*	3	
	4	30	0				45	15	2			6		
v^5F^0	1			25*	30*	25				9*b*	4			
	2		10	25	25				10	8	10			1*K*
	3	25	25	20					12	15*		1*K*	1*K*	
	4	2	30				25	40	3					
	5	30					15†	3						
$58_1{}^0$				15	20	30				2	12		4*B*	2*B*

* These lines are used twice.
† An examination of an arc plate suggests that this intensity is in error. The line is definitely considerably stronger than $a^5F_4-z^5F_4{}^0$.

It is found that the second triad built on ^6D should lie about 2000 wave numbers below the new triad and the one built on ^4D about 7000 above it. If we assume the reverse assignment, we would expect the second member of the series built on ^6D about 1600 wave numbers above the new triad and the one built on ^4D about 3500 above the new triad. It appears therefore that the new triad is probably built on ^6D but it is impossible to say at present with which of the lower triads it is in series. A comparison of the intensities of the transitions between the three triads and low ^5D, ^5F and ^5P also fails to tell us which of the previously known groups goes to the ^6D limit. The possibility that the triad should be assigned to $d^6(^5D)4s4p(^{1,3}P)$ or $d^6(^5D)4p(^{6,4}P, D, F)4s$ instead of $d^6(^5D)4s(^{6,4}D)4p$ was considered. The term intervals for these various possibilities were calculated by the rule of Goudsmit and Humphreys.[6] However in no case was the agreement between the predicted and observed values sufficiently good to warrant an assignment.

Table III contains the new identifications in Fe I. The columns are as follows: column one, the wave-length in vacuum up to λ2200 and in air for longer wave-lengths. When this is poorly determined, it is followed by a small "*p*." If the wave-length of a line below λ2200 can be calculated by means of the combination principle from measures made above λ2240, the calculated decimal is given in the second column. Column three contains the intensity in the arc; column four, the intensity in the He Schüler tube; a "*b*" after the intensity means that the line is a blend. Column five gives the observer, where *G* stands for Green, *BW* for Burns and Walters, *B* for Burns, *S* for Schumacher, and *K* for Kayser. Column six contains "*s*" if the line is regarded as especially suitable as a standard. The final column gives the identification; where this is regarded as uncertain it is followed by a question mark.

Fe II

In the tables below are listed all the new even and odd levels which have been found in Fe II together with six which were previously found by Dobbie[7] and which have been given new assignments on the basis of additional material. The following information is contained in the columns of the tables: in the first, the electron configuration; in the second, the term symbol; in the

[6] S. Goudsmit and C. J. Humphreys, Phys. Rev. **31**, 960 (1928).

[7] J. C. Dobbie, *Proc. Roy. Soc. London* **A151**, 703 (1935).

TABLE III. *New identifications in* Fe I. *In the column S, the source is given and in column st, those lines are designated which are especially suitable as standards.*

λ VAC		INTENSITY				
OBS.	CALC.	ARC	S.T.	S	st	IDENTIFICATION
1862.318	0.324	5	15	G	s	$a^5D_3-z^5P^o_3$
1866.815	.817	2	10	G		$a^5D_2-z^5P^o_1$
1872.359	.369	8	15	G	s	$a^5D_3-z^5P^o_2$
1873.052	.056	8	12	G		$a^5D_4-z^5P^o_3$
1873.259	.256	5	15	G		$a^5D_1-z^5P^o_1$
1876.421	.417	2	10	G		$a^5D_0-z^5P^o_1$
1878.849	.846	1	2	G	s	$a^5D_1-z^5P^o_2$
1887.761	.763	15	20	G		$a^5D_2-z^5P^o_2$
1934.528		25	25	G		$a^5D_4-a^5P^o_3$
1937.274	.266	25	35	G		$a^5D_4-y^5F^o_5$
1940.649		25	25	G		$a^5D_3-a^5P^o_2$
1945.070	.083	10	20b	G		$a^5D_3-y^5F^o_4$
1945.294		20	25	G		$a^5D_2-a^5P^o_1$
1946.219	.225	2	10	G	s	$a^5D_4-y^5F^o_4$
1946.978	.986	30	25	G	s	$a^5D_4-y^5D^o_4$
1950.223		25	20	G		$a^5D_3-a^5P^o_1$
1951.556	.529	25	25	G		$a^5D_2-y^5F^o_3$
						$a^5D_3-a^5P^o_2$
1952.262		25	20	G		$a^5D_1-a^5P^o_1$
1952.596	.586	25	30	G	s	$a^5D_2-y^5D^o_3$
1952.997	3.002	25	20	G		$a^5D_2-y^5F^o_2$
1955.690		20	20	G		$a^5D_2-y^5D^o_1$
						$a^5D_3-a^5P^o_2$
1956.026	.043	25	30	G	s	$a^5D_3-y^5F^o_2$
1957.831	.841	30	25	G	s	$a^5D_4-y^5D^o_3$
1958.598	.567	30	30	G		$a^5D_3-y^5F^o_3$
						$a^5D_1-a^5P^o_2$
1958.739	.724	15	15	G	s	$a^5D_1-y^5D^o_2$
1960.129	.142	30	25	G	s	$a^5D_4-y^5F^o_5$
1961.236		25	20	G		$a^5D_2-a^5P^o_2$
1962.031ρ	.023	25	30	G		$a^5D_3-y^5F^o_4$
1962.100ρ	.108	30		G		$a^5D_3-y^5F^o_3$
1962.746		0	15	G		$a^5D_1-y^5D^o_1$
1962.871	.881	20	20	G	s	$a^5D_2-y^5D^o_2$
1963.110	.113	25	25	G	s	$a^5D_1-y^5F^o_2$
1963.629	.631	10	15	G	s	$a^5D_1-y^5F^o_1$
1964.043	.052	20	20	G		$a^5D_2-y^5F^o_2$
1970.771	.757	—	0	G	s	$a^5D_1-y^5D^o_0$
1973.911	.915	0	1	G	s	$a^5D_2-y^5D^o_2$
1974.059	.043	—	1	G	s	$a^5D_3-y^5D^o_3$
2098.759	.783	15	25b	G		$a^5D_3-5s_1{}^6S^o_{5/2}$
2106.931	.926	20	15	G	s	$a^5D_1-5s_1{}^6S^o_{5/2}$
2110.910	.926	30	25	G		$a^5D_0-5s_1{}^6S^o_{5/2}$
2155.820	.906	1u	10b	S		$a^5F_2-z^5P^o_2$?
2189.997	90.071	1u	12b	S		$a^5F_3-z^5P^o_3$?

λ AIR						
2248.855		25		BW		$a^5F_5-y^5F^o_5$
2255.859		45		BW		$a^5F_4-a^5P^o_3$
2260.860		12		BW		$a^5F_3-a^5P^o_2$

λ VAC		INTENSITY				
OBS.	CALC.	ARC	S.T.	S	st	IDENTIFICATION
λ AIR						
2264.390		45		BW		$a^5F_5-y^5D^o_4$
2265.60		1		S		$a^5F_3-a^5P^o_1$
2266.903		10		BW		$a^5F_3-y^5F^o_3$
2267.465		15		BW		$a^5F_4-y^5F^o_4$
2271.778		40		BW		$a^5F_4-y^5F^o_5$
2272.816		8		BW		$a^5F_4-y^5D^o_4$
2274.087		9		BW		$a^5F_5-y^5F^o_5$
						$a^5D_3-12s^6S^o_{5/2}$
2277.094		9		BW		$a^5F_3-y^5D^o_3$
2277.663		12		BW		$a^5F_2-y^5F^o_2$
2280.222		8		BW		$a^5F_3-y^5F^o_3$
2282.861		4		BW		$a^5F_1-y^5F^o_2$
2283.079		9		BW		$a^5F_1-y^5D^o_1$
2287.628		15		BW		$a^5F_4-y^5D^o_4$
2289.032		10		BW		$a^5F_1-y^5F^o_1$
2290.064		3		BW		$a^5F_2-y^5F^o_2$
2290.546		9		BW		$a^5F_2-y^5D^o_2$
2290.771		3		BW		$a^5F_4-y^5F^o_5$
2291.117		15		BW		$a^5F_3-y^5D^o_3$
						$a^5F_3-y^5F^o_4$
2299.42		1		S		$a^5F_1-y^5D^o_0$
2304.727		5		BW		$a^5F_2-y^5D^o_2$
2306.164		2		BW		$a^5F_2-y^5D^o_1$
2476.654		2		BW		$a^5F_2-5s_1{}^6S^o_{5/2}$
2487.064		12		BW		$a^5F_1-5s_1{}^6S^o_{5/2}$
2734.266		4		BW		$a^5F_3-z^5P^o_2$
2735.611		3		B		$a^5F_3-z^5P^o_1$
2747.553		2		BW		$a^5F_2-z^5P^o_2$
2750.72		1		K		$a^5P_1-z^5P^o_1$?
2762.770		3		BW		$a^5P_1-z^5P^o_2$
2789.477		2		BW		$a^5P_2-z^5P^o_2$
2907.518		5		BW		$a^5P_2-a^5P^o_1$
2920.3		1		K		$a^5P_2-z^5P^o_2$
2924.6		1u		K		$a^5P_1-a^5P^o_1$
2928.11		2		K		$a^5P_3-a^5P^o_2$
2934.4		1		K		$a^5P_2-y^5F^o_2$
2939.072		1		BW		$a^5P_1-y^5D^o_1$
2948.69		2		K		$a^5P_2-y^5D^o_2$
2948.94		1		K		$a^5P_1-y^5F^o_2$
2949.8		1		K		$a^5P_2-y^5F^o_3$
2956.7		1		K		$a^5P_3-y^5D^o_3$
2966.23		2		K		$a^5P_1-y^5D^o_2$
2972.277		3		BW		$a^5P_2-y^5D^o_3$
2981.852		6		BW		$a^5P_3-y^5D^o_4$
3264.522		4		B		$a^5P_2-5s_1{}^6S^o_{5/2}$
3286.026		2		B		$a^5P_1-5s_1{}^6S^o_{5/2}$
3339.588		1b		B		$a^3P_2-z^3P^o_2$
3388.966		1b		B		$a^3P_1-z^3P^o_1$
3935.31		2		K		$b^3P_1-5s_1{}^6S^o_{5/2}$
4804.6		1		K		$a^1P_1-5s_1{}^6S^o_{5/2}$?

TABLE IV. *New even levels in* Fe II.

CONFIG.	DESIG.	J	LEVEL	INTERVAL	NO. OF COMB.	POSSIBLE DESIG.	DOBBIE'S DESIG.
$d^5(^5D)4d$	e^6F	$5\frac{1}{2}$	82853.5		3		
$d^5(^5D)4d$	e^6F	$4\frac{1}{2}$	82978.9	−125.4	6		$f^6D_{4\frac{1}{2}}$
$d^5(^5D)4d$	e^6F	$3\frac{1}{2}$	83136.5	−157.6	7		$f^6D_{3\frac{1}{2}}$
$d^5(^5D)4d$	e^6F	$2\frac{1}{2}$	83308.4	−171.9	8		$f^6D_{2\frac{1}{2}}$
$d^5(^5D)4d$	e^6F	$1\frac{1}{2}$	83459.7	−151.3	7		
$d^5(^5D)4d$	e^6F	$\frac{1}{2}$	83558.5	− 98.8	4		
$d^5(^5D)4d$?	30	$3\frac{1}{2}$	83713.3		4	^6D	
$d^5(^5D)4d$?	31	$4\frac{1}{2}$ or $3\frac{1}{2}$	83726.2		4	^6D	$e^6P_{3\frac{1}{2}}$
$d^5(^5D)4d$?	32	$2\frac{1}{2}$	83812.1		6	^6D	
$d^5(^5D)4d$?	33	$1\frac{1}{2}$	83989.7		4	^6D	
$d^5(^5D)4d$?	34	$\frac{1}{2}$ or $1\frac{1}{2}$	84131.2		3	^6D	
$d^5(^5D)4d$?	35	$2\frac{1}{2}$	84266.9		6		$e^6P_{2\frac{1}{2}}$
$d^5(^5D)4d$?	36	$2\frac{1}{2}$	84327.0		5		$e^6P_{1\frac{1}{2}}$

TABLE V. *New odd levels in* Fe II.

CONFIG.	DESIG.	J	LEVEL	INTERVAL	NO. OF COMB.	POSSIBLE DESIG.
$3d^64s(\ )4p$	y^6P^0	1½	61974.9		3	
				+74.1		
$3d^64s(\ )4p$	y^6P^0	2½	62049.0		3	
				+122.7		
$3d^64s(\ )4p$	y^6P^0	3½	62171.7		3	
$3d^64s(^5S)4p$	x^4P^0	2½	69102.4		3	
				−199.7		
$3d^64s(^5S)4p$	x^4P^0	1½	69302.1		3	
				−124.7		
$3d^64s(^5S)4p$	x^4P^0	½	69426.8		2	
$3d^64s(\ )4p$	x^6P^0	1½	79244.6		3	
				+40.1		
$3d^64s(\ )4p$	x^6P^0	2½	79284.7		4	
				+46.5		
$3d^64s(\ )4p$	x^6P^0	3½	79331.2		4	
$3d^6(^1D)5p$	y^4F^0	5½	87340.4		1	
				−130.4		
$3d^6(^3D)5p$	y^4F^0	4½	87470.8		2	
				−66.1		
$3d^6(^3D)5p$	y^4F^0	3½	87536.9		3	
				−34.9		
$3d^6(^3D)5p$	y^4F^0	2½	87571.8		3	
				−30.1		
$3d^6(^3D)5p$	y^4F^0	1½	87601.9		3	
				−33.3		
$3d^6(^3D)5p$	y^4F^0	½	87635.2		2	
	1^0	3½	88208.6		4	$^4P^0$
	2^0	3½	89127.7		3	$^4P^0$
	3^0	2½	89443.7		3	$^4P^0$
	4^0	1½	89625.0		3	$^4P^0$
	5^0	3½	90300.0		4	
	6^0	4½ or 3½	90385.5		4	
	8^0	½ or 1½	90828.4		2	$^4P^0$
	9^0	1½	90898.2		3	$^4P^0$
	10^0	2½ or 1½	90981.5		2	$^4P^0$
	11^0	2½	91067.1		6	
	w^6F^0	3½	91167.3		4	
				−407.5		
	w^6F^0	2½	91574.8		4	
				−268.3		
	w^6F^0	1½	91843.1		4	
	13^0	3½	93986.9		4	
	14^0	2½	94210.1		5	
	15^0	3½	94762.3		4	
	16^0	3½	106863.2		6	
	17^0	3½ or 2½	107165.6		5	
	18^0	2½	107196.2		4	
	20^0	3½	107886.6		6	$^6D^0$
	21^0	4½ or 3½	107964.7		4	$^6D^0$
	22^0	2½	108130.6		4	$^6D^0$
	23^0	1½	108191.6		3	$^6D^0$
	24^0	3½	108239.2		4	
	25^0	1½	108371.7		4	
	26^0	3½	108373.8		6	
	27^0	1½	108780.0		6	
	28^0	1½	109780.0		4	
	29^0	2½	111929.0		4	

third, the J value; in the fourth, the level value; in the fifth, the interval; in the sixth, the number of combinations which the level makes; in the seventh, a possible term symbol for some of the unclassified levels; in the eighth, the designation previously assigned to the level by Dobbie. Numbers have been given to the unclassified levels. When two J values are possible the more probable one is listed first.

Since there is no place for y^6P^0 or x^6P^0 in the $3d^64p$ configuration, they have been assigned to $3d^54s4p$, which is the only other odd configuration between 60,000 and 80,000. On the other hand, x^4P^0 could be the missing $3d^6(^3D)4p\ ^4P^0$, were it not for the fact that it combines strongly with a^4D. Since neither the ^4D nor the ^4F from $3d^6(^3D)4p$ combines with a^4D, x^4P^0 has also been assigned to $3d^54s4p$. The three terms now appear in the same order as in the isoelectronic spectrum of Mn I; they have also the same arrangement of J values, that is, the sextets are normal and the quartet inverted. An attempt was made to determine by the rule of Goudsmit and Humphreys,[6] whether these terms arise from $3d^54s(^{7,\,5}S)4p$, or $3d^5(^6S)4s4p(^{3,\,1}P)$, or $3d^54p(^{7,\,5}P)4s$. However, in none of the three cases was the agreement between the predicted and observed intervals sufficiently good to warrant an assignment.

The sextet triad of $3d^6(^5D)5p$ would be expected to lie about 88,000 wave numbers above a^6D. The term found in this region appears to be ^6F rather than ^6D. The corresponding triad from $3d^6(^5D)6p$ would be expected in the

TABLE VI. *Intensities of lines in* Fe *spark.*

DOBBIE'S DESIG.	DESIG.	J		z^6D^0				z^6F^0						z^6P^0		
			4½	3½	2½	1½	½	5½	4½	3½	2½	1½	½	3½	2½	1½
$^6P_{1\frac{1}{2}}$	36	2½			4	8				10					1	10
$^6P_{2\frac{1}{2}}$	35	2½		10	5	20				0				6	20	
	34	½ or 1½				4	6									6
	33	1½			10	1	4									0
	32	2½		20	2	10								10	5	5
$^6P_{3\frac{1}{2}}$	31	4½ or 3½	30	30					8					20		
	30	3½	20		30						0			25		
	e^6F	½				8	30					6	3			
	e^6F	1½			20	25	8				10	5	5		0	
$^6D_{3\frac{1}{2}}$	e^6F	2½		25	30	10				15	8	15		1	2	
$^6D_{3\frac{1}{2}}$	e^6F	3½	20	35	25				10	10	5			8		
$^6D_{4\frac{1}{2}}$	e^6F	4½	45	50				20	25	15				3		
	e^6F	5½	80					40	25							

TABLE VII. *Identified* Fe II *lines. In the column S, the source is given and in column st, those lines are designated which are especially suitable as standards.*

λ vac		Intensities					λ vac		Intensities				
obs.	calc.	Ne S.T.	He S.T.	Spark	st	Identification	obs.	calc.	Ne S.T.	He S.T.	Spark	st	Identification
896.504		1	—			$a^6D_{3\frac{1}{2}} - 29_{3\frac{1}{2}}{}^0$	1128.530			10h			$a^6S_{2\frac{1}{2}} - 29_{3\frac{1}{2}}{}^0$
898.776		0	—			$a^6D_{2\frac{1}{2}} - 29_{2\frac{1}{2}}{}^0$	1128.909			20			$a^4D_{3\frac{1}{2}} - 3_{3\frac{1}{2}}{}^0$
900.360		5	—			$a^6D_{1\frac{1}{2}} - 29_{1\frac{1}{2}}{}^0$	1129.777			12			$a^4F_{4\frac{1}{2}} - 6_{4\frac{1}{2}}{}^0$
918.118		—	1			$a^6D_{3\frac{1}{2}} - 28_{3\frac{1}{2}}{}^0$	1130.428			25b			$a^4D_{2\frac{1}{2}} - 2_{2\frac{1}{2}}{}^0$
919.095		—	0			$a^6D_{2\frac{1}{2}} - 28_{2\frac{1}{2}}{}^0$	1130.874			2			$a^4F_{4\frac{1}{2}} - 5_{4\frac{1}{2}}{}^0$
923.884		30	—			$a^6D_{4\frac{1}{2}} - 24_{3\frac{1}{2}}{}^0$	1133.413			25			$a^4F_{3\frac{1}{2}} - 11_{3\frac{1}{2}}{}^0$
924.970		15	—			$c^4D_{3\frac{1}{2}} - 27_{3\frac{1}{2}}{}^0$	1133.678			25			$a^4D_{3\frac{1}{2}} - 1_{3\frac{1}{2}}{}^0$
926.220		60	20			$a^6D_{4\frac{1}{2}} - 21_{4\frac{1}{2}}{}^0$	1138.039			5			$a^4F_{3\frac{1}{2}} - 5_{3\frac{1}{2}}{}^0$
926.618		10	—			$a^6D_{3\frac{1}{2}} - 27_{3\frac{1}{2}}{}^0$	1138.642			25			$a^4D_{2\frac{1}{2}} - 1_{2\frac{1}{2}}{}^0$
926.900		25	—			$a^6D_{4\frac{1}{2}} - 20_{3\frac{1}{2}}{}^0$	1142.334			25			$a^4D_{3\frac{1}{2}} - y^6F_{3\frac{1}{2}}{}^0$
927.176		30	2			$a^6D_{3\frac{1}{2}} - 24_{2\frac{1}{2}}{}^0$							$a^4D_{2\frac{1}{2}} - 1_{2\frac{1}{2}}{}^0$
927.632		8	—			$a^6D_{2\frac{1}{2}} - 27_{2\frac{1}{2}}{}^0$	1143.235			25			$a^4D_{3\frac{1}{2}} - y^6F_{4\frac{1}{2}}{}^0$
928.107		30	1			$a^6D_{4\frac{1}{2}} - 22_{3\frac{1}{2}}{}^0$	1144.946			35hb			$a^4D_{4\frac{1}{2}} - y^6F_{5\frac{1}{2}}{}^0$
928.470		20	—			$a^6D_{3\frac{1}{2}} - 25_{3\frac{1}{2}}{}^0$	1146.963			15			$a^4D_{3\frac{1}{2}} - y^6F_{3\frac{1}{2}}{}^0$
929.538		30	1			$a^6D_{3\frac{1}{2}} - 21_{3\frac{1}{2}}{}^0$	1147.413			25			$a^4D_{3\frac{1}{2}} - y^6F_{2\frac{1}{2}}{}^0$
929.612		30	—			$a^6D_{2\frac{1}{2}} - 24_{2\frac{1}{2}}{}^0$	1148.295			30			$a^4D_{2\frac{1}{2}} - y^6F_{3\frac{1}{2}}{}^0$
930.030		30	1			$a^6D_{3\frac{1}{2}} - 23_{3\frac{1}{2}}{}^0$	1150.292			20			$a^4D_{2\frac{1}{2}} - y^6F_{1\frac{1}{2}}{}^0$
930.165		30	1			$a^6D_{1\frac{1}{2}} - 25_{1\frac{1}{2}}{}^0$	1150.689			20			$a^4D_{1\frac{1}{2}} - y^6F_{2\frac{1}{2}}{}^0$
930.219		30				$a^6D_{2\frac{1}{2}} - 20_{2\frac{1}{2}}{}^0$	1151.163			25			$a^4D_{2\frac{1}{2}} - y^6F_{2\frac{1}{2}}{}^0$
930.558		30	—			$a^6D_{3\frac{1}{2}} - 22_{2\frac{1}{2}}{}^0$	1152.440			15			$a^6D_{4\frac{1}{2}} - y^6F_{5\frac{1}{2}}{}^0$
931.142		25	—			$a^6D_{2\frac{1}{2}} - 25_{2\frac{1}{2}}{}^0$	1152.882			20			$a^4D_{1\frac{1}{2}} - y^6F_{1\frac{1}{2}}{}^0$
931.709		10	—			$a^6D_{1\frac{1}{2}} - 23_{1\frac{1}{2}}{}^0$	1153.281			20			$a^4D_{1\frac{1}{2}} - y^6F_{2\frac{1}{2}}{}^0$
932.244		30	0			$a^6D_{2\frac{1}{2}} - 22_{2\frac{1}{2}}{}^0$	1153.955			15			$a^6D_{\frac{1}{2}} - y^6F_{1\frac{1}{2}}{}^0$
932.687		30	0			$a^6D_{1\frac{1}{2}} - 23_{1\frac{1}{2}}{}^0$	1154.401			20			$a^6D_{1\frac{1}{2}} - y^6F_{1\frac{1}{2}}{}^0$
						$a^4D_{2\frac{1}{2}} - 20_{2\frac{1}{2}}{}^0$	1156.575			2			$a^6S_{2\frac{1}{2}} - 28_{3\frac{1}{2}}{}^0$
935.783		0	—			$a^6D_{4\frac{1}{2}} - 16_{3\frac{1}{2}}{}^0$	1159.347			20			$a^4D_{2\frac{1}{2}} - 14_{2\frac{1}{2}}{}^0$
936.484		8	—			$a^6D_{3\frac{1}{2}} - 17_{2\frac{1}{2}}{}^0$	1162.351			2			$a^4D_{2\frac{1}{2}} - 13_{2\frac{1}{2}}{}^0$
938.967		10	—			$a^4F_{4\frac{1}{2}} - 26_{3\frac{1}{2}}{}^0$	1165.269			12			$a^4D_{2\frac{1}{2}} - 14_{3\frac{1}{2}}{}^0$
						$a^6D_{3\frac{1}{2}} - 17_{2\frac{1}{2}}{}^0$	1175.699			1			$a^6S_{2\frac{1}{2}} - 26_{3\frac{1}{2}}{}^0$
939.159		20	—			$a^6D_{2\frac{1}{2}} - 16_{2\frac{1}{2}}{}^0$							$a^6S_{2\frac{1}{2}} - 25_{3\frac{1}{2}}{}^0$
941.660		12	—			$a^6D_{3\frac{1}{2}} - 16_{3\frac{1}{2}}{}^0$	1213.149			20			$a^4D_{3\frac{1}{2}} - 6_{4\frac{1}{2}}{}^0$
942.589		5	—			$a^4F_{4\frac{1}{2}} - 21_{4\frac{1}{2}}{}^0$	1213.764			20			$a^4D_{3\frac{1}{2}} - 11_{3\frac{1}{2}}{}^0$
943.267		12	—			$a^4F_{4\frac{1}{2}} - 20_{3\frac{1}{2}}{}^0$	1214.409			10			$a^4D_{3\frac{1}{2}} - 5_{3\frac{1}{2}}{}^0$
943.910		15	—			$a^4F_{3\frac{1}{2}} - 27_{3\frac{1}{2}}{}^0$	1220.882			5			$a^4D_{3\frac{1}{2}} - 5_{3\frac{1}{2}}{}^0$
						$a^4F_{3\frac{1}{2}} - 26_{3\frac{1}{2}}{}^0$	1260.542			20			$a^4D_{4\frac{1}{2}} - z^6P_{3\frac{1}{2}}{}^0$
945.095		25	∞			$a^4F_{3\frac{1}{2}} - 24_{3\frac{1}{2}}{}^0$	1266.694			20			$a^4D_{3\frac{1}{2}} - z^6P_{2\frac{1}{2}}{}^0$
946.051		0	—			$a^4F_{3\frac{1}{2}} - 22_{2\frac{1}{2}}{}^0$	1267.437			25			$a^4D_{2\frac{1}{2}} - z^6P_{2\frac{1}{2}}{}^0$
947.564		1	—			$a^4F_{3\frac{1}{2}} - 26_{3\frac{1}{2}}{}^0$	1271.235			1			$a^4D_{2\frac{1}{2}} - z^6P_{1\frac{1}{2}}{}^0$
						$a^4F_{3\frac{1}{2}} - 21_{4\frac{1}{2}}{}^0$	1272.001			25b			$a^6D_{3\frac{1}{2}} - z^6P_{2\frac{1}{2}}{}^0$
952.470		10	—			$a^4F_{4\frac{1}{2}} - 16_{3\frac{1}{2}}{}^0$	1272.638			15			$a^6D_{2\frac{1}{2}} - z^6P_{1\frac{1}{2}}{}^0$
954.496		1	—			$a^4F_{3\frac{1}{2}} - 18_{3\frac{1}{2}}{}^0$	1275.154			15			$a^6D_{1\frac{1}{2}} - z^6P_{2\frac{1}{2}}{}^0$
954.786		2	—			$a^4F_{3\frac{1}{2}} - 17_{2\frac{1}{2}}{}^0$	1275.801			20			$a^6D_{1\frac{1}{2}} - z^6P_{1\frac{1}{2}}{}^0$
995.829		8	—			$a^4D_{2\frac{1}{2}} - 26_{3\frac{1}{2}}{}^0$	1290.204			15			$a^4P_{2\frac{1}{2}} - 10_{3\frac{1}{2}}{}^0$
999.003		1	—			$a^4D_{1\frac{1}{2}} - 27_{2\frac{1}{2}}{}^0$	1291.594			15			$a^4P_{2\frac{1}{2}} - 9_{2\frac{1}{2}}{}^0$
1000.183		2	—			$a^4D_{2\frac{1}{2}} - 26_{3\frac{1}{2}}{}^0$	1293.543			0			$a^4P_{1\frac{1}{2}} - 10_{2\frac{1}{2}}{}^0$
1000.665		1	—			$a^4D_{\frac{1}{2}} - 27_{1\frac{1}{2}}{}^0$	1294.914			12			$a^4P_{1\frac{1}{2}} - 9_{1\frac{1}{2}}{}^0$
						$a^4D_{2\frac{1}{2}} - 20_{2\frac{1}{2}}{}^0$	1296.088			20			$a^4P_{1\frac{1}{2}} - 8_{1\frac{1}{2}}{}^0$
1005.082		1	—			$a^4D_{2\frac{1}{2}} - 20_{3\frac{1}{2}}{}^0$	1298.815			2			$a^4P_{\frac{1}{2}} - 9_{1\frac{1}{2}}{}^0$
1007.657		20	—			$a^4D_{2\frac{1}{2}} - 18_{2\frac{1}{2}}{}^0$	1299.984			0			$a^4P_{\frac{1}{2}} - 8_{1\frac{1}{2}}{}^0$
1007.975		25	—			$a^4D_{2\frac{1}{2}} - 17_{2\frac{1}{2}}{}^0$	1459.311			15			$a^6S_{2\frac{1}{2}} - w^6P_{1\frac{1}{2}}{}^0$
1011.037		25	—			$a^4D_{2\frac{1}{2}} - 16_{2\frac{1}{2}}{}^0$	1465.043			20			$a^6S_{2\frac{1}{2}} - w^6P_{2\frac{1}{2}}{}^0$
1012.088		20	—			$a^4D_{2\frac{1}{2}} - 18_{2\frac{1}{2}}{}^0$	1473.834			20			$a^6S_{2\frac{1}{2}} - w^6P_{2\frac{1}{2}}{}^0$
1012.417		25	1			$a^4D_{2\frac{1}{2}} - 17_{2\frac{1}{2}}{}^0$	1476.054			10			$a^6S_{2\frac{1}{2}} - 11_{2\frac{1}{2}}{}^0$
1015.083		10	—			$a^4D_{1\frac{1}{2}} - 18_{2\frac{1}{2}}{}^0$	1541.011		1	0			$a^6S_{2\frac{1}{2}} - 1_{2\frac{1}{2}}{}^0$
1015.520		20	—			$a^4D_{2\frac{1}{2}} - 16_{2\frac{1}{2}}{}^0$	1550.260	0.273	—	1	—	3	$a^4F_{4\frac{1}{2}} - x^4F_{3\frac{1}{2}}{}^0$
1038.370			1			$a^4P_{2\frac{1}{2}} - 28_{3\frac{1}{2}}{}^0$	1558.543	.538	8	10	—		$a^4F_{3\frac{1}{2}} - y^2D_{2\frac{1}{2}}{}^0$??
1055.269			25			$a^4D_{4\frac{1}{2}} - 15_{3\frac{1}{2}}{}^0$	1558.706	.691	8	10	—		$a^4F_{3\frac{1}{2}} - y^2D_{1\frac{1}{2}}{}^0$??
1059.571			20			$a^6D_{4\frac{1}{2}} - 15_{3\frac{1}{2}}{}^0$	1559.106	.084	25	20	2	3	$a^4F_{4\frac{1}{2}} - x^4F_{4\frac{1}{2}}{}^0$
1062.758			20			$a^6D_{3\frac{1}{2}} - 15_{3\frac{1}{2}}{}^0$	1563.790	.788	25	25	2	3	$a^4F_{3\frac{1}{2}} - x^4F_{3\frac{1}{2}}{}^0$
1063.982			15			$a^6D_{4\frac{1}{2}} - 13_{3\frac{1}{2}}{}^0$	1566.825	.821	20	20	1	3	$a^4F_{4\frac{1}{2}} - x^4G_{4\frac{1}{2}}{}^0$
1068.356			30			$a^6D_{3\frac{1}{2}} - 13_{3\frac{1}{2}}{}^0$	1568.031	.017	5	8	—	3	$a^4F_{3\frac{1}{2}} - x^4F_{3\frac{1}{2}}{}^0$
1069.038			15			$a^6D_{2\frac{1}{2}} - 14_{2\frac{1}{2}}{}^0$	1569.670	.674	10	12	—	3	$a^4F_{4\frac{1}{2}} - x^4G_{5\frac{1}{2}}{}^0$
1071.260			5			$a^6D_{1\frac{1}{2}} - 14_{2\frac{1}{2}}{}^0$	1570.248	.244	20	20	1	3	$a^4F_{3\frac{1}{2}} - x^4F_{2\frac{1}{2}}{}^0$
1071.596			30			$a^6D_{2\frac{1}{2}} - 13_{2\frac{1}{2}}{}^0$	1572.750	.754	3	1	—	3	$a^4F_{3\frac{1}{2}} - x^4F_{4\frac{1}{2}}{}^0$
1076.556			2			$a^4F_{4\frac{1}{2}} - 15_{3\frac{1}{2}}{}^0$	1573.831	.826	2	3	—	3	$a^4F_{3\frac{1}{2}} - x^4F_{3\frac{1}{2}}{}^0$
1096.616			20			$a^6D_{4\frac{1}{2}} - w^6P_{3\frac{1}{2}}{}^0$	1574.778	.769	0	0	—	3	$a^4F_{3\frac{1}{2}} - x^4G_{3\frac{1}{2}}{}^0$
1096.793p			20			$a^6D_{3\frac{1}{2}} - w^6P_{2\frac{1}{2}}{}^0$	1574.931	.921	20	20	1	3	$a^4F_{2\frac{1}{2}} - x^4F_{1\frac{1}{2}}{}^0$
1096.886p			30			$a^6D_{4\frac{1}{2}} - w^6P_{3\frac{1}{2}}{}^0$	1577.158	.167	1	1	—	3	$a^4F_{1\frac{1}{2}} - x^4F_{2\frac{1}{2}}{}^0$
1097.782			2			$a^4F_{3\frac{1}{2}} - 14_{3\frac{1}{2}}{}^0$	1580.635	.627	20	25b	1		$a^4F_{3\frac{1}{2}} - x^4G_{4\frac{1}{2}}{}^0$
1099.117			25h			$a^4D_{1\frac{1}{2}} - w^6P_{1\frac{1}{2}}{}^0$	1581.293	.268	20	8	—		$a^4F_{3\frac{1}{2}} - x^4G_{3\frac{1}{2}}{}^0$
1100.026			20			$a^6D_{2\frac{1}{2}} - w^6P_{2\frac{1}{2}}{}^0$	1584.954	.949	20	15	1	3	$a^4F_{3\frac{1}{2}} - x^4G_{3\frac{1}{2}}{}^0$
1100.525p			20			$a^6D_{\frac{1}{2}} - w^6P_{1\frac{1}{2}}{}^0$	1588.295	.288	8	10	1		$a^4F_{1\frac{1}{2}} - x^4G_{2\frac{1}{2}}{}^0$
1101.538			20			$a^6D_{3\frac{1}{2}} - w^6P_{2\frac{1}{2}}{}^0$	1608.446		40	35	15		$a^6D_{4\frac{1}{2}} - y^6P_{3\frac{1}{2}}{}^0$
1102.385			8			$a^6D_{1\frac{1}{2}} - w^6P_{2\frac{1}{2}}{}^0$	1610.933	.922	8	15h	1		$a^4F_{4\frac{1}{2}} - y^6G_{5\frac{1}{2}}{}^0$
1102.758			1			$a^6D_{2\frac{1}{2}} - 11_{2\frac{1}{2}}{}^0$	1612.814	.803	20	20	8	3	$a^4F_{4\frac{1}{2}} - y^6G_{5\frac{1}{2}}{}^0$
1104.978			1			$a^6D_{2\frac{1}{2}} - w^6P_{2\frac{1}{2}}{}^0$	1618.464		25	25	2		$a^6D_{3\frac{1}{2}} - y^6P_{3\frac{1}{2}}{}^0$
1106.215			15			$a^6D_{2\frac{1}{2}} - 11_{2\frac{1}{2}}{}^0$	1621.685		30	30	10		$a^6D_{3\frac{1}{2}} - y^6P_{2\frac{1}{2}}{}^0$
1106.362			5			$a^6D_{4\frac{1}{2}} - 6_{4\frac{1}{2}}{}^0$	1623.102	.090	8	8	1	3	$a^4F_{3\frac{1}{2}} - y^6G_{3\frac{1}{2}}{}^0$
1111.114			15			$a^6D_{3\frac{1}{2}} - 6_{4\frac{1}{2}}{}^0$	1625.525	.520	15	20	8	3	$a^4F_{4\frac{1}{2}} - y^6G_{4\frac{1}{2}}{}^0$
1121.987			25			$a^6D_{4\frac{1}{2}} - 2_{3\frac{1}{2}}{}^0$	1625.919		12	15	—		$a^6D_{3\frac{1}{2}} - y^6P_{3\frac{1}{2}}{}^0$
1122.858			25			$a^6D_{3\frac{1}{2}} - 3_{3\frac{1}{2}}{}^0$	1629.155		25	30	8		$a^6D_{3\frac{1}{2}} - y^6P_{3\frac{1}{2}}{}^0$
1124.134			20			$a^6D_{2\frac{1}{2}} - 4_{3\frac{1}{2}}{}^0$	1631.124		25	30	2		$a^6D_{2\frac{1}{2}} - y^6P_{2\frac{1}{2}}{}^0$
1126.425			20			$a^6D_{2\frac{1}{2}} - 3_{3\frac{1}{2}}{}^0$	1632.672	.665	2	1	—	3	$a^4F_{3\frac{1}{2}} - y^6G_{3\frac{1}{2}}{}^0$
1126.603			20			$a^6D_{1\frac{1}{2}} - 4_{2\frac{1}{2}}{}^0$	1633.907	.906	15	15	2	3	$a^4F_{3\frac{1}{2}} - y^6G_{3\frac{1}{2}}{}^0$
1126.850			20			$a^6D_{2\frac{1}{2}} - 2_{2\frac{1}{2}}{}^0$	1634.353		20	20	1		$a^6D_{1\frac{1}{2}} - y^6P_{2\frac{1}{2}}{}^0$
1128.074			25b			$a^6D_{\frac{1}{2}} - 4_{1\frac{1}{2}}{}^0$	1635.389		25	35	15		$a^6D_{2\frac{1}{2}} - z^6P_{2\frac{1}{2}}{}^0$
1128.180			5			$a^4F_{4\frac{1}{2}} - 11_{3\frac{1}{2}}{}^0$	1636.334		25	30	5		$a^6D_{1\frac{1}{2}} - y^6P_{1\frac{1}{2}}{}^0$

TABLE VII.—*Continued.*

λ VAC		INTENSITIES					λ VAC		INTENSITIES				
OBS	CALC	Ne S.T.	He S.T.	SPARK	*st*	IDENTIFICATION	OBS	CALC	Ne S.T.	He S.T.	SPARK	*st*	IDENTIFICATION
1637.400	0.398	20	15	2	*s*	$a^4F_{4\frac{1}{2}} - x^4D_{3\frac{1}{2}}^0$	1904.784	.785		15	5	*s*	$a^2D_{2\frac{1}{2}} - x^2F_{2\frac{1}{2}}^0$
1639.403		25	30	2		$a^6D_{\frac{1}{2}} - y^6P_{1\frac{1}{2}}^0$	1910.150	.147		1	—		$a^4H_{6\frac{1}{2}} - w^6H_{4\frac{1}{2}}^0$?
1640.167	.150	12	12	2	*s*	$a^4F_{1\frac{1}{2}} - y^4G_{2\frac{1}{2}}^0$	1917.337	.321		15*b*	8*b*		$a^2G_{4\frac{1}{2}} - y^2H_{4\frac{1}{2}}^0$
1641.761		20	25	8		$a^4D_{3\frac{1}{2}} - x^6P_{3\frac{1}{2}}^0$	1918.114	.100		2	—		$c^2D_{2\frac{1}{2}} - w^4D_{2\frac{1}{2}}^0$
1643.588	.576	15	15	2	*s*	$a^4F_{3\frac{1}{2}} - x^4D_{2\frac{1}{2}}^0$	1922.234	.268		0	—		$a^4H_{4\frac{1}{2}} - w^6H_{4\frac{1}{2}}^0$?
1646.187		10	20	1		$a^4D_{1\frac{1}{2}} - x^4P_{1\frac{1}{2}}^0$	1922.797	.794		20*b*	30*b*		$a^2D_{2\frac{1}{2}} - w^4D_{2\frac{1}{2}}^0$
1647.161		10	25	1		$a^4D_{2\frac{1}{2}} - x^6P_{2\frac{1}{2}}^0$	1925.987	.986		20*b*	25*b*		$a^2H_{5\frac{1}{2}} - x^2H_{4\frac{1}{2}}^0$
1649.444	.423	12	15*b*	1		$a^4F_{3\frac{1}{2}} - x^4D_{4\frac{1}{2}}^0$	1927.481	.485		1*hb*	—		$a^2D_{1\frac{1}{2}} - y^2P_{1\frac{1}{2}}^0$
1649.583		12	20	1		$a^4D_{1\frac{1}{2}} - x^6P_{1\frac{1}{2}}^0$		.548					$a^2D_{1\frac{1}{2}} - y^2P_{\frac{1}{2}}^0$
1650.709		15	20	1		$a^4D_{\frac{1}{2}} - x^4P_{\frac{1}{2}}^0$	1929.194	.191		1	—		$a^2D_{2\frac{1}{2}} - w^4F_{3\frac{1}{2}}^0$?
1652.489	.482	1	0	—	*s*	$a^4F_{2\frac{1}{2}} - x^4D_{2\frac{1}{2}}^0$	1932.477	.483		15	2		$a^2D_{1\frac{1}{2}} - x^2F_{2\frac{1}{2}}^0$
1654.105		20*b*	5	—		$a^4D_{\frac{1}{2}} - x^4P_{1\frac{1}{2}}^0$	1935.296	.297		15	2		$a^2G_{4\frac{1}{2}} - y^2H_{5\frac{1}{2}}^0$
1654.484	.476	10	5	1	*s*	$a^4F_{1\frac{1}{2}} - x^4D_{\frac{1}{2}}^0$	1936.781	.805		20*b*	1*b*		$a^2G_{3\frac{1}{2}} - y^2H_{4\frac{1}{2}}^0$
1655.042		—	1	—		$a^4D_{1\frac{1}{2}} - x^4P_{2\frac{1}{2}}^0$	1938.899	.899		8*b*	25*b*		$b^4F_{1\frac{1}{2}} - x^2D_{2\frac{1}{2}}^0$?
1658.785	.771	10	15	2	*s*	$a^4F_{4\frac{1}{2}} - y^4F_{4\frac{1}{2}}^0$	1948.372	.383		10*b*	5		$a^2H_{4\frac{1}{2}} - x^2H_{4\frac{1}{2}}^0$
1659.487	.479	20	20	10	*s*	$a^4F_{2\frac{1}{2}} - y^4D_{2\frac{1}{2}}^0$	1958.121	.086		5	—		$a^4H_{4\frac{1}{2}} - w^4D_{2\frac{1}{2}}^0$?
1662.369	.357	—	0	—		$a^4F_{1\frac{1}{2}} - x^4D_{2\frac{1}{2}}^0$		.135					$a^4H_{4\frac{1}{2}} - w^4F_{4\frac{1}{2}}^0$?
1663.226	.220	15	15	2	*s*	$a^4F_{2\frac{1}{2}} - y^4D_{1\frac{1}{2}}^0$	1963.110	.093		25*b*	—		$a^4H_{3\frac{1}{2}} - w^4D_{2\frac{1}{2}}^0$?
1670.759	.746	20	25	20		$a^4F_{4\frac{1}{2}} - y^4D_{3\frac{1}{2}}^0$		.142					$a^4H_{3\frac{1}{2}} - w^4F_{4\frac{1}{2}}^0$?
	.787					$a^4F_{3\frac{1}{2}} - y^4D_{2\frac{1}{2}}^0$	1964.330	.339		12	—		$a^4H_{3\frac{1}{2}} - w^4D_{2\frac{1}{2}}^0$?
1671.010	70.990	0	1	—	*s*	$a^4F_{1\frac{1}{2}} - y^4D_{1\frac{1}{2}}^0$	1975.542	.547		1	1		$a^2G_{4\frac{1}{2}} - y^4H_{5\frac{1}{2}}^0$
1673.470	.466	15	15	15		$a^2G_{4\frac{1}{2}} - w^2F_{3\frac{1}{2}}^0$?	1993.289	.298		8*b*	15*b*		$a^2G_{4\frac{1}{2}} - x^4F_{4\frac{1}{2}}^0$
1674.258	.254	10	2	1	*s*	$a^4F_{2\frac{1}{2}} - y^4F_{4\frac{1}{2}}^0$	1994.857	.908		20	1*h*		$b^2P_{1\frac{1}{2}} - w^2F_{2\frac{1}{2}}^0$?
1676.871	.854	1	1	—	*s*	$a^4F_{2\frac{1}{2}} - y^4F_{3\frac{1}{2}}^0$	1999.430	.411		10	25		$b^4F_{4\frac{1}{2}} - w^4D_{4\frac{1}{2}}^0$
1679.388	.379	8	15	10		$a^2G_{3\frac{1}{2}} - w^2F_{2\frac{1}{2}}^0$		.462					$b^4F_{4\frac{1}{2}} - w^4F_{4\frac{1}{2}}^0$
1685.953	.952	8	5	1	*s*	$a^4F_{3\frac{1}{2}} - y^4F_{3\frac{1}{2}}^0$	1999.727	.681		1	1		$a^2G_{3\frac{1}{2}} - x^4F_{3\frac{1}{2}}^0$?
1686.457	.454	2	8	1	*s*	$a^4F_{3\frac{1}{2}} - y^4D_{3\frac{1}{2}}^0$		.730					$a^2D_{2\frac{1}{2}} - x^2G_{3\frac{1}{2}}^0$
1686.717	.690	1	2	—		$a^4F_{2\frac{1}{2}} - x^2D_{1\frac{1}{2}}^0$?	2001.019	.025		30	30	*s*	$a^2H_{5\frac{1}{2}} - x^2G_{4\frac{1}{2}}^0$
1689.821	.832	2	10*b*	—		$a^4P_{2\frac{1}{2}} - w^4D_{2\frac{1}{2}}^0$	2004.533	.556		2	—	*s*	$a^4P_{1\frac{1}{2}} - x^4D_{\frac{1}{2}}^0$
1690.781	.755	2	8	—		$a^4P_{2\frac{1}{2}} - w^4D_{2\frac{1}{2}}^0$	2007.665	.658		12	5		$b^4F_{3\frac{1}{2}} - w^4D_{3\frac{1}{2}}^0$
1691.289	.272	5	8	1	*s*	$a^4F_{1\frac{1}{2}} - y^4F_{1\frac{1}{2}}^0$	2008.105	.088		15*b*	2		$a^4P_{3\frac{1}{2}} - x^4D_{3\frac{1}{2}}^0$
1693.477	.475	0	0	—	*s*	$a^4P_{2\frac{1}{2}} - w^4D_{1\frac{1}{2}}^0$	2008.364	.356		12	5	*s*	$a^4P_{1\frac{1}{2}} - x^4D_{1\frac{1}{2}}^0$
1693.961	.935	—	0	—	*s*	$a^4F_{1\frac{1}{2}} - y^4F_{2\frac{1}{2}}^0$	2011.341	.348		25	30	*s*	$a^2H_{4\frac{1}{2}} - x^2G_{3\frac{1}{2}}^0$
1696.800	0.794	2	8	—	*s*	$a^4F_{4\frac{1}{2}} - x^6G_{4\frac{1}{2}}^0$	2011.635	.602		0	1		$a^2G_{4\frac{1}{2}} - x^2H_{4\frac{1}{2}}^0$
1698.190	.134	—	0	—		$a^6F_{2\frac{1}{2}} - y^4D_{2\frac{1}{2}}^0$?	2013.921	.908		15	5	*s*	$a^4P_{\frac{1}{2}} - x^4D_{\frac{1}{2}}^0$
1699.199	.195	1	2	—	*s*	$a^4P_{1\frac{1}{2}} - w^4D_{1\frac{1}{2}}^0$	2014.318	.365		1*b*	1		$a^2G_{3\frac{1}{2}} - x^4F_{4\frac{1}{2}}^0$?
1701.952	.938	1	2	—		$a^4P_{1\frac{1}{2}} - w^4D_{\frac{1}{2}}^0$	2016.154	.136		20	20	*s*	$a^4P_{1\frac{1}{2}} - x^4D_{2\frac{1}{2}}^0$
1702.045	.044	25	25	25	*s*	$a^4F_{4\frac{1}{2}} - x^6G_{4\frac{1}{2}}^0$	2016.746	.728		10	1	*s*	$b^4F_{2\frac{1}{2}} - w^4D_{1\frac{1}{2}}^0$
1706.179	.144	—	1	—		$a^4F_{3\frac{1}{2}} - x^6G_{3\frac{1}{2}}^0$	2017.744	.743		15	5	*s*	$a^4P_{\frac{1}{2}} - x^4D_{1\frac{1}{2}}^0$
1708.627	.621	8	8	2		$a^4F_{3\frac{1}{2}} - x^6G_{3\frac{1}{2}}^0$	2018.509	.496		2	1	*s*	$b^4F_{3\frac{1}{2}} - w^4F_{2\frac{1}{2}}^0$
	.675					$a^4P_{\frac{1}{2}} - w^4D_{\frac{1}{2}}^0$	2019.427	.429		25	25		$a^2G_{4\frac{1}{2}} - x^2H_{4\frac{1}{2}}^0$
1709.560	.551	—	0	—	*s*	$a^4F_{2\frac{1}{2}} - y^4P_{1\frac{1}{2}}^0$	2021.394	.399		25	25	*s*	$a^4P_{2\frac{1}{2}} - x^4D_{3\frac{1}{2}}^0$
1713.002	2.998	25	20	25	*s*	$a^4F_{3\frac{1}{2}} - x^6G_{4\frac{1}{2}}^0$	2024.370	.355		1	—		$b^4F_{1\frac{1}{2}} - w^4D_{\frac{1}{2}}^0$
1716.569	.576		2	0		$a^4F_{2\frac{1}{2}} - x^2D_{2\frac{1}{2}}^0$?	2028.434	.427		5	1	*s*	$b^4F_{2\frac{1}{2}} - w^4F_{2\frac{1}{2}}^0$
1718.123	.100		2	—	*s*	$a^4F_{3\frac{1}{2}} - x^6G_{3\frac{1}{2}}^0$	2029.838	.839		8	2		$a^2G_{4\frac{1}{2}} - y^6G_{5\frac{1}{2}}^0$
1720.621	.611		20	20	*s*	$a^4F_{3\frac{1}{2}} - x^6G_{3\frac{1}{2}}^0$	2033.064	.060		25	25		$a^2G_{3\frac{1}{2}} - x^2H_{4\frac{1}{2}}^0$
1724.847	.853		8	1		$a^4F_{1\frac{1}{2}} - x^2D_{2\frac{1}{2}}^0$	2035.118	.091		1	—		$b^4F_{1\frac{1}{2}} - w^4F_{1\frac{1}{2}}^0$
1724.963	.962		8	1	*s*	$a^4F_{3\frac{1}{2}} - y^4P_{2\frac{1}{2}}^0$	2037.093	.089		20	25	*s*	$a^2D_{2\frac{1}{2}} - y^2F_{3\frac{1}{2}}^0$
1726.394	.391		12	8	*s*	$a^4F_{1\frac{1}{2}} - x^6G_{2\frac{1}{2}}^0$	2038.506	.429		0	—		$a^4P_{\frac{1}{2}} - y^4D_{1\frac{1}{2}}^0$?
1731.364	.337		1	—		$a^6G_{4\frac{1}{2}} - w^6H_{5\frac{1}{2}}^0$	2040.164	.119		2	*m*		$a^4P_{1\frac{1}{2}} - y^4D_{2\frac{1}{2}}^0$
1749.136	.120		1	—		$a^6G_{4\frac{1}{2}} - x^2F_{3\frac{1}{2}}^0$	2041.345	.346		25	35		$a^4G_{4\frac{1}{2}} - y^4G_{4\frac{1}{2}}^0$
1764.118	.117		1	—		$a^6G_{3\frac{1}{2}} - x^2F_{3\frac{1}{2}}^0$	2049.152	.146		5	1		$a^2H_{4\frac{1}{2}} - y^2F_{3\frac{1}{2}}^0$
1765.325	.320		0	—		$a^6G_{2\frac{1}{2}} - x^2F_{2\frac{1}{2}}^0$	2051.688	.689		25	30		$a^2G_{3\frac{1}{2}} - y^2G_{3\frac{1}{2}}^0$
1772.518	.512		15	20		$a^6G_{4\frac{1}{2}} - x^2H_{4\frac{1}{2}}^0$	2055.931	.922		20	20	*s*	$a^2P_{1\frac{1}{2}} - y^2D_{2\frac{1}{2}}^0$
1776.661	.649		1	—		$a^6G_{4\frac{1}{2}} - x^2H_{4\frac{1}{2}}^0$	2057.993	.988		12	2	*s*	$a^4P_{2\frac{1}{2}} - y^4F_{3\frac{1}{2}}^0$
1781.529	.508		1	—		$a^4P_{2\frac{1}{2}} - y^2F_{3\frac{1}{2}}^0$?	2058.762	.826		0	—		$a^4P_{1\frac{1}{2}} - y^4F_{1\frac{1}{2}}^0$?
1785.262			40	30		$a^6S_{2\frac{1}{2}} - x^6F_{3\frac{1}{2}}^0$	2062.747*p*	.774		0	—		$a^4P_{1\frac{1}{2}} - y^4F_{2\frac{1}{2}}^0$
1786.448	.437		1	—		$a^4P_{1\frac{1}{2}} - y^2F_{2\frac{1}{2}}^0$?	2064.335	.336		25*hb*	20		$a^6G_{4\frac{1}{2}} - x^2F_{3\frac{1}{2}}^0$
1786.738			40	30		$a^6S_{2\frac{1}{2}} - x^6P_{2\frac{1}{2}}^0$	2066.668	.666		15	8		$a^2P_{\frac{1}{2}} - y^2D_{1\frac{1}{2}}^0$
1787.997*p*			35	25		$a^6S_{2\frac{1}{2}} - x^6P_{1\frac{1}{2}}^0$	2068.580	.575		20	20		$a^2D_{1\frac{1}{2}} - y^2F_{2\frac{1}{2}}^0$
1793.371	.366		10	20		$a^6G_{5\frac{1}{2}} - x^2H_{4\frac{1}{2}}^0$	2070.616	.615		10*b*	1		$a^2F_{2\frac{1}{2}} - w^2F_{2\frac{1}{2}}^0$
1815.406	.411		0	1	*s*	$a^2D_{2\frac{1}{2}} - w^2F_{3\frac{1}{2}}^0$	2070.994	.994		8	2	*s*	$a^2F_{3\frac{1}{2}} - w^2F_{3\frac{1}{2}}^0$
1818.509	.516		2	1	*s*	$a^2D_{2\frac{1}{2}} - x^4D_{2\frac{1}{2}}^0$	2072.485	.449		10	2		$a^2P_{1\frac{1}{2}} - x^4F_{1\frac{1}{2}}^0$
1822.150	.120		1	0*h*		$a^4D_{2\frac{1}{2}} - x^4D_{2\frac{1}{2}}^0$		.468					$a^4P_{2\frac{1}{2}} - y^4D_{2\frac{1}{2}}^0$
	.188					$a^4D_{1\frac{1}{2}} - x^4D_{\frac{1}{2}}^0$	2074.860	.850		8*b*	2		$a^6G_{4\frac{1}{2}} - y^6G_{5\frac{1}{2}}^0$
1823.888	.869		1	1		$a^2P_{1\frac{1}{2}} - y^2P_{1\frac{1}{2}}^0$	2076.348	.340		5	1	*s*	$a^2P_{1\frac{1}{2}} - x^2F_{2\frac{1}{2}}^0$
	.925					$a^2P_{1\frac{1}{2}} - y^2P_{\frac{1}{2}}^0$	2078.829	.824		8	5		$a^6G_{4\frac{1}{2}} - y^6G_{4\frac{1}{2}}^0$
1826.991	.994		1	1	*s*	$a^4D_{3\frac{1}{2}} - y^4D_{3\frac{1}{2}}^0$	2080.912	.902		20	20		$a^6G_{3\frac{1}{2}} - x^2F_{3\frac{1}{2}}^0$
1831.261	.263		1	1		$a^2D_{1\frac{1}{2}} - w^2F_{2\frac{1}{2}}^0$	2084.178	.178		0*b*	10*b*		$a^2F_{3\frac{1}{2}} - w^2F_{3\frac{1}{2}}^0$
1831.724	.751		1	—		$a^6D_{\frac{1}{2}} - x^4D_{\frac{1}{2}}^0$	2086.939	.940		0	—		$a^2G_{4\frac{1}{2}} - x^2F_{3\frac{1}{2}}^0$
1833.071	.073		0	—	*s*	$a^4D_{2\frac{1}{2}} - x^4D_{2\frac{1}{2}}^0$	2088.194	.205		25	25		$a^2P_{1\frac{1}{2}} - x^2S_{\frac{1}{2}}^0$
1835.869	.872		15	10		$a^6G_{4\frac{1}{2}} - x^6G_{4\frac{1}{2}}^0$	2095.310	.294		1	1		$a^2P_{\frac{1}{2}} - x^4F_{1\frac{1}{2}}^0$
1841.701	.687		10*h*	1		$a^4D_{2\frac{1}{2}} - y^4D_{2\frac{1}{2}}^0$?	2095.654	.640		2	1		$a^2G_{4\frac{1}{2}} - y^4G_{5\frac{1}{2}}^0$
1842.256	.238		0	—	*s*	$a^4D_{1\frac{1}{2}} - y^4D_{1\frac{1}{2}}^0$		.659					$a^2P_{1\frac{1}{2}} - x^6G_{2\frac{1}{2}}^0$
1846.581	.574		12	2		$a^6G_{3\frac{1}{2}} - x^6G_{3\frac{1}{2}}^0$	2097.659	.686		0*b*	0*b*		$a^6G_{2\frac{1}{2}} - y^6G_{3\frac{1}{2}}^0$
1848.768	.771		12	2	*s*	$a^2D_{2\frac{1}{2}} - x^2D_{2\frac{1}{2}}^0$	2098.181	.175		25*b*	25*b*		$a^2H_{5\frac{1}{2}} - y^2H_{4\frac{1}{2}}^0$
1851.517	.526		1	—	*s*	$a^4D_{1\frac{1}{2}} - y^4D_{2\frac{1}{2}}^0$		.213					$a^4P_{1\frac{1}{2}} - y^4P_{1\frac{1}{2}}^0$
1859.744	.744		15	10	*s*	$a^4D_{2\frac{1}{2}} - y^4D_{2\frac{1}{2}}^0$	2101.633	.673		5*h*	5		$b^2H_{5\frac{1}{2}} - w^2H_{4\frac{1}{2}}^0$
1860.040	.052		20	20		$a^6G_{4\frac{1}{2}} - y^6F_{3\frac{1}{2}}^0$	2102.363	.368		1	—	*s*	$b^2P_{\frac{1}{2}} - x^2D_{1\frac{1}{2}}^0$
1874.931	.970		0	—		$a^4D_{2\frac{1}{2}} - y^4D_{1\frac{1}{2}}^0$	2108.226	.222		10	10		$b^2H_{5\frac{1}{2}} - w^2H_{4\frac{1}{2}}^0$
1876.173	.212		8*h*	—		$a^2D_{1\frac{1}{2}} - x^2D_{2\frac{1}{2}}^0$	2108.529	.461		1	—		$a^4P_{\frac{1}{2}} - y^4P_{1\frac{1}{2}}^0$?
1876.835	.836		15	10		$a^2G_{4\frac{1}{2}} - y^4F_{3\frac{1}{2}}^0$	2109.613	.635		25	—		$b^2P_{1\frac{1}{2}} - y^2P_{1\frac{1}{2}}^0$
1877.462	.470		20	20		$a^2H_{5\frac{1}{2}} - w^2H_{5\frac{1}{2}}^0$	2109.768	.711		10	15		$b^2P_{1\frac{1}{2}} - y^2P_{\frac{1}{2}}^0$
1880.046	.050		2	0		$a^2D_{1\frac{1}{2}} - x^2D_{1\frac{1}{2}}^0$		.770					$b^2H_{4\frac{1}{2}} - w^2H_{4\frac{1}{2}}^0$
1888.729	.734		20	25		$a^2H_{4\frac{1}{2}} - w^2H_{4\frac{1}{2}}^0$	2111.396	.401		15	20		$a^2P_{\frac{1}{2}} - x^2S_{\frac{1}{2}}^0$
1894.006	.022		10*b*	25*b*		$a^2H_{4\frac{1}{2}} - w^2H_{5\frac{1}{2}}^0$	2117.633	.665		25*b*	15		$a^4G_{4\frac{1}{2}} - w^4F_{4\frac{1}{2}}^0$
1898.538	.535		10	2	*s*	$a^2D_{2\frac{1}{2}} - y^6P_{1\frac{1}{2}}^0$	2118.868	.869		8	2	*s*	$a^2H_{4\frac{1}{2}} - y^2H_{4\frac{1}{2}}^0$
1903.370	.384		1	—	*s*	$a^2D_{2\frac{1}{2}} - x^2F_{3\frac{1}{2}}^0$	2119.723	.721		12	8	*s*	$a^2H_{5\frac{1}{2}} - y^2H_{4\frac{1}{2}}^0$

TABLE VII.—*Continued.*

λ vac		Intensities					λ vac		Intensities				
obs	calc	Ne S.T.	He S.T.	Spark	st	Identification	obs	calc	Ne S.T.	He S.T.	Spark	st	Identification
2123.126	.124		0b	—		$a^5G_{4\frac{1}{2}} - x^4D_{3\frac{1}{2}}^0$	2211.643	.607		5	—		$a^5H_{4\frac{1}{2}} - z^5H_{4\frac{1}{2}}^0$
2130.934	.926		15	5	s	$a^5F_{3\frac{1}{2}} - y^4F_{3\frac{1}{2}}^0$		.692					$a^5D_{4\frac{1}{2}} - x^4F_{3\frac{1}{2}}^0$?
2133.213	.208		2	—		$a^5F_{2\frac{1}{2}} - x^5D_{1\frac{1}{2}}^0$?	2211.803	.784		5	1		$b^5G_{4\frac{1}{2}} - w^5F_{3\frac{1}{2}}^0$
2134.666	.685		8b	1h		$a^5G_{4\frac{1}{2}} - w^4F_{4\frac{1}{2}}^0$		.800					$a^5H_{4\frac{1}{2}} - y^4H_{4\frac{1}{2}}^0$
2135.268	.245		2	—		$a^5G_{3\frac{1}{2}} - x^5H_{4\frac{1}{2}}^0$	2214.371	.342		20	25		$a^5H_{3\frac{1}{2}} - y^4H_{3\frac{1}{2}}^0$
	.292					$b^3P_{1\frac{1}{2}} - w^4D_{2\frac{1}{2}}^0$		.409					$a^5H_{2\frac{1}{2}} - y^4H_{2\frac{1}{2}}^0$
2138.412	.419		15b	—		$a^5D_{1\frac{1}{2}} - z^5P_{1\frac{1}{2}}^0$	2214.751			20	10h		$z^5D_{2\frac{1}{2}}^0 - 32_{2\frac{1}{2}}$
2138.780	.723		20	0		$a^3D_{2\frac{1}{2}} - y^5D_{1\frac{1}{2}}^0$?	2215.786			10	2h		$z^5D_{3\frac{1}{2}}^0 - 33_{1\frac{1}{2}}$
2140.353	.311		25b	1		$a^5D_{2\frac{1}{2}} - z^5P_{1\frac{1}{2}}^0$	2216.420			4	1h		$z^5D_{1\frac{1}{2}}^0 - 34_{\frac{1}{2}}$
2141.289	.252		1	—		$a^5G_{4\frac{1}{2}} - x^5H_{4\frac{1}{2}}^0$	2218.982			30	10h		$z^5D_{2\frac{1}{2}}^0 - 31_{2\frac{1}{2}}$
2146.736	.720		10b	2b		$a^5D_{3\frac{1}{2}} - z^5P_{2\frac{1}{2}}^0$	2220.582	.584		20	15	s	$a^5H_{4\frac{1}{2}} - y^4H_{3\frac{1}{2}}^0$
2147.049	.041		1	1		$a^3G_{3\frac{1}{2}} - x^4D_{2\frac{1}{2}}^0$	2221.081	.072		25	25	s	$a^5H_{4\frac{1}{2}} - z^5H_{3\frac{1}{2}}^0$
2148.398	.373		15	20		$a^5G_{4\frac{1}{2}} - w^4F_{3\frac{1}{2}}^0$	2221.146			6	—		$z^5D_{1\frac{1}{2}}^0 - 34_{\frac{1}{2}}$
2151.297	.294		20b	25		$a^3D_{2\frac{1}{2}} - y^5D_{2\frac{1}{2}}^0$	2223.373			1	—		$z^5D_{1\frac{1}{2}}^0 - 33_{1\frac{1}{2}}$
2151.441	.443		10	1		$b^3H_{4\frac{1}{2}} - w^4F_{4\frac{1}{2}}^0$	2224.560			2			$z^5D_{2\frac{1}{2}}^0 - 32_{2\frac{1}{2}}$
2151.774	.765		25	8	s	$a^3P_{1\frac{1}{2}} - z^3P_{1\frac{1}{2}}^0$	2228.164			4			$z^5D_{\frac{1}{2}}^0 - 33_{1\frac{1}{2}}$
2153.053	.044		12	10	s	$a^3P_{1\frac{1}{2}} - z^3P_{\frac{1}{2}}^0$	2229.456			30			$z^5D_{3\frac{1}{2}}^0 - 30_{3\frac{1}{2}}$
2154.554	.578		1	—		$a^5D_{\frac{1}{2}} - z^3P_{1\frac{1}{2}}^0$?	2232.208			10			$z^5D_{1\frac{1}{2}}^0 - 32_{2\frac{1}{2}}$
2156.519	.542		12	1	s	$a^5G_{2\frac{1}{2}} - w^4F_{2\frac{1}{2}}^0$	2238.283			20			$z^5D_{4\frac{1}{2}}^0 - e^6F_{3\frac{1}{2}}$
2159.199	.198		25	—		$a^5G_{3\frac{1}{2}} - y^4F_{3\frac{1}{2}}^0$	2239.752			25			$z^5D_{3\frac{1}{2}}^0 - e^6F_{2\frac{1}{2}}$
2159.833	.835		10b	—		$a^5D_{2\frac{1}{2}} - z^5P_{2\frac{1}{2}}^0$	2242.132			20			$z^5D_{2\frac{1}{2}}^0 - e^6F_{1\frac{1}{2}}$
2161.453	.470		12	—		$a^5H_{4\frac{1}{2}} - y^5H_{4\frac{1}{2}}^0$?	2244.886			8			$z^5D_{1\frac{1}{2}}^0 - e^6F_{\frac{1}{2}}$
2161.842	.836		15b	15b		$a^5G_{2\frac{1}{2}} - w^4F_{2\frac{1}{2}}^0$	2246.171			45			$z^5D_{4\frac{1}{2}}^0 - e^6F_{4\frac{1}{2}}$
	.862					$b^3P_{\frac{1}{2}} - y^3P_{1\frac{1}{2}}^0$	2248.388			35			$z^5D_{3\frac{1}{2}}^0 - e^6F_{3\frac{1}{2}}$
2161.994	1.942		20b	—		$b^3P_{1\frac{1}{2}} - y^3P_{1\frac{1}{2}}^0$	2249.754			30			$z^5D_{2\frac{1}{2}}^0 - e^6F_{2\frac{1}{2}}$
	2.084					$z^5D_{4\frac{1}{2}}^0 - e^6G_{3\frac{1}{2}}$?							$z^5D_{\frac{1}{2}}^0 - e^6F_{\frac{1}{2}}$
2162.263	.218		20	—		$a^3H_{4\frac{1}{2}} - y^4H_{4\frac{1}{2}}^0$?	2249.891			25			$z^5D_{1\frac{1}{2}}^0 - e^6F_{1\frac{1}{2}}$
2162.704	.702		20	30		$a^5G_{4\frac{1}{2}} - z^5G_{4\frac{1}{2}}^0$							$a^5D_{4\frac{1}{2}} - z^5D_{3\frac{1}{2}}^0$?
2164.052	3.996		20	—		$z^5D_{4\frac{1}{2}}^0 - f^5D_{3\frac{1}{2}}$	2252.531			80			$z^5D_{4\frac{1}{2}}^0 - e^6F_{4\frac{1}{2}}$
2165.021	4.990		20	20		$z^5D_{3\frac{1}{2}}^0 - f^5D_{2\frac{1}{2}}$	2254.766			8			$z^5D_{\frac{1}{2}}^0 - e^6F_{1\frac{1}{2}}$
2165.240	.216		25	1		$z^5D_{2\frac{1}{2}}^0 - e^6G_{3\frac{1}{2}}$?	2256.369			50			$z^5D_{3\frac{1}{2}}^0 - e^6F_{4\frac{1}{2}}$
	.288					$a^5G_{2\frac{1}{2}} - w^4F_{2\frac{1}{2}}^0$	2257.576			10			$z^5D_{2\frac{1}{2}}^0 - e^6F_{3\frac{1}{2}}$
2168.084	.105		12	1		$a^3H_{5\frac{1}{2}} - y^4H_{4\frac{1}{2}}^0$?	2258.468			25			$z^5D_{1\frac{1}{2}}^0 - e^6F_{2\frac{1}{2}}$
2168.563	.550		12	10	s	$a^5G_{3\frac{1}{2}} - w^4F_{3\frac{1}{2}}^0$	2375.906			10			$a^5F_{1\frac{1}{2}} - z^5D_{1\frac{1}{2}}^0$
2169.608	.591		8	1		$b^5H_{5\frac{1}{2}} - x^5H_{5\frac{1}{2}}^0$							$z^5F_{5\frac{1}{2}} - 36_{4\frac{1}{2}}$?
2170.114	.178		10	—		$z^5D_{4\frac{1}{2}}^0 - e^6G_{4\frac{1}{2}}$?	2379.264			0			$z^5F_{5\frac{1}{2}} - 35_{5\frac{1}{2}}$
2170.633	.662		12	—		$z^5D_{4\frac{1}{2}}^0 - e^6G_{4\frac{1}{2}}$?	2403.182			8			$z^5F_{4\frac{1}{2}} - 31_{4\frac{1}{2}}$
2170.876	.854		5	—		$a^3P_{1\frac{1}{2}} - z^3F_{2\frac{1}{2}}^0$	2403.355			6			$a^5F_{5\frac{1}{2}} - z^5D_{5\frac{1}{2}}^0$
	.920					$z^5D_{\frac{1}{2}}^0 - f^5D_{\frac{1}{2}}$							$z^5P_{2\frac{1}{2}} - 35_{2\frac{1}{2}}$
2172.233	.247		1	—		$z^5D_{1\frac{1}{2}}^0 - f^5D_{1\frac{1}{2}}$	2416.708			0			$z^5F_{5\frac{1}{2}} - 30_{5\frac{1}{2}}$
2172.739	.726		1	—		$z^5D_{2\frac{1}{2}}^0 - f^5D_{2\frac{1}{2}}$	2429.708			6			$z^5F_{\frac{1}{2}}^0 - e^6F_{\frac{1}{2}}$
2173.363	.352		8	—		$z^5D_{3\frac{1}{2}}^0 - f^5D_{2\frac{1}{2}}$	2429.886			10			$z^5F_{3\frac{1}{2}}^0 - 32_{2\frac{1}{2}}$
2173.673	.661		15	8		$a^5D_{2\frac{1}{2}} - x^4F_{2\frac{1}{2}}^0$	2431.614			10			$z^5F_{3\frac{1}{2}}^0 - e^6F_{1\frac{1}{2}}$
2173.904	.943		20b	0		$b^5H_{4\frac{1}{2}} - w^4F_{3\frac{1}{2}}^0$?	2431.974			3			$z^5F_{1\frac{1}{2}}^0 - e^6F_{\frac{1}{2}}$
2175.533	.531		8	10		$a^5D_{1\frac{1}{2}} - y^5D_{1\frac{1}{2}}^0$	2433.789			1			$z^5F_{2\frac{1}{2}}^0 - 36_{2\frac{1}{2}}$
2176.129	.131		25	30		$a^5G_{2\frac{1}{2}} - z^5G_{2\frac{1}{2}}^0$	2434.791			15			$z^5F_{3\frac{1}{2}}^0 - e^6F_{2\frac{1}{2}}$
2176.708	.789		1	—		$z^5D_{\frac{1}{2}}^0 - f^5D_{1\frac{1}{2}}$?	2434.968			20			$z^5F_{2\frac{1}{2}}^0 - 31_{2\frac{1}{2}}$
2177.048	.002		5hh	—		$a^4H_{4\frac{1}{2}} - y^5H_{4\frac{1}{2}}^0$?	2435.561			5			$z^5F_{1\frac{1}{2}}^0 - e^6F_{1\frac{1}{2}}$
2177.510	.470		20	—		$z^5D_{1\frac{1}{2}}^0 - e^6G_{1\frac{1}{2}}$?	2435.727			25			$z^5F_{2\frac{1}{2}}^0 - 30_{2\frac{1}{2}}$
2177.709	.711		10	5		$a^3P_{\frac{1}{2}} - z^3P_{\frac{1}{2}}^0$	2437.354			20			$z^5F_{2\frac{1}{2}}^0 - 35_{2\frac{1}{2}}$
2180.940	.944		12	—		$z^5D_{2\frac{1}{2}}^0 - e^6G_{2\frac{1}{2}}$?	2437.726			10			$z^5F_{4\frac{1}{2}}^0 - e^6F_{3\frac{1}{2}}$
2181.555	.610		12	—		$z^5D_{4\frac{1}{2}}^0 - e^6G_{4\frac{1}{2}}$?	2437.839			5			$z^5F_{\frac{1}{2}}^0 - e^6F_{1\frac{1}{2}}$
2181.822	.904		8	—		$z^5D_{3\frac{1}{2}}^0 - e^6G_{3\frac{1}{2}}$?	2438.372			20			$z^5F_{3\frac{1}{2}}^0 - e^6F_{4\frac{1}{2}}$
2182.092	.034		5b	—		$z^5D_{\frac{1}{2}}^0 - e^6G_{1\frac{1}{2}}$?	2440.600			8			$z^5F_{3\frac{1}{2}}^0 - e^6F_{3\frac{1}{2}}$
2183.987	.940		12	—		$a^5G_{3\frac{1}{2}} - y^4F_{4\frac{1}{2}}^0$	2444.583			15b			$z^5F_{1\frac{1}{2}}^0 - e^6F_{2\frac{1}{2}}$
2184.154	.201		8	—		$a^3H_{4\frac{1}{2}} - y^4H_{4\frac{1}{2}}^0$?	2445.015			10			$z^5F_{2\frac{1}{2}}^0 - e^6F_{2\frac{1}{2}}$
2184.489	.472		10h	—		$b^3H_{4\frac{1}{2}} - x^5H_{4\frac{1}{2}}^0$	2445.855			40			$z^5F_{3\frac{1}{2}}^0 - e^6F_{3\frac{1}{2}}$
2186.308	.268		8h	—		$a^3F_{2\frac{1}{2}} - x^5F_{2\frac{1}{2}}^0$?	2447.147			25			$z^5F_{4\frac{1}{2}}^0 - e^6F_{4\frac{1}{2}}$
2188.131	.117		12	2		$a^3F_{3\frac{1}{2}} - x^5F_{3\frac{1}{2}}^0$	2450.876			5			$z^5F_{2\frac{1}{2}}^0 - e^6F_{2\frac{1}{2}}$
2188.365	.367		10	2		$a^3G_{3\frac{1}{2}} - y^4F_{3\frac{1}{2}}^0$	2454.490			15			$z^5F_{3\frac{1}{2}}^0 - e^6F_{3\frac{1}{2}}$
2188.555	.540		15	1		$a^3D_{1\frac{1}{2}} - y^5D_{2\frac{1}{2}}^0$	2454.678			25			$z^5F_{4\frac{1}{2}}^0 - e^6F_{4\frac{1}{2}}$
2189.512	.503		1	—		$a^3H_{5\frac{1}{2}} - x^4F_{4\frac{1}{2}}^0$	2456.635			10			$z^5F_{1\frac{1}{2}}^0 - 36_{2\frac{1}{2}}$
2192.622			10	5h		$z^5D_{2\frac{1}{2}}^0 - 35_{2\frac{1}{2}}$	2459.270			1			$z^5F_{2\frac{1}{2}}^0 - e^6F_{2\frac{1}{2}}$
2193.362	.373		5	—	s	$b^5P_{\frac{1}{2}} - w^4D_{1\frac{1}{2}}^0$	2464.645			5			$z^5F_{3\frac{1}{2}}^0 - 32_{2\frac{1}{2}}$
2197.961	.947		5h	—		$b^5P_{\frac{1}{2}} - w^4D_{\frac{1}{2}}^0$	2468.478			6b			$z^5F_{1\frac{1}{2}}^0 - 34_{\frac{1}{2}}$
2199.349			4	2h		$z^5D_{2\frac{1}{2}}^0 - 36_{2\frac{1}{2}}$	2470.459			8			$z^5F_{2\frac{1}{2}}^0 - e^6F_{2\frac{1}{2}}$
2202.284			5	5h		$z^5D_{3\frac{1}{2}}^0 - 35_{2\frac{1}{2}}$	2477.185			0			$z^5F_{1\frac{1}{2}}^0 - 33_{1\frac{1}{2}}$
2206.843			8	15h		$z^5D_{1\frac{1}{2}}^0 - 36_{2\frac{1}{2}}$	2480.134			3			$z^5F_{3\frac{1}{2}}^0 - e^6F_{4\frac{1}{2}}$
2207.272	.277		2	1		$a^3F_{2\frac{1}{2}} - w^4D_{2\frac{1}{2}}^0$?	2486.245			0			$z^5F_{2\frac{1}{2}}^0 - e^6F_{1\frac{1}{2}}$
	.278					$a^2D_{1\frac{1}{2}} - x^4F_{1\frac{1}{2}}^0$	2488.107			5b			$z^5F_{1\frac{1}{2}}^0 - 32_{1\frac{1}{2}}$
2209.110			30	15h		$z^5D_{4\frac{1}{2}}^0 - 31_{4\frac{1}{2}}$	2495.645			2			$z^5F_{2\frac{1}{2}}^0 - e^6F_{2\frac{1}{2}}$
2209.740			20	10h		$z^5D_{4\frac{1}{2}}^0 - 30_{3\frac{1}{2}}$							
						$z^5D_{1\frac{1}{2}}^0 - 35_{2\frac{1}{2}}$							

neighborhood of 106,000 wave numbers. The unclassified odd levels tentatively marked ^6D are in about the proper place.

The use of Dobbie's three even ^6D levels as part of e^6F seems amply justified by the intensity diagram given below in Table VI. His $e^6P_{3\frac{1}{2}}$ has been given a number in place of its name because the $z^6D_{2\frac{1}{2}}^0 - e^6P_{2\frac{1}{2}}$ line is definitely not present on my plates. Since $z^6D_{4\frac{1}{2}}^0 - e^6P_{3\frac{1}{2}}$ and $z^6D_{3\frac{1}{2}}^0 - e^6P_{3\frac{1}{2}}$ are both of intensity 30, it is highly probable that it would appear if it existed. The assignment of $J = 2\frac{1}{2}$ instead of $J = 1\frac{1}{2}$ to level 36 ($^6P_{1\frac{1}{2}}$) depends

TABLE VIII, *Terms of* Fe III.

CONFIGURATION	DESIG.	LEVEL	APPROX. LEVEL	INTERVALS	NO. OF COMB.	CONFIGURATION	DESIG.	LEVEL	APPROX. LEVEL	INTERVALS	NO. OF COMB.
$3d^6$	a^5D_4	0.0			2	$3d^5(^6S)4p$	$z^5P_3^0$	89083.6			4
				−436.1						−249.7	
	a^5D_3	436.1			2		$z^5P_2^0$	89333.3			4
				−302.0						−156.0	
	a^5D_2	738.1			3		$z^5P_1^0$	89489.3			4
				−193.4		$3d^5(^4G)4p$	$z^5G_2^0$	113584.5			2
	a^5D_1	931.5			2					+19.4	
				−95.8			$z^5G_3^0$	113603.9			2
	a^5D_0	1027.3			1					+29.8	
$3d^5(^6S)4s$	a^5S_2	40998.7			3		$z^5G_4^0$	113633.7			3
										+41.7	
$3d^5(^4G)4s$	a^5G_6	63423.1			5		$z^5G_5^0$	113675.4			2
				−41.3						+62.5	
	a^5G_5	63464.4			6		$z^5G_6^0$	113737.9			1
				−20.5							
	a^5G_4	63484.9			7	$3d^5(^4G)4p$	$z^5H_3^0$	114949.2			1
				−7.4						+160.7	
	a^5G_3	63492.3			6		$z^5H_4^0$	115109.9			2
				−2.2						+178.8	
	a^5G_2	63494.5			2		$z^5H_5^0$	115288.7			2
										+184.1	
$3d^5(^4P)4s$	a^5P_3	66463.5			2		$z^5H_6^0$	115472.8			2
				−58.2						+167.9	
	a^5P_2	66521.7			1		$z^5H_7^0$	115640.7			1
				−68.8							
	a^5P_1	66590.5			0	$3d^5(^4G)4p$	$z^5F_1^0$	116315.6			5
										−150.6	
$3d^5(^4D)4s$	b^5D_4	69694.4			2		$z^5F_2^0$	116466.2			6
				−141.2						−8.0	
	b^5D_3	69835.6			2		$z^5F_3^0$	116474.2			5
				−1.2							
	b^5D_2	69836.8			0	$3d^5(^6S)4s$	a^7S_3	0.0	30000		3
				+50.3							
	b^5D_1	69786.5			0	$3d^5(^6S)4p$	$z^7P_2^0$	51912.8			1
				+40.2						+332.3	
	b^5D_0	69746.3			0		$z^7P_3^0$	52245.1			1
										+512.3	
							$z^7P_4^0$	52757.4	83000		1

only upon the identification of the line λ2375.906 as $z^6F_{3\frac{1}{2}}^0 - 36_{2\frac{1}{2}}$. Since this line is also assigned to the transition $a^4F_{1\frac{1}{2}} - z^4D_{\frac{1}{2}}^0$, the evidence is inconclusive.

It is very surprising that a long search has failed to uncover the third member of the d^6s^6D series. Its position can be predicted fairly accurately, and the analogous transitions in Mn II and Cu II give strong lines. I am, therefore, unable to improve the present value of the ionization potential,[8] 16.16 volts.

A list of identified lines of Fe II is given in Table VII. The list is complete for wave-lengths less than λ2220.582 but beyond this only those lines are given which are of interest in connection with new levels and new assignments of high even terms. The first column contains the wave-length of the line in vacuum. When poorly determined, it is followed by a small "p." If the wave-length of a line below λ2225 can be calculated by means of the combination principle from measures made above λ2300, the calculated decimal is given in the second column. Dobbie's[9] level values were used for the calculations. The next three columns give the intensity as observed in the neon Schüler tube, the helium Schüler tube, and the spark. If the line occurs in a region of the plate which has not been measured, the space for the intensity is left blank. A dash in the intensity column means that the region was measured but the line was not present; "*m*" means that the line is masked; "*h*" that it is somewhat hazy; "*b*" that it is a blend. The great increase in the intensity of the spectrum in the neon relative to the helium Schüler tube in the neighborhood of λ930 is readily apparent from a glance at the first part of the list. This region is within 4000 wave numbers of the limit of excitation of Fe II by collisions of the second kind with neon atoms in the normal state of the ion. The next column of the table contains "*s*" if the line is regarded as especially suitable as a standard. The final column gives the identification, followed by a question mark if uncertain. All wave-

[8] J. C. Dobbie, Phys. Rev. **45**, 76 (1934).

[9] J. C. Dobbie, *Annals of the Solar Physics Observatory, Cambridge* (Cambridge University Press, 1938), Vol. V, Part I.

TABLE IX. *Identified* Fe III *lines.*

WAVE-LENGTH	INT.	IDENTIFICATION	WAVE-LENGTH	INT.	IDENTIFICATION	WAVE-LENGTH	INT.	IDENTIFICATION
859.737	15	$a^5D_4-z^5F_5^0$	1892.865	1	$a^5G_4-z^5F_5^0$	1994.355*p*	1*h*	$a^5G_3-z^5G_4^0$
1122.551	25*h*	$a^5D_4-z^5P_3^0$	1895.448	40	$a^7S_3-z^7P_4^0$	1995.249	15	$a^5G_4-z^5G_5^0$
1124.885	25	$a^5D_3-z^5P_3^0$	1914.036	50	$a^7S_3-z^7P_3^0$	1995.549	25	$a^5G_5-z^5G_6^0$
1126.747	8	$a^5D_2-z^5P_1^0$	1915.062	30	$a^5G_6-z^5H_7^0$	1996.408	25*	$a^5G_2-z^5G_2^0$
1128.074	25*b*	$a^5D_3-z^5P_2^0$	1921.182	0	$a^5G_6-z^5H_6^0$			$a^5G_3-z^5G_3^0$
1128.733	20	$a^5D_2-z^5P_2^0$	1922.766	30	$a^5G_5-z^5H_6^0$	1999.570	25	$a^5P_3-z^5F_3^0$
1129.205	20	$a^5D_1-z^5P_1^0$	1926.284	40	$a^7S_3-z^7P_3^0$	1999.872	1	$a^5P_3-z^5F_4^0$
1130.428	25*b*	$a^5D_0-z^5P_1^0$	1929.586	1	$a^5G_4-z^5H_5^0$	2001.904	5	$a^5P_2-z^5F_3^0$
1131.206	10	$a^5D_1-z^5P_2^0$	1930.361	30	$a^5G_4-z^5H_5^0$	2062.203	35	$a^5S_2-z^5P_1^0$
1131.914	8*h*	$a^5D_2-z^5P_3^0$	1937.054	1	$a^5G_4-z^5H_4^0$	2068.899	40	$a^5S_2-z^5P_2^0$
1886.733	25	$a^5G_5-z^5F_4^0$	1937.322	30	$a^5G_3-z^5H_4^0$	2079.642	50	$a^5S_2-z^5P_3^0$
1887.174	10	$a^5G_4-z^5F_5^0$	1943.458	30	$a^5G_3-z^5H_3^0$	2138.038	1	$b^5D_4-z^5F_4^0$
1887.451	8	$a^5G_4-z^5F_4^0$	1987.486	35	$a^5G_5-z^5G_6^0$	2144.151	2	$b^5D_3-z^5F_3^0$
		$a^5G_3-z^5F_3^0$	1989.957	15	$a^5G_6-z^5G_6^0$	2144.504	0	$b^5D_3-z^5F_4^0$
1887.718	2	$a^5G_3-z^5F_4^0$	1991.595	30	$a^5G_5-z^5G_6^0$	2144.960	2	$b^5D_4-z^5F_5^0$
1890.644	30	$a^5G_6-z^5F_5^0$	1993.251	15	$a^5G_5-z^5G_4^0$			
1892.068	5	$a^5G_5-z^5F_5^0$	1994.064	25	$a^5G_4-z^5G_4^0$			

* Measured as double in the Schüler tube.

lengths and intensities in the He Schüler tube are taken from one plate except for lines of wave-length longer than λ2190 arising from transitions between high and middle levels.

Fe III

The known terms of Fe III are collected in Table VIII. The a^5D, a^7S and a^5S, and z^7P^0 and z^5P^0 were found by Bowen.[10] The a^5P and b^5D were found by Swings and Edlén.[11] A search for the multiplet $a^7S-z^5P^0$ has been unsuccessful, and the septet and quintet systems remain unconnected. In the third column of the table the position of z^7P^0 is therefore given with reference to a^7S as zero. An estimate of the probable position of a^5G and a^5S relative to a^7S can be obtained from a plot of the corresponding differences in Cr I and Mn II since the major portion of the change from one spectrum to another along an isoelectronic sequence is linear with atomic number. It is found that a^5S would be expected to be about 11,000 wave numbers above a^7S and a^5G about 34,000 wave numbers above a^7S. The fourth column of the table gives estimated term values for the septets with reference to a^5D as zero. Column six contains the number of times each of the various levels were used in identifying the lines of Table IX.

Table IX contains a list of the identified Fe III lines below λ2200. Column one gives the wave-length. When this is poorly determined, it is followed by a small "*p*." Column two contains the intensity and column three the identification. If the line is hazy or a blend, the intensity is followed by "*h*" or "*b*," respectively. The $a^5D_4-z^5F_5^0$ line and the $a^5D-z^5P^0$ multiplet were taken from a Schüler tube plate, the remainder of the lines from a plate of the spark in nitrogen.

[10] I. S. Bowen, Phys. Rev. **52**, 1153 (1937).
[11] P. Swings and B. Edlén, Astrophys. J. **88**, 618 (1938).

ACKNOWLEDGMENTS

Primarily I wish to thank Professor A. G. Shenstone for his constant interest and help during the course of this work. I also want to extend my thanks to Professor C. H. Willis, Dr. C. W. Lampson, Dr. C. W. Curtis, Professor D. P. Smith, Professor G. H. Shortley and Dr. Charlotte Moore Sitterly. It has been a great privilege to be a student under Professor H. N. Russell and to have his active interest.

Many-Body Interactions in Atomic and Nuclear Systems

H. PRIMAKOFF, *Polytechnic Institute of Brooklyn, Brooklyn, New York*

AND

T. HOLSTEIN,* *New York University, University Heights, New York, New York*

(Received March 28, 1938)

When particles interact with each other through the intervening mechanism of a field, the description of their dynamical behavior by means of action-at-a-distance potentials is only of an approximate nature. Two-body, three-body, $\cdots$, m-body potentials may be regarded as successive stages of this approximation; their relative magnitudes are examined systematically for several types of classical and quantized fields, e.g., electromagnetic, mesotron, etc. It is found that the description of electrons in atomic systems by the customary two-body potentials is an excellent approximation; in nuclei, independent of the details of the field, one finds: three-body potentials $\leqq(v_n/c)\times$(two-body potentials)$\cdots$, m-body potentials $\leqq(v_n/c)^{m-2}\times$(two-body potentials), where v_n is the average velocity of the heavy particles in the nucleus. The usual description of nuclei in terms of two-body potentials cannot therefore be considered satisfactory, except in the case of the deuteron.

INTRODUCTION

IN field theories of particle interaction, an exact description of the dynamical behavior of the particles necessitates the explicit introduction of variables describing the state of the field. A description of particle dynamics in terms of interactions depending only on the instantaneous relative coordinates of the particles[1] (action-at-a-distance) is, therefore, necessarily of an approximate character. In the first stage of this approximation the interactions are of the so-called "two-body" type:

$$V(\mathbf{r}_{12}, \mathbf{r}_{13}, \cdots)=\sum_{i,\,j} V_{ij}(\mathbf{r}_{ij}).$$

In the higher stages, as shown below, one obtains additional interactions of such a nature that the *force* between any *two* particles is dependent on the positions of some of the *others* ("many-body" forces). For example,

$$V=\sum_{i,\,j,\,k} V_{ijk}(\mathbf{r}_{ij}, \mathbf{r}_{jk}, \mathbf{r}_{ik})$$

represents three-body interactions. It is the purpose of this paper to examine the conditions under which a set of two-body interactions constitute an adequate substitute for the explicit use of field variables. It will be found that the use of two-body interactions is an excellent approximation for electronic motions in atomic systems, but a relatively poor one for the heavy particles in nuclei.

CLASSICAL ELECTROMAGNETIC THEORY OF ELECTRON DYNAMICS

(a) Equations of motion

The equation of motion of a given electron in the presence of potentials, φ, $\mathbf{A}$ is

$$m\mathbf{a}_k=e_k\left\{-\text{grad.}_k\,\varphi(\mathbf{r}_k, t)-\frac{1}{c}\frac{\partial}{\partial t}\mathbf{A}(\mathbf{r}_k, t)\right.$$
$$\left.+\frac{\mathbf{v}_k}{c}\times\text{curl}_k\,\mathbf{A}(\mathbf{r}_k, t)\right\},\quad k=1, \cdots, n. \quad (1)$$

Here φ, $\mathbf{A}$, arise from the other electrons, and describe the state of the field; they are determined by the equations:[2]

$$\nabla^2\varphi=-4\pi\sum_j e_j\delta(\mathbf{r}-\mathbf{r}_j(t))-\frac{1}{c}\,\text{div.}\,\frac{\partial\mathbf{A}}{\partial t}, \quad (2)$$

$$\nabla^2\mathbf{A}-\frac{1}{c^2}\frac{\partial^2\mathbf{A}}{\partial t^2}=-4\pi\sum_j e_j\frac{\mathbf{v}_j}{c}\delta(\mathbf{r}-\mathbf{r}_j(t))$$
$$+\text{grad.}\left(\text{div.}\,\mathbf{A}+\frac{1}{c}\frac{\partial\varphi}{\partial t}\right). \quad (3)$$

To obtain an "action-at-a-distance" dynamical description of the particles, one attempts to express φ, $\mathbf{A}$ in terms of the instantaneous relative particle coordinates. Choosing the gauge so

* University Fellow.

[1] One also admits interactions depending on the particle velocity into the action-at-a-distance dynamical description.

[2] W. Heitler, *Quantum Theory of Radiation* (Oxford Univ. Press, 1936), p. 2, Eqs. (8a), (8b).

that div. $\mathbf{A}=0$, one finds:[2a]

$$\varphi(\mathbf{r}_k, t)=\sum_j \frac{e_j}{r_{kj}}; \quad \text{exactly.} \tag{4}$$

$$\mathbf{A}(\mathbf{r}_k, t)=\sum_j \frac{e_j}{2c}\left(\frac{\mathbf{v}_j}{r_{kj}}+\frac{\mathbf{r}_{kj}(\mathbf{v}_j\cdot\mathbf{r}_{kj})}{r_{kj}^3}\right)$$

$$+\text{terms in } \frac{\mathbf{v}_j^2}{c^2}+\text{terms in } \frac{\mathbf{a}_j}{c^2}+\cdots;$$

$$\mathbf{a}_j \equiv \text{acceleration of } j\text{th particle.} \tag{5}$$

The forces acting on the kth particle will be correct to the second order in v_j/c, and the first order in a_j/c^2, if all terms in $\mathbf{A}$ except those in v_j/c, are neglected.[2b]

With this approximation, the equations of motion (1) for the system of electrons, become:

$$m\mathbf{a}_k=\sum_j \frac{e_k e_j \mathbf{r}_{kj}}{r_{kj}^3}-\sum_j \frac{e_k e_j}{2c^2}\left(-\frac{v_j^2\mathbf{r}_{kj}}{r_{kj}^3}+\frac{3(\mathbf{v}_j\cdot\mathbf{r}_{kj})^2\mathbf{r}_{kj}}{r_{kj}^5}\right)$$

$$+\sum_j \frac{e_k\mathbf{v}_k}{c}\times\left(\frac{e_j}{c}\frac{\mathbf{v}_j\times\mathbf{r}_{kj}}{r_{kj}^3}\right)$$

$$+\sum_j \frac{e_k e_j}{2c^2}\left(\frac{\mathbf{a}_j}{r_{kj}}+\frac{(\mathbf{a}_j\cdot\mathbf{r}_{kj})\mathbf{r}_{kj}}{r_{kj}^3}\right)$$

$$\equiv \mathbf{f}_c(k)+\mathbf{f}_v(k)+\mathbf{f}_m(k)+\mathbf{f}_a(k), \quad k=1, \cdots, n. \tag{6}$$

Here, $\mathbf{f}_c(k)$, $\mathbf{f}_v(k)$, $\mathbf{f}_m(k)$, represent, in order, the Coulomb force, a velocity-dependent correction to the Coulomb force, and the magnetic force. $\mathbf{f}_a(k)$ is the force on the kth particle determined by the acceleration of the others.

Since there are n equations of motion (4), the n unknown accelerations are given in terms of the positions and velocities. To the zeroth order in v/c,

$$\mathbf{a}_j=\frac{1}{m}\sum_l \frac{e_j e_l}{r_{jl}^3}\mathbf{r}_{jl}, \tag{7}$$

whence, to v^2/c^2

$$\mathbf{f}_a(k)=\sum_{j,\,l}\frac{e_k e_j}{2mc^2}\left(\frac{e_j e_l \mathbf{r}_{jl}}{r_{kj}r_{jl}^3}+\frac{e_j e_l(\mathbf{r}_{jl}\cdot\mathbf{r}_{kj})\mathbf{r}_{kj}}{r_{kj}^3 r_{jl}^3}\right)$$

$$\leqq \frac{e^2}{mc^2}\frac{1}{r}\frac{e^2}{r^2}\leqq\frac{e^2}{mc^2}\frac{1}{r}|\mathbf{f}_c|. \tag{8}$$

Thus $\mathbf{f}_a(k)$ is of the three-body type. The three-body forces become appreciable whenever the relative distances between the electrons are not large in comparison with their classical electromagnetic radii.

It is a general fact that "acceleration-dependent" forces, when expressed in terms of coordinates and velocities, are of the many-body type.

(b) Lagrangian and Hamiltonian of the particle system

The equations of motion, (6), are derivable from a two-body Lagrangian:[3]

$$L=\sum_k \tfrac{1}{2}m\mathbf{v}_k^2-\tfrac{1}{2}\sum_{k,\,j}\frac{e_k e_j}{r_{kj}}$$

$$+\tfrac{1}{2}\sum_{k,\,j}\frac{e_k e_j}{2c^2}\left(\frac{\mathbf{v}_k\cdot\mathbf{v}_j}{r_{kj}}+\frac{(\mathbf{v}_k\cdot\mathbf{r}_{kj})(\mathbf{v}_j\cdot\mathbf{r}_{kj})}{r_{kj}^3}\right)$$

$$\equiv \sum_k \tfrac{1}{2}m\mathbf{v}_k^2-\tfrac{1}{2}\sum_k e_k\varphi(\mathbf{r}_k)+\tfrac{1}{2}\sum_k \frac{e_k}{c}\mathbf{v}_k\cdot\mathbf{A}(\mathbf{r}_k), \tag{9}$$

from which one obtains the Hamiltonian:

$$H=\sum_k \tfrac{1}{2}m\mathbf{v}_k^2+\tfrac{1}{2}\sum_{k,\,j}\frac{e_k e_j}{r_{kj}}$$

$$+\tfrac{1}{2}\sum_{k,\,j}\frac{e_k e_j}{2c^2}\left(\frac{\mathbf{v}_k\cdot\mathbf{v}_j}{r_{kj}}+\frac{(\mathbf{v}_k\cdot\mathbf{r}_{kj})(\mathbf{v}_j\cdot\mathbf{r}_{kj})}{r_{kj}^3}\right)$$

$$\equiv \sum_k \tfrac{1}{2}m\mathbf{v}_k^2+\tfrac{1}{2}\sum_k e_k\varphi(\mathbf{r}_k)+\tfrac{1}{2}\sum_k \frac{e_k\mathbf{v}_k}{c}\cdot\mathbf{A}(\mathbf{r}_k), \tag{10}$$

where the $\mathbf{v}$'s are to be expressed in terms of the

[2a] The gauge div. $\mathbf{A}=0$, and the subsequent approximate solution for $\mathbf{A}$ from the field equations, has been used by Breit in his derivation of the velocity dependent interaction between two electrons. See Phys. Rev. **39**, 616 (1932).

[2b] For further discussion of this neglect, see Addendum.

[3] This Lagrangian was first given by C. G. Darwin, Phil. Mag. **39**, 537 (1920). All relativistic terms in the kinetic energy, such as $\sum_k m_k v_k^4/8c^2$, are consistently omitted in what follows, since they introduce no essential modification in the derivation of many-body potentials. A further discussion of the approximations involved in this Lagrangian is given in the Addendum.

p's, by the equations

$$\mathbf{v}_k=\frac{1}{m}\left[\mathbf{p}_k-\sum_j\frac{e_ke_j}{2c^2}\left(\frac{\mathbf{v}_j}{r_{kj}}+\frac{\mathbf{r}_{kj}(\mathbf{v}_j\cdot\mathbf{r}_{kj})}{r_{kj}^3}\right)\right]$$
$$\equiv\frac{1}{m}\left(\mathbf{p}_k-\frac{e_k}{c}\mathbf{A}(\mathbf{r}_k)\right),\quad k=1,\cdots,n. \quad (11)$$

Substituting into (10), the value of $\mathbf{v}_k$ given by (11), one obtains

$$H=\sum_k\frac{\mathbf{p}_k^2}{2m}+\tfrac{1}{2}\sum_k e_k\varphi(\mathbf{r}_k)-\tfrac{1}{2}\sum_k\frac{e_k}{c}\frac{\mathbf{p}_k}{m}\cdot\mathbf{A}(\mathbf{r}_k) \quad (12)$$

with the **A**'s given in terms of the **p**'s, by (cf. (5) and (11))

$$\mathbf{A}(\mathbf{r}_k)=\sum_j\frac{e_j}{2mc}\left[\frac{(\mathbf{p}_j-(e_j/c)\mathbf{A}(\mathbf{r}_j))}{r_{kj}}+\frac{\mathbf{r}_{kj}(\mathbf{p}_j-(e_j/c)\mathbf{A}(\mathbf{r}_j))\cdot\mathbf{r}_{kj}}{r_{kj}^3}\right]$$
$$\equiv\sum_j\frac{e_j}{2mc}\left(\frac{\mathbf{p}_j}{r_{kj}}+\frac{\mathbf{r}_{kj}(\mathbf{r}_{kj}\cdot\mathbf{p}_j)}{r_{kj}^3}\right)$$
$$-\sum_j\frac{e_j^2}{2mc^2r_{kj}}\left(\mathbf{A}(\mathbf{r}_j)+\frac{\mathbf{r}_{kj}(\mathbf{r}_{kj}\cdot\mathbf{A}(\mathbf{r}_j))}{r_{kj}^2}\right), \quad (13)$$
$$k=1,\cdots,n.$$

The n linear inhomogeneous vector equations (13), may be solved, either exactly, with determinants, or approximately, with $e_j^2/2mc^2r_{kj}$ as an expansion parameter. The latter method leads to

$$\mathbf{A}(\mathbf{r}_k)=\sum_j\frac{e_j}{2mc}\left(\frac{\mathbf{p}_j}{r_{kj}}+\frac{\mathbf{r}_{kj}(\mathbf{r}_{kj}\cdot\mathbf{p}_j)}{r_{kj}^3}\right)$$
$$-\sum_{j,\,l}\frac{e_j^2}{2mc^2r_{kj}}\frac{e_l}{2mc}\left[\left(\frac{\mathbf{p}_l}{r_{jl}}+\frac{\mathbf{r}_{jl}(\mathbf{p}_l\cdot\mathbf{r}_{jl})}{r_{jl}^3}\right)+\frac{\mathbf{r}_{kj}}{r_{kj}^2}\mathbf{r}_{kj}\cdot\left(\frac{\mathbf{p}_l}{r_{jl}}+\frac{\mathbf{r}_{jl}(\mathbf{p}_l\cdot\mathbf{r}_{jl})}{r_{jl}^3}\right)\right]$$
$$+\sum_{j,\,l,\,s}\text{terms in}\left(\frac{e^2}{mc^2}\frac{1}{r}\right)^2\frac{e}{c}\frac{\mathbf{p}}{mr}$$
$$+\sum_{j,\,l,\,s,\,t}\text{terms in}\left(\frac{e^2}{mc^2}\frac{1}{r}\right)^3\frac{e}{c}\frac{\mathbf{p}}{mr}+\cdots, \quad (14)$$

whence, neglecting terms in $[(e^2/mc^2)(1/r)]^3$, $[(e^2/mc^2)(1/r)]^3$, $\cdots$, and substituting for $\mathbf{A}(\mathbf{r}_k)$ into the Hamiltonian (12), one obtains

$$H=\sum_k\frac{\mathbf{p}_k^2}{2m}+\tfrac{1}{2}\sum_{k,\,j}\frac{e_ke_j}{r_{kj}}$$
$$-\tfrac{1}{2}\sum_{k,\,j}\frac{e_ke_j}{2m^2c^2}\left(\frac{\mathbf{p}_k\cdot\mathbf{p}_j}{r_{kj}}+\frac{(\mathbf{p}_k\cdot\mathbf{r}_{kj})(\mathbf{p}_j\cdot\mathbf{r}_{kj})}{r_{kj}^3}\right)$$
$$+\sum_{k,\,j,\,l}\frac{e_ke_j^2e_l}{8m^3c^4}\left[\frac{\mathbf{p}_k\cdot\mathbf{p}_l}{r_{kj}r_{jl}}+\frac{(\mathbf{p}_k\cdot\mathbf{r}_{jl})(\mathbf{p}_l\cdot\mathbf{r}_{jl})}{r_{kj}r_{jl}^3}+\frac{(\mathbf{p}_k\cdot\mathbf{r}_{kj})(\mathbf{p}_l\cdot\mathbf{r}_{kj})}{r_{kj}^3r_{jl}}+\frac{(\mathbf{r}_{kj}\cdot\mathbf{r}_{jl})(\mathbf{p}_k\cdot\mathbf{r}_{kj})(\mathbf{p}_l\cdot\mathbf{r}_{jl})}{r_{kj}^3r_{jl}^3}\right]$$
$$\equiv H(\text{kinetic})+H(\text{Coulomb})+H(\text{Darwin})+H'. \quad (15)$$

The interaction H' contains "velocity-dependent" three-body potentials (for $j\neq l$). These are:

$$H'(\text{three-body vel.-depend})\leqq\sum_{k,\,j,\,l}\frac{e_ke_j^2e_l}{8m^3c^4}\frac{\mathbf{p}_k\cdot\mathbf{p}_l}{r_{kj}r_{jl}}\leqq\left(\frac{e^2}{mc^2}\frac{1}{r}\right)\left(\frac{v^2}{c^2}\right)\frac{e^2}{r}. \quad (16)$$

Thus one obtains a three-body Hamiltonian from the two-body Lagrangian because of the peculiar relation between the **p**'s and **v**'s, in (11), and the consequent peculiar relation between the **A**'s and **p**'s (Eq. (13)). While the use of the three-body Hamiltonian is somewhat artificial in classical mechanics, the same equations of motion (6), being derivable from the two-body Lagrangain (9), its introduction is essential in quantum mechanics, since the **p**'s, not the **v**'s, enter into the fundamental commutation relationships.

The terms in **A**, of order

$$[(e^2/mc^2)(1/r)]^2ep/mcr,\quad[(e^2/mc^2)(1/r)]^3ep/mcr,$$
$$\cdots,\quad[(e^2/mc^2)(1/r)]^{m-2}ep/mcr,$$

when substituted into the

$$-\tfrac{1}{2}\Sigma_k(e_k/c)(\mathbf{p}_k/m)\cdot\mathbf{A}(\mathbf{r}_k)$$

term of the Hamiltonian give 4, 5, $\cdots$, m-body-potentials. The ratio of the magnitudes of the individual terms in the m-body and Coulomb potentials is $\leqq[(e^2/mc^2)(1/r)]^{m-2}v^2/c^2$.

If one considers the classical electron to have a spin $\mathbf{s}_k$ and a magnetic moment $\boldsymbol{\mu}_k$, proportional

to $\mathbf{s}_k$, then[3a]

$$\mathbf{A}(\mathbf{r}_k)=\sum_j \frac{e_j}{2c}\left(\frac{\mathbf{v}_j}{r_{kj}}+\frac{\mathbf{r}_{kj}(\mathbf{v}_j\cdot\mathbf{r}_{kj})}{r_{kj}^3}\right)+\sum_j \frac{\boldsymbol{\mu}_j\times\mathbf{r}_{kj}}{r_{kj}^3}, \quad (17)$$

$$L=\sum_k \frac{m\mathbf{v}_k^2}{2}-\tfrac{1}{2}\sum_{k,j}\frac{e_ke_j}{r_{kj}}+\left[\tfrac{1}{2}\sum_{k,j}\frac{e_ke_j}{2c^2}\left(\frac{\mathbf{v}_k\cdot\mathbf{v}_j}{r_{kj}}+\frac{(\mathbf{v}_k\cdot\mathbf{r}_{kj})(\mathbf{v}_j\cdot\mathbf{r}_{kj})}{r_{kj}^3}\right)+\tfrac{1}{2}\sum_{k,j}\frac{e_k\mathbf{v}_k}{c}\cdot\frac{\boldsymbol{\mu}_j\times\mathbf{r}_{kj}}{r_{kj}^3}\right]$$
$$+\left[\tfrac{1}{2}\sum_{k,j}\boldsymbol{\mu}_k\cdot\left(\frac{e_j\mathbf{v}_j\times\mathbf{r}_{kj}}{cr_{kj}^3}\right)+\tfrac{1}{2}\sum_{k,j}\boldsymbol{\mu}_k\cdot\mathrm{curl}_k\left(\frac{\boldsymbol{\mu}_j\times\mathbf{r}_{kj}}{r_{kj}^3}\right)\right]$$
$$\equiv\sum_k \frac{m\mathbf{v}_k^2}{2}-\tfrac{1}{2}\sum_k e_k\varphi(\mathbf{r}_k)+\tfrac{1}{2}\sum_k\frac{e_k\mathbf{v}_k}{c}\cdot\mathbf{A}(\mathbf{r}_k)+\tfrac{1}{2}\sum_k\boldsymbol{\mu}_k\cdot\mathrm{curl}_k\,\mathbf{A}(\mathbf{r}_k), \quad (18)$$

$$\mathbf{v}_k=\frac{1}{m}\left(\mathbf{p}_k-\sum_j\frac{e_j}{2c}\left(\frac{\mathbf{v}_j}{r_{kj}}+\frac{\mathbf{r}_{kj}(\mathbf{v}_j\cdot\mathbf{r}_{kj})}{r_{kj}^3}\right)-\sum_j\frac{\boldsymbol{\mu}_j\times\mathbf{r}_{kj}}{r_{kj}^3}\right)\equiv\frac{1}{m}\left(\mathbf{p}_k-\frac{e_k}{c}\mathbf{A}(\mathbf{r}_k)\right), \quad (19)$$

$$H=\sum_k\frac{m\mathbf{v}_k^2}{2}+\tfrac{1}{2}\sum_k e_k\varphi(\mathbf{r}_k)+\tfrac{1}{2}\sum_k\frac{e_k}{c}\mathbf{v}_k\cdot\mathbf{A}(\mathbf{r}_k)-\tfrac{1}{2}\sum_k\boldsymbol{\mu}_k\cdot\mathrm{curl}_k\,\mathbf{A}(\mathbf{r}_k) \quad (20)$$
$$=\sum_k\frac{\mathbf{p}_k^2}{2m}+\tfrac{1}{2}\sum_k e_k\varphi(\mathbf{r}_k)-\tfrac{1}{2}\sum_k\frac{e_k}{c}\frac{\mathbf{p}_k}{m}\cdot\mathbf{A}(\mathbf{r}_k)-\tfrac{1}{2}\sum_k\boldsymbol{\mu}_k\cdot\mathrm{curl}_k\,\mathbf{A}(\mathbf{r}_k).$$

Using (19), one may express $\mathbf{A}$ in (17), in terms of the $\mathbf{p}$'s, just as before. Thus

$$\mathbf{A}=\sum_j\frac{e_j}{2mc}\left(\frac{\mathbf{p}_j}{r_{kj}}+\frac{\mathbf{r}_{kj}(\mathbf{p}_j\cdot\mathbf{r}_{kj})}{r_{kj}^3}\right)+\sum_j\frac{\boldsymbol{\mu}_j\times\mathbf{r}_{kj}}{r_{kj}^3}$$
$$-\sum_{j,l}\frac{e_j^2}{2mc^2r_{kj}}\frac{e_l}{2mc}\left[\left(\frac{\mathbf{p}_l}{r_{jl}}+\frac{\mathbf{r}_{jl}(\mathbf{p}_l\cdot\mathbf{r}_{jl})}{r_{jl}^3}\right)+\frac{\mathbf{r}_{kj}}{r_{kj}^2}\mathbf{r}_{kj}\cdot\left(\frac{\mathbf{p}_l}{r_{jl}}+\frac{\mathbf{r}_{jl}(\mathbf{p}_l\cdot\mathbf{r}_{jl})}{r_{jl}^3}\right)\right]-\sum_{j,l}\frac{e_j^2}{2mc^2r_{kj}}$$
$$\times\left[\frac{\boldsymbol{\mu}_l\times\mathbf{r}_{jl}}{r_{jl}^3}+\frac{\mathbf{r}_{kj}}{r_{kj}^2}\mathbf{r}_{kj}\cdot\left(\frac{\boldsymbol{\mu}_l\times\mathbf{r}_{jl}}{r_{jl}^3}\right)\right]. \quad (21)$$

[3a] A moving magnetic dipole gives rise to an electric dipole with moment $\cong\mathbf{v}_j/c\times\boldsymbol{\mu}_j$. The interaction of this electric dipole with the electric field due to the other particles is of the same order in v/c as the spin-orbit term appearing in the Lagrangian (18). It is omitted for reasons of simplicity since its inclusion introduces nothing essentially new.

Upon substitution of this expression for $\mathbf{A}$ into the Hamiltonian (20), the term:

$$-\tfrac{1}{2}\textstyle\sum_k(e_k/c)(\mathbf{p}_k/m)\cdot\mathbf{A}(\mathbf{r}_k)$$

gives the Darwin two-body potential, and the three-body potential obtained before, and in addition, a "spin-orbit" two-body potential and a "spin-orbit" three-body potential. The term: $-\frac{1}{2}\sum_k\boldsymbol{\mu}_k\cdot\mathrm{curl}_k\,\mathbf{A}(\mathbf{r}_k)$ gives "spin-orbit" and "spin-spin" two-body potentials; and "spin-orbit" and "spin-spin" three-body potentials. The "spin-spin" three-body potential is

$$H'(\text{three-body spin-spin})=\sum_{k,j,l}\frac{e_j^2}{4mc^2}\boldsymbol{\mu}_k\cdot\mathrm{curl}_k\left[\frac{1}{r_{kj}}\left(\frac{\boldsymbol{\mu}_l\times\mathbf{r}_{jl}}{r_{jl}^3}\right)+\frac{\mathbf{r}_{kj}}{r_{kj}^3}\mathbf{r}_{kj}\cdot\left(\frac{\boldsymbol{\mu}_l\times\mathbf{r}_{jl}}{r_{jl}^3}\right)\right]\cong\frac{e^2}{mc^2r}\frac{\mu^2}{r^3}. \quad (23)$$

It will be seen below that a three-body potential, with the same spin dependence, as in (23), is of considerable importance in the mesotron field theory of nuclear forces.

In concluding this section it may be pointed out that when the $\mathbf{A}$'s in the Hamiltonian are expressed in terms of $\mathbf{p}_k$, $\mathbf{r}_k$, $\mathbf{s}_k$ one need only apply the commutation relations to these variables, to obtain a quantum-mechanical action-at-a-distance theory of electronic motion.

Quantum Electromagnetic Theory of Electron Dynamics

In the preceding section the classical electromagnetic field was eliminated, to a certain degree of approximation, from the equations of motion of the electrons. The resulting action-at-a-distance Hamiltonian (15), could then be quantized. In the following section the procedure will be reversed: one first quantizes the electromagnetic field, as well as the matter, and then proceeds to an approximate action-at-a-distance description of electronic motion, by means of a quantum-mechanical perturbation method. This method will give not only the same many-body potentials found above ("classical"), but also, many-body potentials explicitly dependent on $\hbar$ ("specifically quantum-mechanical").

The Hamiltonian for the total system, field

and matter, is: (Fourier representation of the quantized field variables[4])

$$H=\{\tfrac{1}{2}\sum_\rho P_\rho^2+\nu_\rho^2 Q_\rho^2\}+\left\{\sum_k \frac{\mathbf{p}_k^2}{2m}+\sum_{k,\,j}{}'\tfrac{1}{2}\frac{e_k e_j}{r_{kj}}\right\}$$
$$+\left\{-\sum_k \frac{e_k}{c}\frac{\mathbf{p}_k}{m}\cdot\mathbf{A}(\mathbf{r}_k)+\sum_k \frac{e_k^2}{2mc^2}(\mathbf{A}(\mathbf{r}_k))^2\right.$$
$$\left.-\sum_k \boldsymbol{\mu}_k\cdot\operatorname{curl}_k \mathbf{A}(\mathbf{r}_k)\right\}$$
$$\equiv H(\text{field})+H(\text{matter})+H(\text{interaction}) \quad (24)$$

with

$$\mathbf{A}(\mathbf{r})=\sum_\rho (4\pi c^2)^{\frac{1}{2}}\mathbf{a}_\rho\left(Q_\rho\cos(\mathbf{k}_\rho\cdot\mathbf{r})-\frac{P_\rho}{\nu_\rho}\sin(\mathbf{k}_\rho\cdot\mathbf{r})\right)$$
$$=\sum_\rho (4\pi c^2)^{\frac{1}{2}}\mathbf{a}_\rho(q_\rho\exp(i\mathbf{k}_\rho\cdot\mathbf{r}) \quad (25)$$
$$+q_\rho^*\exp(-i\mathbf{k}_\rho\cdot\mathbf{r}))$$
$$=\sum_\rho q_\rho\mathbf{A}_\rho+q_\rho^*\mathbf{A}_\rho^*,$$
$$\text{div. }\mathbf{A}=0;\quad |\mathbf{a}_\rho|^2=1. \quad (26)$$

In the eigenstates $\Psi(Q_\rho, \mathbf{r}_j)$ of H, the number of light quanta is not specified, i.e.

$$\Psi(Q_\rho,\mathbf{r}_j)=\sum_{a;\,n_\rho} c_{a,\,n_\rho}\psi_a(\mathbf{r}_j)\varphi_{n_\rho}(Q_\rho) \quad (27)$$

with

$$H(\text{matter})\ \psi_a(\mathbf{r}_j)=\epsilon_a\psi_a(\mathbf{r}_j),$$
$$H(\text{field})\ \varphi_{n_\rho}(Q_\rho)=[\sum_\rho (n_\rho+\tfrac{1}{2})\hbar\nu_\rho]\varphi_{n_\rho}(Q_\rho). \quad (28)$$

The elimination of the field variables, and the consequent action-at-a-distance dynamical description of the particles, corresponds, in quantum mechanics, to the consideration of transitions of the system among states, where the number of light quanta is always zero, i.e., states of type

$$\Psi(Q_\rho,\mathbf{r}_j)=\{\sum_{a',\,0_\rho} c_{a',\,0_\rho}\psi_{a'}(\mathbf{r}_j)\}\varphi_{0_\rho}(Q_\rho). \quad (29)$$

In particular, one may limit the discussion to transitions among the matter eigenstates, i.e., $c_{a',\,0_\rho}=\delta_{a',\,a}$. The transitions among the states ψ_a, caused by H(interaction), i.e., by the virtual emission and absorption of light quanta, are now to be regarded as caused by an equivalent action-at-a-distance potential H'. The dependence of H' on the particle coordinates is to be such that the transition probabilities between the matter states ψ_a, with H' as perturbing potential, are identical to any desired approximation, with those arising from H(interaction) in the complete field theory.

It is to be noted that the quantum-mechanical method of eliminating the field variables, is necessarily of a perturbation character of successive approximations, since one must consider transitions between states in which no quanta are present. Such a treatment, as already observed above, leads to two types of many-body potentials, "classical" and "specifically quantum-mechanical," which are discussed in order.

(a) Classical many-body potentials

In a system, consisting, for simplicity, of only *three* electrons and the radiation field, the following type of transition takes place: The first electron, say, *simultaneously* emits two virtual light quanta, by means of the $(e^2/2mc^2)(\mathbf{A}(\mathbf{r}_1))^2$ term in the perturbation; one of these virtual light quanta is absorbed by the second electron by means of the $-(e\mathbf{p}_2/cm)\cdot\mathbf{A}(\mathbf{r}_2)$ term, while the other is absorbed by the third electron by means of the $-(e\mathbf{p}_3/cm)\cdot\mathbf{A}(\mathbf{r}_3)$ term. The matrix element for this transition, which depends on the instantaneous coordinates of all the three electrons, is given by

$$\sum_{n,\,n'}{}'\frac{\left(i\left|\frac{e^2}{2mc^2}(\mathbf{A}(\mathbf{r}_1))^2\right|n\right)\left(n\left|-\frac{e}{c}\frac{\mathbf{p}_2}{m}\cdot\mathbf{A}(\mathbf{r}_2)\right|n'\right)\left(n'\left|-\frac{e}{c}\frac{\mathbf{p}_3}{m}\cdot\mathbf{A}(\mathbf{r}_3)\right|f\right)}{(E_i-E_n)(E_i-E_{n'})}. \quad (30)$$

The initial and final states i, and f, are characterized by no virtual light quanta present and matter wave functions ψ_i and ψ_f; the intermediate states n, n' have, respectively, two and one virtual light quanta present, and matter wave functions ψ_n, $\psi_{n'}$.

[4] W. Heitler, reference 1, paragraphs 6 and 7.

Employing the customary expressions for the matrix elements of emission and absorption of the virtual light quanta,[5] neglecting recoil energies of the electrons, using the completeness relations for the matter wave functions, and adding over the possible polarization directions of the virtual light quanta, as well as over all possible permutations of the order of their emission and absorption, one obtains for the matrix element (30):

$$\int \psi_i^* \left\{ \sum_{\rho\rho'} \frac{16\pi^2 e^4 \exp(i\mathbf{k}_\rho \cdot \mathbf{r}_{12}) \exp(i\mathbf{k}_{\rho'} \cdot \mathbf{r}_{13})(\mathbf{p}_2 - \mathbf{k}_\rho(\mathbf{p}_2 \cdot \mathbf{k}_\rho)/k_\rho^2)(\mathbf{p}_3 - \mathbf{k}_{\rho'}(\mathbf{p}_3 \cdot \mathbf{k}_{\rho'})/k_{\rho'}^2)}{m^3 \nu_\rho^2 \nu_{\rho'}^2} \right\} \psi_f d\tau_1 d\tau_2 d\tau_3. \quad (31)$$

Thus, the equivalent action-at-a-distance three-body potential, H', becomes

$$\left(\nu_\rho = ck_\rho; \quad \sum_\rho f(\mathbf{k}_\rho) \rightarrow \frac{1}{(2\pi)^3} \int f(\mathbf{k}_\rho) d\mathbf{k}_\rho \right)$$

$$H'(r_{12}, r_{13}) = \sum_{\rho, \rho'} \frac{16\pi^2 e^4 \exp(i\mathbf{k}_\rho \cdot \mathbf{r}_{12}) \exp(i\mathbf{k}_{\rho'} \cdot \mathbf{r}_{13})(\mathbf{p}_2 - \mathbf{k}_\rho(\mathbf{p}_2 \cdot \mathbf{k}_\rho)/k_\rho^2)(\mathbf{p}_3 - \mathbf{k}_{\rho'}(\mathbf{p}_3 \cdot \mathbf{k}_{\rho'})/k_{\rho'}^2)}{m^3 \nu_\rho^2 \nu_{\rho'}^2}$$

$$= \frac{1}{4\pi^4} \frac{e^4}{m^3 c^4} \int \frac{\exp(i\mathbf{k}_\rho \cdot \mathbf{r}_{12})}{k_\rho^2} \left(\mathbf{p}_2 - \frac{\mathbf{k}_\rho(\mathbf{p}_2 \cdot \mathbf{k}_\rho)}{k_\rho^2} \right) d\mathbf{k}_\rho \int \frac{\exp(i\mathbf{k}_{\rho'} \cdot \mathbf{r}_{13})}{k_{\rho'}^2} \left(\mathbf{p}_3 - \frac{\mathbf{k}_{\rho'}(\mathbf{p}_3 \cdot \mathbf{k}_{\rho'})}{k_{\rho'}^2} \right) d\mathbf{k}_{\rho'}. \quad (32)$$

Now

$$\int \frac{\exp(i\mathbf{k}_\rho \cdot \mathbf{r}_{12})}{k_\rho^2} \left(\mathbf{p}_2 - \frac{\mathbf{k}_\rho(\mathbf{p}_2 \cdot \mathbf{k}_\rho)}{k_\rho^2} \right) d\mathbf{k}_\rho = \pi^2 \frac{1}{r_{12}} \left(\mathbf{p}_2 + \frac{\mathbf{r}_{12}(\mathbf{p}_2 \cdot \mathbf{r}_{12})}{r_{12}^2} \right),$$

whence

$$H'(r_{12}, r_{13}) = \frac{e^4}{4m^3 c^4} \left(\frac{\mathbf{p}_2}{r_{12}} + \frac{\mathbf{r}_{12}(\mathbf{p}_2 \cdot \mathbf{r}_{12})}{r_{12}^3} \right) \left(\frac{\mathbf{p}_3}{r_{13}} + \frac{\mathbf{r}_{13}(\mathbf{p}_3 \cdot \mathbf{r}_{13})}{r_{13}^3} \right), \quad (33)$$

which is just the term obtained in the classical treatment, above.[6] (Cf. Eq. (15).)

If one considers three-body potentials arising from the same type of transition as before, except that $-\boldsymbol{\mu}_2 \cdot \mathrm{curl}_2 \mathbf{A}(\mathbf{r}_2)$, and $-\boldsymbol{\mu}_3 \cdot \mathrm{curl}_3 \mathbf{A}(\mathbf{r}_3)$ replace $-(e\mathbf{p}_2/cm) \cdot \mathbf{A}(\mathbf{r}_2)$, and $-(e\mathbf{p}_3/cm) \cdot \mathbf{A}(\mathbf{r}_3)$, one obtains "spin-spin" three-body potentials, which again, are just the same as those obtained in classical theory. (Cf. Eq. (23).)

(b) Specifically quantum-mechanical many-body potentials

Consider, again, a system of three electrons and the radiation field. In addition to the transitions discussed above, the following type of process also takes place: one electron emits two virtual light quanta, *in succession;* one of these quanta is absorbed by the second electron, the other by the third. The perturbation energy responsible for any one of these single absorptions or emissions is either

$$-\boldsymbol{\mu}_k \cdot \mathrm{curl}_k \mathbf{A}(\mathbf{r}_k), \quad \text{or} \quad -(e\mathbf{p}_k/cm) \cdot \mathbf{A}(\mathbf{r}_k).$$

Only the first of these perturbations will be treated explicitly, since in the mesotron field theory of nuclear interaction, which has a formalism almost identical with that of electromagnetic theory, the term analogous to

$$-\boldsymbol{\mu}_k \cdot \mathrm{curl}_k \mathbf{A}(\mathbf{r}_k),$$

gives by far the largest effect.

The matrix element corresponding to the transition described in the preceding paragraph, is

$$\sum_{n, n', n''} \frac{(i|\boldsymbol{\mu}_1 \cdot \mathrm{curl}_1 \mathbf{A}(\mathbf{r}_1)|n)(n|\boldsymbol{\mu}_1 \cdot \mathrm{curl}_1 \mathbf{A}(\mathbf{r}_1)|n')(n'|\boldsymbol{\mu}_2 \cdot \mathrm{curl}_2 \mathbf{A}(\mathbf{r}_2)|n'')(n''|\boldsymbol{\mu}_3 \cdot \mathrm{curl}_3 \mathbf{A}(\mathbf{r}_3)|f)}{(E_i - E_n)(E_i - E_{n'})(E_i - E_{n''})}, \quad (34)$$

[5] W. Heitler, reference 1, pp. 95 and 96, Eqs. (12) and (13).

[6] A symmetrical expression in the indices 1, 2, 3, is obtained by interchanging the roles which the particles play in the transition process.

The initial and final states, i and f, are characterized by no virtual light quanta present and matter wave functions ψ_i and ψ_f; the intermediate states have, respectively, one, two, and one virtual light quanta present, and matter wave functions ψ_n, $\psi_{n'}$, $\psi_{n''}$.

The matrix element of $-\boldsymbol{\mu}_1\cdot\mathrm{curl}_1\,\mathbf{A}(\mathbf{r}_1)$ for the emission of a light quantum of frequency ν_ρ, and the transition of the three electrons, from ψ_i to ψ_n, is:

$$-\int\psi_n^*\boldsymbol{\mu}_1\cdot\mathrm{curl}_1\left((4\pi c^2)^{\frac{1}{2}}(\hbar/2\nu_\rho)^{\frac{1}{2}}\mathbf{a}_\rho\exp\left(i\mathbf{k}_\rho\cdot\mathbf{r}_1\right)\right)\times\psi_i d\mathbf{r}_1 d\mathbf{r}_2 d\mathbf{r}_3 \quad (35)$$

and similarly for the other emissions and absorptions.

Substituting (35) into (34), neglecting recoil energies, and making use of the completeness relations for the matter wave functions, one obtains for (34):

$$-\int\psi_i^*\left\{\frac{4\pi^2c^4}{\hbar}\left(\boldsymbol{\mu}_1\cdot\mathrm{curl}_1\sum_\rho\mathbf{a}_\rho\exp\left(i\mathbf{k}_\rho\cdot\mathbf{r}_1\right)\boldsymbol{\mu}_2\cdot\mathrm{curl}_2(\mathbf{a}_\rho\exp\left(-i\mathbf{k}_\rho\cdot\mathbf{r}_2\right)\right)\times\left(\boldsymbol{\mu}_1\cdot\mathrm{curl}_1\sum_{\rho'}\frac{\mathbf{a}_{\rho'}\exp\left(i\mathbf{k}_{\rho'}\cdot\mathbf{r}_1\right)\boldsymbol{\mu}_3\cdot\mathrm{curl}_3(\mathbf{a}_{\rho'}\exp\left(-i\mathbf{k}_{\rho'}\cdot\mathbf{r}_3\right))}{(\nu_\rho\nu_{\rho'})(\nu_\rho(\nu_\rho+\nu_{\rho'})\nu_{\rho'})}\right)\right\}\psi_f d\mathbf{r}_1 d\mathbf{r}_2 d\mathbf{r}_3. \quad (36)$$

Summing over the possible polarization directions of the virtual light quanta, one obtains

$$-\int\psi_i^*\left\{\frac{4\pi^2c^4}{\hbar}\boldsymbol{\mu}_1\cdot\mathrm{curl}_1\sum_\rho\mathrm{curl}_2\left(\boldsymbol{\mu}_2\cdot\exp\left(i\mathbf{k}_\rho\cdot\mathbf{r}_{12}\right)\boldsymbol{\mu}_1\cdot\mathrm{curl}_1\sum_{\rho'}\frac{\mathrm{curl}_3\left(\boldsymbol{\mu}_3\exp\left(i\mathbf{k}_{\rho'}\cdot\mathbf{r}_{13}\right)\right)}{\nu_\rho^2\nu_{\rho'}^2(\nu_\rho+\nu_{\rho'})}\right\}\psi_f d\mathbf{r}_1 d\mathbf{r}_2 d\mathbf{r}_3. \quad (37)$$

The equivalent action-at-a-distance three-body potential, corresponding to a process where ν_ρ is the first to be emitted, and first to be absorbed, is thus given by the quantity inside the curly brackets in (37). Taking into account all possible orders of emission and absorption of the virtual light quanta ν_ρ, $\nu_{\rho'}$, one obtains, for the three-body potential, $H''(r_{12}, r_{13})$:

$$H''(r_{12}, r_{13})=-\frac{4\pi^2}{\hbar c}\left[\boldsymbol{\mu}_1\cdot\mathrm{curl}_1\sum_\rho\frac{\mathrm{curl}_2\left(\boldsymbol{\mu}_2\exp\left(i\mathbf{k}_\rho\cdot\mathbf{r}_{12}\right)\right)}{\nu_\rho^3/c^3}\right]\times\left[\boldsymbol{\mu}_1\cdot\mathrm{curl}_1\sum_{\rho'}\frac{\mathrm{curl}_3\left(\boldsymbol{\mu}_3\exp\left(i\mathbf{k}_{\rho'}\cdot\mathbf{r}_{13}\right)\right)}{\nu_{\rho'}^3/c^3}\right] \quad (38)$$

+same term with indices 2 and 3 interchanged.

With $\nu_\rho/c=k_\rho$, and $\sum_\rho f(\mathbf{k}_\rho)\rightarrow\frac{1}{(2\pi)^3}\int f(\mathbf{k}_\rho)d\mathbf{k}_\rho$

the first bracket becomes

$$\frac{1}{(2\pi)^2}\boldsymbol{\mu}_1\cdot\mathrm{curl}_1\left(\frac{\mathbf{r}_{12}\times\boldsymbol{\mu}_2}{r_{12}^2}\right), \quad (38a)$$

while the second bracket is equal to

$$-\frac{1}{4\pi}\boldsymbol{\mu}_1\cdot\mathrm{curl}_1^2\left(\frac{\boldsymbol{\mu}_3}{r_{13}}\right), \quad (38b)$$

being, apart from the numerical factor $1/4\pi$, just the spin-spin two-body potential between the first and third particle.

Thus,

$$H''(r_{12}, r_{13})=\frac{1}{2\pi\hbar c}\left[\boldsymbol{\mu}_1\cdot\mathrm{curl}_1\left(\frac{\mathbf{r}_{12}\times\boldsymbol{\mu}_2}{r_{12}^2}\right)\right]\times\left[\boldsymbol{\mu}_1\cdot\mathrm{curl}_1^2\left(\frac{\boldsymbol{\mu}_3}{r_{13}}\right)\right] \quad (39)$$

+same term with indices 2 and 3 interchanged $\leqq\mu^4/\hbar c r^6$.

Orders of Magnitude of Electromagnetic Many-Body Potentials in Atomic Systems

The magnitudes of the many-body potentials, in particular of the three-body potentials, will now be estimated. Suppose the three electrons are orbital electrons in an atom. Then, on the average, the distances $r_{kj}\leqq r$, between the electrons are of the order of Bohr radii, and are related to the electronic velocities, v, by: $r\leqq\hbar/mv$; the electronic magnetic moments μ are $\leqq e\hbar/mc\leqq erv/c$. Thus, from Eqs. (15), (16), (33), the relation between the magnitudes of the individual terms in the velocity-dependent three-body po-

tential and in the Coulomb two-body potential, is

$$H'(\text{three-body vel.-depend.}) \leqq \frac{e^2}{mc^2 r}\frac{v^2}{c^2}\frac{e^2}{r} \leqq \frac{1}{137}\left(\frac{v}{c}\right)^3 H(\text{Coulomb}). \quad (40)$$

Further, from Eq. (23),

$$H'(\text{three-body spin-spin}) \leqq \frac{e^2}{mc^2 r}\frac{\mu^2}{r^3} \leqq \frac{e^2}{mc^2 r}\left(\frac{\hbar/mc}{r}\right)^2\frac{e^2}{r} \leqq \frac{1}{137}\left(\frac{v}{c}\right)^3 H(\text{Coulomb}). \quad (41)$$

Finally, for the specifically quantum three-body potential (cf. Eq. (39)),

$$H'' \leqq \frac{\mu^4}{\hbar c}\frac{1}{r^5} \leqq \frac{e^2}{\hbar c}\left(\frac{\hbar/mc}{r}\right)^4\frac{e^2}{r} \leqq \frac{1}{137}\left(\frac{v}{c}\right)^4 H(\text{Coulomb}). \quad (42)$$

It is therefore clear that the description of the electromagnetic interaction of electrons in atomic systems, by means of action-at-a-distance two-body potentials, is an extraordinarily good approximation,[6a] since $v/c \leqq Z/137$.[6b]

Mesotron Field Theory of Nuclear Interaction

(a) Elimination of field variables for the "classical" mesotron field

The mesotron theory of the interaction of nuclear heavy particles[7] (protons and neutrons) is closely modeled upon the electromagnetic theory of electron interaction. Here the variables of the system also fall into two categories: those describing the motion of the heavy particles and those describing the state of the field. The dynamical relations between these two sets of variables are given by equations analogous to the Maxwell equations and the Lorentz force formula; the heavy particles act as sources of the field, and the field in turn affects the motion of the heavy particles. The characteristic difference between this theory and that of Maxwell is the appearance of a fundamental length, R, in the field equations; a consequence of this new constant in the quantized form of the theory, is the existence of "quanta" of rest mass, $m_0 = \hbar/cR$.

The mesotron field due to mesotron-charge, mesotron-current, mesotron-magnetization and mesotron-polarization densities of the heavy particles,[8] ρ, $\boldsymbol{I}$, $\boldsymbol{M}$, $\boldsymbol{P}$ is specified by two six-vectors[9] $\boldsymbol{E}$, $\boldsymbol{B}$; $\boldsymbol{E}^*$, $\boldsymbol{B}^*$, and two four-vectors Φ, $\boldsymbol{A}$; Φ^*, $\boldsymbol{A}^*$ satisfying the equations:

$$\boldsymbol{B} = \text{curl } \boldsymbol{A}, \quad (43)$$

$$\boldsymbol{E} = -\frac{1}{c}\frac{\partial \boldsymbol{A}}{\partial t} - \text{grad. } \Phi, \quad (44)$$

$$\text{curl } \boldsymbol{B} = \frac{4\pi \boldsymbol{I}}{c} + \frac{4\pi}{c}\frac{\partial \boldsymbol{P}}{\partial t} + 4\pi \text{ curl } \boldsymbol{M} + \frac{1}{c}\frac{\partial \boldsymbol{E}}{\partial t} - \frac{1}{R^2}\boldsymbol{A}, \quad (45)$$

$$\text{div. } \boldsymbol{E} = 4\pi\rho - 4\pi \text{ div. } \boldsymbol{P} - \frac{1}{R^2}\Phi. \quad (46)$$

Taking the div. of (45) and the time derivative of (46), one obtains:

$$0 = \text{div. } \boldsymbol{I} + \frac{\partial \rho}{\partial t} - \frac{1}{R^2}\left(\frac{\partial \Phi}{\partial t} + \text{div. } \boldsymbol{A}\right) \quad (47)$$

[6a] See, however, the Addendum.

[6b] Z is the effective nuclear charge for the electron in question.

[7] The "vector" mesotron field theory will be used, since it gives the correct sign for the neutron-proton two-body potential. For a general discussion of mesotron theory, see H. Yukawa, Proc. Phys.-Math. Soc. Jap. **17**, 48 (1935); **19**, 1084 (1937); **20**, 320 (1938); also H. Bhabha, Proc. Roy. Soc. **166**, 501 (1938); N. Kemmer, Proc. Roy. Soc. **166**, 127 (1938); Frohlich, Heitler and Kemmer, Proc. Roy. Soc. **166**, 154 (1938). The use of a linear combination of the "scalar," "vector," "pseudo vector" and "pseudo scalar" charged mesotron fields, and/or of uncharged mesotrons, would not essentially alter any of the results on many-body interactions obtained below. (See section .n present paper on general field theory.)

It may be pointed out that the singularities in the mesotron field equations are exactly of the same type as the singularities in the electromagnetic field equations. Hence, the mesotron theory convergence difficulties are no better, and no worse, than those of electromagnetism; cf, H. Bhabha, Nature **143**, 276 (1939).

[8] $\rho = |\rho|\Pi$; $\rho^* = |\rho|\Pi^*$ where the Π and Π^* are operators (complex conjugate to each other) changing the heavy particle from a proton to a neutron, and from a neutron to a proton, respectively. Similarly for $\boldsymbol{I}$, $\boldsymbol{M}$, $\boldsymbol{P}$.

[9] Here the asterisks denote complex conjugates.

and so, if charge-current is to be conserved, the potentials must satisfy the "Lorentz" condition.

$$\frac{\partial\Phi}{\partial t}+\text{div. } \boldsymbol{A}=0. \tag{48}$$

Second-order equations for the potentials may be obtained in the usual way:

$$\nabla^2\Phi-\frac{1}{R^2}\Phi-\frac{1}{c^2}\frac{\partial^2\Phi}{\partial t^2}=-4\pi(\rho-\text{div. } \boldsymbol{P}), \tag{49}$$

$$\nabla^2\boldsymbol{A}-\frac{1}{R^2}\boldsymbol{A}-\frac{1}{c^2}\frac{\partial^2\boldsymbol{A}}{\partial t^2}=-4\pi\left(\frac{\boldsymbol{I}}{c}+\text{curl } \boldsymbol{M}+\frac{1}{c}\frac{\partial\boldsymbol{P}}{\partial t}\right). \tag{50}$$

Finally, the equation of motion of a heavy particle in presence of potentials Φ, $\boldsymbol{A}$ is[10]

$$M\mathbf{a}_k=\left\{g_k^*\left(-\text{grad. }\Phi-\frac{1}{c}\frac{\partial\boldsymbol{A}}{\partial t}\right)+g_k^*\frac{\mathbf{v}_k}{c}\times\text{curl } \boldsymbol{A}+\text{grad. }(\boldsymbol{\mu}_k^*\cdot\text{curl } \boldsymbol{A})+\text{grad.}\left(\boldsymbol{p}_k^*\cdot\left(-\text{grad. }\Phi-\frac{1}{c}\frac{\partial\boldsymbol{A}}{\partial t}\right)\right)+\text{comp. conj.}\right\},\quad k=1,\cdots,n, \tag{51}$$

where $g_k^*=g\Pi_k^*$, $\boldsymbol{\mu}_k^*=\boldsymbol{\mu}\Pi_k^*$, $\boldsymbol{p}^*=\boldsymbol{p}\Pi_k^*$ (see footnote 8) with g, $\boldsymbol{\mu}$, $\boldsymbol{p}$, the mesotron-charge, mesotron-magnetic moment, mesotron-electric moment of the heavy particle. Terms involving $\boldsymbol{p}\cong\mathbf{v}/c\times\boldsymbol{\mu}$ will be consistently omitted in what follows, since they do not essentially affect any of the subsequent results.

The potentials Φ, $\boldsymbol{A}$ arise from the other heavy particles. As in electromagnetic theory, to obtain an action-at-a-distance description, one attempts to express Φ, $\boldsymbol{A}$ in terms of the instantaneous relative heavy-particle coordinates. Approximate solutions of (49), (50), for point sources, are[11]

$$\Phi(\mathbf{r}_k,t)=\sum_j g_j\frac{e^{-r_{kj}/R}}{r_{kj}}+\text{terms in }\frac{\mathbf{v}_j^2}{c^2},\ \frac{\mathbf{a}_j}{c^2},\text{ etc.} \tag{52}$$

$$\boldsymbol{A}(\mathbf{r}_k,t)=\sum_j\frac{g_j\mathbf{v}_j}{c}\frac{e^{-r_{kj}/R}}{r_{kj}}+\sum_j\boldsymbol{\mu}_j\times\text{grad.}_j\left(\frac{e^{-r_{kj}/R}}{r_{kj}}\right)+\text{terms in }\frac{\mathbf{v}_j^2}{c^2},\ \frac{\mathbf{a}_j}{c^2},\ \frac{d\boldsymbol{\mu}_j}{dt},\ \frac{d^2\boldsymbol{\mu}_j}{dt^2},\text{ etc.} \tag{53}$$

The equations of motion (51), with Φ and $\boldsymbol{A}$ expressed by means of the sums in (52), (53), are derivable from the following Lagrangian and Hamiltonian:

$$L=\sum_k\frac{M\mathbf{v}_k^2}{2}+\left\{-\tfrac{1}{2}\sum_k g_k^*\Phi(\mathbf{r}_k)+\tfrac{1}{2}\sum_k\frac{g_k^*}{c}\mathbf{v}_k\cdot\boldsymbol{A}(\mathbf{r}_k)+\tfrac{1}{2}\sum_k\boldsymbol{\mu}_k^*\cdot\text{curl}_k\,\boldsymbol{A}(\mathbf{r}_k)+\text{c.c.}\right\}, \tag{54}$$

$$H=\sum_k\frac{\boldsymbol{p}_k^2}{2M}+\left\{\tfrac{1}{2}\sum_k g_k^*\Phi(\mathbf{r}_k)-\tfrac{1}{2}\sum_k\frac{g_k^*}{c}\frac{\boldsymbol{p}_k}{M}\cdot\boldsymbol{A}(\mathbf{r}_k)-\tfrac{1}{2}\sum_k\boldsymbol{\mu}_k^*\cdot\text{curl}_k\,\boldsymbol{A}(\mathbf{r}_k)+\text{c.c.}\right\}. \tag{55}$$

In H, the $\boldsymbol{A}$'s are to be expressed in terms of the $\mathbf{p}$'s by means of the equations:

$$\boldsymbol{A}(\mathbf{r}_k)=\sum_j\frac{g_j}{cM}\frac{(\mathbf{p}_j-((g_j^*/c)\boldsymbol{A}(\mathbf{r}_j)+\text{c.c.}))e^{-r_{kj}/R}}{r_{kj}}+\sum_j\boldsymbol{\mu}_j\times\text{grad.}_j\left(\frac{e^{-r_{kj}/R}}{r_{kj}}\right)=\sum_j\frac{g_j}{c}\frac{\mathbf{p}_j}{M}\frac{e^{-r_{kj}/R}}{r_{kj}}+\sum_j\boldsymbol{\mu}_j\times\text{grad.}_j\left(\frac{e^{-r_{kj}/R}}{r_{kj}}\right)-\sum_{j,\,l}\frac{g_jg_j^*e^{-r_{kj}/R}}{Mc^2r_{kj}}\frac{g_l\mathbf{p}_l}{Mc}\frac{e^{-r_{jl}/R}}{r_{jl}}-\sum_{j,\,l}\frac{g_jg_j^*e^{-r_{kj}/R}}{Mc^2r_{kj}}\boldsymbol{\mu}_l\times\text{grad.}_l\left(\frac{e^{-r_{jl}/R}}{r_{jl}}\right)+\text{terms of higher order in }g^2/Mc^2r_{kj}. \tag{56}$$

[10] The classical equation of motion (51) can be considered in quantum mechanics, as an equation of motion between operators; in this sense it is equivalent to the wave equation (11) given by Bhabha, reference 7.

[11] These solutions, including explicit expressions for the terms in $\mathbf{v}_j^2/c^2$, $\mathbf{a}_j/c^2$, $d\boldsymbol{\mu}_j/dt$, $d^2\mathbf{u}_j/dt^2$ are obtained in Appendix I. The only terms which are treated in the text are those explicitly written out in Eqs, (52), (53), For a discussion of the acceleration-dependent terms, see the Addendum.

Substituting for $A(\mathbf{r}_k)$, one obtains for the Hamiltonian (55):

$$H=\sum_k \frac{\mathbf{p}_k^2}{2M}+\left\{\left[\tfrac{1}{2}\sum_{k,j}\frac{g_k^* g_j}{r_{kj}}e^{-r_{kj}/R}\right]\right.$$

$$+\left[-\tfrac{1}{2}\sum_{k,j}\boldsymbol{\mu}_k^*\cdot\mathrm{curl}_k\left(\boldsymbol{\mu}_j\times\mathrm{grad}._j\left(\frac{e^{-r_{kj}/R}}{r_{kj}}\right)\right)\right]$$

$$+\left[-\tfrac{1}{2}\sum_{k,j}\boldsymbol{\mu}_k^*\cdot\mathrm{curl}_k\left(\frac{g_j}{c}\frac{\mathbf{p}_j}{M}\frac{e^{-r_{kj}/R}}{r_{kj}}\right)\right.$$

$$\left.-\tfrac{1}{2}\sum_{k,j}\frac{g_k^*}{c}\frac{\mathbf{p}_k}{M}\cdot\boldsymbol{\mu}_j\times\mathrm{grad}._j\left(\frac{e^{-r_{kj}/R}}{r_{kj}}\right)\right]$$

$$+\left[-\tfrac{1}{2}\sum_{k,j}\frac{g_k^* g_j}{M^2c^2}\frac{\mathbf{p}_k\cdot\mathbf{p}_j}{r_{kj}}e^{-r_{kj}/R}\right]$$

$$+\left[\tfrac{1}{2}\sum_{k,j,l}\frac{g_j g_l^*}{Mc^2}\boldsymbol{\mu}_k^*\cdot\mathrm{curl}_k\left(\frac{e^{-r_{kj}/R}}{r_{kj}}\boldsymbol{\mu}_l\right.\right.$$

$$\left.\left.\times\mathrm{grad}._l\left(\frac{e^{-r_{jl}/R}}{r_{jl}}\right)\right)\right]$$

$$+\left[\tfrac{1}{2}\sum_{k,j,l}\frac{g_k^* g_j g_l^*}{M^2c^4}\frac{\mathbf{p}_k\cdot\mathbf{p}_l e^{-r_{kj}/R}e^{-r_{jl}/R}}{r_{kj}r_{jl}}\right]$$

$$+\left[\tfrac{1}{2}\sum_{k,j,l}\frac{g_k^* g_j g_l^*}{M^2c^3}\mathbf{p}_k\left(\frac{e^{-r_{kj}/R}}{r_{kj}}\right)\cdot\boldsymbol{\mu}_l\times\mathrm{grad}._l\left(\frac{e^{-r_{jl}/R}}{r_{jl}}\right)\right.$$

$$\left.+\tfrac{1}{2}\sum_k\frac{g_j g_l^* g_l}{M^2c^3}\boldsymbol{\mu}_k^*\cdot\mathrm{curl}_k\left(\mathbf{p}_l\frac{e^{-r_{kj}/R}}{r_{kj}}\frac{e^{-r_{jl}/R}}{r_{jl}}\right)\right]$$

$$\left.+\text{terms of higher order in }\frac{g^2}{Mc^2r}+\text{c.c.}\right\} \quad (57)$$

$$\equiv H(\text{kinetic})+H(\text{two-body "Coulomb"})$$
$$+H(\text{two-body spin-spin})$$
$$+H(\text{two-body spin orbit})$$
$$+H(\text{two-body vel.-depend.})$$
$$+H(\text{three-body spin-spin})$$
$$+H(\text{three-body vel.-depend})$$
$$+H(\text{three-body spin-orbit}).$$

The two-body "Coulomb" and two-body spin-spin interaction Hamiltonians have already been discussed by the authors of reference 7.[11a] The order of magnitude of the other two-body interactions, as well as of all of the three-body interactions, will be given in a later section.

[11a] The procedure of solving the equations of the mesotron potentials in order to obtain two-body Coulomb and two-body spin-spin interactions was introduced by Yukawa, reference 7. Recently these interactions have been derived by Stueckelberg by a method of canonical transformation; Phys. Rev. **54**, 889 (1938). A treatment similar to Stueckelberg's has been reported by E. Feenberg, December meeting of the American Physical Society, 1938.

(b) Quantum mesotron theory

In the preceding section, the unquantized mesotron field was approximately eliminated, and an action-at-a-distance dynamical description of the heavy particles obtained in terms of a Hamiltonian (Eq. (57)) which could then be quantized. The elimination of the *quantized* mesotron field gives results similar to the corresponding treatment in electromagnetic theory; on the one hand the classical Hamiltonian (57) is confirmed, and on the other hand, additional specifically quantum many-body potentials are obtained.

Since the Hamiltonian formalism of the quantized mesotron theory is somewhat different from the formalism of electrodynamics (due to the fundamental length), it will be discussed briefly.

In the Fourier representation of the field:

$$\Phi(\mathbf{r},t)=\sum_\sigma a_\sigma(t)\Phi_\sigma(\mathbf{r})$$

$$=\sum_\sigma a_\sigma(t)(4\pi c^3)^{-\frac{1}{2}}\exp(i\mathbf{k}_\sigma\cdot\mathbf{r}), \quad (58)$$

$$\boldsymbol{A}_L(\mathbf{r},t)=\sum_\sigma q_\sigma(t)\boldsymbol{A}_\sigma(r)=\sum_\sigma q_\sigma(t)\frac{1}{k_\sigma}\mathrm{grad}.\,\Phi_\sigma(\mathbf{r});$$

$$\mathrm{curl}\,\boldsymbol{A}_L=0, \quad (59)$$

$$\boldsymbol{A}_T(\mathbf{r},t)=\sum_\rho q_\rho(t)\boldsymbol{A}_\rho(r)$$

$$=\sum_\rho q_\rho(t)(4\pi c^3)^{-\frac{1}{2}}\mathbf{a}_\rho\exp(i\mathbf{k}_\rho\cdot\mathbf{r});$$

$$\mathrm{div}.\,\boldsymbol{A}_T=0,\ |\mathbf{a}_\rho|^2=1, \quad (60)$$

$$\boldsymbol{A}(\mathbf{r},t)=\boldsymbol{A}_L(\mathbf{r},t)+\boldsymbol{A}_T(\mathbf{r},t). \quad (61)$$

The potential equations (49), (50), and the Lorentz condition (48), become:

$$\ddot{a}_\sigma+\nu_\sigma^2 a_\sigma=\sum_k g_k\Phi_\sigma^*(\mathbf{r}_k), \quad (62)$$

$$\ddot{q}_\sigma+\nu_\sigma^2 q_\sigma=\sum_k \frac{g_k}{c}\mathbf{v}_k\cdot \boldsymbol{A}_\sigma^*(\mathbf{r}_k), \tag{63}$$

$$\ddot{q}_\rho+\nu_\rho^2 q_\rho=\sum_k \frac{g_k}{c}\mathbf{v}_k\cdot \boldsymbol{A}_\rho^*(\mathbf{r}_k) +\sum_k \boldsymbol{\mu}_k^*\cdot \mathrm{curl}_k\, \boldsymbol{A}_\rho^*(\mathbf{r}_k), \tag{64}$$

$$\dot{a}_\sigma=ck_\sigma q_\sigma, \tag{65}$$

$$\nu^2=c^2k^2+\frac{c^2}{R^2}. \tag{66}$$

The equations of motion of the heavy particles (51), are:

$$M\mathbf{a}_k=\Big\{g_k^*\Big(-\mathrm{grad.}_k \sum_\sigma a_\sigma\Phi_\sigma(\mathbf{r}_k)-\frac{1}{c}\sum_\sigma \dot{q}_\sigma \boldsymbol{A}_\sigma(\mathbf{r}_k) -\frac{1}{c}\sum_\rho \dot{q}_\rho \boldsymbol{A}_\rho(\mathbf{r}_k)\Big)+\frac{g_k^*}{c}\mathbf{v}_k\times\mathrm{curl}_k \sum_\rho q_\rho \boldsymbol{A}_\rho(\mathbf{r}_k), +\mathrm{grad.}_k\Big(\boldsymbol{\mu}_k^*\cdot\mathrm{curl}_k \sum_\rho q_\rho \boldsymbol{A}_\rho(\mathbf{r}_k)\Big)+\mathrm{c.c.}\Big\}, \tag{67}$$

$$k=1,\ \cdots,\ n.$$

Inspection indicates that the above equations of motion, for field and matter, are derivable from the following Lagrangian and Hamiltonian:[12]

$$L=\sum_\rho(\dot{q}_\rho^*\dot{q}_\rho-\nu_\rho^2 q_\rho^* q_\rho)+\sum_\sigma(\dot{q}_\sigma^*\dot{q}_\sigma-\nu_\sigma^2 q_\sigma^* q_\sigma) -\sum_\sigma(\dot{a}_\sigma^*\dot{a}_\sigma-\nu_\sigma^2 a_\sigma^* a_\sigma)+\sum_k\frac{M\mathbf{v}_k^2}{2} +\Big\{\sum_k\Big(-g_k^*\sum_\sigma a_\sigma\Phi_\sigma(\mathbf{r}_k) +\frac{g_k^*}{c}\mathbf{v}_k\cdot\sum_\sigma q_\sigma \boldsymbol{A}_\sigma(\mathbf{r}_k)+\frac{g_k^*}{c}\mathbf{v}_k\cdot\sum_\rho q_\rho \boldsymbol{A}_\rho(\mathbf{r}_k) +\boldsymbol{\mu}_k^*\cdot\mathrm{curl}_k\sum_\rho q_\rho \boldsymbol{A}_\rho(\mathbf{r}_k)\Big)+\mathrm{c.c.}\Big\}, \tag{68}$$

$$H=\sum_\rho(p_\rho^* p_\rho+\nu_\rho^2 q_\rho^* q_\rho)+\sum_\sigma(p_\sigma^* p_\sigma+\nu_\sigma^2 q_\sigma^* q_\sigma) -\sum_\sigma(b_\sigma^* b_\sigma+\nu_\sigma^2 a_\sigma^* a_\sigma)+\sum_k\frac{1}{2M} \times\Big(\mathbf{p}_k-\Big[\frac{g_k^*}{c}\Big(\sum_\sigma q_\sigma \boldsymbol{A}_\sigma(\mathbf{r}_k)+\sum_\rho q_\rho \boldsymbol{A}_\rho(\mathbf{r}_k)\Big)+\mathrm{c.c.}\Big]\Big)^2 +\Big(\sum_k g_k^*\sum_\sigma a_\sigma\Phi_\sigma(\mathbf{r}_k)+\mathrm{c.c.}\Big) -\Big(\sum_k \boldsymbol{\mu}_k^*\cdot\mathrm{curl}_k\sum_\rho q_\rho \boldsymbol{A}_\rho(\mathbf{r}_k)+\mathrm{c.c.}\Big). \tag{69}$$

Now, a peculiarity of the system of Eqs. (62)–(67) is that the variables q_σ and a_σ are not independent, the connection between them being given by the Lorentz condition (65). Making use of this relation and of (62), one can completely eliminate the variables a_σ from the equation of motion (67), obtaining:[13]

$$M\mathbf{a}_k=\Big\{g_k^*\Big(-\mathrm{grad.}_k \sum_j g_j\frac{e^{-r_{kj}/R}}{r_{kj}} -\frac{1}{c}\sum_\sigma\frac{c^2}{R^2\nu_\sigma^2}\dot{q}_\sigma \boldsymbol{A}_\sigma(\mathbf{r}_k)-\frac{1}{c}\sum_\rho \dot{q}_\rho \boldsymbol{A}_\rho(\mathbf{r}_k)\Big) +\frac{g_k^*}{c}\mathbf{v}_k\times\mathrm{curl}_k\sum_\rho q_\rho \boldsymbol{A}_\rho(\mathbf{r}_k) +\mathrm{grad.}_k\Big(\boldsymbol{\mu}_k^*\cdot\mathrm{curl}_k\sum_\rho q_\rho \boldsymbol{A}_\rho(\mathbf{r}_k)\Big)+\mathrm{c.c.}\Big\},$$

$$k=1,\ \cdots,\ n. \tag{70}$$

$$\ddot{q}_\sigma+\nu_\sigma^2 q_\sigma=\sum_k\frac{g_k}{c}\mathbf{v}_k\cdot \boldsymbol{A}_\sigma^*(\mathbf{r}_k), \tag{71}$$

$$\ddot{q}_\rho+\nu_\rho^2 q_\rho=\sum_k\frac{g_k}{c}\mathbf{v}_k\cdot \boldsymbol{A}_\rho^*(\mathbf{r}_k)+\sum_k \boldsymbol{\mu}_k\cdot\mathrm{curl}_k\, \boldsymbol{A}_\rho^*(\mathbf{r}_k). \tag{72}$$

The new set of equations of motion: (70), (71), (72), as may be directly verified, are derivable from the following Lagrangian and Hamiltonian:[14]

[12] In deriving the equations of motion (62)–(67) from the Lagrangian (68), q_ρ, q_ρ^*, q_σ, q_σ^*, a_σ, a_σ^*, $\mathbf{r}_k$ are to be treated as independent variables. Eq. (65) must then be assumed as an auxiliary relation. Also $p_\rho\equiv\partial L/\partial\dot{q}_\rho$, etc.

[13] Equation (70) is derived in Appendix II.

[14] In the limit $R\to\infty$, the variables describing the longitudinal field disappear completely from the Lagrangian (73), and the equations of motion (70). Since in this limit, the mesotron field equations are identical with the Maxwell equations (apart from the complex character of the field variables) one obtains the well-known result of electro-

$$L_1=\sum_\rho(\dot{q}_\rho^*\dot{q}_\rho-\nu_\rho^2q_\rho^*q_\rho)+\sum_\sigma\frac{c^2}{R^2\nu_\sigma^2}(\dot{q}_\sigma^*\dot{q}_\sigma-\nu_\sigma^2q_\sigma^*q_\sigma)$$
$$+\sum_k\frac{M\mathbf{v}_k^2}{2}+\left\{-\frac{1}{2}\sum_{k,j}g_k^*g_j\frac{e^{-r_{kj}/R}}{r_{kj}}\right.$$
$$+\sum_k\frac{g_k^*}{c}\mathbf{v}_k\cdot\sum_\sigma\frac{c^2}{R^2\nu_\sigma^2}q_\sigma\boldsymbol{A}_\sigma(\mathbf{r}_k)+\sum_k\frac{g_k^*}{c}\mathbf{v}_k\cdot\sum_\rho q_\rho\boldsymbol{A}_\rho(\mathbf{r}_k)$$
$$\left.+\sum_k\boldsymbol{\mu}_k^*\cdot\mathrm{curl}_k\sum_\rho q_\rho\boldsymbol{A}_\rho(\mathbf{r}_k)+\mathrm{c.c.}\right\},\quad(73)$$

$$H_1=\left\{\sum_\rho(p_\rho^*p_\rho+\nu_\rho^2q_\rho^*q_\rho)+\sum_\sigma\left(\frac{p_\sigma^*p_\sigma}{c^2/R^2\nu_\sigma^2}\right.\right.$$
$$\left.\left.+\left(\frac{c^2}{R^2\nu_\sigma^2}\right)\nu_\sigma^2q_\sigma^*q_\sigma\right)\right\}+\left\{\sum_k\frac{\mathbf{p}_k^2}{2M}\right.$$
$$\left.+\left(\frac{1}{2}\sum_{k,j}g_k^*g_j\frac{e^{-r_{kj}/R}}{r_{kj}}+\mathrm{c.c.}\right)\right\}$$
$$+\left\{\left[-\sum_k\frac{g_k^*}{c}\frac{\mathbf{p}_k}{M}\cdot\left(\sum_\sigma\frac{c^2}{R^2\nu_\sigma^2}q_\sigma\boldsymbol{A}_\sigma(\mathbf{r}_k)\right.\right.\right.$$
$$\left.\left.\left.+\sum_\rho q_\rho\boldsymbol{A}_\rho(\mathbf{r}_k)\right)+\mathrm{c.c.}\right]+\sum_k\frac{1}{2Mc^2}\right.$$
$$\times\left[g_k^*\sum_\sigma\frac{c^2}{R^2\nu_\sigma^2}q_\sigma\boldsymbol{A}_\sigma(\mathbf{r}_k)+g_k^*\sum_\rho q_\rho\boldsymbol{A}_\rho(\mathbf{r}_k)+\mathrm{c.c.}\right]^2$$
$$\left.-\left[\sum_k\boldsymbol{\mu}_k^*\cdot\mathrm{curl}_k\sum_\rho q_\rho\boldsymbol{A}_\rho(\mathbf{r}_k)+\mathrm{c.c.}\right]\right\}$$
$$\equiv H(\text{mesotron-field})+H(\text{heavy-particles})$$
$$+H(\text{interaction}).\quad(74)$$

Numerically,

$H_1=H=$[Volume Integral of Energy Density of Field+Heavy Particle Kinetic Energy+Magnetic Moment Interaction Energy].

The Hamiltonian H_1, plays a role in the quantized mesotron theory, completely analogous to the role of the Hamiltonian (24) in quantum electrodynamics. It is to be noted that quantum perturbation calculations, in particular, the derivation of action-at-distance two-body and many-body potentials, will not involve that part of the longitudinal interaction already exactly expressed by the "Coulomb" term:

$$\frac{1}{2}\sum_{k,j}g_k^*g_j\frac{e^{-r_{kj}/R}}{r_{kj}}+\mathrm{c.c.}$$

(c) Many-body potentials obtained in classical mesotron theory

Three-body potentials can now be obtained just as in electrodynamics, by a perturbation treatment of transitions in which one has *simultaneous* emission (by means of the g^2A^2/Mc^2 interaction term) of two virtual mesotrons by the first heavy particle, one of the mesotrons being absorbed by the second heavy particle and the other by the third. The absorptions take place by means of either the $-(g\mathbf{p}/cM)\cdot\boldsymbol{A}$ or the $-\boldsymbol{\mu}\cdot\mathrm{curl}\,\boldsymbol{A}$ interaction terms.

In this way, one obtains exactly the three-body potentials already found in the Hamiltonian of Eq. (57).[15]

(d) Specifically quantum-mechanical many-body potentials

The largest specifically quantum-mechanical three-body potential is obtained by a transition of the following type:

The first heavy particle emits two virtual mesotrons *in succession*; one of these is absorbed by the second heavy particle, and the other by the third. All individual absorptions and emissions are due to the $-\boldsymbol{\mu}\cdot\mathrm{curl}\,\boldsymbol{A}$ interaction term.

Since the expression for the transverse field energy: $\Sigma_\rho(p_\rho^*p_\rho+\nu_\rho^2q_\rho^*q_\rho)$, and for the magnetic moment interaction term:

$$-[\Sigma_k\boldsymbol{\mu}_k^*\cdot\mathrm{curl}_k\,\Sigma_\rho q_\rho\boldsymbol{A}_\rho(\mathbf{r}_k)+\mathrm{c.c.}]$$

are formally alike in the electromagnetic and mesotron theories,[16] the calculation of the three-body potential proceeds in the same way as the calculation of the corresponding three-body potential in electrodynamics. (Cf. Eqs. (34) to (38) and accompanying text.)

Thus the specifically quantum three-body potential arising from the transition outlined above

magnetism, *vis:* The effect of the longitudinal waves may be completely expressed by means of action-at-a-distance two-body Coulomb potentials.

[15] One can also obtain H (two-body spin-spin) and H (two-body spin-orbit) by a second-order quantum perturbation calculation with neglect of heavy particle recoil energies. The results, naturally, are identical with those obtained in Eq. (57).

[16] Compare the Hamiltonians (24) and (74). The complex nature of the field variables in mesotron theory introduces only trivial modifications in this connection.

is: (cf. the analogous electrodynamical Eq. (38)).

$$H''(\mathbf{r}_{12},\mathbf{r}_{13}) = \left\{\frac{-4\pi^2}{\hbar c}\left[\boldsymbol{\mu}_1^*\cdot\mathrm{curl}_1\sum_{\rho}\frac{\mathrm{curl}_2\,(\boldsymbol{\mu}_2\exp(i\mathbf{k}_\rho\cdot\mathbf{r}_{12})}{\nu_\rho^3/c^3}\right]\right.$$
$$\times\left[\boldsymbol{\mu}_1\cdot\mathrm{curl}_1\sum_{\rho'}\frac{\mathrm{curl}_3\,(\boldsymbol{\mu}_3^*\exp(i\mathbf{k}_{\rho'}\cdot\mathbf{r}_{13})}{\nu_{\rho'}^2/c^2}\right]$$
$$+\text{same term with indices 2 and 3}$$
$$\left.\text{interchanged}\right\}+\text{c.c.}\quad(75)$$

The characteristic difference between the two theories (the existence of the fundamental length R), now makes itself felt in the circumstance that the frequency ν_ρ is no longer proportional to the wave number k_ρ; the relation between them is in this case:

$$\nu_\rho^2/c^2 = k_\rho^2 + 1/R^2. \quad (76)$$

Converting the sums to integrals by the relation

$$\sum_\rho f(\mathbf{k}_\rho)\rightarrow\frac{1}{(2\pi)^3}\int f(\mathbf{k}_\rho)d\mathbf{k}_\rho$$

one observes that the second square bracket in (75) is equal to:

$$-\frac{1}{4\pi}\boldsymbol{\mu}_1\cdot\mathrm{curl}_1^2\left(\boldsymbol{\mu}_3^*\frac{e^{-r_{13}/R}}{r_{13}}\right) \quad (76)$$

and is, apart from the numerical factor $1/4\pi$ just the spin-spin two-body potential between the first and third particles. The first square bracket becomes:

$$\frac{1}{(2\pi)^3}\boldsymbol{\mu}_1^*\cdot\mathrm{curl}_1\,\boldsymbol{\mu}_2\times\int\frac{i\mathbf{k}_\rho\exp(i\mathbf{k}_\rho\cdot\mathbf{r}_{12})}{(k_\rho^2+1/R^2)^{\frac{1}{2}}}d\mathbf{k}_\rho. \quad (77)$$

Introducing the dimensionless variable, $\mathbf{Q}=\mathbf{k}_\rho r_{12}$, one obtains

$$\frac{1}{(2\pi)^3}\boldsymbol{\mu}_1^*\cdot\mathrm{curl}_1\frac{\boldsymbol{\mu}_2}{r_{12}}\times\int\frac{i\mathbf{Q}\exp(i\mathbf{Q}\cdot\mathbf{r}_{12}/r_{12})}{[Q^2+(r_{12}/R)^2]^{\frac{1}{2}}}d\mathbf{Q}.$$

The integral is finite and is of the order of $\mathbf{r}_{12}/r_{12}$ for $r_{12}\leqq R$. (For $r_{12}\ll R$, we have the electrodynamic case and the integral is $-4\pi(\mathbf{r}_{12}/r_{12})$; for $r_{12}\gg R$ the integral is very small.) Thus the specifically quantum three-body potential becomes for $r_{12}\leqq R$

$$H''(\mathbf{r}_{12},\mathbf{r}_{13})\leqq\left\{\frac{1}{\hbar c}\left[\boldsymbol{\mu}_1^*\cdot\mathrm{curl}_1\left(\frac{\mathbf{r}_{12}\times\boldsymbol{\mu}_2}{r_{12}^2}\right)\right]\right.$$
$$\times\left[\boldsymbol{\mu}_1\cdot\mathrm{curl}_1^2\left(\frac{\boldsymbol{\mu}_3^*e^{-r_{13}/R}}{r_{13}}\right)\right]$$
$$+\text{same term with indices 2 and 3}$$
$$\left.\text{interchanged}\right\}+\text{c.c.}\quad(78)$$

Order of Magnitude of Nuclear Potentials, from Mesotron Field Theory

The orders of magnitude of the nuclear potentials obtained in the mesotron theory will now be estimated. The average distances, $r_{kj}\leqq r$, between the nuclear heavy particles, are $\leqq R\equiv\hbar/m_0c$, the average nuclear heavy particle velocities, $v_n\leqq\hbar/MR\leqq m_0c/M$. The mesotron charge g determines the magnitude of the various interactions. The mesotron-magnetic moment μ, is $\leqq gR\leqq g\hbar/m_0c$. It is to be noted that the mass occurring in the Compton wave-length in μ, is the mass of the *emitted* mesotron, and not of the *emitting* heavy particle. The resulting anomalously large value of μ, is needed if one is to have in Eq. (57): H(two-body "Coulomb") $\leqq H$(two-body spin-spin);[17] which is necessary for a proper description of the strong spin-dependence of the total two-body potential.[18]

The heavy particle mesotron charge g, is related to the mesotron rest mass m_0. Thus:

$$Mv_n\frac{\hbar}{MR}\leqq\frac{Mv_n^2}{2}\leqq\text{Average Potential Energy}\leqq\frac{g^2}{R},$$

whence $$v_n/c\leqq g^2/\hbar c. \quad (79)$$

Thus $$m_0/M\leqq g^2/\hbar c. \quad (80)$$

The order of magnitude of the individual terms in the various potentials in Eq. (57), and of the specifically quantum three-body potential H''

[17] See Eqs. (81), (82). Also, compare papers cited in reference 7.

[18] Direct experimental evidence for a strong spin-dependence of the total two-body potential follows from the transparency of para-H_2 and the opaqueness of ortho-H_2 for slow neutrons. See E. Teller, Phys. Rev. **49**, 420 (1936); J. Schwinger and E. Teller, Phys. Rev. **52**, 286 (1937); F. G. Brickwedde *et al.*, Phys. Rev. **54**, 266 (1938); W. F. Libby and E. A. Long, Phys. Rev, **55**, 339 (1939).

(Eq. (78)) can now be estimated. Thus:

$$H(\text{two-body "Coulomb"}) \leqq g^2/R, \tag{81}$$

H(two-body spin-spin)

$$\leqq \frac{\mu^2}{R^3} \leqq \frac{g^2}{R} \leqq H(\text{two-body "Coulomb"}), \tag{82}$$

H(two-body spin-orbit)

$$\leqq g\frac{v_n}{c}\frac{\mu}{R^2} \leqq \frac{v_n}{c} H(\text{two-body "Coulomb"}), \tag{83}$$

H(two-body vel.-dep.)

$$\leqq \frac{v_n^2}{c^2}\frac{g^2}{R} \leqq \frac{v_n^2}{c^2} H(\text{two-body "Coulomb"}), \tag{84}$$

$$H(\text{three-body spin-spin}) \leqq \frac{g^2}{Mc^2}\frac{\mu^2}{R^4} \leqq \frac{g^2}{Mc^2R}\frac{g^2}{R}$$

$$\leqq \frac{v_n^2}{c^2} H(\text{two-body "Coulomb"}), \tag{85}$$

$$H(\text{three-body vel.-dep.}) \leqq \frac{g^4}{Mc^4}\frac{v_n^2}{R^2} \leqq \frac{g^2}{Mc^2R}\frac{v_n^2}{c^2}\frac{g^2}{R}$$

$$\leqq \frac{v_n^4}{c^4} H(\text{two-body "Coulomb"}), \tag{86}$$

$$H(\text{three-body spin-orbit}) \leqq \frac{g^3}{Mc^3}\frac{\mu v_n}{R^3} \leqq \frac{g^2}{Mc^2R}\frac{v_n}{c}\frac{g^2}{R}$$

$$\leqq \frac{v_n^3}{c^3} H(\text{two-body "Coulomb"}), \tag{87}$$

$$H''(\text{three-body quant.-mech.}) \leqq \frac{\mu^4}{\hbar c R^5} \leqq \frac{g^2}{\hbar c}\frac{g^2}{R}$$

$$\leqq \frac{v_n}{c} H(\text{two-body "Coulomb"}). \tag{88}$$

It is especially to be noted that the anomalously large mesotron-magnetic moment $\mu \leqq gR$ and the approximate equality of the average distances between the particles, and the range R, gives rise to a specifically quantum three-body potential and a spin-orbit two-body potential[19] both $\leqq (v_n/c)H$(two-body "Coulomb").

[19] A two-body interaction of the spin of the particle with its own orbit, arises from the mesotron-polarization term:

$$\tfrac{1}{2}\sum_k \mathfrak{p}_k^* \cdot \text{grad.}_k \Phi(\mathfrak{r}_k) + \text{c.c.}$$

$$= \tfrac{1}{2}\sum_{k,j}\left(\frac{\nabla_k}{c}\times\mathfrak{y}_k^*\right)\cdot\text{grad.}_k\left(\frac{g_j e^{-r_{kj}/R}}{r_{kj}}\right) + \text{c.c.}$$

$$\leqq \frac{v_n}{c}\mu\frac{g}{R^2} \leqq \frac{v_n}{c} H \text{ (two-body "Coulomb").}$$

The numerical value of v_n/c is determined by the details of the magnitude and spatial dependence of the interactions and may be estimated to lie within the following limits: (for light nuclei)

$$\frac{1}{3} \geqq \frac{v_n}{c} \geqq \frac{1}{10}. \tag{89}$$

Many-Body Potentials for a General Field Theory[20]

It will now be shown that three-body potentials $\leqq v_n/c \times$(two-body potentials), etc., are obtained in a general field theory satisfying the conditions:

(a) The Hamiltonian H of the total system may be written as

$$H(\text{field}) + H(\text{heavy-particles}) + H(\text{interaction}), \tag{90}$$

where, H(interaction) can be considered as a perturbation.

(b) Two-body potentials obtained from H(interaction) in the second approximation of the quantum perturbation calculation, are, at least of the same order of magnitude, as any two-body potentials which may already be contained in H(heavy-particles), due to an elimination procedure analogous to that performed in the electromagnetic and mesotron field theories.

The matrix element for the emission of a virtual light particle of mass m_0 and wave number k_ρ by one of the heavy particles will be denoted by

$$\int \psi_i^*(\mathfrak{r}_j)\varphi_{0\rho}^*(q_\rho) H(\mathfrak{r}_j, q_\rho; \text{interaction}) \times \varphi_{1\rho}(q_\rho)\psi_n(\mathfrak{r}_j)\, d\mathfrak{r}_j\, dq_\rho$$

$$\equiv \int \psi_i^*(\mathfrak{r}_j)\, V_\rho \exp(i\mathbf{k}_\rho\cdot\mathfrak{r}_j)\psi_n(\mathfrak{r}_j)\, d\mathfrak{r}_j, \tag{91}$$

where $\psi_i(\mathfrak{r}_j)$, $\psi_n(\mathfrak{r}_j)$ are material states, and $\varphi_{n\rho}(q_\rho)$ is a state of the field with n_ρ light particles of wave number $\mathbf{k}_\rho$ present.

The usual quantum perturbation method employed previously,[20a] now gives the following

[20] The contents of this section were first presented by one of the authors (H. P.) at the Washington meeting of the American Physical Society, April 28, 1938; Abstract No. 126, Phys. Rev. **53**, 938 (1938).

[20a] Again, with neglect of heavy particle recoil energies.

two-body and three-body action-at-a-distance potentials:

$$H(r_{12};\ \text{two-body})=\sum_{\rho}\frac{V_\rho V_\rho^*\exp(i\mathbf{k}_\rho\cdot\mathbf{r}_{12})}{(\hbar^2c^2k_\rho^2+m_0^2c^4)^{\frac{1}{2}}},\quad(92)$$

$$H(r_{12},r_{13};\ \text{three-body})=\sum_{\rho,\rho'}\frac{V_\rho V_\rho^*\exp(i\mathbf{k}_\rho\cdot\mathbf{r}_{12})}{[(\hbar^2c^2k_\rho^2+m_0^2c^4)^{\frac{1}{2}}]^2}$$

$$\times\frac{V_{\rho'}V_{\rho'}^*\exp(i\mathbf{k}_{\rho'}\cdot\mathbf{r}_{13})}{(\hbar^2c^2k_{\rho'}^2+m_0^2c^4)^{\frac{1}{2}}}+\text{same terms}$$

with indices 2 and 3 interchanged

$$=\left[\frac{1}{\hbar c[k_\rho^2+(\hbar/m_0c)^{-2}]^{\frac{1}{2}}}\right]_{kr}H(r_{12};\ \text{two-body})$$

$$\times H(r_{13};\ \text{two-body})+\text{same term}$$

with indices 2 and 3 interchanged. (93)

Here, $\hbar/m_0c\equiv R$, must be the range of H(two-body), by a general argument due to Wick,[21] relating the rest mass of the virtually emitted particles and the range of the resulting interaction. Further, for $r_{12}\leqq R$,

$$\left[\frac{1}{(k_\rho^2+1/R^2)^{\frac{1}{2}}}\right]_{kr}\leqq R\quad(94)$$

since R is the only parameter characterizing the r space dependence of H(two-body), and consequently, the k space dependence of $V_\rho V_\rho^*/(\hbar^2c^2k_\rho^2+m_0^2c^4)^{\frac{1}{2}}$. Thus:

$$H(r_{12},r_{13};\ \text{three-body})\leqq(R/\hbar c)H(r_{12};\ \text{two-body})\times H(r_{13};\ \text{two-body}).\quad(95)$$

For nuclear systems, $(r_{12}\leqq r_{13}\leqq R)$

$$v_n(\hbar/R)\leqq Mv_n^2/2\leqq H(R;\ \text{two-body}),\quad(96)$$

$$\text{whence}\quad H(\text{three-body})\leqq\frac{v_n}{c}H(\text{two-body}).\quad(97)$$

Similarly, higher order quantum perturbation calculations lead to:

$$H(m\text{-body})\leqq[(R/\hbar c)(H(\text{two-body}))]^{m-2}\leqq(v_n/c)^{m-2}H(\text{two-body}).\quad(98)$$

[21] C. G. Wick, Nature **142**, 994 (1938).

Conclusions

These investigations indicate that the replacement of field interactions by two-body action-at-a-distance potentials is a poor approximation in nuclear problems. The error made is at least of the order of v_n/c, if one compares the magnitudes, term by term, of two- and three-body potentials. Furthermore, the number of terms in the m-body interaction of an n-body nucleus: $n!/m!(n-m)!$, is, in general, many times larger than the number of two-body interaction terms: $n!/2!(n-2)!=n(n-1)/2$, but, a direct estimate of the magnitude of the total m-body interaction ((number of m-body terms)$\times$(average magnitude of each)) is complicated by the fact that the m-body interactions are, at least in part, of an exchange and spin-dependent character. It seems therefore, that a satisfactory description of nuclei, other than the deuteron, can be obtained only by an explicit consideration from the very beginning of the role played by the field.[22]

Addendum

The electromagnetic two-body Lagrangian (9) is correct to the second order in v/c and to the zero order in time-derivatives of the velocity. If, however, one wishes to consider the acceleration terms previously neglected in the vector potential (5),[23] and hence terms in the time-derivative of the acceleration in the equations of motion,[24] there are two alternatives:

(1) To retain the time-derivative of the acceleration *explicitly* in the equations of motion. Now, if these equations are to be derivable from a variational principle, the "Lagrangian" must contain the accelerations explicitly. This involves an action-at-a-distance particle mechanics beyond the scope of the present canonical formalism, and, consequently renders impossible the transition to quantum-mechanics.

[22] It may be added that a description of nuclei in terms of many-body interactions, or, more hypothetically, in terms of an integrated field energy density is consistent with the nuclear model proposed by Bohr.

[23] A vector potential correct to the first order in v/c leads immediately to the equations of motion (6), which are, in turn, derivable from the two-body Lagrangian (9).

[24] The "self-force" term in the equations of motion is proportional to the time-derivative of the electron's *own* acceleration, and represents dissipation of its energy by radiation. Naturally such "self-force" terms (along with all other "self" terms) are beyond the scope of the mutual interaction problem, whether or not, the mutual interactions themselves are capable of Lagrangian-Hamiltonian description. This is formally indicated by the fact that the vector potential of the kth electron depends on the velocities, accelerations, $\cdots$, of the $n-1$ *others*. Thus the sum in Eq. (5) is extended over all j except $j=k$.)

(2) To express the accelerations and their time derivatives in the equations of motion by means of the coordinates and velocities of the particles. This can be done to a first approximation by setting the acceleration equal to the Coulomb force divided by the mass. If the resulting equations of motion are to be the basis of a quantum-mechanical treatment, they should be capable of reduction to a Lagrangian, and hence, Hamiltonian form. If such a reduction proves to be impossible, then the *canonical* action-at-a-distance description of acceleration-retardation effects must be renounced. On the other hand, if these equations of motion can be deduced from a Lagrangian and Hamiltonian, then additional many-body interactions will be obtained.

A counterpart of the explicit appearance of accelerations in the classical vector potential is the presence of particle recoil energies in the energy denominators of the quantum perturbation scheme involved in the elimination of the quantized field variables. An attempt to consider the effects of these recoil energies to a first approximation leads to problems in connection with the canonical action-at-a-distance description of the particles, similar to those arising in classical theory from the acceleration-retardation effects.

The questions raised in this addendum are being investigated both for the electromagnetic and the mesotron field theories, and it is intended to make a more detailed report in the near future.

Appendix I

To obtain a solution of (49), in the form of an expansion in v/c it is simplest to make a Fourier resolution of Φ and ρ.

$$\Phi(\mathbf{r}, t)=\int \Phi_\nu(\mathbf{r})e^{i\nu t}d\nu, \tag{A1}$$

$$\rho(\mathbf{r}, t)=\int \rho_\nu(\mathbf{r})e^{i\nu t}d\nu. \tag{A2}$$

Substituting into (49),

$$\nabla^2\Phi_\nu-\frac{1}{R^2}\Phi_\nu+\frac{\nu^2}{c^2}\Phi_\nu=-4\pi\rho_\nu, \tag{A3}$$

whence

$$\Phi_\nu(\mathbf{r})=\int \rho_\nu(\mathbf{r}')\frac{\exp(-\kappa|\mathbf{r}-\mathbf{r}'|)}{|\mathbf{r}-\mathbf{r}'|}d\mathbf{r}' \tag{A4}$$

with $$\kappa\equiv(1/R^2-\nu^2/c^2)^{\frac{1}{2}}. \tag{A5}$$

For $$\frac{v}{c}\ll 1, \quad \nu \text{ is } \ll\frac{c}{R},$$

for all $\rho_\nu(\mathbf{r})$ which contribute appreciably to $\rho(\mathbf{r}, t)$. Expanding κ, one obtains,

$$\Phi_\nu(\mathbf{r})\cong\int \rho_\nu(\mathbf{r}')\frac{\exp[-1/R(1-\nu^2R^2/2c^2)|\mathbf{r}-\mathbf{r}'|]}{|\mathbf{r}-\mathbf{r}'|}d\mathbf{r}'$$

$$\cong\int \rho_\nu(\mathbf{r}')\frac{\exp(-1/R|\mathbf{r}-\mathbf{r}'|)}{|\mathbf{r}-\mathbf{r}'|}d\mathbf{r}'$$

$$+\frac{\dot{R}}{2c^2}\int \nu^2\rho_\nu(\mathbf{r}')\exp(-1/R|\mathbf{r}-\mathbf{r}'|)d\mathbf{r}' \tag{A6}$$

and

$$\Phi(\mathbf{r}, t)=\int \rho(\mathbf{r}', t)\frac{\exp(-1/R|\mathbf{r}-\mathbf{r}'|)}{|\mathbf{r}-\mathbf{r}'|}d\mathbf{r}'$$

$$-\frac{R}{2c^2}\int\left(\frac{d^2}{dt^2}\rho(\mathbf{r}', t)\right)\exp(-1/R|\mathbf{r}-\mathbf{r}'|)d\mathbf{r}'$$

$$+\text{terms of higher order in the time derivatives of } \rho. \tag{A7}$$

For point sources located at $\mathbf{r}_j(t)$ and having velocities, accelerations, $\mathbf{v}_j(t)$, $\mathbf{a}_j(t)$,

$$\rho(\mathbf{r}', t)=\sum_j g_j\delta(\mathbf{r}'-\mathbf{r}_j(t))$$

and $\Phi(\mathbf{r}, t)$ becomes

$$\Phi(\mathbf{r}, t)=\sum_j g_j\frac{\exp(-1/R|\mathbf{r}-\mathbf{r}_j|)}{|\mathbf{r}-\mathbf{r}_j|}$$

$$-\frac{R}{2c^2}\sum_j g_j\frac{d^2}{dt^2}\exp(-1/R|\mathbf{r}-\mathbf{r}_j|)+\text{terms}$$

$$\text{of higher order in } \frac{\mathbf{v}_j}{c}, \frac{\mathbf{a}_j}{c}, \text{ etc.}$$

$$=\sum_j g_j\frac{\exp(-1/R|\mathbf{r}-\mathbf{r}_j|)}{|\mathbf{r}-\mathbf{r}_j|}$$

$$-\frac{R}{2c^2}\Big\{\sum_j g_j(\mathbf{v}_j\cdot\text{grad.}_j)$$

$$\times(\mathbf{v}_j\cdot\text{grad.}_j)\exp(-1/R|\mathbf{r}-\mathbf{r}_j|)$$

$$+\sum_j g_j(\mathbf{a}_j\cdot\text{grad.}_j)\exp(-1/R|\mathbf{r}-\mathbf{r}_j|)\Big\}$$

$$+\text{terms of higher order in } \frac{\mathbf{v}_j}{c}, \frac{\mathbf{a}_j}{c}, \text{ etc.} \tag{A8}$$

One may solve Eq. (50) for $\boldsymbol{A}$ in an entirely similar manner. Thus:

$$\boldsymbol{A}(\mathbf{r},t)=\sum_j \frac{g_j}{c}\mathbf{v}_j \frac{\exp(-1/R|\mathbf{r}-\mathbf{r}_j|)}{|\mathbf{r}-\mathbf{r}_j|}$$
$$+\sum_j \boldsymbol{\mu}_j \times \text{grad.}_j\left(\frac{\exp(-1/R|\mathbf{r}-\mathbf{r}_j|)}{|\mathbf{r}-\mathbf{r}_j|}\right)$$
$$+\frac{R}{2c^2}\Bigg\{\sum_j \text{curl}_j[(\mathbf{v}_j\cdot\text{grad.}_j)$$
$$\times(\mathbf{v}_j\cdot\text{grad.}_j)\boldsymbol{\mu}_j \exp(-1/R|\mathbf{r}-\mathbf{r}_j|)]$$
$$+\sum_j \text{curl}_j[(\mathbf{a}_j\cdot\text{grad.}_j)\boldsymbol{\mu}_j \exp(-1/R|\mathbf{r}-\mathbf{r}_j|)]$$
$$+\sum_j \text{curl}_j\left[\frac{d\boldsymbol{\mu}_j}{dt}(\mathbf{v}_j\cdot\text{grad.}_j)\exp(-1/R|\mathbf{r}-\mathbf{r}_j|)\right]$$
$$+\sum_j \text{curl}_j\left[\frac{d^2\boldsymbol{\mu}_j}{dt^2}\exp(-1/R|\mathbf{r}-\mathbf{r}_j|)\right]\Bigg\}$$
$$+\text{terms of higher order in}$$
$$\frac{\mathbf{v}_j}{c},\ \frac{\mathbf{a}_j}{c},\ \frac{d\boldsymbol{\mu}_j}{dt},\ \frac{d^2\boldsymbol{\mu}_j}{dt^2},\ \text{etc.} \quad \text{(A9)}$$

Appendix II

To eliminate the variables a_σ from (67), in order to obtain (70), one makes use of (62) and (65). The latter two equations give:

$$a_\sigma=\frac{\sum_j g_j\Phi_\sigma^*(\mathbf{r}_j)-\dot{a}_\sigma}{\nu_\sigma^2}=\frac{\sum_j g_j\Phi_\sigma^*(\mathbf{r}_j)-ck_\sigma\dot{q}_\sigma}{\nu_\sigma^2}. \quad \text{(A10)}$$

The second expression for a_σ, is just the equation div. $\boldsymbol{E}=4\pi\rho-(1/R^2)\Phi$ written in terms of the Fourier components a_σ, q_σ. Substituting this value for a_σ into (67), one obtains:

$$M\mathbf{a}_k=\Bigg\{g_k^*\Bigg[-\text{grad.}_k\sum_j\sum_\sigma\frac{g_j\Phi_\sigma^*(\mathbf{r}_j)\Phi_\sigma(\mathbf{r}_k)}{\nu_\sigma^2}$$
$$+\frac{1}{c}\sum_\sigma\dot{q}_\sigma\left(\frac{c^2k_\sigma}{\nu_\sigma^2}\text{grad.}_k\Phi_\sigma(\mathbf{r}_k)-\boldsymbol{A}_\sigma(\mathbf{r}_k)\right)\Bigg]$$
$$-\frac{g_k^*}{c}\sum_\rho\dot{q}_\rho\boldsymbol{A}_\rho(\mathbf{r}_k)+\frac{g_k^*}{c}\mathbf{v}_k\times\text{curl}_k\sum_\rho q_\rho\boldsymbol{A}_\rho(\mathbf{r}_k)$$
$$+\text{grad.}_k\left(\boldsymbol{\mu}_k^*\cdot\text{curl}_k\sum_\rho q_\rho\boldsymbol{A}_\rho(\mathbf{r}_k)\right)+\text{c.c.}\Bigg\}. \quad \text{(A11)}$$

From (59), (66)

$$\frac{c^2k_\sigma}{\nu_\sigma^2}\text{grad.}_k\Phi_\sigma(\mathbf{r}_k)-\boldsymbol{A}_\sigma(\mathbf{r}_k)$$
$$=\left(\frac{c^2k_\sigma^2}{\nu_\sigma^2}-1\right)\boldsymbol{A}_\sigma(\mathbf{r}_k)=-\frac{c^2}{R^2\nu_\sigma^2}\boldsymbol{A}_\sigma(\mathbf{r}_k). \quad \text{(A12)}$$

Also,

$$(\nabla_k^2-1/R^2)\sum_\sigma\frac{\Phi_\sigma^*(\mathbf{r}_j)\Phi_\sigma(\mathbf{r}_k)}{\nu_\sigma^2}$$
$$=-\sum_\sigma\frac{\Phi_\sigma^*(\mathbf{r}_j)(k_\sigma^2+1/R^2)\Phi_\sigma(\mathbf{r}_k)}{\nu_\sigma^2}=-4\pi\delta(\mathbf{r}_k-\mathbf{r}_j).$$

Thus
$$\sum_\sigma\frac{\Phi_\sigma^*(\mathbf{r}_j)\Phi_\sigma(\mathbf{r}_k)}{\nu_\sigma^2}=\frac{e^{-r_{kj}/R}}{r_{kj}}. \quad \text{(A13)}$$

Substituting (A12) and (A13) into (A11), gives Eq. (70).

The Positive Column of the Nitrogen Arc at Atmospheric Pressure

EDWARD S. LAMAR, ALBERT M. STONE AND KARL T. COMPTON
George Eastman Research Laboratory, Massachusetts Institute of Technology, Cambridge, Massachusetts

(Received April 20, 1939)

Extending earlier work by one of us,[1] a theory of the positive column in an arc has been developed, from considerations of energy balance, from which good values of nitrogen arc parameters are calculated from known properties of the gas. The power generation per unit volume is obtained in terms of the potential gradient, the electron mobility and the electron concentration. The electron concentration is computed with the aid of the Saha equation for thermal ionization. The power loss is calculated in terms of a generalized heat conductivity which includes the heat transport that results from the diffusion of dissociated atoms. Convection is neglected, so that the theory applies only to low current arcs in ordinary space or to arcs below 30 amperes in gravity-free space. Equating power generation and power loss leads to a differential equation that can be solved numerically once the center temperature is known. Without solving the equation a change of variable is evident, which shows the potential gradient to be independent of the total power. This gives an arc equation of the Ayrton type. The arc is shown to be free from certain constraints which might otherwise set the center temperature. However, the center temperature is determined by introducing the additional consideration that the arc operates to make the power loss a maximum. The agreement with experiment is satisfactory. The inclusion of convection in a more complete theory is discussed, and it can be asserted that departure from the above simplified theory, for arcs of larger currents, is qualitatively of the type to be expected from the influence of convection. These results supply convincing evidence that the mechanism of the positive column of arcs is now understood.

INTRODUCTION

THE electric arc can be divided into three distinct regions; one is near the cathode, one near the anode, and one between the two. The middle region is known as the positive column. The present investigation is concerned with the positive column of an arc running steadily between electrodes placed one above the other. The electrodes are of such a nature, or so cooled, as to prevent vapors or gases given off by them from being present in the positive column in greater than negligible amounts. In the arc at atmospheric pressure, the longitudinal potential gradient is known to be constant throughout the positive column; the apparent diameter of the arc is constant throughout the column, and the temperatures of both electrons and gas are several thousands of degrees.

Evidence for these statements can be found throughout the literature of the subject. Even for arcs less than ten millimeters in length, voltage *vs.* length plots show considerable straight portions for most of the current range investigated. This can be seen from the measurements taken by Nottingham[2] in air. Suits,[3] from the same type of measurement and by a more direct method applied to a wide variety of arcs, concludes that the longitudinal potential gradient in the positive column is constant.

Suits[3] as a result of his measurements on arcs of various lengths states definitely that the arc diameter is independent of length over the positive column. Further evidence on this point is to be found from various photographs appearing in the literature on the subject. Even for arcs as short as six millimeters,[4] as can be seen from Nottingham's Fig. 4, an approximately uniform portion extends over several millimeters in the center.

A number of different methods have been employed for the measurement of temperatures in the positive column. Ornstein[5] and his coworkers have obtained values for both electron and gas temperatures from spectroscopic measurements. The electron temperatures were deduced from the relative intensities of atomic lines and of electronic bands. The gas temperatures were obtained from relative intensities of the rotational lines in the bands and of the vibrational band heads. From these measurements the indications are that, within experimental error, the electron and gas temperatures

[1] E. S. Lamar, Phys. Rev. **49**, 861 (1936).
[2] W. B. Nottingham, Phys. Rev. **28**, 764 (1926).
[3] C. G. Suits, Phys. Rev. **55**, 561 (1939).
[4] W. B. Nottingham, J. Frank. Inst. **206**, 52 (1928).
[5] *L. S. Ornstein: His Life and Work* (Utrecht, 1933).

are equal.[6] In air or nitrogen the value of each temperature is independent of current. The best spectroscopic measurements on d.c. arcs give temperatures in air ranging from 5700°K to 6700°K with an average of 6200°K.

Electron temperatures deduced from probe measurements are in disagreement with the spectroscopic values by as much as a factor of three in some cases.[7] It has been shown by Mason[8] that the probe constitutes a serious disturbing factor when introduced into the arc. Quantitative deductions from such probe measurements, therefore, remain open to criticism in the absence of further analysis.

Values of the gas temperature in the positive column have been deduced from indirect measurements of the gas density. Engel and Steenbeck[9] obtained the gas density from measurements of the absorption coefficient of soft x-rays and from the range of α particles.[10] Ramsauer[11] performed similar measurements using 100-kv beta-rays. The values obtained from these density measurements were somewhat lower than the spectroscopic ones but hardly more than the probable experimental error.

The latest and perhaps the most reliable values of gas temperature are those deduced by Suits[12] from measurements of the velocity of sound through the arc. His value for nitrogen is 6100°K with little or no dependence on arc current.

Three concepts underlie the present theory of the arc positive column. First is the theory of thermal ionization following the Saha equation, introduced by Compton[13] and found not inconsistent with experimental observations. Second is the application of an energy-extreme principle, introduced into arc studies by Compton and Morse[14] who, however, applied it differently and only to the region of the cathode. Third is the application of heat balance, earlier applied to the cathode region, but first applied with any rigor to the positive column by Lamar,[1] who also applied the energy-extreme principle to this region. Armed with further experimental evidence, Ornstein and Brinkmann[15] further justified the assumption of thermal ionization and the use of the Saha equation.

Energy balance equations have been used by many investigators.[16] In particular, Elenbaas by ingenious experiments was able to obtain sufficient boundary conditions to arrive at a satisfactory solution in the case of the high pressure mercury arc. Suits has enjoyed great success in correlating arc data from dimensional considerations following similar treatment of heat losses from solids.[17] At very low currents Lamar,[1] using an energy extreme hypothesis and no arbitrary constant, obtained temperature and power dissipation per unit length for the nitrogen positive column. The present paper carries forward this type of analysis in greater detail and precision.

Simple Theory of the Positive Column

Following Compton,[13] the arc current density can be written as

$$J=J_{+}+J_{-}=n_{+}e\mu_{+}E+n_{-}e\mu_{-}E. \qquad (1)$$

The absence of an appreciable second derivative of the potential leads from Poisson's equation to the equality of n_{+} and n_{-}. Hence, since the electron mobility greatly exceeds that of the positive ions, the first term on the right of Eq. (1) can be neglected and with it the necessity for subscripts in the second. The power generation per unit length in the ring element between r and $r+dr$, therefore, can be written as

$$dW=2\pi JErdr=2\pi E^{2}ne\mu rdr. \qquad (2)$$

[6] R. Mannkopf, Zeits. f. Physik **86**, 161 (1933); H. Witte, Zeits. f. Physik **88**, 415 (1934).
[7] W. B. Nottingham, J. Frank. Inst. **206**, 43 (1928); **207**, 299 (1929).
[8] R. C. Mason, Phys. Rev. **51**, 28 (1937).
[9] A. von Engel and M. Steenbeck, Phys. Rev. **37**, 1554 (1931); Wiss. Veroff. Siemens K. **XII**, 1, 81 (1933).
[10] A. von Engel and M. Steenbeck, Wiss. Veroff. Siemens K. **XII**, 1, 74 (1933).
[11] C. Ramsauer, Electrotech. u. Maschinenbau **51**, 189 (1933).
[12] C. G. Suits, Physics **6**, 190, 196, 315 (1935); Proc. Nat. Acad. **21**, 48 (1935); G. E. Rev. **39**, 194 (1936).
[13] K. T. Compton, Phys. Rev. **21**, 266 (1923); J. A.I.E.E. **46**, 868 (1927).
[14] K. T. Compton and P. M. Morse, Phys. Rev, **30**, 305 (1927).
[15] L. S. Ornstein and H. Brinkmann, Physica **1**, 797 (1934).
[16] Ter Horst, Brinkmann and Ornstein, Physica **2**, 652 (1935); W. Elenbaas, Physica **1**, 211, 673 (1934); **2**, 757 (1935); B. Kirschstein and F. Koppelmann, Wiss. Veroff. Siemens K. **XVI**, 3, 56 (1937); C. G. Suits, Phys. Rev. **52**, 245 (1937); G. E. Rev. **39**, 194 (1936); Physics **6**, 196 (1935); C. G. Suits and H. Poritsky, Phys, Rev. **52**, 136 (1937).
[17] W. J. King, Mech. Engin. May (1932).

The assumption of thermal ionization as the only process contributing to the electron concentration n permits n to be expressed as a function of temperature only, by the Saha[18] equation. The electron mobility μ is computed from kinetic theory[19] and hence is a function of temperature only. Eq. (2) can be rewritten, therefore, as

$$dW = 2\pi E^2 F r dr, \tag{3}$$

where $F = ne\mu$, a function of temperature only.

In the nitrogen positive column there are five processes by means of which energy is lost: (1) radiation; (2) the radial drift of ions and electrons, each pair taking with it the ionization energy; (3) convection; (4) the diffusion of atoms out from the arc, each pair taking with it the dissociation energy of the molecule; and (5) thermal conduction. Concerning radiation, Holm and Lotz,[20] from measurements of the total radiation from the positive column of a long carbon arc with large alternating currents flowing, give the radiation loss as five percent at 30 amperes. Extrapolation of their experimental curve below 10 amperes indicates completely negligible radiation loss in this range. Hence radiation is neglected here. As will be seen later, the radial drift of ions and electrons accounts for only negligible power loss and hence is neglected. Convection within the radius occupied by the arc, discussed later, is neglected in the simple theory, making this first treatment applicable only to cases in which convection losses in the arc are known to be small. The term representing the power loss by diffusion of atoms has the form of a conduction term and hence is included in a generalized conductivity Θ.

Neglecting convection, therefore, the power loss can be written as

$$dW = -2\pi \frac{d}{dr}\left(r\Theta \frac{dT}{dr}\right) dr = 2\pi E^2 F r dr, \tag{4}$$

which, integrated and rearranged, gives

$$dT/dr = -(E^2/r\Theta)\int_0^r F r dr. \tag{5}$$

It is possible to integrate Eq. (5) for any value of E to give the temperature distribution, W and hence the current I. The temperature gradient in the arc center must be zero, however, and the temperature T_e known. The problem then resolves itself into one of determining this temperature T_e along the axis of the positive column.

In a pure conduction problem of this kind one difficulty arises immediately. The boundary condition $dT/dr = 0$ must be satisfied when $T = T_0$, the ambient temperature. This cannot be done unless W is zero or T_e is infinity. Hence, although convection is neglected within the radius occupied by the arc, it must be considered outside of this radius in any argument for determining T_e.

Further information for use in determining T_e can be obtained from consideration of a similar thermal problem; namely, that of the heat losses from solid cylinders immersed in a fluid.

Dimensional arguments[17] applied to heat losses from solid cylinders lead to the conclusion that

$$H/K = f(g\alpha\theta d^3/\nu^2), \tag{6}$$

where H is the heat loss per unit length per degree temperature excess; K, the thermal conductivity; g, the acceleration of gravity; α, the thermal expansion coefficient of the fluid; θ, the temperature excess of cylinder above surroundings; d, the cylinder diameter; and ν, the kinematical viscosity (the ratio of viscosity to density).

This formula has been applied successfully to cases in which θ is small in comparison with T, with α, K and ν evaluated at the average temperature. A similar relation has been found by Suits and Poritsky to hold for the arc if α is evaluated at ambient temperature, and K and ν at the temperature of the arc.

From the plot of H/K *vs.* $g\alpha\theta d^3/\nu^2$ presented in King's review[17] it can be seen that H/K does not change very rapidly with changes in the abscissa. This should be true for the arc also.

The arc differs from the solid cylinders just considered in that it has no sharp solid boundary. Hence it may be possible to find a diameter d, which includes the arc and at which the dimensional relationship is satisfied, for a wide range of assumed values of T_e rather than for only one. This seems to be true of the atmospheric arc

[18] R. H. Fowler, *Statistical Mechanics* (Cambridge, 1929), p. 281.
[19] K. T. Compton and I. Langmuir, Rev. Mod. Phys, 2, 218 (1930).
[20] R. Holm and A. Lotz, Wiss. Veroff. Siemens K. XIII, 2, 87 (1934).

and hence so far as external conditions are concerned, this arc is free to select any value of T_e within the allowed range. It is by no means certain that arcs having small values of $g\alpha\theta d^3/\nu^2$ at pressures other than atmospheric can be treated without regard for the boundary condition at T_0.

In order to fix the value of T_e within the allowed range it is assumed that the arc will adjust itself so as to operate with extreme power dissipation. The adjustment is possible because the outer boundary condition does not constitute a constraint. The integration indicated by Eq. (5) was carried out numerically for each of a number of assumed values of T_c. The values of W resulting from these integrations were plotted as a function of T_c. Within the range of temperatures permitted by the absence of constraints, there is one maximum and one minimum. The maximum provides better agreement with experiment than does the minimum. Before carrying out the integration it was necessary to compute the two functions F and Θ occurring in Eq. (5).

The function $F=ne\mu$ is a function of temperature only. The mobility μ, occurring in F, was computed by means of Eq. (107) in Compton and Langmuir's paper.[19] For molecular nitrogen the value of λ_0, given on page 208 of that article, was used. The kinetic theory mean free path for atomic nitrogen is not known. It seems reasonable to suppose, however, that the ratios of atomic to molecular mean free paths should not differ greatly from gas to gas. For hydrogen this ratio is known to be 1.183. If this ratio is used and each gas is weighted according to its partial pressure in obtaining λ_0, the mobility of a mixture of atomic and molecular nitrogen turns out to be

$$\mu=\{4.52(10^2)T^{\frac{1}{2}}/P\}\{1+0.183P_a/P\}, \quad (7)$$

where μ is in cm²/sec. volt, P is the total gas pressure, and P_a the partial pressure of atoms; both pressures are in atmospheres.

Fowler[18] writes the Saha equation for a single gas as

$$\frac{n^-n^+}{n}=\frac{\omega^-\omega^+}{\omega}\left(\frac{2\pi mkT}{h^2}\right)^{\frac{3}{2}}e^{-V_i e/kT}, \quad (8)$$

where n^-, n^+ and n are the concentrations of electrons, ions and neutral gas, respectively. The ω's are the respective statistical weights, V_i is the ionization potential, and the other symbols have their usual meanings. The derivation of Eq. (8) involves the assumption that the neutral gas has no excited states below ionization and that the positive ions have only a ground state. With nitrogen over the temperature range considered here, the population of the ground state greatly exceeds the combined populations of the other states for both neutral gas and positive ions. Eq. (8), in which the ω's are the multiplicities of the respective ground states, can then be used.

Substituting for the various statistical weights and introducing subscripts for the molecular and atomic gases, we obtain

$$\frac{n^-n_m^+}{n_m}=4\left(\frac{2\pi mkT}{h^2}\right)^{\frac{3}{2}}e^{-V_m e/kT}$$

and

$$\frac{n^-n_a^+}{n_a}=\tfrac{1}{2}\left(\frac{2\pi mkT}{h^2}\right)^{\frac{3}{2}}e^{-V_a e/kT}.$$

If we remember that $n_m^+ + n_a^+ = n^-$, and drop the $^-$ superscript,

$$n=\left(\frac{2\pi mkT}{h^2}\right)^{\frac{3}{2}}(4n_m e^{-V_m e/kT}+\tfrac{1}{2}n_a e^{-V_a e/kT})^{\frac{1}{2}}. \quad (9)$$

Both n_m^+ and n_a^+ are known to be small in comparison with n_m and n_a. Hence the latter two can be computed directly from the partial pressures of atoms and molecules, respectively. The ionization potentials $V_m=16.5$ volts[21] and $V_a=14.5$ volts[22] were selected. Numerically, therefore,

$$n=3.006(10^{18})T^{\frac{1}{2}}\times(P_a e^{-168300/T}+8(P-P_a)e^{-191500/T})^{\frac{1}{2}} \quad (10)$$

and finally,

$$F=2.17(10^2)T^{\frac{1}{2}}\times\{P_a e^{-168300/T}+8(P-P_a)e^{-191500/T}\}^{\frac{1}{2}}\times(1+0.183P_a/P)/P. \quad (11)$$

[21] W. Jevons, *Band Spectra of Diatomic Molecules* (Cambridge, 1932), p. 81.
[22] R. F. Bacher and S. Goudsmit, *Atomic Energy States* (McGraw-Hill, 1932), p. 293.

The partial pressure P_a was computed from the data of Giauque and Clayton,[23] a plot of which yields the equilibrium constant

$$K=P_a^2/P_m=1.36(10^7)e^{-94700/T}. \quad (12)$$

Since $P_a+P_m=P$, we have

$$P_a=(K/2)\{(1+4P/K)^{\frac{1}{2}}-1\}. \quad (13)$$

The functions F, P_a and n are given in Table I computed for a total pressure of one atmosphere.

The generalized conductivity Θ is the sum of two terms, one the ordinary thermal conductivity and the other a term contributed by atomic diffusion with its accompanying energy transfer. The gas under consideration is, of course, a mixture of molecules and atoms. With regard to the ordinary conductivity, a sufficiently good approximation for the mixture is given by an average of the separate conductivities of the two gases in the mixture, each weighted in proportion to its partial pressure.[24] The diffusion term will be considered later.

Measurements of thermal conductivity are not available at extremely high temperatures. Furthermore, there are difficulties inherent in the experiments which limit the reliability of thermal conductivity measurement in gases even at easily available temperatures. Hence, following Langmuir[25] the conductivity is obtained by means of the kinetic theory relationship connecting conductivity and viscosity, i.e., $K=\epsilon\eta C_V$. Here η is the viscosity, C_V is the specific heat at constant volume, and $\epsilon=\frac{1}{4}(9\gamma-5)$, where γ is the ratio of specific heats.[26]

Viscosity measurements are available for molecular nitrogen up to about 1000°K. Two different formulas have been considered for use in extrapolating these data to higher temperatures: the familiar Sutherland formula, and that due to Hassé and Cook.[27] The first of these has been employed here, since its use provides better agreement with experiment than does the second. Constants obtained from Landolt-Bornstein give the formula,

$$\eta=138(10^{-7})T^{\frac{1}{2}}/(T+104.7). \quad (14)$$

The values of η given by the Sutherland formula are lower than those given by Hassé

[23] W. F. Giauque and J. D. Clayton, J. Am. Chem. Soc. **55**, 4887 (1933).

[24] E. H. Kennard, *Kinetic Theory of Gases* (McGraw-Hill, 1938), p. 183.

[25] I. Langmuir, Phys. Rev. **34**, 401 (1912).

[26] J. H. Jeans, *Dynamical Theory of Gases* (Cambridge, 1925), p. 302.

[27] H. R. Hassé and W. R. Cook, Proc. Roy. Soc. **A125**, 196 (1929).

TABLE I. *Values of the current density per unit potential gradient $F(T)$; atomic nitrogen pressure P_a; electron concentration n; and generalized conductivity Θ.*

T°K	$F(T)$ AMP./VOLT-CM	P_a ATMOSPHERE	n (CM)$^{-3}$	$\Theta(T)$ WATT/CM-DEG.
2900	1.160×10^{-9}	2.99×10^{-4}	2.987×10^{5}	1.235×10^{-3}
3100	1.065×10^{-8}	8.454×10^{-4}	2.653×10^{6}	1.309×10^{-3}
3300	7.612×10^{-8}	2.170×10^{-3}	1.846×10^{7}	1.418×10^{-3}
3500	4.437×10^{-7}	4.906×10^{-3}	1.039×10^{8}	1.579×10^{-3}
3700	2.160×10^{-6}	1.015×10^{-2}	4.916×10^{8}	1.829×10^{-3}
3900	9.144×10^{-6}	1.949×10^{-2}	2.023×10^{9}	2.205×10^{-3}
4100	3.390×10^{-5}	3.496×10^{-2}	7.299×10^{9}	2.750×10^{-3}
4300	1.132×10^{-4}	5.922×10^{-2}	2.368×10^{10}	3.504×10^{-3}
4500	3.382×10^{-4}	9.454×10^{-2}	6.873×10^{10}	4.473×10^{-3}
4700	9.293×10^{-4}	1.438×10^{-1}	1.832×10^{11}	5.646×10^{-3}
4900	2.358×10^{-3}	2.086×10^{-1}	4.500×10^{11}	6.940×10^{-3}
5100	5.532×10^{-3}	2.888×10^{-1}	1.024×10^{12}	8.218×10^{-3}
5300	1.221×10^{-2}	3.822×10^{-1}	2.174×10^{12}	9.276×10^{-3}
5500	2.520×10^{-2}	4.835×10^{-1}	4.329×10^{12}	9.894×10^{-3}
5700	4.890×10^{-2}	5.860×10^{-1}	8.114×10^{12}	9.952×10^{-3}
5900	8.987×10^{-2}	6.811×10^{-1}	1.441×10^{13}	9.393×10^{-3}
6100	1.563×10^{-1}	7.633×10^{-1}	2.435×10^{13}	8.417×10^{-3}
6300	2.595×10^{-1}	8.293×10^{-1}	3.937×10^{13}	7.287×10^{-3}
6500	4.135×10^{-1}	8.791×10^{-1}	6.127×10^{13}	6.205×10^{-3}
6700	6.369×10^{-1}	9.154×10^{-1}	9.243×10^{13}	5.320×10^{-3}
6900	9.309×10^{-1}	9.409×10^{-1}	1.326×10^{14}	4.664×10^{-3}
7100	1.383×10^{0}	9.581×10^{-1}	1.936×10^{14}	4.178×10^{-3}
7300	1.967×10^{0}	9.702×10^{-1}	2.711×10^{14}	3.862×10^{-3}
7500	2.743×10^{0}	9.786×10^{-1}	3.726×10^{14}	3.653×10^{-3}

and Cook, and undoubtedly the truth is somewhere between. The use of the Sutherland formula together with a high estimate of the conductivity of atomic nitrogen leads to a reasonable value for the net conductivity.

The specific heat C_V was obtained from the values of C_P given by Giauque and Clayton[28] up to 5000°K. A plot of the data shows little curvature at that temperature. No great error was anticipated, therefore, in extrapolating to higher temperatures.

Using subscript 1 for quantities characteristic of atomic, and 2 for those characteristic of molecular, nitrogen, we may write

$$\frac{K_1}{K_2}=\frac{9\gamma_1-5}{9\gamma_2-5}\cdot\frac{\eta_1}{\eta_2}\cdot\frac{C_{V_1}}{C_{V_2}}. \tag{15}$$

Simple kinetic theory relationships were used in evaluating this ratio, i.e., $\gamma_1=5/3$; $\gamma_2=7/5$; $C_{V_1}=3R/2M_1$; $C_{V_2}=5R/2M_2$, and

$$\eta_1/\eta_2=(M_1/M_2)^{\frac{1}{2}}d_2^2/d_1^2.$$

The ratio d_2^2/d_1^2, as before, is taken as 1.183. Putting in the remaining constants gives $K_1/K_2=1.33$. The argument, however, does not justify use of more than two significant figures. As was stated earlier, the ordinary conductivity arrived at by using the Sutherland formula does not increase with temperature with sufficient rapidity to conform with experimental data. This deficiency can be approximately compensated for by increasing the ratio of atomic to molecular conductivities. This is done and the ratio is reasonably taken as 1.5 instead of the 1.33 computed from kinetic theory. Hence

$$K=K_2(1+0.5P_a/P). \tag{16}$$

The number of atoms diffusing across unit area per second is given by Chapman[28] as ND grad. (n_a/N) in the absence of gradients of temperature or total pressure. In this formula N is the total gas concentration, D the coefficient of ordinary diffusion, and n_a the atomic concentration. In the present case n_a is a function of temperature only and hence the diffusion term can be written as $ND(d/dT)(n_a/N)dT/dr$. On substituting for N and for n_a in terms of P and P_a, respectively, this becomes

$$[73.85(10^{20})P/T]D(d/dT)(P_a/P).$$

This term does not include so-called thermal diffusion, which is neglected here for reasons to be presented later. Each pair of atoms diffusing carries with it the dissociation energy $2q$. Hence the generalized conductivity (the coefficient which multiplies the temperature gradient) becomes

$$\Theta=K+\frac{73.85(10^{20})P}{T}qD\frac{d}{dT}(P_a/P). \tag{17}$$

Of the quantities appearing in Eq. (17) K has been discussed already. The dissociation energy $2q$ was taken as 7.90 electron volts per molecule.[28] The coefficient of diffusion has been calculated by Amdur[29] for the case of hydrogen, following Enskog and Chapman. The formula given there is

$$D_{12}=\frac{3R^{\frac{1}{2}}T^{\frac{1}{2}}}{8(2\pi)^{\frac{1}{2}}N_1\{\frac{1}{2}(d_1+d_2)\}^2}\left(\frac{1}{M_1}+\frac{1}{M_2}\right)^{\frac{1}{2}}\times\frac{1}{P}\left(\frac{1.0364-0.0303\alpha}{1+C_{12}/T}\right), \tag{18}$$

where N_1 is Avogadro's number; R is the gas constant; d_1 and d_2 the atomic and molecular diameters, respectively; M_1 and M_2 the corresponding atomic weights; P the total pressure, and α the degree of dissociation. The constant C_{12} is the Sutherland constant for the mixture and is given by

$$C_{12}=\frac{(C_1C_2)^{\frac{1}{2}}}{\{\frac{1}{2}[(d_1/d_2)^{\frac{1}{2}}+(d_2/d_1)^{\frac{1}{2}}]\}^6}. \tag{19}$$

Equation (18) is applied here to obtain the diffusion coefficient of nitrogen. From viscosity data Landolt-Bornstein give $d_2=3.90$A. The atomic diameter is not given but is computed here on the assumption that the ratio d_2/d_1 is the same for nitrogen as for hydrogen. As was mentioned earlier, the ratio is given by Amdur as 1.088. An average value of $\frac{1}{2}$ is taken for α. Since α goes from 0 to 1, the maximum error thus introduced is 1.5 percent. Assuming that C_1/C_2

[28] S. Chapman, Phil. Trans. **217**, 158 (1918).

[29] I. Amdur, J. Chem. Phys. **4**, 339 (1936).

is the same for nitrogen as for hydrogen, and using $C_2=104.7$, we obtain $C_1=87.8$. Thus, $C_{12}=96.0$ from Eq. (19). Putting in the other numerical factors gives, finally,

$$D=\frac{44.1(10^{-6})T^{\frac{1}{2}}}{P(1+96/T)} \tag{20}$$

and hence

$$\Theta=K+0.205\frac{T^{\frac{1}{2}}}{1+96/T}\frac{d}{dT}(P_e/P). \tag{21}$$

Values of Θ, computed with the aid of Eq. (21) for $P=1$ atmosphere, are presented in Table I. Eq. (21) is a Sutherland type of equation. As was mentioned earlier, the Sutherland equation gives values of the viscosity too low at high temperatures. Since the diffusion coefficient is proportional to the viscosity, the diffusion coefficient also should be too low at high temperatures. Thermal diffusion is opposite in direction to ordinary diffusion and is neglected here deliberately to compensate approximately for the diffusion deficiency known to exist.

The radial diffusion of electrons and ions is limited by the rate at which ions diffuse out. The coefficient of diffusion for the ions is about the same as for the atoms. The ionization potential is of the same order of magnitude as the dissociation energy expressed in electron volts, so that each pair of electron and ion carries with it about the same energy as does a pair of atoms. The concentration gradient of electrons and ions is small in comparison with that of the atoms, as can be seen from Table I. Hence the power carried out by electrons and ions can be neglected in comparison to that lost by generalized conduction.

Instead of carrying out the integration indicated by Eq. (5) a change of variable was introduced, namely, $x=Er$. With this change Eq. (5) becomes

$$dT/dx=-(1/x\Theta)\int_0^x Fxdx, \tag{22}$$

and W, the power input per unit length, becomes

$$W=EI=2\pi\int_0^\infty Fxdx. \tag{23}$$

Hence Eq. (23) leads to the arc characteristic $E=\text{const}/I$, an equation of the Ayrton type, for cases in which convection heat losses within the arc are small in comparison with those due to conduction..

Equation (22) was integrated numerically in order to evaluate the constant occurring in Eq. (23), starting with a number of different assumed values of T_e, the center temperature. In the calculation of dT/dx, the values of x and F characteristic of the center of a zone of width dx were used in the numerator of Eq. (22). In the denominator of Eq. (22) the values of x and Θ were characteristic of the edge of the zone. The resulting value of dT/dx referred to the edge of the zone, and its use in computing the temperature of the center of the next zone amounted to a three-term Taylor expansion of ΔT.

Results and Conclusions

The values of W resulting from the integrations described above are presented as a function of T_e in Fig. 1. Any inaccuracy in the function Θ appears directly as an inaccuracy in W. Inaccuracies in F appear in W to some power smaller than the first. This is easy to see, since a decrease in F both decreases the contribution of each zone to the power integral and increases the number of zones contributing by altering the temperature distribution.

There are two extremes represented in Fig. 1, one maximum and one minimum. Of these the maximum provides the better agreement with experiment.

The results of the simple theory should apply to cases in which convection is negligible, i.e., when $g\alpha\theta d^3/\nu^2$ is small. This variable can be made small by decreasing the arc diameter, which is done by going to low currents. In Fig. 2 W is plotted as a function of I. The horizontal line, curve A, is the theoretical curve and the other, curve B, is experimental. The solid line was obtained from Suits'[8] data for pure nitrogen. The vertical lines represent unpublished data taken by Mr. J. J. Hopkins in this laboratory. The length of each vertical line indicates the probable error. In the figure the experimental curve approaches the theoretical at low currents, and

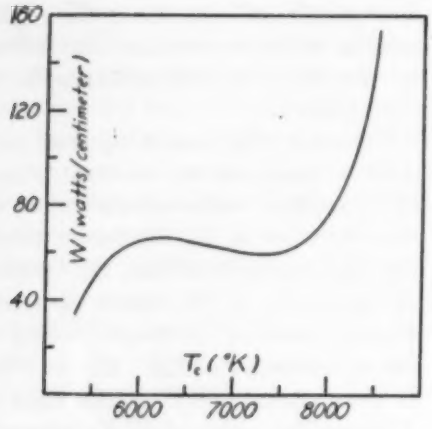

FIG. 1. Power loss per unit length, W, as a function of axial temperature, T_c.

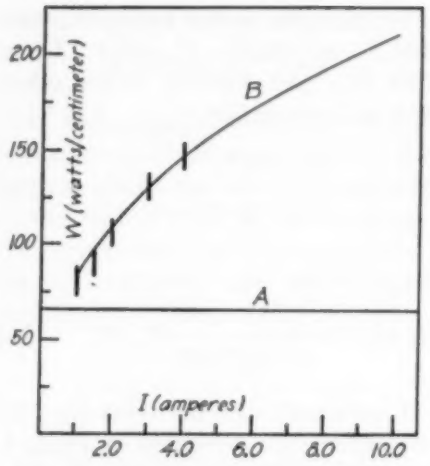

FIG. 2. Power loss per unit length, W, as a function of current, I.

the two coincide within experimental error, if the former is extrapolated to zero current.

The temperature distribution is shown by the plot of T *vs.* x in Fig. 3. Experimentally, the arc appears to have a well-defined edge, so that the apparent arc diameter can be determined either visually or photographically. Lacking values for the light emitted from unit volume of the arc as a function of temperature, this diameter has not been determined from theory. It has been found,[11] however, that the product of the visual cross-sectional area, the electric intensity E, and the F value characteristic of the measured temperature equals the measured current. This being the case, the apparent arc diameter should equal the theoretical root-mean-square diameter defined by Eq. (24) below.

$$d^2=4\int_0^\infty Fr^3dr\Big/\int_0^\infty Frdr. \qquad (24)$$

In the literature one usually finds values of current density J as a function of total current rather than values of d. Remembering that $x=Er$ and $W=EI$, we find Eq. (24) leads to

$$J=W^2/\pi\langle x^2\rangle_{Av}I=9.65/I, \qquad (25)$$

where $\langle x^2\rangle_{Av}$ is the average value of x^2.

A plot of Eq. (25) is shown as curve A, Fig. 4. Curve B is a plot of the experimental values taken from Suits' paper.[3] The comparison of theoretical and experimental current densities is difficult, for several reasons. In the first place, one would like experiments below one ampere in order to see whether or not the trend toward increased current density at decreased currents is anything like as marked experimentally as theoretically. In the second place, errors in the function F appear directly in computations of current density. These errors may be quite large because of uncertainties in the mobility and because of the fact that slight changes in temperature are amplified in changes in F.

The value of the function F required for the average current density given by Eq. (25) is that corresponding to a temperature of 6080°K. This temperature agrees remarkably well with the value of 6100°K given by Suits[12] as the temperature of the atmospheric arc in nitrogen determined from measurements of the velocity of sound. The center temperature T_c, on which the computations are based, is that temperature at which the maximum in W occurs, namely, 6200°K, again not far from the 6100°K given by Suits.

EFFECT OF CONVECTION*

The variable $g\alpha\theta d^3/\nu^2$, which brings in convection effects, can be made small by effectively

* *Note added in proof.*—Dr. Joseph Slepian has kindly pointed out that although $g\alpha\theta d^3/\nu^2$ must be small, it cannot be zero if the present theory is to apply. In future experiments it will be interesting to see how far g can be reduced without the need for considering longitudinal changes in the positive column.

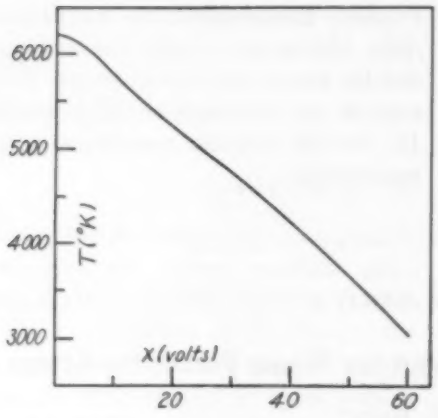

FIG. 3. Temperature distribution curve —temperature T as a function of $x = Er$, the product of longitudinal potential gradient and radius.

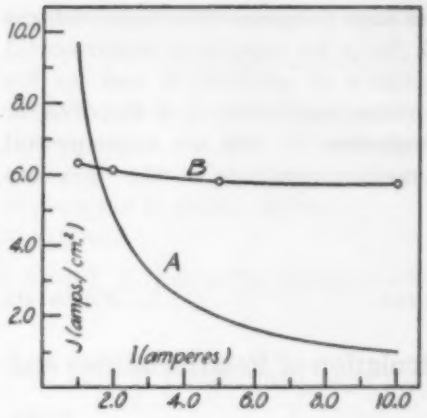

FIG. 4. Current density, J, as a function of current, I.

reducing the acceleration of gravity. The present theory should apply, therefore, to the results of experiments performed in gravity-free space. Steenbeck,[30] in a most ingenious set of experiments, has investigated an arc operating in a freely-falling container. His measurements were for air, not nitrogen, and were more qualitative than quantitative.

The air and nitrogen arcs do not differ greatly one from the other. Hence a comparison of Steenbeck's experiments in air with the present theory developed for nitrogen should at least prove instructive. Steenbeck concludes that the arc drop is less in gravity-free space than in ordinary space and mentions a factor of 2 or 3. His current range was from 1 to 8 amperes. He does not state at which of the various currents the factor of 2 or 3 is observed. It is interesting to note, however, that in Fig. 2 the experimental and theoretical values of W observed at 8 amperes bear the ratio, one to the other, of almost exactly 3. The diameter of the arc is observed by Steenbeck to increase when gravity is removed. The current density corresponding to a total current of 7 or 8 amperes is less than 1 amp./cm². The theoretical value observed at 8 amperes in Fig. 4 is 1.2 amp./cm². For currents below 4 amperes Steenbeck gives the current density as somewhere between 1 and 3 amp./cm². Fig. 4 shows 2.4 amp./cm² at 4 amperes. If we consider the uncertainties in the theoretical determination of current density and the qualitative nature of the experiments, the agreement seems satisfactory.

From Steenbeck's measurements it is safe to conclude that the theoretical results show the same trends as do the experiments with respect to the influence of convection, and that theory and experiment are not in quantitative disagreement. Quantitative measurements in nitrogen are greatly needed. In a private communication Dr. Suits has expressed an interest in such measurements, and it is sincerely hoped that he will carry them out.

A few preliminary computations on the arc at 10 atmospheres indicates about 80 watts per centimeter for W. The curve of W *vs.* T_e is almost flat over a wide temperature range. Hence the determination of T_e and of J awaits further computations.

Some attempts have been made at atmospheric pressure with a view toward including convection in developing a more complete theory of the arc. To date several empirical functions have been tried for representing convection heat loss. Each is subject to certain restrictions as to form, imposed by dimensional arguments, and hence none are entirely arbitrary. Any one of the three functions tried is satisfactory within the arc, but none of them behave properly at large radii. Work is still in progress, however, and it is hoped that an entirely satisfactory function will be developed before very long.

[30] M. Steenbeck, Physik. Zeits. **38**, 1019 (1937).

The authors wish to express their indebtedness to Dr. C. G. Suits for supplying experimental results in advance of publication and for his excellent criticisms, and to Mr. J. J. Hopkins for his kind permission to use his experimental results. To various members of the Institute Physics Department, in particular Professors Allis, Morse and Frank, the authors' thanks are due for many useful discussions. We wish also to express our gratitude to Mr. George H. Lamar, Jr., for his valuable assistance in preparing the manuscript.

JUNE 15, 1939 PHYSICAL REVIEW VOLUME 55

On the Calculation of Polarizabilities and Van der Waals Forces for Atoms in *S* States

JULIAN K. KNIPP*
Laboratory of Physics, University of Wisconsin, Madison, Wisconsin
(Received April 26, 1939)

The perturbation scheme of Møller and Plesset, which has as its basis a complete set of solutions of the Fock single-electron differential-integral equation, is extended to the calculation of atomic polarizabilities and van der Waals force constants. The present treatment differs in three respects from the previous treatments of Kirkwood and Buckingham. First, the Hartree-Fock model is used consistently throughout the calculation. Additional functions are introduced to complete the set of single-electron functions. Sum rules are developed for these functions with the aid of their common Hamiltonian. These replace the Kuhn-Reiche sum rules, which do not apply in their usual form. Second, atomic polarizabilities are expressed as a sum of sums in the perturbation scheme. An ordered set of lower bounds is derived for the first of these sums and also for similar expressions for van der Waals force constants. Third, the contribution of each electron is considered separately. The lower bounds are evaluated exactly with the help of the sum rules developed. In this way are obtained for the approximate values of the atomic polarizability of beryllium and argon 4.14×10^{-24} cm^3 and 1.28×10^{-24} cm^3, respectively. Likewise the constant μ in the van der Waals energy, $-\mu/R^6$, is found to be about 222×10^{-60} erg cm^6 for two beryllium atoms and 63.7×10^{-60} erg cm^6 for two argon atoms. The observed atomic polarizability of argon is 1.63×10^{-24} cm^3.

Sum Rules for the Fock Equation

IN the Hartree-Fock method[1] of dealing with the Schrödinger equation there is assigned to a state of the system an approximate wave function having the proper symmetry and made up of products of single-particle functions. For an atom with N electrons in a nondegenerate state, the approximate wave function has the form

$$\Phi(A)=\mathfrak{A}u_1(a^1)u_2(a^2)\cdots u_N(a^N). \tag{1}$$

A stands for the collection of quantum symbols $a^1, a^2, \cdots, a^N$; the functions $u(a)$ are orthogonal normalized functions of the space and spin coordinates, $xyz\sigma$, of a single electron; and $\mathfrak{A}$ is the normalized antisymmetrizing operator.[2]

For the purpose of Hartree-Fock calculations the atomic Hamiltonian is assumed to be

$$\begin{aligned} H&=\sum_{i=1}^{N}H_i^0+Q;\\ H_i^0&=(1/2m)p_i^2-Ze^2/r_i,\\ Q&=\tfrac{1}{2}\sum_{i\neq j}q_{ij},\quad q_{ij}=e^2/r_{ij}. \end{aligned} \tag{2}$$

In terms of the two expressions

$$\begin{aligned} (a|H^0|a)&=\sum_{\sigma}\int d\tau u^*(a)H^0u(a),\\ (ab|q|cd)&=\sum_{\sigma_1\sigma_2}\int d\tau_1\int d\tau_2 u_1^*(a)u_2^*(b)\\ &\qquad\times q_{12}u_1(c)u_2(d), \end{aligned} \tag{3}$$

* On leave from Purdue University, 1937–38.

[1] D. R. Hartree, Proc. Camb. Phil. Soc. **24**, 89 (1928); V. Fock, Zeits. f. Physik **61**, 126 (1930); P. A. M. Dirac, Proc. Camb. Phil. Soc. **26**, 376 (1930).

[2] $\mathfrak{A}=[N!]^{-\frac{1}{2}}\Sigma_P(-)^pP$, where P is a permutation of parity p of both positional and spin coordinates of the electrons. The notation of this paper follows more or less that of Condon and Shortley, *Theory of Atomic Spectra*. It is an adaptation of the general Dirac notation to atomic problems. Coordinates are usually indicated through subscripts which indicate the particles to which functions belong. Quantum symbols appear in the main line of print.

the average value of H for the function (1) is

$$E_A=(A|H|A)$$
$$=\sum_a(a|H^0|a)+\tfrac{1}{2}\sum_{aa'}[(aa'|q|aa')-(aa'|q|a'a)]. \quad (4)$$

The single-electron functions $u(a^1), \cdots, u(a^N)$ are chosen to give the lowest possible value for E_A. The approximate atomic function then is, for the purpose of calculation of the energy, the best possible consistent with the restriction (1). On minimizing E_A with respect to variations in the functions $u(a)$, it is found that these functions must satisfy the Fock equations,

$$F_1(A)u_1(a)\equiv(H_1^0+P_1)u_1(a)-\sum_{\sigma_2}\int d\tau_2 K_{12}u_2(a)$$
$$=\lambda(a)u_1(a), \quad a=a^1, a^2, \cdots, a^N. \quad (5)$$

Here

$$P_1=\sum_{a'}\sum_{\sigma_2}\int d\tau_2 u_2^*(a')q_{12}u_2(a'),$$
$$K_{12}=\sum_{a'}u_2^*(a')q_{12}u_1(a'). \quad (6)$$

These are N simultaneous nonlinear differential-integral equations. Solutions for particular atoms have been obtained by Fock and Petraschen, Hartree and Hartree and others using numerical methods. When the solutions of the Fock equations are used in (4), E_A becomes the Hartree-Fock energy,

$$E_{HF}=\sum_a\lambda(a)-D(A), \quad (4a)$$

where

$$D(A)=\tfrac{1}{2}\sum_{aa'}[(aa'|q|aa')-(aa'|q|a'a)]. \quad (7)$$

The differential-integral operator $F(A)$ is completely defined as a one-electron operator once the fundamental set of functions $u(a^1), \cdots, u(a^N)$ is defined. After one has obtained the fundamental set for the state A, $F(A)$ can be used as a linear operator for the determination of other solutions, as has been pointed out by Møller and Plesset.[3] In this way is obtained the Fock single-electron differential-integral equation

$$F_1(A)u_1(c)=\lambda(c)u_1(c). \quad (8)$$

N of the normalized orthogonal solutions $u(c)$ of this equation are the N fundamental solutions $u(a^1), \cdots, u(a^N)$ obtained from (5). When written out in detail, (8) is

$$\left[H_1^0+\sum_{a'}\sum_{\sigma_2}\int d\tau_2 u_2^*(a')q_{12}u_2(a')-\lambda(c)\right]u_1(c)$$
$$-\sum_{a'}\sum_{\sigma_2}\int d\tau_2 u_2^*(a')q_{12}u_1(a')u_2(c)=0. \quad (8a)$$

For $u(c)$ the characteristic value is

$$\lambda(c)=(c|H^0|c)+\sum_{a'}[(ca'|q|ca')-(ca'|q|a'c)], \quad (9)$$

where, as before, a' goes over the values $a^1, \cdots, a^N$. It is convenient to denote by $b^{N+1}, \cdots, b, \cdots$ those quantum symbols which do not belong to the fundamental set. A complete set of solutions of (8) can be written as $u(a^1), \cdots, u(a), \cdots, u(a^N), u(b^{N+1}), \cdots, u(b), \cdots$; by $u(c)$ is meant any one of these solutions. It should be pointed out that these functions do *not* become hydrogenic functions in the case of one electron ($N=1$). In the one-electron case (8a) differs from the real Hamiltonian, H^0, through the density and exchange integrals, which cancel only for the lowest characteristic value. The real Hamiltonian and (8a) have the lowest characteristic value and its characteristic function in common but the other characteristic values and functions are different for the two Hamiltonians.

By the use of the completeness relation the following sums over the set of solutions just considered are obtained

$$g(a)\equiv\sum_c|(c|z|a)|^2=(a|z^2|a),$$
$$f(a)\equiv\sum_c[\lambda(c)-\lambda(a)]|(c|z|a)|^2,$$
$$=(a|z[F,z]|a),$$
$$=\frac{\hbar^2}{2m}+\sum_{a'}(aa'|s|a'a), \quad (10)$$

where $[F,z]$ is the commutator $Fz-zF$ and $s=q_{12}(z_1^2-z_1z_2)$. The sum over a' in the second

[3] C. Møller and M. S. Plesset, Phys. Rev. **46**, 618 (1934).

TABLE I. *Sums for beryllium (Hartree units).*

nl	$g_+(nl)$	$f_+(nl)$
$1s$	0.2329	1.801
$2s$	8.43	3.377

expression comes from the exchange integral in $F(A)$, which integral does not commute with the coordinate z. The sums $g(a)$ and $f(a)$ have been reduced to expressions which contain only the fundamental solutions $u(a^1), \cdots, u(a^N)$ of the Fock equation.

For an atom in a state with only complete (nl) groups, the operator $F(A)$ will not affect the spin, as one sees if delta-functions are taken for the spin parts of the single-electron functions, $u(c)$. For such an atomic state the solutions of the associated Fock equation can be taken in the form

$$u(c)=(1/r)R(n^cl^c)P(l^cm_l{}^c)\delta(m_s{}^c,\sigma), \tag{11}$$

with $c=n^cl^cm_s{}^cm_l{}^c$, the usual four quantum numbers of a single particle in a central field. With functions of this form (8) can be separated after substituting the expansion for e^2/r_{12} in the exchange integral and carrying out the integrations over the angles. The equation for $R(n^cl^c)$ is

$$\left[-\frac{\hbar^2}{2m}\left(\frac{d^2}{dr_1{}^2}-\frac{l^c(l^c+1)}{r_1{}^2}\right)-\frac{e^2}{r_1}\left(Z-\int_0^\infty dr_2\frac{r_1}{r_>}\sum_{n'l'}2(2l'+1)R_2(n'l')^2\right)-\lambda(n^cl^c)\right]R_1(n^cl^c)$$

$$-e^2\sum_k\sum_{n'l'}\tfrac{1}{2}C_{l^cl'k}(2l'+1)R_1(n'l')\int_0^\infty dr_2\frac{r_<{}^k}{r_>{}^{k+1}}R_2(n'l')R_2(n^cl^c)=0, \tag{8c}$$

where $C_{lcl'k}$ is the integral of the product of three Legendre polynomials,

$$C_{uvw}=\int_{-1}^{1}dzP_u(z)P_v(z)P_w(z)$$

and $r_<$ is the lesser, $r_>$ the greater, of r_1 and r_2. The fundamental solutions $R(n^al^a)$ of this equation are already available for some atoms. It would be valuable to have in addition some of the Møller-Plesset solutions $R(n^bl^b)$ with lowest characteristic values. Then the first, and often principal, terms in perturbation expressions could be evaluated exactly and the remaining terms approximated with the help of sum rules after the manner described in the last section.

In this representation the matrix of z has nonzero elements only where l changes by unity. Sums like (10) can be separated into two parts, a sum over c_+, in which $l^c=l+1$, and a sum over c_-, in which $l^c=l-1$; $(a=nlm_sm_l)$. Each part can be evaluated separately since there is a different radial equation for each.[4] Let

$$\begin{aligned}
g_+(a)&=\sum_{c_+}|(c_+|z|a)|^2=\frac{(l-m_l+1)(l+m_l+1)}{(2l+3)(2l+1)}g_+(nl),\\
g_-(a)&=\sum_{c_-}|(c_-|z|a)|^2=\frac{(l^2-m_l{}^2)}{(2l+1)(2l-1)}g_-(nl),\\
f_+(a)&=\sum_{c_+}[\lambda(c_+)-\lambda(a)]|(c_+|z|a)|^2=\frac{(l-m_l+1)(l+m_l+1)}{(2l+3)(2l+1)}f_+(nl),\\
f_-(a)&=\sum_{c_-}[\lambda(c_-)-\lambda(a)]|(c_-|z|a)|^2=\frac{(l^2-m_l{}^2)}{(2l+1)(2l-1)}f_-(nl),
\end{aligned} \tag{10a}$$

[4] See E. Wigner, Physik. Zeits. **32**, 451 (1931).

TABLE II. *Sums for argon (Hartree units). In this table and in Table I the effect of the exchange integral which occurs in the Fock equation is very noticeable. Eq. (12a) shows that if the exchange terms were absent $f_+(ns)$ would have the value 1.5, $f_+(np)$ the value 2.5, and $f_-(np)$ the value -0.5. The effect is greater the more loosely bound the electron.*

nl	$g_\pm(nl)$	$f_+(nl)$	$f_-(nl)$
$1s$	0.0101	1.555	
$2s$	0.201	1.656	
$2p$	0.174	2.827	−0.531
$3s$	2.348	2.007	
$3p$	3.310	3.943	−0.484

where

$$g_+(nl)=\sum_{n^cl}|(n^cl+1|r|nl)|^2,$$
$$f_+(nl)=\sum_{n^cl}[\lambda(n^cl+1)-\lambda(nl)]|(n^cl+1|r|nl)|^2, \tag{12}$$

with similar expressions for $g_-(nl)$ and $f_-(nl)$. Then $g(a)=g_+(a)+g_-(a)$ and $f(a)=f_+(a)+f_-(a)$. By using the completeness relation there result

$$g_+(nl)=(nl|r^2|nl)=g_-(nl),$$
$$f_+(nl)=\frac{\hbar^2}{2m}(2l+3)+\sum_{n'l'k}\left(\frac{2l'+1}{2}\right)[C_{ll'k}G_k^{(20)}(nl,n'l')-C_{l+1l'k}G_k^{(11)}(nl,n'l')], \tag{12a}$$
$$f_-(nl)=\frac{-\hbar^2}{2m}(2l-1)+\sum_{n'l'k}\left(\frac{2l'+1}{2}\right)[C_{ll'k}G_k^{(20)}(nl,n'l')-C_{l-1l'k}G_k^{(11)}(nl,n'l')],$$

where[5]

$$G_k^{(ij)}(nl,n'l')=e^2\int_0^\infty dr_1\int_0^\infty dr_2 r_1^i r_2^j R_1(nl)R_1(n'l')R_2(nl)R_2(n'l')\frac{r_<^k}{r_>^{k+1}},$$

in which $r_<$ is the lesser and $r_>$ the greater of r_1 and r_2.

The sums (12) have been calculated by numerical integration for the ground states of beryllium and argon using the functions calculated by Hartree and Hartree.[6] The results are given in Tables I and II. The effect of the exchange terms on $f_+(nl)$ is very large for outer shells and progressively less important for inner shells. In $f_-(nl)$ the coefficients of the negative terms are larger than they are in the corresponding $f_+(nl)$. The result is that the exchange terms more nearly cancel in $f_-(nl)$.

THE MØLLER-PLESSET HAMILTONIAN

Let $\Phi(C)=\mathfrak{A}u_1(c^1)u_2(c^2)\cdots u_N(c^N)$. Then $\Phi(C)$ satisfies the equation

$$H(A)\Phi(C)=E(C)\Phi(C), \tag{13}$$

where
$$H(A)=\sum_{i=1}^N F_i(A)-D(A).$$

The characteristic value is
$$E(C)=\sum_c\lambda(c)-D(A).$$

[5] This quantity reduces to the familiar $G_k(nl,n'l')$ for $i=j=0$.

[6] Hartree and Hartree, Proc. Roy. Soc. **150**, 9 (1935), Be with exchange; Proc. Roy. Soc. **166**, 450 (1938), *A* with exchange, partially interpolated.

In particular for $C=A$, $E(A)=E_{HF}$ as defined in (4a). The functions $\Phi(C)$ form a complete set of functions in the $4N$ space-spin variables of the atomic system.

Møller and Plesset introduce the Hamiltonian $H(A)$ and its solutions $\Phi(C)$ with characteristic values $E(C)$ for use as the starting point of a perturbation calculation of the atomic energy. The perturbing term in their scheme is the difference between H, the actual Hamiltonian of the system, and $H(A)$, a Hamiltonian to which the Hartree-Fock wave function belongs. It is convenient to introduce a parameter ϵ, which is later put equal to unity. The perturbing term is $\epsilon[H-H(A)]$. The actual function and energy of the state can be developed in powers of ϵ with $\Phi(A)$ and $E(A)$ as the zero-order terms. The first-order perturbation energy is obviously zero.

Atomic Polarizabilities

In the presence of an electric field of strength $\mathcal{E}$, directed along the z axis, the Hamiltonian is $H'=H+e\mathcal{E}Z$, where Z is the sum of the z coordinates of the electrons; $Z=z_1+z_2+\cdots+z_N$. By taking an approximate wave function of the form $\mathcal{A}u_1'(e^1)u_2'(e^2)\cdots u_N'(e^N)$ in which the single-electron functions depend on $\mathcal{E}$, new Fock equations are obtained. They are

$$F_1'u_1'(e)\equiv(H_1^0+P_1'+e\mathcal{E}z_1)u_1'(e)-\sum_{\sigma_1}\int d\tau_2 K_{12}'u_2'(e)=\lambda'(e)u_1'(e),\quad e=e^1,\cdots,e^N, \tag{14}$$

where P' and K_{12}' are expressions (6) calculated with the functions $u'(e^1),\cdots,u'(e^N)$. The approximate (Hartree-Fock) energy is $\sum_e\lambda'(e)-D'$. The coefficient of $-\frac{1}{2}\mathcal{E}^2$ in this expression might be called the Hartree-Fock polarizability, α_{HF}. It is the polarizability of an imaginary atom the Hamiltonian of which is minimized by the Hartree-Fock field dependent wave function. It would be advantageous if the solutions of (14) could be conveniently expressed in terms of the complete set of solutions of the field-free equation. An attempt to obtain such relations by perturbation methods led to expressions from which objectionable degeneracy terms could not readily be removed because of the nonlinearity of the equations.

Another approach is through the Møller-Plesset Hamiltonian $H(A)$ and the perturbing function $\epsilon[H-H(A)]+e\mathcal{E}z$. The exact wave function, energy and polarizability of the atom, Ψ', E' and α are developed in powers of the parameters ϵ and $\mathcal{E}$,

$$\begin{aligned}\Psi'&=[\Phi(A)+\mathcal{E}\Phi^{(01)}+\cdots]+\epsilon[\Phi^{(10)}+\mathcal{E}\Phi^{(11)}+\cdots]+\cdots,\\ E'&=[E(A)+\mathcal{E}^2E^{(02)}+\cdots]+\epsilon[\mathcal{E}^2E^{(12)}+\cdots]+\cdots,\\ \alpha&=\alpha^{(0)}+\epsilon\alpha^{(1)}+\cdots.\end{aligned} \tag{15}$$

Expressions for the coefficients of the various powers of ϵ and $\mathcal{E}$ are given by the regular perturbation theory. These expressions involve only elements of the matrices of $[H-H(A)]$ and eZ, in the representation scheme belonging to $H(A)$, and the corresponding energy differences.

The expression for $\alpha^{(0)}$ is

$$\alpha^{(0)}=2e^2\sum_B\frac{|(B|Z|A)|^2}{E(B)-E(A)}. \tag{16}$$

The sum is restricted to terms B which differ from A in only one single-electron quantum number set since all other terms give zero. The terms can be separated into N groups, one for each of the N elements of $A: a^1,\cdots,a^N$. (16) becomes

$$\alpha^{(0)}=2e^2\sum_{ab}\frac{|(b|z|a)|^2}{\lambda(b)-\lambda(a)}, \tag{16a}$$

where a runs over $a^1,\cdots,a^N$ and b over all other single-electron quantum number sets necessary to

specify the complete set of functions $u(c)$. Similarly $\alpha^{(1)}$ can be shown to be

$$\alpha^{(1)}=2e^2\sum_{aa'bb'}\frac{\cdot\ (a'|z|b')X(b|z|a)}{[\lambda(b')-\lambda(a')][\lambda(b)-\lambda(a)]}, \tag{17}$$

where $$X=(ab'|q|a'b)-(ab'|q|ba')+(aa'|q|b'b)-(aa'|q|bb').$$

The right side of (16a) can be obtained from the exact expression for the polarizability by replacing the exact atomic functions and energies by the Møller-Plesset functions and energies. $\alpha^{(0)}$ cannot be expected to be a good approximation when the number of electrons is very small. The difficulty comes from the Fock equation. Even when there is but one electron the Møller-Plesset functions and energies are not the exact functions; even in this case $\alpha^{(0)}$ is only a first approximation to α.

Van der Waals Forces

If two atoms are far enough apart that overlapping and accompanying exchange effects can be neglected, their interaction can be calculated by starting with a complete set of functions for each atom and expanding the Hamiltonian in inverse powers of the separation distance. A state of the system is represented by the wave function $\mathfrak{A}'\Psi(\Gamma')\Psi^0(\Gamma^{0\prime})$, where $\Psi(\Gamma')$ and $\Psi^0(\Gamma^{0\prime})$ are functions for the first and second atoms, respectively. The operator $\mathfrak{A}'$ antisymmetrizes the product for all permutations of the $N+N^0$ electrons.[7] Let $\mathbf{H}$ be the Hamiltonian of the system, that is, of the two atoms with fixed centers a distance R apart and $N+N^0$ electrons. Then since $\mathbf{H}$ is symmetrical in all the electrons, it commutes with the operator $\mathfrak{A}'$ and can be expanded in inverse powers of the internuclear distance,

$$\mathbf{H}\mathfrak{A}'\Psi\Psi^0=\mathfrak{A}'[H+H^0+(e^2W_2/R^3)+(e^2W_3/R^4)+(e^2W_4/R^5)+\cdots]\Psi\Psi^0. \tag{18}$$

All monopole terms drop out since the atoms are assumed to be neutral. W_2 is the dipole-dipole coefficient; W_3 is the dipole-quadrupole coefficient; and W_4 contains the dipole-octopole and quadrupole-quadrupole coefficients. In particular, the dipole-dipole coefficient is

$$W_2=-\sum_m a(m)F(m)F^0(-m),\quad a(-1)=a(1)=1,\quad a(0)=2. \tag{19}$$

Here $F(m)=\sum f(m)$, and $F^0(m)$ is defined for the second atom similarly, with the summation in each case over the electrons of the particular atom. The single-electron functions are

$$f(-1)=(x-iy)/\sqrt{2},\quad f(0)=z,\quad f(1)=-(x+iy)/\sqrt{2}.$$

The van der Waals interaction energy, $-\mu/R^6$, is a second-order effect coming from the dipole-dipole term. It was first calculated by Wang for two hydrogen atoms.[8] Generalizations were made by London[9] using perturbation expressions and introducing average denominators equal to the sum of the first ionization potentials of the two atoms in question. He obtained the simple result that μ is roughly equal to three halves the product of the polarizabilities of the atoms divided by the sum of the reciprocals of the ionization potentials. Hassé, Kirkwood and others[10] have used variational procedures to obtain similar expressions. Hellmann has used a combination of methods in his estimates of van der Waals constants. The most elaborate calculations have recently been made by Buckingham[11] using the methods of Kirkwood but taking into account the exclusion principle.

---

[7] $\mathfrak{A}'=[N!N^0!/(N+N^0)!]^{\frac{1}{2}}\Sigma_Q(-)^qQ$, where Q is an exchange of parity q, that is a permutation of the $N+N^0$ electrons leading to an ordered assignment in each atom.

[8] S. Wang, Physik. Zeits. **28**, 663 (1927).

[9] F. London, Zeits. f. Physik **63**, 245 (1930); Zeits. f. physik. Chemie **11**, 222 (1930).

[10] H. R. Hassé, Proc. Camb. Phil. Soc. **27**, 66 (1931); J. G. Kirkwood, Physik. Zeits. **33**, 57 (1932); L. Pauling and J. Y. Beach, Phys. Rev. **47**, 686 (1935); H. Hellmann, Acta Phys. Chem. USSR **2**, 273 (1935).

[11] R. A. Buckingham, Proc. Roy. Soc. **160**, 113 (1937).

TABLE III. *Sums for argon (Hartree units). The sums of Table II corrected as required by the exclusion principle.*

nl	$\zeta_+(nl)$	$\zeta_-(nl)$	$\eta_+(nl)$	$\eta_-(nl)$
$1s$	0.0061		0.924	
$2s$	0.046		1.142	
$2p$	0.174	0.015	2.827	0.382
$3s$	0.103		0.554	
$3p$	3.310	1.065	3.943	1.200

An exact expression for μ is

$$\mu=e^4\sum_{\Gamma'\Gamma^{0\prime}}\frac{|(\Gamma\Gamma^0|W_2|\Gamma'\Gamma^{0\prime})|^2}{E(\Gamma')+E^0(\Gamma^{0\prime})-E(\Gamma)-E^0(\Gamma^0)}, \tag{20}$$

provided exact solutions of the atomic problem are used. Here

$$(\Gamma\Gamma^0|W_2|\Gamma'\Gamma^{0\prime})=-\sum_m a(m)(\Gamma|F(m)|\Gamma')(\Gamma^0|F^0(-m)|\Gamma^{0\prime}).$$

If Hartree-Fock functions are used, μ can be thought of as a sum of terms, $\mu=\mu^{(0)}+\mu^{(1)}+\cdots$, in a perturbation scheme which starts with the Hartree-Fock approximation for the lowest states. The first nonzero contribution to μ is similar in form to the exact expression and can be obtained by substituting the Møller-Plesset functions and energies in (20). There results

$$\mu^{(0)}=e^4\sum_{BB^0}\frac{|(AA^0|W_2|BB^0)|^2}{E(B)+E^0(B^0)-E(A)-E^0(A^0)}, \tag{21}$$

where

$$(AA^0|W_2|BB^0)=-\sum_m a(m)(A|F(m)|B)(A^0|F^0(-m)|B^0)$$

$$=\pm\sum_m a(m)(a|f(m)|b)(a^0|f^0(-m)|b^0).$$

This can be easily transformed into

$$\mu^{(0)}=6e^4\sum_{aa^0}\sum_{bb^0}\frac{|(a|z|b)|^2|(a^0|z^0|b^0)|^2}{\lambda(b)+\lambda^0(b^0)-\lambda(a)-\lambda^0(a^0)}. \tag{21a}$$

APPROXIMATE VALUES

The exclusion principle operates in (16a), (17) and (21a) to limit the infinite sums to unoccupied states (the sums are over b, b', etc.). It is convenient to introduce sums which are limited in this way and correspond to the sums (10) and (12) of the first section. The first of these are

$$\zeta(a)=g(a)-\sum_{a'}|(a|z|a')|^2,\quad \eta(a)=f(a)-\sum_{a'}[\lambda(a')-\lambda(a)]|(a|z|a')|^2; \tag{10b}$$

and in addition

$$\zeta(a)_{nl}=(1/2(2l+1))\sum_{m_a m_l}\zeta(a),\quad \eta(a)_{nl}=(1/2(2l+1))\sum_{m_a m_l}\eta(a). \tag{10c}$$

TABLE IV. *Sums for argon (Hartree units).*

a	$\zeta_+(a)$	$\zeta_-(a)$	$\zeta(a)$	$\zeta(a)_{hy}$	$\eta_+(a)$	$\eta_-(a)$	$\eta(a)$	$\eta(a)_{hy}$
$1s\pm\frac{1}{2}0$	0.002		0.002	0.002	0.308		0.308	0.308
$2s\pm\frac{1}{2}0$	0.015		0.015	0.015	0.381		0.381	0.381
$2p\pm\frac{1}{2}\pm1$	0.035		0.035		0.565		0.565	
$2p\pm\frac{1}{2}0$	0.046	0.005	0.051	0.040	0.754	0.127	0.881	0.670
$3s\pm\frac{1}{2}0$	0.034		0.034	0.034	0.185		0.185	0.185
$3p\pm\frac{1}{2}\pm1$	0.662		0.662		0.789		0.789	
$3p\pm\frac{1}{2}0$	0.883	0.355	1.238	0.854	1.052	0.400	1.452	1.010

Here, as before, the four quantum numbers nlm_lm_l are introduced for a. Next are

$$\zeta_+(a)=g_+(a)-\sum_{a_+'}|(a|z|a_+')|^2=\frac{(l-m_l+1)(l+m_l+1)}{(2l+3)(2l+1)}\zeta_+(nl),$$
$$\eta_+(a)=f_+(a)-\sum_{a_+'}[\lambda(a_+')-\lambda(a)]|(a|z|a_+')|^2=\frac{(l-m_l+1)(l+m_l+1)}{(2l+3)(2l+1)}\eta_+(nl), \tag{10d}$$

and similar expressions for $\zeta_-(a)$ and $\eta_-(a)$. In these expressions

$$\zeta_+(nl)=g_+(nl)-\sum_{n'}|(n'l+1|r|nl)|^2,$$
$$\eta_+(nl)=f_+(nl)-\sum_{n'}[\lambda(n'l+1)-\lambda(nl)]|(n'l+1|r|nl)|^2, \tag{12b}$$

and similarly for $\zeta_-(nl)$ and $\eta_-(nl)$. In (12b) the precaution must be taken to sum only over the principal quantum numbers for which there are occupied shells having $l'=l+1$. The sums of this paragraph have been evaluated for argon and are given in Tables III and IV.

Lower bounds to $\alpha^{(0)}$ and $\mu^{(0)}$ will next be obtained by the use of the Schwarz inequality. It will be supposed that $\lambda(b)-\lambda(a)>0$, a condition which is fulfilled for an atom in its lowest state. The Schwarz inequality can be applied in different ways leading to several lower bounds denoted by $\beta_1, \beta_2, \beta_3, \cdots$. Some of these will be seen to be related to expressions previously proposed, while others are quite new. The lower bounds form an ordered set, as will be seen in (27).

Consider the lower bounds which can be completely evaluated using the functions of the fundamental set, $u(a^1), \cdots, u(a^N)$. When the Schwarz inequality is applied to the entire sum in (16a), there is obtained the first lower bound

$$\beta_1=\frac{2e^2[\sum_{ab}|(b|z|a)|^2]^2}{\sum_{ab}[\lambda(b)-\lambda(a)]|(b|z|a)|^2}=2e^2\frac{[\sum_a\zeta(a)]^2}{\sum_a\eta(a)}\leq\alpha^{(0)}. \tag{22}$$

This expression is closely related to the formula obtained by Kirkwood.[12] If, instead of the sum rules which have been developed, the Kuhn-Reiche sum rule is used (or one-electron functions which satisfy the Kuhn-Reiche sum rule are employed) and if the terms missing in the sums because of the exclusion principle are introduced, then by replacing $\zeta(a)$ by $g(a)$ and $\eta(a)$ by $\hbar^2/2m$ there is obtained from (22) Kirkwood's formula, which is

$$(e^2m/\hbar^2)(4/9N)[\sum_a(a|r^2|a)]^2\leq\alpha^{(0)}. \tag{22a}$$

[12] J. G. Kirkwood, Physik. Zeits. **33**, 57 (1932).

This expression was obtained by Kirkwood by a variational type of calculation using a single-product atomic function. It was also obtained by Vinti[13] with the aid of the Kuhn-Reiche sum rule.

If in (16a) the Schwarz inequality is applied separately to terms with different principal quantum numbers n, there is obtained

$$\beta_2=2e^2\sum_n\Big[\sum_{lm_sm_l}\zeta(a)\Big]^2/\sum_{lm_sm_l}\eta(a). \tag{23}$$

In a similar way treating each (nl) group separately gives

$$\beta_3=2e^2\sum_a\zeta(a)_{nl}^2/\eta(a)_{nl}. \tag{24}$$

The most extensive calculations of atomic polarizabilities have been made by Buckingham,[14] who has obtained expressions by starting with the variational method. He follows Hassé's procedure of adding terms to the wave function which have the same form as the perturbing terms of the Hamiltonian. Because of certain terms which he neglects, the expression for the energy which is obtained is not an upper bound to the energy as required by the variational principle. For this reason his result does not represent a lower bound for the atomic polarizability. The expression which Buckingham obtains when a different parameter is used for each (nl) group in the atom is related to β_3. The average value of $\zeta(a)$ over a complete (nl) group can be transformed to give

$$\zeta(a)_{nl}=\tfrac{1}{3}\Big[(a|r^2|a)-\sum_{a'}|(a|\mathbf{r}|a')|^2\Big],$$

where
$$|(a|\mathbf{r}|a')|^2=|(a|x|a')|^2+|(a|y|a')|^2+|(a|z|a')|^2.$$

Substituting this in β_3 and replacing $\eta(a)_{nl}$ by $\hbar^2/2m$, there results

$$4me^2/9\hbar^2\sum_a\Big[(a|r^2|a)-\sum_{a'}|(a|\mathbf{r}|a')|^2\Big]^2\leqq\alpha^{(0)}, \tag{24a}$$

which is the expression obtained by Buckingham.[15] It contains corrections due to the exclusion principle, which are missing in Kirkwood's formula, because Buckingham's functions were properly antisymmetrized. Values calculated from this expression are very large. This is to be expected since $\eta(a)_{nl}$ is much larger than $\hbar^2/2m$ for an outer shell.

If each of the N terms in the summation over a in (16a) is treated separately, there is obtained the lower bound

$$\beta_4=2e^2\sum_a\zeta(a)^2/\eta(a). \tag{25}$$

Still another expression is obtained by separating the terms with $l'=l+1$ from those with $l'=l-1$,

$$\beta_5=2e^2\sum_a\big[\zeta_+(a)^2/\eta_+(a)+\zeta_-(a)^2/\eta_-(a)\big]. \tag{26}$$

These five expressions stand in the relation

$$\beta_1\leqq\beta_2\leqq\beta_3\leqq\beta_4\leqq\beta_5\leqq\alpha^{(0)}. \tag{27}$$

The lower bounds for beryllium can be calculated directly from the data of Table I. β_1 is $19.3a_0^3$ (a_0 = radius of first Bohr orbit of hydrogen); β_2 is $28.1a_0^3$; and β_3, β_4 and β_5 are the same as β_2. Kirk-

[13] P. Vinti, Phys. Rev. **41**, 813 (1932).
[14] R. A. Buckingham, Proc. Roy. Soc. **160**, 94 (1937); see also R. Eisenschitz and F. London, Zeits f. Physik **60**, 491 (1930); H. R. Hassé, Proc. Camb. Phil. Soc. **26**, 542 (1930); H. Hellmann, Acta Phys. Chem. USSR **2**, 273 (1935).
[15] More complicated expressions are obtained by Buckingham on introducing a second function and second parameter for each shell.

wood's formula (22a) gives $33.3a_0^3$ and Buckingham's formula (24a) gives $63.2a_0^3$. In β_2 the $2s$ electrons contribute $28.05a_0^3$ and the $1s$ electrons $0.04a_0^3$ to the total. In ordinary units β_2 is 4.14×10^{-24} cm^3.

For argon β_1, β_2 and β_3 are $5.05a_0^3$, $8.41a_0^3$, and $8.72a_0^3$, respectively. β_3, β_4 and β_5 are almost the same, but differences can be calculated with some accuracy; thus $\beta_5-\beta_3$ is only $3.4\times10^{-3}a_0^3$. Kirkwood's formula gives $16.7a_0^3$ and Buckingham's formula gives $17.5a_0^3$. In β_3 the $3p$ electrons contribute $8.69a_0^3$; the $2s$ and $2p$ electrons contribute $3.1\times10^{-2}a_0^3$; and the $1s$ electrons contribute $5.2\times10^{-5}a_0^3$. In ordinary units β_3 is 1.28×10^{-24} cm^3. The value of the polarizability obtained from the experimental data of C. and M. Cuthbertson[16] is 1.63×10^{-24} cm^3.

In each case even the best of these lower bounds may not be very close to the true value of $\alpha^{(0)}$; the major contribution always comes from one of the groups of terms and the sum for each group has been approximated by the use of an average denominator. Better lower bounds could be obtained if some of the functions $u(b^{N+1})$, $\cdots$ were obtained and used to calculate the first terms in (16a). The sum of the remaining terms could be approximated by the use of sum rules in the way the entire sums have been treated.[17]

Estimates of the next term in the polarizability, $\alpha^{(1)}$, have been made and indicate that this term may not be small. If in (17) each (nl) group is treated separately and average denominators are introduced (the same approximation as β_3), an expression is obtained which has the value $3.07a_0^3$ for beryllium and $-4.53a_0^3$ for argon. The exchange terms, which give positive contributions, are for s electrons larger than the direct terms, which give negative contributions. For p electrons the relative contribution of the exchange terms is cut down and the combined effect is negative. These are not lower bounds to $\alpha^{(1)}$.

Lower bounds to $\mu^{(0)}$ can be obtained from (21a). If the electrons of each atom are all grouped together, there results

$$\nu_1=\frac{6e^4[\sum_a\zeta(a)]^2[\sum_{a^0}\zeta^0(a^0)]^2}{\sum_a\eta(a)\sum_{a^0}\zeta^0(a^0)+\sum_{a^0}\eta^0(a^0)\sum_a\zeta(a)}. \tag{28}$$

The corresponding formula of Kirkwood is

$$\frac{e^4m}{\hbar^2}\frac{4}{9}\frac{[\sum_a(a|r^2|a)]^2[\sum_{a^0}(a^0|r^{02}|a^0)]^2}{[N\sum_{a^0}(a^0|r^2|a^0)+N^0\sum_a(a|r^2|a)]}. \tag{28a}$$

If in each atom electrons with the same principal quantum number are grouped together, there is obtained

$$\nu_2=6e^4\sum_{nn^0}\frac{[\sum_{lm_sm_l}\zeta(a)]^2[\sum_{l^0m_s^0m_l^0}\zeta^0(a^0)]^2}{[\sum_{lm_sm_l}\eta(a)\sum_{l^0m_s^0m_l^0}\zeta^0(a^0)+\sum_{l^0m_s^0m_l^0}\eta^0(a^0)\sum_{lm_sm_l}\zeta(a)]}. \tag{29}$$

Treating each (nl) group separately gives

$$\nu_2=6e^4\sum_{aa^0}\frac{\zeta(a)_{n_a}^2\zeta^0(a^0)_{n_0}^2}{\eta(a)_{n_a}\zeta^0(a^0)_{n_0}+\eta^0(a^0)_{n_0}\zeta(a)_{n_a}}. \tag{30}$$

[16] C. and M. Cuthbertson, Proc. Roy. Soc. **84**, 13 (1911).

[17] In addition upper bounds could be obtained. The terms of (16a) could be grouped and the denominators of the group replaced by the smallest denominator in the group. For example if $\lambda^{(4)}(a)$ is the lowest $\lambda(b)$ which occurs in (16a) for a given a, an upper bound is $\beta^{(4)}=2e^2\Sigma_a\zeta(a)/[\lambda^{(4)}(a)-\lambda(a)]$.

The corresponding formula of Buckingham is

$$\frac{12e^4m}{\hbar^2}\sum_{aa^0}\frac{\zeta(a)_{kl}^2\zeta^0(a^0)_{kl}^2}{\zeta(a)_{kl}+\zeta^0(a^0)_{kl}}. \tag{30a}$$

Similarly, if each electron is treated separately, an expression ν_4 is obtained; and if each electron is treated separately and the sum separated according to the changes in l, an expression ν_5 results. It is found for argon that ν_4 and ν_5 differ but slightly from ν_3. The above expressions have the relation $\nu_1 \leq \nu_2 \leq \nu_3 \leq \mu^{(2)}$.

The results for beryllium are: $\nu_1 = 167.2h_0a_0^6$ ($h_0 = me^4/\hbar^2$ = twice the ionization energy of hydrogen); Kirkwood's formula (28a), gives $288.6h_0a_0^6$; $\nu_2 = 237.8h_0a_0^6$; Buckingham's formula (30a), gives $534.0h_0a_0^6$. In ordinary units ν_2 is 222.3×10^{-60} erg cm^6. The interactions of $2s$ with $2s$ electrons contribute $236.5h_0a_0^6$ to ν_2 and the interactions of $2s$ with $1s$ and $1s$ with $1s$ contribute 1.286 and $0.00935h_0a_0^6$, respectively.

The results for argon are: $\nu_1 = 41.5h_0a_0^6$; Kirkwood's formula gives $217.5h_0a_0^6$; $\nu_2 = 66.2h_0a_0^6$; $\nu_3 = 68.1h_0a_0^6$; Buckingham's formula gives $135.9h_0a_0^6$. In ordinary units ν_3 is 63.7×10^{-60} erg cm^6. The interactions of $3p$ with $3p$ electrons contribute $66.6h_0a_0^6$ to ν_3; the interactions of $3p$ with $3s$, with $2p$, with $2s$, and with $1s$ contribute 0.65, 0.83, 0.073 and $0.0017h_0a_0^6$, respectively. The interactions of $3s$ with $3s$ contribute only $0.0026h_0a_0^6$. The interactions of $2p$ with $2p$ contribute 0.0096, etc.

A very extensive study of the nature of the interaction of two argon atoms has recently been made by Buckingham.[18] He has used the magnitude and temperature dependence of the second virial coefficient of argon gas and the lattice energy and lattice constant of solid argon as experimental data to fix the constants in various assumed potential functions. It is found that the temperature dependence of the second virial coefficient is given satisfactorily for a wide range of the parameters. For the Lennard-Jones interaction $\lambda R^s - \mu R^{-6}$, the lattice energy is given best for $s = 13.6$ and $\mu = 90\times10^{-60}$ erg cm^6. This interaction then gives a lattice constant which is about three percent too small. The Born-Mayer interaction $be^{-R/\rho} - \mu R^{-6}$ with $\mu = 102\times10^{-60}$ erg cm^6 and appropriate values of the other constants is found to reproduce all the experimental data fairly well. The Wasatjerna interaction $cR^7e^{-R/\rho} - \mu R^{-6}$ is also found to give good results; the best value of μ for it is 105×10^{-60} erg cm^6. It is pointed out by Buckingham that higher order van der Waals terms, terms in R^{-8}, R^{-10}, etc., are probably important at the distances considered and that they would, if included, have the effect of reducing the magnitude of the estimated value of μ. Herzfeld and Goeppert-Mayer[19] give an interaction of the Born-Mayer type with $\mu = 110\times10^{-60}$ erg cm^6, which gives a somewhat smaller lattice energy than used by Buckingham, but about the same lattice constant and very good values for the second virial coefficient. Hirschfelder, Ewell and Roebuck[20] have shown that the temperature dependence of the Joule-Thomson coefficient is given fairly well by a variety of possible potential curves.

The writer is indebted to Professor Breit and Professor Wigner for discussion of this work and many suggestions regarding it. He wishes to thank the Wisconsin Alumni Research Foundation for its support.

[18] R. A. Buckingham, Proc. Roy. Soc. **168**, 264 (1938).
[19] K. F. Herzfeld and M. Goeppert-Mayer, Phys. Rev. **46**, 995 (1934); K. F. Herzfeld, Phys. Rev. **52**, 374 (1937).
[20] Hirschfelder, Ewell and Roebuck, J. Chem. Phys. **6**, 205 (1938).

Conservation of Momentum in Electrical Conductivity

W. V. HOUSTON
California Institute of Technology, Pasadena, California
(Received December 21, 1938)

In the theory of the electrical conductivity of metals, the conservation theorem of Peierls establishes the invariance of the sum of the electron wave numbers and a function of the lattice vibrations. This is shown to be accompanied by other related conservation theorems based on the periodicity of the system. One of these refers to the difference between Peierls' integral and the total momentum of the system. The connection between Peierls' integral and the integral of momentum has usually been obscured by the use of electron states that do not represent a definite value of the momentum. When the system is treated as a whole it can be shown that the transfer of momentum from the electrons to the lattice need not be a process involving one electron at a time, but may involve a large number. One can say that the *umklapprozesse* involve a whole group of electrons rather than a single one. As a result one can understand the establishment of a steady state in a conducting metal without considering the *umklapprozesse* of single electrons as introduced by Peierls.

1. INTRODUCTION

SINCE the work of Peierls[1] the theory of the electrical conductivity of metals has been marred by the presence of a conservation theorem whose physical significance has not been clearly understood. It has been interpreted as indicating that the conductivity of a metal should be very much larger, at low temperatures, than is observed, unless the electron energy as a function of wave number is restricted to a closely prescribed form. This seems an undue restriction, especially in the case of the alkalis. It is proposed to show here that this interpretation of the theorem is not justified, and that Peierls' conservation law presents no real obstacle to the understanding of the processes of conduction and resistance.

The theorem in question is that, in the absence of an external electric field, the quantity

$$I_1=(1/G)\{\Sigma k_j+\Sigma f m_f\}, \qquad (1)$$

is a constant of the motion, or can change by integral amounts only. Eq. (1) is written for the special case of a one-dimensional lattice in which d is the distance between the equilibrium positions of the ions, G is the number of ions in one cycle, f is the integer characterizing a lattice vibration, and m_f is an integer associated with the excitation of the vibration f. A positive value of m_f represents a wave traveling through the lattice in the positive direction. The quantities k_j are integers that characterize the wave functions of the individual electrons. These functions are of the form $u(x_j)\exp(2\pi i/Gd)k_j x_j$, where $u(x_j)$ is periodic with the period d. To satisfy the Pauli exclusion principle the k_j must be different for different electrons. Since the k_j for each electron changes under the influence of an electric field, and since an electric field cannot directly set up vibrations in the lattice, there has seemed to be no way to prevent I_1 from increasing indefinitely during the flow of a current. For the same reason, after a current has been started and the electric field removed, there has seemed to be no way in which the interaction with the lattice could stop the current without establishing a value of $\Sigma f m_f$ far different from the equilibrium value of zero.

To avoid these difficulties, Peierls invoked the processes by which a single k_j changes by the amount G. Such transitions are not prohibited by the conservation theorem, and since they may represent a reversal in the direction of motion, Peierls called them *umklapprozesse*. However, he also showed that the effective intervention of such processes at low temperatures requires a prescribed form of the electron energy as a function of the wave number k. That all metals, and in particular the alkalis, should have this particular form seems quite improbable.

It will be shown here, however, that the restriction imposed by Peierls' theorem applies

[1] R. Peierls, Ann. d. Physik **12**, 154 (1932).

to all of the electrons together and not to each one by itself. In addition to the *umklapprozesse* of Peierls there can take place processes by which a number of electrons change their total Σk_j by the amount G. Such a process does not require the presence of a lattice vibration, but is due to the interaction with the undisturbed lattice. This provides a tremendous number of processes in which different numbers of electrons take part. Included in them are the processes in which each electron present changes its k_j by a single unit.

Transitions involving two or more electrons might be regarded as very improbable if the interaction between the lattice and the electrons were really a small perturbation. It is, however, a very large interaction, and conclusions characteristic of only the first-order perturbation treatment are not necessarily valid. The fact that the theorem of Peierls imposes a restriction on only the sum of the k_j can be shown by consideration of the properties of the Hamiltonian function.

The treatment of the complete problem shows other integrals of the motion in addition to I_1. One of these is trivial since it expresses merely the cyclic boundary condition. It is that

$$I_2 = k_j \tag{2}$$

can change by integral amounts only. Since k_j is restricted from the beginning to integral values, this is of little importance. The origin of this integral, however, is very similar to that of the others. The third is that

$$I_3 = (1/G)(s - \sum_f f m_f) \tag{3}$$

can change by integral amounts only. In this, s is an integer that represents the momentum of the lattice as a whole. The last is the sum of two others,

$$I_4 = I_1 + I_3 = (1/G)(\sum_j k_j + s), \tag{4}$$

and is associated with the motion of the system as a whole. The presence, in this sum, of both Σk_j and s indicates that all of these integrals are closely connected with the momentum integral.

2. The Hamiltonian Function

The most satisfactory treatment of the theorem of Peierls was given by Bloch,[2] and is based on the invariance of the Hamiltonian function to various transformations. His general procedure will be followed here.

The problem can be treated adequately in one dimension as the other dimensions add only non-essential complications. Let the lattice be composed of G ions of mass m_I, arranged in a straight line, and separated by a distance d, in their equilibrium positions. These equilibrium positions will have the coordinates nd, with n an integer. Only displacements that lie in the line of the ions will be considered. Transverse waves need not be treated since they are of little consequence in the resistance. Let u_n be the displacement of the nth ion from its equilibrium position, and assume that the interaction between the ions can be represented by springs connecting them. It is immaterial whether this interaction is restricted to adjacent ions or whether it extends also to those more distant. It is essential, however, that the lattice as a whole be free to move. This interaction, which is represented by springs, is in addition to that produced by the interaction with the conduction electrons, and it can be regarded as caused by the electrons in the closed shells. Such a specification makes, of course, a very much idealized model of a metal crystal, but it contains the elements essential to the present discussion and it is desirable to be very specific as to the model that is under consideration. In particular it is to be emphasized that only harmonic forces between the ions are being considered. It is also to be understood that the problem is treated as cyclic, and that the G ions constitute one cycle.

If p_j and x_j are respectively the momentum and the coordinate of the jth electron, the Hamiltonian function for the system in the absence of any external field, is

$$H = (m_I/2)\sum_{n=1}^{G} \dot{u}_n^2 + \sum_{n,\,n'} b_{nn'} u_n u_{n'} + \sum_{j=1}^{G} \{(p_j^2/2m) + \sum_{n=1}^{G} V(x_j - nd - u_n) + \sum_{j'=1}^{G} V_e(x_j - x_{j'})\}. \tag{5}$$

The $b_{nn'}$ are constants that can be expressed in

[2] F. Bloch, J. de phys. et rad. **4**, 486 (1933).

terms of the force constants of the springs. $V(x_j-nd-u_n)$ is the potential energy of interaction between the jth electron and the nth ion. The use of a general function, instead of the first few terms of a power series expansion, is necessary to give a Hamiltonian function that guarantees the conservation of momentum.

Following Bloch we may introduce new coordinates ξ_f and η_f defined by the equations

$$u_n=\sum_{f=0}^{G/2}\{\xi_f\cos(2\pi fn/G)+\eta_f\sin(2fn/G)\}. \quad (6)$$

The apparent presence of $G+2$ coordinates for the specification of the positions of G ions need not overdetermine them, since η_0 and $\eta_{G/2}$ are always multiplied by zero coefficients in Eqs. (6). They may therefore be set equal to zero without imposing any restriction on the motion of the ions. Expressed in these coordinates the Hamiltonian function is

$$H=(M/2)\{\dot\xi_0^2+(\tfrac{1}{2})\sum_{f=1}^{G/2-1}[\dot\xi_f^2+\dot\eta_f^2+\omega_f^2(\xi_f^2+\eta_f^2)]$$
$$+\dot\xi_{G/2}^2+\omega_{G/2}^2\xi_{G/2}^2\}+\sum_{j=1}^{G}\{(p_j^2/2m)$$
$$+\sum_{n=1}^{G}V(x_j-nd-\sum_{f=0}^{G/2}[\xi_f\cos(2\pi fn/G)$$
$$+\eta_f\sin(2\pi fn/G)])+\sum_{j'}V_s(x_j-x_{j'})\}, \quad (7)$$

with $M=Gm_I$.

Now let

$$\xi_f=\rho_f\cos\varphi_f, \quad \text{and} \quad \eta_f=\rho_f\sin\varphi_f,$$

with the special provision that $\varphi_0=0$, and $\varphi_{G/2}$ is an integral multiple of π. These provisions preserve the zero values of η_0 and $\eta_{G/2}$. It will also be convenient to introduce the center of mass of the electrons. Hence let

$$X=(1/G)\sum_{j=1}^{G}x_j, \quad \text{and} \quad \xi_i=x_i-X.$$

These coordinates are not all independent since $\Sigma_1{}^G\xi_j=0$. When it is necessary to guard against any ambiguity due to this fact, ξ_1 will be replaced by $-\Sigma_2{}^G\xi_j$. With these coordinates the Hamiltonian function becomes

$$H=(M/2)\{\dot\rho_0^2+(\tfrac{1}{2})\sum_{f=1}^{G/2-1}[\dot\rho_f^2+\rho_f^2\dot\varphi_f^2+\omega_f^2\rho_f^2]$$
$$+\dot\rho_{G/2}^2+\omega_{G/2}^2\rho_{G/2}^2+(Gm/2)\dot X^2$$
$$+(m/2)\sum^{G}\dot\xi_i^2+(m/2)(\sum^{G}\dot\xi_j)^2$$
$$+\sum_{i,\,i'}{}^{i\neq i'}V_s(\xi_i-\xi_{i'})+\sum_{i,\,n}{}^{i\neq i}V(X+\xi_i-nd$$
$$-\sum_{f=0}^{G/2}\rho_f\cos[(2\pi fn/G)-\varphi_f]). \quad (8)$$

This is not strictly the Hamiltonian function since it contains the velocities instead of the momenta, but the transformation is easily made and does not affect any of the conclusions to be drawn.

In the presence of a uniform electric field there is the extra term

$$H'=GeE(\rho_0-X)=GeEZ, \quad (9)$$

where $Z=\rho_0-X$.

Peierls' conservation theorem is associated with the invariance of H under the transformation

$$x_j\to x_j+d, \quad \varphi_f\to\varphi_f+(2\pi f/G), \qquad T_1$$

for all values of j and of f. The increase of all of the x_j by the amount d is equivalent to the increase of X by d with all of the ξ_j unchanged. The terms in the Hamiltonian that are affected by this transformation are those comprising the interaction between the electrons and the lattice. Their invariance under T_1 is due to the cyclic boundary conditions which provide that $V_{n,\,j}=V_{n+G,\,j}$. With this provision, the transformation T_1 effects a rearrangement of the terms in the sum.

However the Hamiltonian function is also invariant under the transformations

$$X\to X+d, \quad \xi_j\to\xi_j-d, \quad (j\neq i), \qquad T_2$$
$$\rho_0\to\rho_0+d, \quad \varphi_f\to\varphi_f-(2\pi f/G), \qquad T_3$$
$$X\to X+d, \quad \rho_0\to\rho_0+d. \qquad T_4$$

The transformation T_2 is equivalent to $x_i\to x_i+Gd$. The invariance of the Hamiltonian func-

tion, as well as all wave functions, under this transformation is due to the cyclic boundary conditions and is merely an expression of them. The transformation T_3 represents the displacement of the lattice through the distance d in one direction, and the displacement of all the elastic waves the same distance in the opposite direction. It can be seen from the forms of the transformations that

$$T_4 = T_1 T_3, \tag{10}$$

and that T_4 is associated with the total momentum of the system. To understand the full significance of these transformations it is helpful to examine the behavior of the wave functions under them.

3. Integrals of the Motion

Let the wave function for each electron be of the usual form indicated above. The total electronic wave function can be built up out of products of these of the form

$$U(x_1, \cdots, x_G) = \prod_{j=1}^{G} \exp\left[(2\pi i/Gd) k_j x_j\right] u_j(x_j)$$

$$= \exp\left[(2\pi i/Gd) \sum k_j x_j\right] \prod_{j=1}^{G} u_j(x_j). \tag{11}$$

The wave function of the lattice can be written in terms of the normal coordinates introduced into the Hamiltonian function

$$U(\rho_f, \varphi_f) = \exp\left[(2\pi i/Gd) s \rho_0\right] \times \prod_{f=1}^{G/2} R(\rho_f, s_f) \exp\left(i m_f \varphi_f\right), \tag{12}$$

where the $R(\rho_f, s_f)$ are the radial functions for a two-dimensional harmonic oscillator, and the s_f and m_f are integers. The Pauli exclusion principle requires that all of the k_j in the electron function be different, but this fact is unimportant for the present considerations. The set of products of these two functions provides a basis for the representation of any state of the combined system.

The above functions have been selected to be characteristic of the operators T_1, T_2, T_3 and T_4. The characteristic values are evident from the following equations:

$$T_1 U(k_j, m_f, s_f, s) = \exp\left[(2\pi i/Gd)\left(\sum_j k_j + \sum_f f m_f\right)\right] U(k_j, m_f, s_f, s),$$

$$T_2 U(k_j, m_f, s_f, s) = U(k_j, m_f, s_f, s),$$

$$T_3 U(k_j, m_f, s_f, s) = \exp\left[(2\pi i/Gd)\left(s - \sum_f f m_f\right)\right] \times U(k_j, m_f, s_f, s),$$

$$T_4 U(k_j, m_f, s_f, s) = \exp\left[(2\pi i/Gd)\left(s + \sum_j k_j\right)\right] \times U(k_j, m_f, s_f, s).$$

Since these operators commute with the Hamiltonian function, any stationary state that is a product of the functions (10) and (12) can be specified by a characteristic value of each of these operators. Furthermore, if the system is in a state represented by any one of the above products, it will make transitions to only those other states that have the same characteristic values of the above four operators. In such transitions the integrals I_1, I_2, I_3 and I_4 either do not change at all or change by integral amounts.

4. Discussion of the Conservation Laws

It is important to notice that the integrals I_1 and I_4 contain the sum of the k_j, and not the individual k_j themselves. The Hamiltonian function is not invariant to the operation which increases one of the x_j by the amount d, changes the φ's by the amount indicated in T_1, and leaves the other x_j unchanged. The same thing is true of the operation on the angles φ_f. It is only when they are all changed that the Hamiltonian function is restored to its original condition. This is not due essentially to the presence of a term giving the interaction between the electrons but is due to the form of the interaction between the electrons and the lattice. It is because all of the electrons interact with all of the modes of vibration. It is true that this interaction consists of a sum over the electrons, so that if the interaction is treated as a perturbation and only the first approximation is considered, the electrons act independently. Since the interaction is really a large one, this apparent independence may be quite misleading.

The original derivation of the integral I_1 was based upon this independent treatment of the electrons and so suggested that changes in I_1 by the amount G must be made up of a change in one m_f and one k_f only. Such an interpretation is not at all required by the general treatment given above. Nevertheless it remains to be shown that transitions involving two or more electrons actually do occur. For this purpose it will suffice to treat a special case.

Consider the situation in which all of the s_f and m_f are zero and do not change, and let the electron functions be those for free electrons. The second-order treatment will involve the square of the interaction energy and this will contain terms which are products of the interaction with two electrons. Such matrix elements have the form

$$(k_1', k_2', s' | V^2 | k_1, k_2, s)$$

$$\sim \sum_{n_1, n_2} \int \exp [(2\pi i/Gd)\{(k_1-k_1')x_1 + (k_2-k_2')x_2 + (s-s')\rho_0\}] \prod_{f=1}^{G/2} |R(\rho_f, 0)|^2$$

$$\times V(x_1 - n_1 d - \sum_0^{G/2} \rho_f \cos [(2\pi f n_1/G) - \varphi_f])$$

$$\times V(x_2 - n_2 d - \sum_0^{G/2} \rho_f \cos [(2\pi f n_2/G) - \varphi_f])$$

$$\times \rho_f d\rho_f d\varphi_f dx_1 dx_2. \quad (14)$$

For ease in computation take the special case in which the interaction between an ion and an electron is limited to a very small region and let it be approximated by a δ-function. Then integration over x_1 and x_2 gives

$$(k_1', k_2', s' | V^2 | k_1, k_2, s)$$

$$\sim \sum_{n_1, n_2} \int \exp [(2\pi i/Gd)\{(k_1-k_1')$$

$$\times (n_1 d + \rho_0 + \sum_1^{G/2} \rho_f \cos [(2\pi f n_1/G) - \varphi_f])$$

$$+ (k_2-k_2')(n_2 d + \rho_0 + \sum_1^{G/2} \rho_f \cos [(2\pi f n_2/G) - \varphi_f])$$

$$+ (s-s')\rho_0\}] \prod_{f=1}^{G/2} |R(\rho_f, 0)|^2 \rho_f d\rho_f d\varphi_f d\rho_0. \quad (15)$$

Let $x_f = \rho_f \cos \varphi_f$, and $y_f = \rho_f \sin \varphi_f$. In the state of the oscillators for $s_f = 0$,

$$R(\rho_f, 0) = \exp [-\alpha_f (x_f^2 + y_f^2)/2].$$

The integrals over x_f and y_f can then be carried out. The constancy of I_4 is evident from the coefficient of ρ_0 in the exponent. The integral over ρ_0 vanishes unless

$$(k_1' + k_2' + s') = (k_1 + k_2 + s).$$

If this condition is satisfied the integral can be evaluated to give

$$(k_1', k_2', s' | V^2 | k_1, k_2, s)$$

$$\sim \exp [-(\pi/Gd)^2\{(k_1-k_1')^2 + (k_2-k_2')\}]$$

$$\sum_{f=1}^{G/2} (1/4\alpha_f) \sum_{n_1, n_2} \exp [(2\pi i/Gd)$$

$$\times \{(k_1-k_1')n_1 + (k_2-k_2')n_2\}$$

$$- (\pi/Gd)^2 \sum_1^{G/2} \{(k_1-k_1')(k_2-k_2')/2\alpha_f\}$$

$$\times \cos (2\pi f/G)(n_1-n_2)]. \quad (16)$$

Since α_f increases with f, the sum in the last exponent decreases rapidly with the absolute value of (n_1-n_2). For $n_1 = n_2$ there remains the sum

$$\sum_{n=1}^{G} \exp [(2\pi i/G)(k_1-k_1'+k_2-k_2')n],$$

which vanishes unless $(k_1'+k_2') - (k_1+k_2) = wG$, with w an integer. The same is true for any fixed value of (n_1-n_2). This represents the conservation of I_1 when there is no change in the state of vibration of the lattice. When the conservation laws are satisfied, the above matrix element is not generally zero, and such transitions can be expected to take place.

The change of a single k_j by the amount G has often been compared to Bragg reflection from the undisturbed lattice. This is true for a single particle. The change of the sum of the k_j for a group of electrons may be likened to the Bragg reflection of an atom or molecule from the lattice. In the case at hand, however, the interaction between the electrons need not be con-

sidered as due to their Coulomb fields, but merely as taking place through their interaction with the lattice.

Some of the difficulty in understanding the significance of Peierls' conservation theorem has been associated with the fact that the electron functions ordinarily used, $u(x)e^{(2\pi i/Gd)kx}$, are not characteristic of momentum. The conservation law involves the k, which represents momentum for a free particle but not for a particle in a periodic field. However, it must be remembered that even though the function used is not characteristic of momentum, it is a sum of momentum characteristic functions whose momenta differ by just the amount h/d. Such a sum is just the ordinary Fourier expansion,

$$u(x) \exp (2\pi i/Gd)kx = \sum_{n=-\infty}^{\infty} A_n \exp (2\pi i/Gd)(k+nG)x.$$

Since all of the conservation theorems apply to k modulo G, the distinction between the k and the momentum is not really significant. The distribution of the momentum over the various values is not at all restricted by the integrals.

The connection of Σk_j with the momentum is demonstrated by the existence of the integral I_4. Any change in Σk_j (modulo G) is accompanied by a corresponding change in s, and s clearly represents the momentum of the lattice. According to I_3, s and Σfm_f must increase together so that the conservation of momentum can be expressed in the form of I_1. It is the integral I_2 that gives the connection between Σfm_f and the momentum of the lattice. This integral shows that it is impossible for the electrons to excite an elastic traveling wave without a transfer of momentum to the lattice.

When the whole interaction between the electrons and the lattice is treated as a perturbation it is quite clear that the magnitude of the interaction is such that a first-order treatment is inadequate. However, the usual procedure has been to consider the unperturbed system as including the interaction between the electrons and the lattice in its equilibrium configuration. The departures from regularity were then treated as the perturbation. This procedure tends to obscure the momentum relations, since the lattice is usually treated as fixed.

Another difficulty with the usual method is that the contribution, to the perturbation, of the term proportional to the first power of the displacement of the ions is very small. Because of the symmetry of the interaction between an ion and an electron, the average of the first derivative will vanish. If the second derivative is considered, terms in the square of the displacement must be included. This leads at once to processes in which two of the m_f change together. As a matter of fact it can be shown that unless an infinite series is used to express the interaction between one electron and one ion, the Hamiltonian function cannot have the proper periodicity and at the same time provide for the conservation of momentum.

The principal consequence of the above considerations is that it is not necessary to give a special treatment of the *umklapprozesse* of a single electron in computing the resistance of a metal. Since, as Peierls showed, such processes require very special circumstances for their effective occurrence at low temperatures, they will be very rare, and will be replaced by processes in which a number of electrons make transitions at the same time. Most of the treatments of resistance have not included the *umklapprozesse* of a single electron in a very satisfactory way at the low temperatures where they would be of importance. In his original work Bloch[3] neglected them entirely. Peierls[4] criticized this neglect and undertook to estimate the effect of their inclusion. This was not very precise, but he showed that their inclusion, with the special circumstances under which they might be expected to occur, would not seriously change the temperature dependence of the resistance from that otherwise estimated. In a recent treatment by Peterson and Nordheim[4] they were neglected on the ground that they would be unimportant at high temperatures, although still later they were considered by Bardeen[5] at the same high temperatures. Since the last two papers were principally devoted to

[3] F. Bloch, Zeits. f. Physik **52**, 555 (1938); **59**, 208 (1930).
[4] E. L. Peterson and L. W. Nordheim, Phys. Rev. **51**, 355 (1937).
[5] J. Bardeen, Phys. Rev. **52**, 688 (1937).

the determination of the proper form for the lattice-electron interaction energy, their results do not throw much light on the role played by the single electron *umklapprozesse*.

Another consequence of these considerations is the suggestion of a different approach to the problem of computing the resistance. It would seem that the treatment of the electrons as independent, and the inclusion of the Pauli exclusion principle in the integral equation for the electron distribution, might not be the best procedure. It might be possible to treat the motion of the center of mass of all the electrons and to compute the probability of a change of its motion under the influence of the electric field and of the lattice interaction.

JUNE 15, 1939 PHYSICAL REVIEW VOLUME 55

The Meson Theory of Nuclear Forces

H. A. BETHE
Cornell University, Ithaca, New York
(Received May 13, 1939)

THE meson[1] theory of nuclear forces[2,3] predicts two kinds of interactions between heavy particles (protons and neutrons). The first kind does not depend on the spin of the heavy particles and has the form

$$U = g_1^2 e^{-\lambda r}/r, \tag{1}$$

where r is the distance between the two interacting heavy particles, g_1 is a constant, λ the reciprocal Compton wave-length of the meson,

$$\lambda = \mu c/\hbar \tag{2}$$

and μ the meson mass. Besides (1), there will be a spin-dependent force,

$$V = V_1 + V_2, \tag{3}$$

$$V_1 = \tfrac{2}{3} g_2^2\, \boldsymbol{\sigma}_1 \cdot \boldsymbol{\sigma}_2\, e^{-\lambda r}/r, \tag{3a}$$

$$V_2 = -g_2^2 \left(3 \frac{\boldsymbol{\sigma}_1 \cdot \mathbf{r}\, \boldsymbol{\sigma}_2 \cdot \mathbf{r}}{r^2} - \boldsymbol{\sigma}_1 \cdot \boldsymbol{\sigma}_2 \right) \times \frac{e^{-\lambda r}}{\lambda^2 r^3} (1 + \lambda r + \tfrac{1}{3}\lambda^2 r^2), \tag{3b}$$

where $\boldsymbol{\sigma}_1$ and $\boldsymbol{\sigma}_2$ are the spin operators of the two heavy particles, and $\mathbf{r}$ the vector from one to the other. The constant g_2 has the same value in (3a) and (3b) but is independent of g_1 in (1).

The spin-dependent interaction has been split into one part, V_1, which does not depend upon the relative position of the two particles (direction of $\mathbf{r}$), and another part, V_2, whose average over all directions of $\mathbf{r}$ gives zero. It is usually argued[2,3] that the latter part has no influence on spherically symmetrical states such as the ground state of the deuteron so that only the spherically symmetrical interactions U and V_1 are considered. In order to obtain agreement with the observed positions of the singlet and triplet states of the deuteron, it is then necessary[3] to choose $g_1 \approx 0.6 g_2$.

The neglecting of V_2 cannot actually be justified. This interaction destroys the spherical symmetry of nuclear states and makes the ground state of the deuteron a mixture of an S and a D state. Quite generally, the orbital momentum L of the nucleus will cease to be quantized when a "tensor" interaction of the type V_2 is present. V_2 vanishes identically only for singlet states of the two-body problem; for any triplet state, including the ground state of the deuteron, it must be considered.

In fact, V_2, as it stands, will give an infinite binding energy for the ground state of the deuteron, for it represents an inverse cube potential which is attractive for a certain linear combination of an S and a D state, and for such a potential the Schrödinger equation does not possess a lowest eigenvalue. The only remedy seems to be to "cut off" the interaction potential at a small

[1] For the name "meson" and the arguments in its favor, see H. J. Bhabha, Nature **143**, 276 (1939).
[2] H. Fröhlich, W. Heitler and N. Kemmer, Proc. Roy. Soc. **166**, 154 (1938); H. J. Bhabha, Proc. Roy. Soc. **166**, 501 (1938).
[3] N. Kemmer, Proc. Camb. Phil. Soc. **34**, 354 (1938).

distance, r_0. This is not very satisfactory from the esthetic point of view but seems justifiable in view of the large size of the interaction constant $g(g_2^2/hc \approx 1/10)$. The cutting-off distance r_0 turns out to be about 0.3 to 0.45 of the "range" of the nuclear forces, $1/\lambda$.

If the potential V_2 is cut off at a certain distance r_0, the lowest eigenvalue of the deuteron will be finite, its exact value depending on r_0 and g_2. The tensor interaction V_2 will tend to lower the triplet state but it will not influence the singlet level. *This interaction can therefore be used to obtain the correct relative position of singlet and triplet state of the deuteron without introducing the spin-independent interaction U at all.* This would mean a great simplification of nuclear theory: There would be only a single force V, given by (3), between nuclear particles, instead of the four different forces (Wigner, Majorana, Heisenberg and Bartlett) used previously.

It seems very probable that the meson potential (3) satisfies the saturation requirement since its average over the spins of the interacting particles is zero. It also appears likely that the relative positions of the energy levels of heavier nuclei will remain qualitatively the same as with the old forces. The meson potential is superior to the old forces in *predicting a quadrupole moment for the deuteron* because the ground state of this nucleus will now be a mixture of an S and a D state rather than a pure S state. Such a quadrupole moment has been observed by Kellogg, Rabi, Ramsey and Zacharias.[4] This cannot be explained on the basis of the old "central" nuclear forces (Majorana, etc.) but requires the introduction of a fifth force, of the same tensor character as our V_2 (Schwinger[5]).

The forces (1), (3) are based on the assumption that heavy particles interact only with neutral mesons (neutral theory). It is also possible to assume interaction with charged as well as neutral mesons. A theory of this type, symmetrical in positive, negative and neutral mesons, was proposed by Kemmer[3] (symmetrical theory) and leads to a force between heavy particles differing from (1), (3) by a factor $\tau_1 \cdot \tau_2$ where τ_1 is the operator of isotopic spin for the first heavy particle. For states "symmetrical in charge" such as the ^1S state of the deuteron, $\tau_1 \cdot \tau_2 = 1$; for states antisymmetrical in charge, such as the ^3S state, $\tau_1 \cdot \tau_2 = -3$.

Both in the neutral and the symmetrical theory, the force between two neutrons (n-n) is equal to that between two protons (p-p), and in the ^1S state the force between neutron and proton (p-n) is also equal to the n-n and p-p force. The equality $(n\text{-}n) = (p\text{-}p)$ is required by general nuclear theory while $(n\text{-}p) = (p\text{-}p)$ follows from the comparison of the scattering of slow neutrons and of protons by protons. With respect to the ground state of the deuteron, the two theories differ: In the neutral theory, the interaction (3a) is repulsive, in the symmetrical theory, it is attractive and equal to the ^1S interaction. The influence of (3b) must therefore be greater in the neutral theory.

In the neutral theory, V_2 is attractive when the spins $\sigma_1\sigma_2$ are in line with the axis $\mathbf{r}$ of the deuteron. Therefore the theory predicts a "cigar shape" for the deuteron, i.e., greater probability of finding the axis $\mathbf{r}$ parallel to the total spin σ than perpendicular to it. In the symmetrical theory, the factor $\tau_1 \cdot \tau_2 = -3$ reverses the sign of V_2 so that a "pill-box" shape results. The experiments of Kellogg, Rabi, Ramsey and Zacharias[4] give a cigar shape.[6]

We have solved the Schrödinger equation for the ground state of the deuteron using the potential V, both for the symmetrical and the neutral theory. The solution was obtained by numerical integration without neglecting any terms. The interaction constant g_2 and the cutting-off radius r_0 were determined so as to give the correct position for both the singlet and the triplet level of the deuteron. The latter was assumed to be -2.17 Mev, the former was deduced from a slow neutron cross section of $18.3 \cdot 10^{-24}$ cm^2. The meson mass was taken equal to 177 electron masses, in approximate[7] agree-

[4] J. M. B. Kellogg, I. I. Rabi, N. F. Ramsey and J. R. Zacharias, Phys. Rev. **55**, 318 (1939).

[5] J. Schwinger, in course of publication.

[6] In order to obtain sign and magnitude of the quadrupole moment from the experiments, it is necessary to know the inhomogeneity of the electric field in the hydrogen molecule near one nucleus. This inhomogeneity has been calculated by Nordsieck using Wang wave functions. It is not known how much error is introduced by the use of such approximate wave functions. Even a reversal of sign can not be completely excluded at present.

[7] The value 177 is convenient for calculation because it makes $h/\mu c$ equal to one-half of the "radius" of the deuteron.

TABLE I. *Summary of results obtained on the basis of the two theories and the two ways of cutting off.*

CUT-OFF	NEUTRAL THEORY ZERO	NEUTRAL THEORY STRAIGHT	SYMMETRICAL THEORY ZERO	SYMMETRICAL THEORY STRAIGHT
$g^2/\hbar c$	0.081_2	0.080_0	0.250	0.154
$r_0/(\hbar/\mu c)$	0.320	0.436	1.679	1.733
Quadrupole moment	2.73	2.67	−24.7	−17.8 $\times 10^{-27}$ cm^2
Percent "D" function	6.88	6.68	23.46	18.52

ment with the latest determination of Nishina, Takeuchi and Ichimya[8] (170±9). The cutting off was made in two different ways, *viz.* (a) the potential was taken to be zero inside of r_0 (zero cut-off), (b) the potential for $r<r_0$ was taken equal to $V(r_0)$ (straight cut-off). In case (a), the radius r_0 must, of course, be taken smaller than in (b) in order to obtain the correct binding energy for the deuteron, but the final value for the quadrupole moment of the deuteron is changed very little.

In Table I, the results[9] are summarized for the two theories and the two ways of cutting off. The values of the cutting-off radius obtained in the neutral theory (0.320 and 0.436 $\hbar/\mu c$) are very reasonable, while those for the symmetrical theory ($\sim 1.7\hbar/\mu c$) are unbelievably high. Correspondingly, the symmetrical theory gives improbably high values for the quadrupole moment (in addition to the wrong sign, i.e., pill-box shape). The neutral theory, on the other hand, gives a value for the quadrupole moment ($\sim 2.7\cdot 10^{-27}$ cm^2) in close agreement with that obtained from the experiments of Kellogg, Ramsey, Rabi and Zacharias with the use of Wang wave functions[6, 10] ($2.5\cdot 10^{-27}$ cm^2). Although the evaluation of the experiments with Wang functions may not be very accurate, present evidence is definitely in favor of the "neutral theory." In this theory, it is of course difficult to explain the β-decay and the magnetic moments of proton and neutron.

The last line of Table I gives the percentage of ^3D wave function contained in the eigenfunction of the ground state of the deuteron.

[8] Y. Nishina, M. Takeuchi and T. Ichimiya, Phys. Rev. **55**, 585 (1939).

[9] The values given previously (Phys. Rev. **55**, 1130 (1939)) were erroneous.

[10] I am indebted to Dr. Nordsieck and Professor Rabi for communicating this value to me.

LETTERS TO THE EDITOR

Prompt publication of brief reports of important discoveries in physics may be secured by addressing them to this department. Closing dates for this department are, for the first issue of the month, the eighteenth of the preceding month, for the second issue, the third of the month. Because of the late closing dates for the section no proof can be shown to authors. The Board of Editors does not hold itself responsible for the opinions expressed by the correspondents.

Communications should not in general exceed 600 words in length.

Excitation Function for Iron by Energetic Deuterons

When pure iron is bombarded by deuterons, several radioactive products[1] are formed. Two of these isotopes are radioactive cobalt of half-life 18 hours and radioactive manganese of half-life 25 minutes, both emitting positrons. These two radioactive isotopes are of particular interest since both are formed from the same parent isotope of iron (mass 54); the former by a (D, n) reaction and the latter by (D, α) reaction. It is thus possible to compare the most probable nuclear reaction, that is, the loss of a neutron, with the less probable transition, the loss of an alpha-particle. These excitation functions have previously been observed[2] up to 5.5 Mev.

With the increased energy now available from our cyclotron these observations can be extended to the more interesting region of higher voltages. When a wave-length of 27.5 meters is used the range of the deuterons outside a window of 2 cm air equivalence is quite sharply 61 cm in air. This beam was made incident upon a stack of uniform iron foils, and after exposure the radioactivity of each foil was studied by a string electrometer with ionization chamber.

Figure 1 shows the 18-hour cobalt activity expressed in relative units as a function of the average exciting energy for each foil. The equivalent air range of each foil was determined directly by observing its stopping power for deuterons. The range-energy relationship given by Bethe and Livingston was employed.

The striking result is apparent that at about 7 Mev a saturation occurs, so that no appreciable gain in radioactivity is obtained at higher voltages for this reaction. This subject has been treated theoretically by Konopinski and Bethe.[3] They predict a leveling of the excitation curve at somewhat higher voltages, 10 to 12 Mev. It should be mentioned that for other heavier elements of atomic number 40 or more an enormous increase in yield for the (D, n) reaction occurs as the exciting energy is increased from 7.5 to 10 Mev. The data for the (D, α) reaction will be reported later.

J. M. Cork
B. R. Curtis

Department of Physics,
University of Michigan,
Ann Arbor, Michigan,
May 23, 1939.

[1] B. T. Darling, B. R. Curtis and J. M. Cork, Phys. Rev. **51**, 110 (1937); J. Livingood and G. T. Seaborg, Phys. Rev. **54**, 51 (1938).
[2] J. M. Cork and B. R. Curtis, Phys. Rev. **53**, 946 (1938).
[3] E. J. Konopinski and H. A. Bethe, Phys. Rev. **54**, 130 (1938).

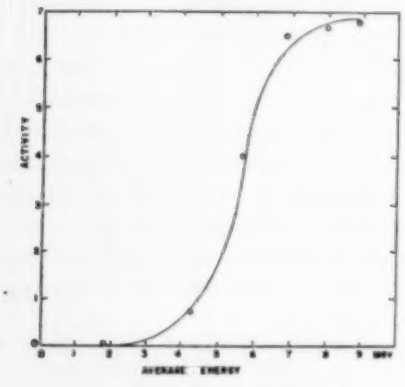

FIG. 1. Excitation curve of Fe(D, n).

On the Angular Distribution of the Fast Neutrons Scattered by Atoms

Recently, Aoki[1] has found that the scattering of 2.9-Mev neutrons by lead, copper and aluminum atoms cannot be spherically symmetric, as the differential scattering cross section measured by the ring scatterer method at the scattering angle of $40° \pm 15°$ is much larger than the value expected from the total absorption scattering cross section determined by the transmission method on the assumption of spherically symmetric scattering. On the other hand, the results for carbon were consistent with the view that the scattering is spherically symmetric.

To test these points more directly, the differential cross sections at different scattering angles were determined for lead and carbon by using ring scatterers of different size.

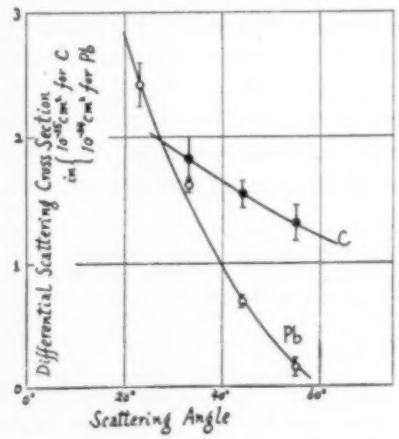

FIG. 1. Scattering cross section in Pb and C.

TABLE I. *Differential scattering cross section in 10^{-25} cm².*

SCATTERING ANGLE	23°	33°	44°	55°
C	——	1.83±0.17	1.55±0.10	1.32±0.14
Pb	24.2±1.8	16.2 ±0.6	6.9 ±0.5	1.6 ±0.7

Our results are tabulated in Table I and illustrated in Fig. 1. The asymmetry in the case of lead is very astonishing; the differential cross section at 55°±5° is less than one-tenth of that at 23°±5°. In the case of carbon we see that the departure from the symmetric scattering is not marked in accordance with the observation of Aoki. The small departure from the symmetry in the case of carbon seems to be real.

SEISHI KIKUCHI
HIROO AOKI
TETUO WAKATUKI

The Physical Institute of Osaka Imperial University,
Osaka, Japan,
April 28, 1939.

[1] H. Aoki, Proc. Phys. Math. Soc. Japan, in press.

Powder Patterns on Permalloy Crystals

If the origin of the inhomogeneities of surface magnetization is merely a magnetostriction effect, there will be no powder pattern formed on a ferromagnetic having no magnetostriction. On the other hand, if McKeehan and Elmore's[1] model for silicon iron is also applicable to the ferromagnetics in general, it should be expected that a magnetic substance even without magnetostriction should also show powder patterns. So it is interesting to investigate this problem with a permalloy crystal of a certain composition which has practically no magnetostriction.

Permalloy of 84 percent nickel and 16 percent iron was chosen. Several disks about 6 mm in diameter and 0.5 mm in thickness, parallel to (110) or (100) planes, were cut from the large crystals grown in an induction furnace. They were polished with Al_2O_3 powder in the usual way. By using a water solution of Fe_2O_3 with a little gum arabic a microscopic view of the patterns in either parallel or normal magnetic field was easily observed or photographed by means of a "panphot" microphotographic camera. The patterns consist of two sets of broken lines inclined to one another at about 130°, one set being more regular and distinct than the other. The (110) plane developed better patterns than the (100) plane, but of the same type. The average space between the lines is about 7μ. When the parallel or normal field was reversed (the former was mostly used in our investigation), the lines moved through a distance of about one-half to one space. They could be brought back and forth without disturbing the sharpness of the lines. This shifting effect was first observed by McKeehan and Elmore on silicon iron crystals with normal field. After the specimens were annealed at about 600°C for six hours the patterns disappeared. However they could be recovered by polishing again. They were not affected by increasing the field strength except that the lines became fainter and fainter until all the powders were attracted to the sides of the specimen. We found no patterns of other types no matter how strong the field.

Because the pattern lines form tees and ells but never cross each other, and because they are also shifted by the reversal of an applied field, one may say that the origin of the lines is of the same nature as that of the maze patterns on silicon iron crystals. In other words, McKeehan and

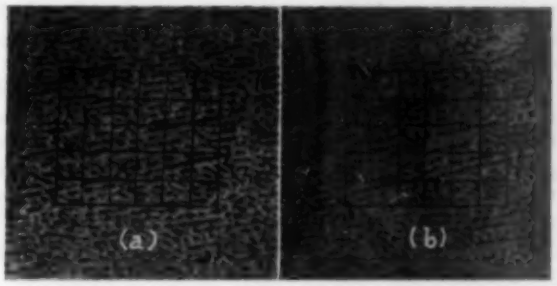

FIG. 1 (a) Powder pattern on (110) plane with a field parallel to the surface, magnification 190×. (b) same as (a) with field reversed.

Elmore's model may explain the general results. They are also similar to Sixtus'[2] patterns of the first type, since for both of them the surface condition produced by polishing is necessary. Mechanical polishing might affect a metallic surface in two ways as pointed out by Elmore.[3] It sets up stresses varying from tension to compression, and produces fragment structure in the surface just underneath the Beilby layer. In the case of permalloy the surface stresses should not be effective because there is no magnetostriction. So the magnetization directions of the elementary domains in the different districts, and hence those of the lines, are not controlled by the stresses, as may be argued in the case of iron crystals. We may, therefore, conclude that the second effect of polishing seems to be the essential one in the formation of the patterns and magnetostriction has little relation with them.

The absence of the patterns of other types is probably due to the fact that the magnetic anisotropy in the crystals of the above composition is very small,[4] yet the existence of the preferential direction of magnetization is one of the necessary conditions for producing patterns.

We wish to thank Professor L. W. McKeehan of Yale University and Dr. W. C. Elmore of Massachusetts Institute of Technology for help in preparing this note. Its publication has been delayed considerably by circumstances beyond our control.

J. W. SHIH
TSU-YEN CHAI

National Research Institute of Physics,
Academia Sinica,
Kunming, Yunnan, China,
February 15, 1939.

[1] L. W. McKeehan and W. C. Elmore, Phys. Rev. **46**, 226 (1934).
[2] K. J. Sixtus, Phys. Rev. **51**, 870 (1937).
[3] W. C. Elmore, Phys. Rev. **51**, 982 (1937).
[4] F. Lichtenberger, Ann. d. Physik **15**, 45 (1932).

Search for Heavy Cosmic-Ray Particles with a Cloud Chamber

Beacuse of the relativistic increase of masses with velocity, the determination of the rest mass of charged particles with a cloud chamber becomes impossible if their energies are very large. To investigate the nature of cosmic-ray particles a special anticoincidence amplifying set was used to trip the cloud chamber only by those cosmic-ray particles whose further path lies below a given range. By this method one makes sure to investigate only those particles which are of low energy and in which differences of mass can be detected by the ionization produced in a cloud chamber.

With a big rectangular Wilson chamber of 12 by 24 inches area and a magnetic field of 2000 gauss, 118 successful photographs have been taken. In 104 expansions the particles traversing the cloud chamber had a range less than 5 mm of lead. In five pictures this range was less than 17 mm. Nine additional expansions were taken with 15 cm of lead above the whole arrangement to count only the penetrating component.

No case was found which showed any observable difference of ionization from fast electrons. This result is in qualitative agreement with similar experiments published in the meantime by Street and Stevenson,[1] and emphasizes the rarity of occurrence of the terminal portion of a mesotron track.

The experiments were performed at the Swiss Institute of Technology in Zurich, and I would like to acknowledge the support and many discussions by Dr. P. Scherrer.

G. HERZOG

University of Chicago,
Chicago, Illinois,
May 18, 1939.

[1] J. C. Street and E. C. Stevenson, Phys. Rev. 52, 1003 (1937).

Zenith Angle Distribution of the Hard Component of Cosmic Rays and the Mass of the Mesotron

In a recent publication,[1] a formula was derived for the relation between the path of decay L of mesotrons and the vertical angle distribution of the hard component of cosmic radiation which is supposed to consist of mesotrons. Regarding both, radioactive decay and absorption due to ionization, we get

$$-d \ln N/d \sec \vartheta = \mu_A(H+H_p)+H_f/L, \qquad (1)$$

where N is the intensity of the radiation, H the mass of the earth atmosphere, H_p the additional mass of the absorber, H_f[2] the height of formation of mesotrons and μ_A the absorption coefficient of the hard component.

Measurements of Brackertz[3] on the zenith angle distribution behind different thicknesses of absorber were used to draw new conclusions on the energy and mass of the hard component.

The difference in value of the absorption coefficient behind different thicknesses of absorber has to be considered. Introducing the relation

$$\mu_A \approx 1/\text{thickness of absorber}_{(\text{m } H_2O)} \qquad (1a)$$

found by Auger for the first few meters of water equivalent of absorber, and taking into consideration the inclination, we have

$$\mu_A \approx 1/(H+H_p) \sec \vartheta.$$

With formula (1) this gives

$$-d \ln N/d \sec \vartheta \approx \cos \vartheta + H_f/L.$$

This formula means that the distribution of the hard component can be found without any assumption about the absorption coefficient if L and H_f are known, since μ_A does not appear in it.

Since L is proportional to the energy according to the law

$$L = E\tau_0/mc,$$

and as the height of formation H_f can be found[4] from $\cos \vartheta/10 = \exp(-H_f/H)$ and is

$$H_f = H(2.3+\ln \sec \vartheta),$$

the general formula

$$-d \ln N/d \sec \vartheta \approx \cos \vartheta + (1/E)H(2.3+\ln \sec \vartheta)mc/\tau_0$$

is obtained, or

$$E \approx mc/\tau_0 H(2.3+\ln \sec \vartheta)/(-d \ln N/d \sec \vartheta - \cos \vartheta), \qquad (2)$$

which gives the energy distribution of the penetrating rays. The data given by Brackertz for $(H+H_p)=19.4$ m may be used to investigate the energy distribution by applying formula (2) (Table I). As a simplification ln sec ϑ will be taken as constant, and the difference quotient will be used in place of the more accurate differential quotient. This shows an increase of the energy with greater angle of inclination as was to be expected.

As Brackertz gives as data on the inclination effect behind different thicknesses of absorber, we may also apply formula (2) to find the energy curve for different thicknesses of dense absorber for a constant angle of inclination as for example the vertical rays ($\vartheta=0°$). Then $(-d \ln N/d \sec \vartheta)$ may be found by extrapolation of the values found for $-\Delta \ln N/\Delta \sec \vartheta$ for $\Delta\vartheta = 30°\to 0°$, $20°\to 0°$, $10°\to 0°$ toward $0°\to 0°$. This was done in the first publication[1] on this subject.

This result (Table II) is in absolute disagreement with the well-known fact that the mean energy of the cosmic radiation increases with the mass of absorber.

The simple law for the vertical angle distribution as represented by formula (1) has been found experimentally to be correct especially near $\vartheta=0°$. The formula (1a) has

TABLE I. *Energy distribution calculated from Eq. (2).*

ϑ	N	$\frac{\Delta \ln N}{\Delta \sec \vartheta}$	$\cos \vartheta$	Denominator	Increase of E by Formula (2)
	283				
0–10°		2.079	0.996	1.083	——
	274				
10–20°		2.055	0.966	1.089	—— (−0.4)
	248				
20–30°		1.996	0.906	1.090	—— (−0.4)
	207				
30–40°		1.796	0.819	0.977	10%
	158				
40–50°		1.631	0.707	0.924	17%
	105				
50–60°		1.418	0.574	0.844	30%
	56				

TABLE II. *Change in E predicted by Eq. (2).*

$(H+H_p)$M H_2O	$-\frac{d \ln N}{d \sec \vartheta}-1$	INCREASE OF E BY FORMULA (2)
10.1	0.89	—
19.4	1.09	$\sim -20\%$
25.2	1.00	$\sim -15\%$

also been found by experiment. There were no other assumptions made to find formula (2), except for the constancy of c, τ_0, m. As we have sufficient proof that c and τ_0 are constants, our results may point to the existence of mesotron particles of different mass. The average mass has to be assumed to increase at least 30 percent, in order that formula (2) should yield the measured increase of energy when about 10 m absorbing mass is added.

I am indebted to Professor W. Kolhoerster for his interest in this work, part of which has been carried on at the Institut für Hoehenstrahlenforschung of the University of Berlin, Germany.

PAUL WEISZ

Cullman, Alabama,
May 7, 1939.

[1] P. Weisz, Naturwiss. **27**, 132 (1939).
[2] In the first publication (reference 1), H_f was falsely assumed as $0.9H$ instead of about $2.4H$ because of the pressure distribution in the earth's atmosphere. Then, L will be found as about 24 km (behind about 10m H_2O additional absorber).
[3] E. Brackertz, doctor's thesis, University of Berlin, Germany (1936).
[4] P. M. S. Blackett, Nature **142**, 992 (1938).

Collision Cross Sections of K Atoms and K_2 Molecules in Gases*

Measurements of effective collision cross sections are here reported for the neutral potassium atom, K, and for the neutral potassium molecule, K_2, scattered in hydrogen, in deuterium, in helium, in argon and in nitrogen. A molecular beam method has made it possible to measure the effective collision cross sections of the K atom and the K_2 molecule under identical conditions.

A beam of neutral potassium, the source of which is an oven at a temperature of approximately 500°K, is predominantly composed of K atoms, but is found to contain a small number of K_2 molecules. The molecules are sorted from the atoms by utilizing the fact that the K atom possesses a much larger magnetic moment than the K_2 molecule. The beam is passed through a strong magnetic field the gradient of which is sufficiently high to deflect the atoms completely out of the beam, while the K_2 molecules suffer no appreciable deflection.

The beam is scattered by a gas whose pressure and temperature (approximately 300°K) are measured. The scattering gas is confined to a region small compared to the total length of the beam. The mean free path is determined by measuring the intensity of that part of the beam which traverses the scattering region without being deflected by more than 45 seconds of arc. Thus the geometric resolution of the apparatus enables a collision between a beam particle and a particle of the scattering gas to be defined as any encounter which deviates the beam particle by more than 45 seconds of arc.

The collision cross sections are calculated from the mean free paths by using Tait's expression [1, 2] for a mixture of two systems, modified to take account of the v^3 velocity distribution characteristic of effusion from a slit. The results are expressed in Table I as effective mutual collision cross sections, i.e., $\pi\sigma^2$.

TABLE I. *Cross sections of* K *and* K_2.

	EFFECTIVE COLLISION CROSS SECTION $cm^2 \times 10^{15}$	PERCENT ACCURACY	RATIO OF CROSS SECTION OF K_2 MOLECULE TO K ATOM
K in H_2	197.5	1.6	1.264
K_2 in H_2	249.6	2.5	
K in D_2	252.4	2.0	1.36
K_2 in D_2	343	5.9	
K in He	170.8	2.3	1.214
K_2 in He	207.3	3.9	
K in A	587.1	1.8	1.197
K_2 in A	702.7	2.5	
K in N_2	613	5.4	1.21
K_2 in N_2	741	5.5	

The intensity of the beam of K_2 molecules is 0.5 percent of the total intensity of the parent beam. This low intensity makes it difficult to measure the mean free paths of the K_2 molecule as accurately as the mean free paths of the K atom, as is reflected in the estimates of accuracy in Table I.

Values of the effective collision cross sections of the K atom in these gases have been reported by Mais[3] and by Rosin and Rabi.[4] In the present experiments the estimated accuracy of the results is much higher than in the experiments of Mais and of Rosin and Rabi, and the angular resolution has been increased.

The last column of Table I gives the ratio of the effective collision cross section of the K_2 molecule to the cross section of the K atom for each scattering gas. Perhaps the most interesting result in these experiments is the small difference in cross section between the K atom and K_2 molecule even though the internuclear distance in the K_2 molecule is large (3.91×10^{-8} cm from band spectra). The ratios in the last column of Table I are about 1.2 except for a ratio of 1.36 in the case of D_2. It is noteworthy that no two of these ratios differ from each other by a factor of more than 0.13 although the cross sections change by a factor of as much as 2.58 as we go from one scattering gas to another.

It also should be noted that both the K atom and the K_2 molecule have considerably larger cross sections in deuterium than in hydrogen.

A complete account of these experiments will be published in this journal.

PAUL ROSENBERG

Department of Physics,
Columbia University,
New York, New York,
May 31, 1939.

* Publication assisted by the Ernest Kempton Adams Fund for Physical Research of Columbia University.
[1] Tait, Trans. Roy. Soc. Edinburgh **33**, 65 (1886).
[2] J. H. Jeans, *The Dynamical Theory of Gases* (fourth edition, 1925), p. 254.
[3] W. H. Mais, Phys. Rev. **45**, 773 (1934).
[4] S. Rosin and I. I. Rabi, Phys. Rev. **48**, 373 (1935).

The Variation of the Adiabatic Elastic Constants of Polycrystalline Ammonium Chloride with Temperature between 200°K and 273°K*

The data which follow were obtained with the dynamical method described in this journal by Balamuth[1] and Rose.[2] The form of specimen required by this method is a right circular cylinder 4.6 mm in diameter and about 3 cm long. Such cylinders are cut from a block of material prepared by compressing dry powdered ammonium chloride to 50,000 lb./in.^{2} in a steel cylinder at room temperature. The result is a coherent isotropic array of microcrystals whose average linear dimensions are 5×10^{-3} cm. The densities of different blocks at 24°C vary slightly about the value 1.520 g/cm^3, which is slightly less than the density of crystalline ammonium chloride as measured by Wulf and Cameron,[3] namely 1.527 g/cm^3. It is found, however, that small changes in density are very nearly without effect on the *temperature variation* of the elastic constants, expressed in percent change per degree.

The temperature of the specimen is kept constant to 0.01°C during a measurement by manually controlling the temperature of an enveloping well stirred methanol bath. The temperature of the bath is measured with a platinum resistance thermometer, certificated by the National Bureau of Standards, used in connection with a Mueller bridge.

The curves of Fig. 1 show the observed variation of the adiabatic Young's and rigidity modulus with temperature through the phase transition which occurs at 242.8°K. The corresponding variations of the adiabatic compressibility and Poisson's ratio, as calculated from these data, are given in Fig. 2. The absolute values of the Young's modulus, rigidity modulus, compressibility and Poisson's ratio at 273.2°K are, respectively, 2.733×10^{11} dynes/cm^2, 1.096×10^{11} dynes/cm^2, 5.54×10^{-12} cm^2/dynes, and 0.246.

The temperature of the transition point has been deduced from observations on the temperature variation of the specific heat at constant pressure by Simon, v. Simson and Ruheman,[4] and of the coefficient of thermal expansion by Smits and Gillavry[5] and Adenstadt.[6] Both quantities show a pronounced maximum at 242.8°K, which is exactly the temperature here found for the occurrence of the minimum value of Young's modulus and the maximum

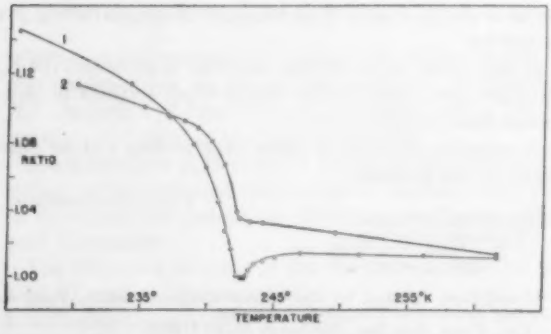

FIG. 1. The variation of the Young's modulus (curve 1) and the rigidity modulus (curve 2) with temperature near the transition point. The ordinates are the ratios of the values at the given temperature to the values at 273.2°K.

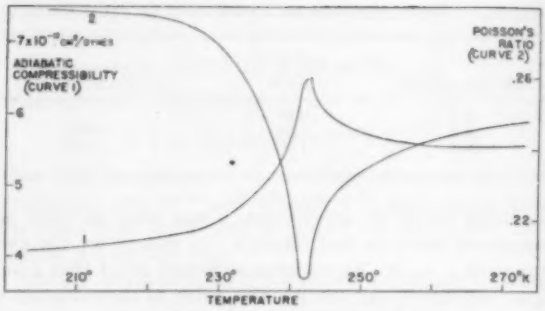

FIG. 2. The variation of the adiabatic compressibility (curve 1) and Poisson's ratio (curve 2) with temperature.

value of the compressibility. May[7] has computed the isothermal compressibility of ammonium chloride at 273°K from supplementary unpublished data supplied him by Bridgman.[8] The value given is 5.60×10^{-12} cm^2/dynes.

The present measurements, together with those on the temperature variation of the coefficient of thermal expansion[5, 6] and on the heat of transition[9], indicate that the values of both c_p and the ratio c_p/c_v at the transition point may be much larger than has hitherto been believed. Measurements similar to the above on the variation of the isothermal moduli with temperature will settle the matter, and apparatus designed for this purpose is now under construction in this laboratory. Data will then be available for comparison with Fowler's theoretical calculation of the variation of c_v with temperature.[10]

A. W. LAWSON
RICHARD SCHEIB

Pupin Physics Laboratories,
Columbia University,
New York, New York,
May 31, 1939.

* Publication assisted by the Ernest Kempton Adams Fund for Physical Research of Columbia University.

[1] Balamuth, Phys. Rev. **45**, 715 (1934).
[2] Rose, Phys. Rev. **49**, 50 (1935).
[3] Wulf and Cameron, Zeits. f. physik. Chemie **B10**, 347 (1930).
[4] Simon, *et al.*, Zeits. f. physik. Chemie **A129**, 339 (1927).
[5] Smits and Gillavry, Zeits. f. physik. Chemie **A166**, 97 (1933).
[6] Adenstadt, Ann. d. Physik **26**, 69 (1936).
[7] May, Phys. Rev. **52**, 339 (1937).
[8] Bridgman, Phys. Rev. **38**, 182 (1931).
[9] Eucken, Physik. Zeits. **35**, 954 (1934).
[10] Fowler, Proc. Roy. Soc. **A149**, 1 (1935).

Long-Lived Radioactive Fe^{55}

In a previous paper[1] we have discussed the production of radioactive iron isotopes Fe^{53} and Fe^{59}, with half-lives 9 minutes and 47 days, respectively. Failure to observe any activity attributable to Fe^{55} led to the conclusion that its lifetime was either very short or extremely long. (The mass numbers of the stable iron isotopes[2] are 54, 56, 57 and 58.)

Continued observations over a period of 22 months on the chemically separated iron fractions from deuteron-bombarded iron samples show that the 47-day period is accompanied by a much weaker and very much longer-lived activity. That this cannot be ascribed to incompletely removed long-lived isotopes of cobalt[3] (~250 days) or manganese[4] (310 days), which are also produced by deuteron-bombardment of iron, is shown by the absence

of the very strong short-lived cobalt and manganese activities in these same iron samples. A particularly rigorous chemical separation, designed to remove all elements other than iron, was made on a more recently activated specimen; this precipitate, now 10 months old, has already departed from the 47-day period and is now going into one much longer.

These facts assure us that Fe^{55} has been formed through $Fe^{54}(d, p)Fe^{55}$ with the activity probably leading to stable Mn^{55} either by positron emission or by K-electron capture. An absorption curve on one of the old samples (unfortunately very weak) shows that the radiation has a soft component with half-thickness 3 to 5 mg/cm^2 of aluminum. This suggests the existence of an internally converted gamma-ray.

It is too early to give a reliable value for the half-life of this activity. The observed decay curves, which are still going through the transition interval from the 47-day period to the long period, set a lower limit of 1 year for the half-life. A comparison of the intensities of the 47 day and the longer activity (assuming equal cross sections for their production and equal ionizing powers for their radiations, and allowing for the abundances of the primary isotopes involved) predicts that the half-life will exceed 10 years.

It is a pleasure to acknowledge the generous support of the Research Corporation.

J. J. LIVINGOOD*
G. T. SEABORG

Radiation Laboratory, Department of Physics (J. J. L.),
Department of Chemistry (G. T. S.),
University of California,
Berkeley, California,
May 30, 1939.

* Now at Harvard University.

[1] J. J. Livingood and G. T. Seaborg, Phys. Rev. **54**, 51 (1938).
[2] A. O. Nier, Bull. Am. Phys. Soc. **14**, 40 (1939).
[3] J. J. Livingood and G. T. Seaborg, Phys. Rev. **53**, 847 (1938).
[4] J. J. Livingood and G. T. Seaborg, Phys. Rev. **54**, 391 (1938).

Stability of Uranium and Thorium for Natural Fission

The question of the occurrence of possible natural fission processes among the heavy nuclei is one of considerable importance to both nuclear physics and geophysics. The characteristics of the neutron-induced splitting of the uranium and thorium nuclei which have recently been studied so intensively by many workers seem to indicate that a naturally occurring explosion process probably would form radioactive isotopes of elements of medium atomic number with convenient half-lives. Further, the emission of neutrons by uranium in the artificial process suggests that neutron emission might accompany the natural process. Finally, natural fission might be detected by disparities between the results of the various calculations of the age of the oldest rocks based on the observed abundances of the elements and the intensities of the ordinary radioactive emissions from uranium and thorium.

It is the purpose of this letter to point out how well evidence on these three points excludes natural fission. In all of the numerous experiments which have been done on the neutron-produced activities of uranium and thorium control separations must have been made without neutron irradiation to exclude the possibility of contamination by natural activities. In order to have definite data for a typical calculation for this type of evidence the experiments[1, 2] on extraction of radioiodine from irradiated uranium were repeated with 0.90 mole of uranyl nitrate which had not been disturbed chemically for at least five years. The iodine, extracted by adding a little solid iodine to a slightly acidified aqueous solution of the uranyl nitrate, shaking with CCl_4, and precipitating AgI in a thin layer was counted in a screen wall counter so no beta-radiation harder than 20,000 electron volts would have been missed. The result was zero within 20 counts per minute. If it is assumed that each ten explosions produced at least one radioactive iodine on the average this result requires that the half-life for natural fission be at least as long as 10^{13} years. Similar results must apply for the other elements which have been separated, so we can conclude that natural fission to produce any of the radioactive elements found in the artificial process must correspond to a half-life of the order of or greater than 10^{14} years. A similar test was performed on thorium with the same results.

In order to investigate possible natural neutron emission from uranium and thorium a BF_3-filled counter was surrounded with paraffin and standardized with 200 mg of $RaBr_2$ mixed with Be powder. Seven and one-half moles of uranium salts were found to give less than two counts per minute whereas the Ra-Be source in the same position gave 4600 counts per minute. If it is assumed that the Ra-Be source gives 17,000 neutrons per second per millicurie,[3] the half-life for fission must be at least as large as 10^{14} years if at least one neutron were emitted per explosion. Similar measurements on a smaller amount of thorium gave a lower limit of 5×10^{13} years.

The agreement between the uranium and thorium age determinations on old rocks and the agreement of these with other estimates of the age of the oldest strata, e.g., the Sr^{87} : Rb^{87} ratio found by Hahn, Strassmann and Walling[4] in lepidolite from the Canadian shield indicate that the age of the earth is at least 2×10^9 years and that no fission process with a half-life less than 5×10^9 years occurs, unless uranium and thorium have been or are now being generated by some terrestrial process. In the absence of any evidence for such a generation we must conclude that the half-life for any possible fission exceeds 5×10^9 years.

Consideration of all these points leads to the conclusion that no fission similar to those induced by neutron absorption can occur naturally for either uranium or thorium at a rate greater than that corresponding to a half-life of 10^{14} years and that no natural fission of any sort has a life less than 5×10^9 years.

W. F. LIBBY

Department of Chemistry,
University of California,
Berkeley, California,
May 31, 1939.

[1] P. Abelson, Phys. Rev. **55**, 670 (1939).
[2] R. W. Dodson and R. D. Fowler, Phys. Rev. **55**, 880 (1939).
[3] E. T. Booth, J. R. Dunning and F. G. Slack, Phys. Rev. **55**, 876 (1939). Their figure of 15,000 for radon has been increased for the extra alpha-particle from radium.
[4] O. Hahn, F. Strassmann and E. Walling, Naturwiss. **25**, 189 (1937). F. Strassmann and E. Walling, Berichte **71**, 1 (1938).

Secondary Emission of Electrons from Sodium Films Contaminated by Gas*

Nelson[1] has given results showing rapid variation of secondary electron emission from thin oxidized films bombarded with primaries of low energy. This occurs as the secondary emission coefficient changes from less than to greater than unity, and he has suggested a reasonable explanation in terms of the charging of the surface. In this connection graphs presented by the writer[2] at Indianapolis may be of interest, since they show a similar phenomenon for high primary energies.

The logarithms of the secondary to primary ratios are shown in Fig. 1. The data shown in curve 2 were obtained after the following treatment. Upon a tantalum base, giving the secondary emission indicated by curve 1 of the figure, a thin film of sodium was condensed. This deposit was allowed to stand in the vacuum produced by the pumps for approximately one hour. A fresh deposit of sodium was then distilled over to the target, and immediately thereafter the secondary emission data shown in curve 2 were obtained. It will be seen that the secondary emission remains at a high value, about 2.5 secondaries per primary, until a primary energy of 2000 electron volts is attained, and then it decreases very rapidly to a value of less than 0.4 for primary energies of about 4000 electron volts. From the first it was evident that this peculiar behavior (which was not common to other data obtained in the investigation) was due to the chemical combination of the sodium in the first film with gas. Nelson's hypothesis suggests a suitable mechanism for its explanation. Throughout the high emission region the outermost layers of the surface film have a positive charge which assists the secondaries in escaping. At a critical primary energy, this positive charge rapidly disappears and is replaced by a negative charge in the outermost layers; hence the rapid decrease of the secondary emission. It is of interest to notice that the total secondary emission is about 2.5 secondaries per primary when the critical value is reached. This would seem to indicate that a large proportion of the secondaries originate at considerable depths in the surface, and, even though many escape, enough are trapped in the surface layers to account for the rapid change of the surface charge necessary to explain this curve on this basis. At the end of the secondary emission observations, a microtitration of the sodium in the film revealed that it contained about 6 micrograms of sodium per square centimeter of surface area.

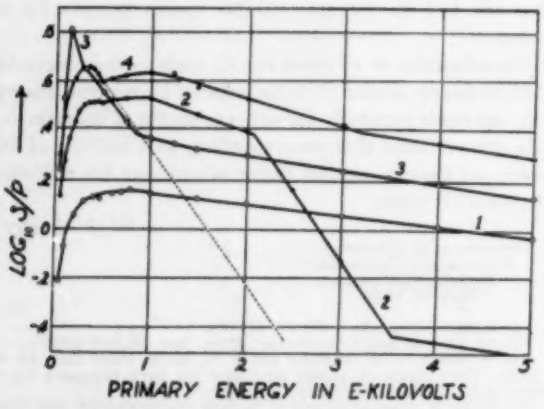

FIG. 1. Secondary electron emission from sodium on tantalum.

It is interesting to notice that rapid changes in secondary emission for primaries of high energy do not necessarily involve a transit through unit secondary emission ratio (or through zero on the semi-logarithmic plot). Curve 3 of the graph was obtained with a target formed by a single condensation of sodium under conditions such that considerable gas was present. The decrease of the secondary emission in the range from 200 to 1000 volts primary energy is so similar to that in curve 2 that the same cause is naturally suggested, but in this case the secondary emission coefficient remains greater than unity. The results shown in curve 4 give a dip whose slope is similar to that of curves 2 and 3, as shown by the dotted line extension of the trend, but in this case the secondary emission drops only a small amount before it again increases.

The total secondary emission is the integrated result of secondary excitation at various depths within the surface. Where the primary energy is high there is evidence[3] that conditions at considerable depths in the target influence the results. In the high energy region, therefore, certain layers might acquire a positive charge at the same time that other layers acquire a negative charge. If the results shown in Fig. 1 are to be explained on the basis of Nelson's hypothesis, this probably does occur in a target containing compounds of sodium bombarded with primaries of high energy. It would, of course, be interesting to measure the potential at various layers in such a surface, or, failing in that, to measure at least the potential of the outermost layer together with the resulting secondary emission as one check on Nelson's hypothesis. Related work on surface films is being continued in this laboratory.

PAUL L. COPELAND

Armour Institute of Technology,
Chicago, Illinois,
May 27, 1939.

* The writer is indebted to the National Research Council for a grant-in-aid under which this work was done.

[1] H. Nelson, Phys. Rev. **55**, 958 (1939).
[2] P. L. Copeland, Phys. Rev. **53**, 328 (1938).
[3] P. L. Copeland, Phys. Rev. **48**, 96 (1935).

The Possible Use of Superconductivity for Radiometric Purposes

The limitations of radiometry, particularly in the infrared region, are given by the magnitude of the thermal indeterminacy of the produced effect itself and that of the indicating device caused by $\frac{1}{2}nkT$ for the n degrees of freedom of the system at the temperature level at which the radiation is received and indicated. The obvious way of decreasing this indeterminacy is to lower the temperature for the receiver of the radiation. In general this fails, however, for most indicative phenomena decrease at a rate comparable to the gain of thermal determinacy (e.g., thermal e.m.f., temperature coefficient of conductivity, thermal dilatation, etc.). Although some improvement may

still be expected, the total gain does not appear to justify the inconveniences connected with the application of low temperatures.

Two effects, however, exist within the lower end of the temperature scale ($T \lesssim 4°K$) which do not follow the mentioned trend: the paramagnetic susceptibility of certain salts and the superconductivity of metal crystals, of which two effects the latter appears to fulfill the conditions of a radiometer favorably for the following reasons: aside from the practical nonexistence of thermal indeterminacy, the atomic heat is decreased to about 10^{-3} and the transition from the superconductive to the conductive state lies within $10^{-2}-10^{-3}$ degrees for good crystals (Sn). The further advantage of this transition lies in its nearly infinite temperature coefficient.

The calculated sensitivity of such a radiometer approaches, with generous allowance for practical deficiencies, $10^{-11}-10^{-12}$ cal./sec., i.e., 50–500 times better than the present radiometric limit. The application of the single adiabatic expansion technique for He does not restrict the use of this apparatus to a cryogenic laboratory, as only liquid air and a limited (transportable) quantity of liquid hydrogen will be required.

ALEXANDER GOETZ

Cryogenic Laboratory,
California Institute of Technology
Pasadena, California,
May 26, 1939.

Anomalies in the Directional Intensity Distribution of Cosmic Rays*

From the banded structure of the penumbra[1] of the Lemaitre-Vallarta allowed cone, Schremp[2] some years ago inferred the existence of an anomalous directional intensity pattern in the sky, the analysis of which might be expected to yield detailed information concerning the identity of the primary cosmic rays, their energy spectra at infinity, and their interaction with absorbing matter. An east-west directional intensity survey has recently been carried out at Washington University, St. Louis, to test these predictions with apparatus of improved angular resolution. The predictions are confirmed by the results of this survey; and these results, in turn, are in complete accord with earlier results[3] extracted from the data of Johnson[4] and Johnson and Stevenson[5] for the same geomagnetic latitude and atmospheric depth.

The intensities $I(z)$ which were recorded against the zenith angle z in the east-west plane roughly follow the well-known empirical relation

$$I(z) = I_0 \cos^2 z. \tag{1}$$

The observed anomalies, which may be considered as deviations $\Delta(z)$ from this empirical curve, are presented in Fig. 1. The quantity $\Delta(z)$ plotted here is the percent deviation of

$$I_0(z) = I(z) \sec^2 z \tag{2}$$

from the mean value of $I_0(z)$ over all angles. The results were taken in such a way as to be essentially independent

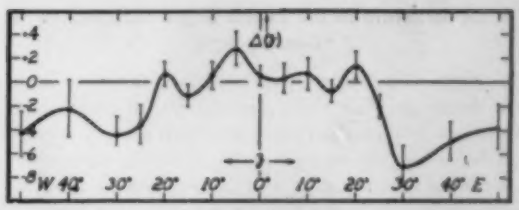

FIG. 1. East-west section of the cosmic-ray directional intensity pattern. $\Delta(z)$ is the percent deviation of the observed east-west distribution from the empirical $\cos^2 z$ distribution.

of secular variations in the counter sensitivity. The telescope was shifted in direction periodically so that the counts taken at any one direction were contributed to on at least twenty separate occasions. The succession of directions was deliberately made random. The probable errors shown in Fig. 1 were computed, not from the total counts at each zenith angle, but rather from residuals, which included any secular variations in the counter sensitivity.

Our results[6] definitely establish the existence of symmetrical prominences at $z = \pm 20°$ and further indicate other symmetrical prominences in the neighborhood of $z = \pm 10°$ and $z = \pm 40°$. The east-west symmetry[7] of these prominences confirms the symmetry which was earlier pointed out[3] to exist in the data of Johnson. According to the theory, this symmetry indicates the presence, in the primary cosmic radiation, of comparable numbers of particles of the same mass and opposite charge, and has been interpreted by Schremp[2] as furnishing evidence that the observed primaries are exclusively positrons and negatrons.

In view of these results it appears quite certain that the complete directional intensity pattern in the sky, obtained at one or more localities by an extension of this type of survey to a number of azimuthal planes, will provide in the future a highly refined method of analysis of the primary rays, their spectra, and their behavior under absorption.

H. S. RIBNER

Wayman Crow Hall of Physics,
Washington University,
St. Louis, Missouri,
May 26, 1939.

* This work is the subject of a Ph.D. dissertation, a full account of which will be published shortly.

[1] M. S. Vallarta, J. Frank. Inst. **227**, 1 (1939). Cf. also E. J. Schremp, Phys. Rev. **54**, 156 (1938); R. Albagli Hutner, Phys. Rev. **55**, 15 (1939), **55**, 614 (1939).

[2] E. J. Schremp, Phys. Rev. **53**, 915A (1938); **54**, 157 (1938).

[3] These reduced results, which do not appear in the original articles cited, form a part of certain unpublished calculations of Dr. E. J. Schremp, which he kindly made available to the writer.

[4] T. H. Johnson, Phys. Rev. **48**, 287 (1935).

[5] T. H. Johnson and E. C. Stevenson, Phys. Rev. **44**, 125 (1933).

[6] Similar results in the eastern azimuthal plane, obtained independently by Mr. Denzil M. Cooper, are described in an accompanying letter. A comparison of the present two surveys shows quantitative agreement with respect to the 10° and 20° prominences. Cooper's minimum at 25° and prominence at 30° compare qualitatively with our minimum at 30° and prominence at 40°. The relative displacement of our respective patterns at large angles may possibly be ascribed to secular fluctuations in the intensity pattern arising from magnetic and barometric disturbances. The existence of such fluctuations has already been indicated by the successive results compiled in the course of this survey.

[7] The symmetry alluded to here refers to the *positional symmetry* of the prominences, and is not to be confused with the well-known east-west *asymmetry of intensities*. The latter asymmetry, which is also demonstrated by Fig. 1, is of noticeably smaller magnitude than the intensity pattern fine structure sought for here.

Fine Structure in the Zenith Angle Distribution of Cosmic Rays

Multiple coincidence Geiger-Müller counting systems have made possible the measurement of cosmic-ray intensities in definite directions, and such systems have been used extensively by various investigators to determine the variation of cosmic rays with zenith angle.[1] If θ is the zenith angle, it is found that the intensity of cosmic rays is proportional essentially to $\cos^2\theta$. It is generally true, however, that these investigations have been carried out to determine the gross shape of the curve representing the angular distribution of intensity, so that the experimental systems and the methods of observations were not especially suited to detect fine structure in this distribution. An attempt has been made in the present work to search for small variations from the $\cos^2\theta$ law in the hope that if they are present, information might be obtained concerning the energies of incoming cosmic rays.

Certain features of the experimental set-up and procedure require special attention for an investigation of this sort. First, it is desirable to have the direction as well defined as is practicable; second, it is desirable to take readings at frequent angular intervals; third, it is desirable to have instantaneous readings at all angles; and fourth, it is desirable to have a large total number of counts at all the angles investigated. The direction may be better defined by placing the counters far apart in relation to their lengths and widths. In the present work, counters of 8.8 cm diameter and 36 cm active length were used with the distance between centers of adjacent ones, 50 cm. With a train of three counters, this gives a maximum divergence of 40° due to their lengths, and of less than 10° due to their widths. Readings were taken at angular intervals of 5°, from the vertical to 45° towards the east. Instantaneous values of cosmic-ray intensity cannot be obtained for all angles. However, it seems desirable to vary the direction of observation periodically and in a cyclic fashion in order to minimize the effect of drift in sensitivity of the instrument. Thus, readings were taken at a given angle for 15 minutes, the outfit was rotated through 5° and readings were again taken for 15 minutes, and so on. The total number of counts recorded at a given angle is between 3000 and 4000 for most angles, though three points have been included which are based on only about 900 counts.

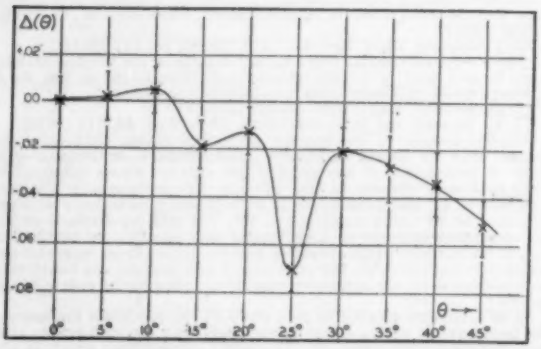

FIG. 1. The deviation, $\Delta(\theta)$, of the experimentally observed intensity from the $\cos^2\theta$ curve as a function of the zenith angle θ.

Since the difference between the observed intensity at a given angle and the general background of intensity is desired, the counting rates for each angular setting were reduced to unity for zero degrees, and the differences between $\cos^2\theta$ and the observed values are obtained as a function of θ. The preliminary results are plotted in Fig. 1 where $\Delta(\theta)$ is the difference between the observed results and the $\cos^2\theta$ curve. Although the effect is small, it appears that there is some experimental support for the conclusion that there is fine structure in the angular distribution of cosmic-ray intensities. Further work is being carried out to improve the reliability of these results and to extend the angles of investigation.

Mr. Ribner has carried out a similar experiment independently, and his more extensive results are reported in a companion letter. It is a pleasure to acknowledge the cooperation and advice of Dr. E. J. Schremp and of Professor N. S. Gingrich.

DENSIL M. COOPER

University of Missouri,
Columbia, Missouri,
May 26, 1939.

[1] D. K. Froman and J. C. Stearns, Can. J. Research **16**, 29 (1938).

On Alfvén's Hypothesis of a "Cosmic Cyclotron"

In a recent paper,[1] Alfvén has suggested that charged primary cosmic rays might acquire their high energy by being accelerated in the magnetic field of double stars, by a process somewhat analogous to that which takes place in an ordinary cyclotron.

If we assume with Alfvén that the field of a double star is the field of two parallel dipoles, and that a charged particle can really describe in their common equatorial plane the motion assumed by him, which is questionable, there remain three important objections to the mechanism he suggests.

(1) The electric field, created by the rotation of the second dipole relative to the first, vanishes for a charged particle rotating synchronously around the first, since then there is manifestly no relative motion between the charged particle and the second star.

(2) The magnetic flux linking the elementary circular path of the charged particle, in Alfvén's analysis, is constant so long as the condition of synchronism still obtains. Therefore, there is no induced e.m.f. along the path and hence no acceleration.

(3) Finally, so far as Alfvén's analysis goes, there is no way for the particle to leave the field of the double star.

In a more extended paper,[2] Alfvén has endeavored to analyze the more general case where synchronism does not obtain. It seems, however, that his calculations are erroneous. In particular, his Eq. (17), fundamental for his calculation of the energy, does not take into account the first dipole; since the particle does not, in general, describe a circle around the first dipole, there is no reason to neglect the latter's influence. But even assuming his calculations were correct, his conclusion is that in the case of parallel dipoles the orbits are closed, so that obviously when the particle returns to its initial position it must have the same momentum, and the total change of kinetic energy along

the orbit must vanish. Thus, the fundamental idea of cyclotron action is untenable.

To be sure such a mechanism entails a periodic change of the particle's energy, which varies from a minimum V_A, at a certain point A on its orbit, to a maximum V_B, at a point B, later to return to V_A. In a favorable case, and with dipole moments 16 times the sun's (10^{34} e.m.u.),

$$V_B = 10\ V_A.$$

A double star might be a generator of cosmic rays *if* two conditions, both difficult to accept, were realized: (1) In the field of the double star there must be already particles of very high energy (about 10^{10} ev), and (2) by an unknown mechanism, particles must be released just at the moment when they go through the point of maximum energy.

Alfvén also considers the case of two antiparallel dipoles. Qualitative, and somewhat obscure, considerations lead him again to expect synchronism, so that the objections already discussed again apply with full force.

I wish to thank Professor M. S. Vallarta for suggesting this problem and for worthwhile discussions. I thank also Dr. F. Cernuschi for his criticism.

E. R. SABATO*

Massachusetts Institute of Technology,
Cambridge, Massachusetts,
May 25, 1939.

* Fellow of the Argentine Association for the Progress of Sciences.

[1] H. Alfvén, Nature **136**, 761 (1936).
[2] H. Alfvén, Zeits. f. Physik **105**, 319 (1937).

Raman Effect of Fluorochloromethane

Using our previously described technique and apparatus,[1] we have determined the Raman shifts for fluorochloromethane. Eastman Spectroscopic Plates Type 1J were used. Two plates were run with exposure times of 8.25 and 36 hours. The results are shown in Table I. The material boils at −9.1°C, and the determinations were made at an average temperature of −30°C.

The plates were completely free from background. Hence, the sample must have been almost completely dust-free. No filters were used, and no photodecomposition was observed.

The material was furnished by the E. I. duPont de Nemours Company, and was specified "Fractionated in the laboratory in an efficient column, boiling range about 0.2°C." About 43 grams of sample were available. We wish to express our gratitude to Dr. A. F. Benning of the Jackson Laboratory for the loan of this substance. Further details regarding the data will be published later.

TABLE I. *Raman shifts of fluorochloromethane.* $a = 4358$A; $b = 4046$A; $c = 4078$A.

cm^{-1}	Exciting Lines	Percent Mean Deviation	Relative Intensity
385.3	*a*, b	0.241	10
742.8	*a*, *b*, *c*	.170	10(*b*)
1004.3	*a*, *b*	.176	0.5
1045.6	*a*, *b*, *c*	.170	2(*b*)
1352.5	*a*, *b*	.104	2
1467.9	*a*, *b*	.067	2
2910.6	*a*, *b*	.053	4
2993.1	*a*, *b*, *c*	.036	10(*b*)
3048.3	*a*, *b*	.059	6(*b*)

GEO. GLOCKLER
J. H. BACHMANN

University of Minnesota,
Minneapolis, Minnesota,
April 26, 1939.

[1] Geo. Glockler and J. H. Bachmann, Phys. Rev. **55**, 669 (1939).

Erratum: Range Distribution of the Uranium Fission Fragments*

(Phys. Rev. **55**, 982 (1939))

Because of an oversight, a Letter to the Editor which appeared in the May 15, 1939 issue of the *Physical Review* was sent in signed incorrectly. The Letter, entitled "Range Distribution of the Uranium Fission Fragments," which appears on page 982, should have been signed: E. T. Booth, J. R. Dunning and F. G. Slack instead of E. T. Booth, J. R. Dunning and G. N. Glasoe, as it appears.

E. T. BOOTH
J. R. DUNNING
F. G. SLACK

Department of Physics,
Columbia University,
New York, New York,
May 29, 1939.

* Publication assisted by the Ernest Kempton Adams Fund for Physical Research of Columbia University.

Author Index to Volume 55

References with (A) are to abstracts of papers presented at meetings of the American Physical Society.
References with (L) are to Letters to the Editor.

Abelson, Philip. Cleavage of the uranium nucleus—418(L)
—— Further products of uranium cleavage—670(L)
—— Identification of some of the products of uranium cleavage—876(L)
—— Identification of x-rays emitted during the decay of radioactive elements—424(A)
Abramson, Harold A. Electrophoretic demonstration of patent pores of human skin—676(A)
Aebersold, Paul C. Collimation of fast neutrons—596(A)
—— **and Gladys A. Anslow.** Ionization produced in gases by fast neutron irradiation—680(A)
—— **and Gladys A. Anslow.** Ionization produced in thimble chambers by fast neutrons—1134(A)
Albagli, R. (see Hutner, R. Albagli)—15, 109(L), 614
Albertson, W. E. and G. R. Harrison. Normal electron configuration of singly ionized cerium—1119(A)
Alder, Robert L. (see Evans, Robley D.)—1134(A)
Alfvén, Hannes. On the motion of cosmic rays in interstellar space—425
Alichanian, A. I. and V. Berestezky. On the interpretation of β-disintegration data—978(L)
Alleman, R. S. Dissipative acoustic reflection coefficients in gases by ultrasonic interferometry—87
Allen, H. W. (see Holmes, R. M.)—593(A)
Allen, James S. Detection of single positive ions, electrons and photons by a secondary electron multiplier—966, 1133(A)
—— Emission of secondary electrons from metals bombarded with protons—336
—— Secondary emission of electrons due to protons—236(A)
—— (see Haxby, R. O.)—140, 598(A)
Allison, Samuel K. Masses of Li^6, Li^7, Be^8, Be^9, B^{10} and B^{11}—624
——, **Elizabeth R. Graves, Lester S. Skaggs and Nicholas M. Smith, Jr.** Precise measurement of the mass difference $_4Be^9-{}_4Be^8$; Stability of $_4Be^8$—107(L), 599(A)
Almy, G. M., H. Q. Fuller and G. D. Kinzer. Fluorescence and absorption of diacetyl—238(A)
Alter, B. E. K. and R. T. K. Murray. Field currents at high and low pressures—672(A)
Alvarez, Luis W. (see Green, G. K.)—417(L)
—— **and Kenneth S. Pitzer.** Scattering of ultra-slow neutrons in ortho- and parahydrogen—596(A)
Anderson, H. L., E. T. Booth, J. R. Dunning, E. Fermi, G. N. Glasoe and F. G. Slack. Fission of uranium—511(L)
—— **and E. Fermi.** Simple capture of neutrons by uranium—1106(L)
——, **E. Fermi and H. B. Hanstein.** Production of neutrons in uranium bombarded by neutrons—797(L)
Anderson, Wilmer C. Velocity of light apparatus—1128(A)
Anslow, Gladys A. (see Aebersold, Paul C.)—680(A), 1134(A)
Aoki, Hiroo. On the scattering of fast neutrons of different energy—795(L)
—— (see Kikuchi, Seishi)—108(L), 1264(L)
Aradine, P. W. (see Barnes, S. W.)—50
Archibald, W. J. Specific heat of monatomic liquids—1139(A)
Astin, Allen V. Negative power factors in air capacitors—594(A)
—— (see Curtis, Harvey L.)—594(A)
—— (see Curtiss, L. F.)—600(A)

Bacher, R. F. Elastic scattering of fast neutrons—679(A)
Bachmann, J. H. (see Glockler, George)—669(L), 1273(L)
Baker, Richard F. and John T. Tate. Ionization and dissociation of $CHBrF_2$ by electron impact—236(A)
Baltzer, O. J. and E. M. McNatt. Diffuse scattering of Cu $K\alpha$ x-rays from single zinc crystals—237(A)
Baños, Alfredo, Jr. On asymptotic orbits of primary cosmic rays—621
Barber, A. (see Champion, F. C.)—111(L)
Barkas, Walter H. Analysis of nuclear binding energies—691
Barker, E. F. Perpendicular vibrations of the ammonia molecule—657
—— (see Owens, Ralph G.)—1119(A)
Barnes, S. W. Proton reactions of $_{48}Cd$ and $_{49}In$—241(A)
—— **and P. W. Aradine.** Radioactivity induced by nuclear excitation. II. Excitation by protons—50
Barnóthy, J. and M. Forró. Cosmic-ray particles at great depth—870
—— **and M. Forró.** Diurnal and sidereal effects and the meteorologic influences on shower and vertical intensity of cosmic rays—868
Baroody, E. M. Anistropy of electric conductivity of metals—1140(A)
Barry, J. G. (see Johnson, T. H.)—503(L)
Barschall, H. H., W. T. Harris, M. H. Kanner and Louis A. Turner. Penetrating beta-particles from uranium activated by neutrons—989(L)
Bartlett, James H., Jr. Stopping power of mercury and of nitrogen for cosmic-ray electrons—803
Bartlett, J. H. and R. E. Watson. Scattering of fast electrons—235(A)
Barton, Charles A. (see Whitaker, Martin D.)—793(L)
Bassoe, Else (see Cashman, R. J.)—63
Bath, Jean (see Ellis, Joseph W.)—1098
Baudisch, Oskar (see Welo, Lars A.)—1143(A)
Bayley, D. S. (see Ellett, A.)—1129(A)
Beams, J. W. Separation of gases by centrifuging—591(A)
—— (see Masket, A. Victor)—674(A)
—— (see Skarstrom, C.)—591(A)
—— (see Snoddy, L. B.)—663(L), 879(L), 1145(A)
—— **and L. B. Snoddy.** Electrical discharge between a stationary and a rotating electrode—504(L)

Bearden, J. A. Spectroscopic and free electron values of e/m—584(L)
Beck, C. A. and W. F. Radle, Experimental study of intensities in benzene vapor absorption in the region 2200–2600A—1120(A)
Becker, R. A. (see McLean, W. B.)—796(L)
Beeck, Otto (see Smith, A. E.)—602(A)
——, **A. Wheeler and A. E. Smith.** Catalytic activity and crystal orientation of metal films—601(A)
Beeman, W. W. (see Friedman, H.)—1115(A)
—— **and H. Friedman.** X-ray evidence on the band structure of copper and nickel—1115(A)
Beese, N. C. Response of several fluorescent materials to short wave-length ultraviolet radiations—1126(A)
Bell, Maurice E. Probability of ionization of mercury atoms by collision with low velocity electrons—201
Bell, P. R. (see Harkins, W. D.)—1110(A)
Berestezky, V. (see Alichanian, A. I.)—978(L)
Berkner, L. V. Concerning the nature of radio fade-out—536
Bernard, René. Presence of the nitrogen forbidden line $^2P \rightarrow 4S$ in the auroral spectrum—511(L)
Bethe, H. A. Energy production in stars—103(L), 434
—— Meson theory of nuclear forces—1261
—— Meson theory of nuclear forces and the quadrupole moment of the deuteron—1130(A)
—— Self-energy of the electron—681(A)
—— (see Marshak, R. E.)—681(A)
—— (see Rose, M. E.)—277, 601(A)
Beutler, H. Absence of new exchange forces in H_2 as shown from band spectra—1118(A)
—— (see Metropolis, N.)—1113(A)
Beyer, Harold G. (see Whitaker, Martin D.)—1101(L), 1124(A)
Bidwell, C. C. Method of determining thermal conductivity suitable for solid or molten metals. Values for zinc from −250°C to 720°C.—1139(A)
Birge, Raymond T. The $L_{II}L_{III}$ spin doublet and the value of the fine structure constant—1119(A)
Bitter, Francis (see Harrison, George R.)—1125(A)
—— **and A. R. Kaufmann.** Susceptibility measurements of Cu-Fe alloys in fields from 0–40,000 gauss—1142(A)
Blewett, J. P. Time changes in emission from oxide-coated cathodes—713
——, **H. A. Liebhafsky and E. F. Hennelly.** Vapor pressure and rate of evaporation of barium oxide—1138(A)
Bloch, F. On the temperature dependence of the scattering of slow neutrons in ferromagnetics—1118(A)
Blodgett, Katharine B. Use of interference to extinguish reflection of light from glass—391
Bohn, J. Lloyd and Francis H. Nadig. Determination of the radon content of the spring waters of Fairmount Park—685(A)
Bohr, N. and John A. Wheeler. Mechanism of nuclear fission—1124(A)
—— Resonance in uranium and thorium disintegration and the phenomenon of nuclear fission—418(L)
Bolt, Richard H. Distribution of eigentones at low frequencies—420(A)
Bonner, L. G. (see Kirby-Smith, J. S.)—1114(A)
——, **A. P. Cleaves and H. Sponer.** Absorption of methylamine vapor in the photographic infra-red—1113(A)
Booth, E. T. (see Anderson, H. L.)—511(L)
——, **J. R. Dunning and G. N. Glasoe.** Range distribution of the uranium fission fragments—982(L)
——, **J. R. Dunning and F. G. Slack.** Delayed neutron emission from uranium—876(L)
——, **J. R. Dunning and F. G. Slack.** Energy distribution of uranium fission fragments—981(L)
——, **J. R. Dunning and F. G. Slack.** Erratum: Range distribution of the uranium fission fragments—1273(L)
——, **J. R. Dunning and F. G. Slack.** Fission of uranium and production of delayed emission by slow neutron bombardment—1124(A)
Boothby, O. L. (see Cioffi, P. P.)—673(A)
Borst, L. P. (see Harkins, W. D.)—1110(A)
Bowersox, Ralph B. Efficiency of production of short range particles from lithium and of 4.4-cm alpha-particles from boron under proton bombardment—323
—— Excitation functions of lithium and boron—240(A)
Boyd, Edward and William D. Harkins. Viscosity in two-dimensional systems—1131(A)
Boyd, George and William D. Harkins. Molecular aspect of the energies of adhesion between various liquids and solids: Adsorption as the result of electrostatic forces—237(A)
Bozorth, R. M. (see Williams, H. J.)—673(A)
Brackett, F. S. (see Kuper, J. B. H.)—1128(A)
—— **and Alexander Hollaender.** Physical factors governing biological action of radiation—1120(A)
Bradbury, N. E. Nocturnal E layer ionization—423(A)
Brady, James J. and William H. Moore. Actinoelectric effects in tartaric acid crystals—308
—— **and William H. Moore.** Photoconductivity of crocoite crystals—424(A)
Brady, Lynn J. Automatically recording Geiger-Müller counter circuit—1133(A)
Bramley, Arthur (see Brewer, A. Keith)—590(A)
Breit, G. (see Share, S.)—1130(A)
——, **L. E. Hoisington, S. S. Share and H. M. Thaxton.** Approximate equality of the proton-proton and proton-neutron interactions for the meson potential—1103(L)
——, **H. M. Thaxton and L. Eisenbud.** Analysis of experiments on the scattering of protons by protons—1018
——, **H. M. Thaxton and L. Eisenbud.** Interpretation of experiments on proton-proton scattering—603(A)
Brewer, A. Keith. Constancy of K^{40}—669(L)
—— **and Arthur Bramley.** Thermal-gravitational method for the separation of gases and isotopes—590(A)
Brickwedde, F. G. and R. B. Scott. Some physical properties of liquid and solid HD—672(A)
Brieger, L. C. (see Vitter, A. L.)—416(L)
Bright, William C. (see Whitaker, Martin D.)—793(L)
Brillouin, Léon. On thermal dependence of elasticity in solids—1139(A)
Brown, B. W. (see Curtiss, L. F.)—600(A)
Brown, George H. Velocity of radio waves in air—1100(L)
Brown, Harrison and D. R. Inglis. Coulomb energies and nuclear models—1182

Brown, Sanborn C. and Robley D. Evans. Discharge counters of unconventional geometry—1133(A)
Brown, S. LeRoy. Complex roots of fifteenth-degree polynomials—604(A)
Brown, William Fuller, Jr. Theory of reversible magnetization in ferromagnetics—568
Broxon, James W. and George T. Merideth. Gamma-ray ion currents in air at high pressures and high gradients at high and low temperatures—883
Brubaker, Gordon. Erratum: Scattering of alpha-particles by argon, oxygen and neon—877(L)
—— (see Slepian, Joseph)—1147(A)
Bruce, W. A. Thermal distribution and temperature gradient in the arc welding of cylindrical tubing—594(A)
Buck, John H. (see Livingston, Stanley M.)—1110(A)
Buechner, W. W. (see Hill, A. G.)—463
Buehl, R. C. and A. von Hippel. Temperature dependence of the electrical breakdown in single crystals—1122(A)
Burbank, Cecil J. Faint *L* series lines from *K* auger transitions in silver—421(A)

Cacciapuoti, B. N. Radioactive isotopes of element 43—110(L)
Campbell, J. S. and J. R. Davis. Hyperfine structure in the spectrum of indium III—1125(A)
Carlson, J. Franklin. Interactions of heavy electrons—599(A)
Carpenter, B. (see Harkins, W. D.)—1110(A)
Carr, H. E. (see Skarstrom, C.)—591(A)
Carroll, K. G. Binding energy of Li^7—1128(A)
—— (see Tyrrell, W. A.)—790(L)
Cartwright, C. Hawley. LiF achromats for covering large spectral ranges—606(A)
—— **and A. Francis Turner.** Reducing the reflection from glass by evaporated films—595(A)
—— **and A. Francis Turner.** Reducing the reflection from glass by multilayer films—675(A)
—— **and A. Francis Turner.** Multilayer films of high reflecting power—1128(A)
Cashman, R. J. and Else Bassoe. Surface and volume photoelectric emission from barium—63
Castleman, R. A., Jr. On the mechanism of air-blast atomization (air-injection; ante-chamber methods)—592(A)
Chai, Tsu-Yen (see Shih, J. W.)—1265(L)
Champion, F. C. and A. Barber. Elastic scattering of fast β-particles by atomic nuclei—111(L)
Chenault, W. L. (see Ramsey, R. R.)—239(A)
Chodorow, Marvin. Band structure of metallic copper—675(A)
Christy, R. F. and S. Kusaka. Electric quadrupole moment of the deuteron—665(L)
Chu, Djen-Yuen. Fine structure of the line λ4686 of ionized helium—175, 423(A)
Cioffi, P. P. and O. L. Boothby. Preparation of single crystals of iron, cobalt, nickel and their alloys—673(A)
Clark, J. S. (see Hill, A. G.)—463
Cleaves, A. P. and E. K. Plyler. Infra-red absorption spectrum of methylamine vapor—1113(A)
—— (see Bonner, L. G.)—1113(A)
Cleveland, Forrest F. and M. J. Murray. Raman spectra of phenyl-1-propyne-1 and chloro-2-phenyl-1-acetylene—600(A)
—— **and M. J. Murray.** Use of Polaroid in depolarization measurements on Raman lines—1113(A)
—— **M. J. Murray, Julia Shackelford and Herschel H. Haney.** Displacements and depolarization factors of the Raman lines of di-normal- and di-iso-ethers—1146(A)
Coblentz, W. W. and R. Stair. Distribution of ozone in the stratosphere—590(A)
Cohen, Victor W. (see Goldsmith, H. H.)—1124(A)
—— (see Seely, S.)—679(A)
—— **and H. H. Goldsmith.** Scattering of neutrons by protons—597(A)
—— **H. H. Goldsmith and Julian Schwinger.** Neutron-proton scattering cross section—106(L)
Cole, Peter A. Ultraviolet microscopy as a means of determining chemical structure in the cell—597(A)
—— (see Hollaender, Alexander)—597(A)
Collins, George B. (see Waldman, B.)—1129(A)
——, **Bernard Waldman and William R. Polye.** Electrodisintegration of beryllium—412(L), 1123(A)
——, **Bernard Waldman, Edward M. Stubblefield and M. Goldhaber.** Nuclear excitation of indium by x-rays—507(L)
Collins, J. R. New infra-red absorption band of liquid water at 2.52μ—470
Colwell, R. C., J. K. Stewart and A. W. Friend. Chladni patterns on circular plates—595(A)
Compton, A. H. and P. S. Gill. Significance of sidereal time variations of cosmic rays—233(A)
Compton, Karl T. (see Lamar, Edward S.)—1235
—— (see Stone, Albert M.)—1145(A)
Constant, F. W. and J. W. Formwalt. Investigations of ferromagnetic impurities in metals—1143(A)
Coolidge, Albert Sprague (see James, Hubert M.)—184, 234(A)
—— (see James, H. M.)—873
Coomes, Edward A. Total secondary electron emission from tungsten and thorium-coated tungsten—519
—— (see Hughes, J. M.)—1138(A)
Cooper, Densil M. Fine structure in the zenith angle distribution of cosmic rays—1272(L)
Cooper, F. S. (see Pollock, H. C.)—593(A)
Copeland, Paul L. Secondary emission of electrons from sodium films contaminated by gas—1270(L)
—— Variation of the anode effect with temperature—1145(A)
Cork, J. M. and B. R. Curtis. Excitation function for iron by energetic deuterons—1264(L)
—— **and J. L. Lawson.** Radioactivity in cadmium and indium—1136(A)
Corson, D. R. and R. L. Thornton. Disintegration of uranium—509(L)
Cowie, D. B. (see Montgomery, C. G.)—1117(A)
Crane, H. R. Attempt to observe the absorption of neutrinos—501
—— (see Halpern, J.)—236(A), 258, 260, 415(L), 1123(A)
—— **and J. Halpern.** On the creation of pairs or positrons by fast electrons—838

—— **and N. L. Oleson.** New type of low voltage, high current ion tube for the production of neutrons—1110(A)
Creutz, Edward C. Resonance scattering of protons by lithium—679(A), 819
—— (see Fox, J. B.)—1106(L)
Curtis, B. R. Gamma-radiation from radioactive cobalt—1136(A)
—— (see Cork, J. M.)—1264(L)
Curtis, Harvey L. and Allen V. Astin. Explanation of the negative power factors in air capacitors—594(A)
Curtiss, L. F., A. V. Astin, L. L. Stockmann and B. W. Brown. Cosmic-ray measurements in the stratosphere by Geiger-Müller counters in an integrating circuit—600(A)

Dahlstrom, R. K. (see Henderson, Joseph E.)—473
Dancoff, S. M. On radiative corrections for electron scattering—959
—— **and P. Morrison.** Calculation of internal conversion coefficients—122, 423(A)
Danforth, W. E. (see Korff, S. A.)—675(A), 980(L)
Danielson, G. C. (see Lanczos, C.)—242(A)
Dart, F. E. and E. Guth. Dependency of the stress-strain relationship for rubber upon the rates of stretching—1141(A)
Davis, Francis J. (see Winans, J. Gibson)—242(A), 1126(A)
Davis, J. R. (see Campbell, J. S.)—1125(A)
Davis, L. and W. V. Houston. Hall effect and change of resistance in a magnetic field—1143(A)
Dawson, L. H. and E. O. Hulburt. Scattering of light by water as a function of angle—1128(A)
Delsasso, L. A. (see Fox, J. G.)—1106(L)
——, **L. N. Ridenour, R. Sherr and M. G. White.** Artificial radioactivity produced by protons—113
Dempster, Arthur J. Isotopic constitution of hafnium, yttrium, lutetium and tantalum—794(L)
—— (see Sherwin, C. W.)—582(L)
Dennison, D. M. (see Fuson, N.)—590(A)
DeVault, Don C. and W. F. Libby. Evidence for the gamma-radioactivity of a 4.5 hour Br^{80} from radiobromate—322(L)
Dieke, G. H. (see Wood, R. W.)—1120(A)
Dietrich, J. R. Effect of wall charge on the progressive breakdown in long discharge tubes—1145(A)
—— **and L. B. Snoddy.** Impulse breakdown in long discharge tubes—591(A)
Distad, Merril. Dielectric anomalies of zincblende crystals—1147(A)
—— Effect of electron bombardment on the electrical conductivity of zincblende crystals—1146(A)
Dodson, R. W. (see Fowler, R. D.)—417(L)
—— **and R. D. Fowler.** Radioactive halogens produced by the neutron bombardment of uranium and thorium—880(L)
Doermann, F. W. (see Halpern, O.)—681(A), 1077
—— **and O. Halpern.** Theoretical evaluation of a wide-angle interference experiment—486
Dorsey, N. Ernest. Quiet boiling—594(A)
Dow, R. B. Crystallization and melting of rubber at high pressure—1141(A)
DuBridge, L. A. Nuclear reactions produced by 6.5 Mev protons—603(A)
Duffendack, O. S. (see Lifschutz, Harold)—412(L), 1133(A)
—— **and O. G. Koppius.** The variation with the density of mercury vapor of the intensity of the spectral lines of mercury excited by electron impact—1199
Dunlap, Henry (see Hudspeth, Emmett)—587(L)
Dunning, J. R. (see Anderson, H. L.)—511(L)
—— (see Booth, E. T.)—876(L), 981(L), 982(L), 1124(A), 1273(L)
—— (see Goldsmith, H. H.)—1124(A)
—— (see Witcher, C.)—1135(A)
Dunnington, Frank G. Re-evaluation of the atomic constants—683(A)

Eaton, J. R. (see Maxfield, F. A.)—592(A)
Eggleston, Forrest C. (see Stewart, John Q.)—1102(L)
Ehrenkranz, Florence. Spark breakdown potentials as a function of the product of the pressure by the plate separation in A, N_2 and H_2 for Pt and Na cathodes—219
Ehrhardt, C. H. (see Lark-Horovitz, K.)—605(A)
Ehrke, Louis F. and Charles M. Slack. Investigation into the gettering powers of various metals for the gases hydrogen, oxygen, nitrogen, CO_2, and air—684(A)
Eichelberger, J. F. (see Green, J. B.)—1126(A)
Eisenbud, L. On the photoelectric effect of the deuteron—1129(A)
—— (see Breit, G.)—603(A), 1018
Elenbaas, W. Temperature distribution in the high pressure mercury discharge tube—294
Ellett, A., J. A. Van Allen and D. S. Bayley. Distribution in angle of protons from the deuteron-deuteron reaction—1129(A)
Elliott, R. M. and J. Wulff. Hyperfine structure of gold—170
Ellis, Cecil B. Crystal field energy levels in Pr salts—1114(A)
Ellis, Joseph W. Infra-red absorption bands of some perturbed hydroxyl groups—597(A)
—— **and Jean Bath.** Infra-red pleochroism and Fermi resonance associated with CH_2 groups in crystal—1098
Elsasser, Walter M. On the origin of the earth's magnetic field—489
Engstrom, R. W. Townsend ionization coefficients and glow potentials in an argon-barium phototube—239(A)
Enns, T. Disintegration of the isomers of Ag^{106}—1118(A)
Eskin, S. G. (see Huxford, W. S.)—1146(A)
Essig, Sanford E. Silver films on a mica crystal face—229(L)
Evans, Robley D. (see Brown, Sanborn C.)—1133(A)
—— (see Livingston, Stanley M.)—1110(A)
—— **and Robert L. Alder.** Improvements in the counting rate meter—1134(A)
——, **Clark Goodman, N. B. Keevil, A. C. Lane and W. D. Urry.** Intercalibration and comparison in two laboratories of measurements incident to the determination of the geological ages of rocks—931
Ewing, D. H. (see Weisskopf, V. F.)—241(A)
——, **Tom Perry and Ralph McCreary.** Radioactivities induced in molybdenum by gas protons—1136(A)

Failla, G. Some new features in the million-volt x-ray installation at the Memorial Hospital—677(A)
—— (see White, T. N.)—676(A)
Fan, Hsu Yun. Transition from glow discharge to arc—769
Feenberg, Eugene. Detonation of nitrogen iodide by nuclear fission—980(L)
—— On the derivation of nuclear forces from field theories—602(A)
—— On the shape and stability of heavy nuclei—504(L)
Fermi, E. (see Anderson, H. L.)—511(L), 797(L), 1106(L)
Feynman, R. P. (see Vallarta, M. S.)—506(L)
Field, J. E. (see Gehman, S. D.)—594(A)
Finck, J. L. General equation of state: Equations for ammonia and steam—682(A)
Fireman, Peter. Inertial mass—683(A)
Fisher, Russell A. Properties of the hyperfine structure of a multiplet—1112(A)
—— **and Edson R. Peck.** Hyperfine structure of manganese I and nuclear magnetic moment—270
Fisk, J. B. Transmutation of boron by slow neutrons with the emission of α-particles and protons—1117(A)
—— (see Hill, A. G.)—463
Florence, Robert T. and William D. Harkins. Effect of molecular shape on molecular attraction in monolayers—237(A)
Forbush, S. E. On world-wide changes in cosmic-ray intensity—233(A)
Formwalt, J. M. (see Constant, F. W.)—1143(A)
Forró, M. (see Barnóthy, J.)—868, 870
Fountain, C. R. and E. G. Pigg. Absorption and reradiation by resonators—592(A)
Fowler, R. D. (see Dodson, R. W.)—880(L)
—— **and R. W. Dodson.** Intensely ionizing particles produced by neutron bombardment of uranium and thorium—417(L)
Fowler, W. A. (see Gaerttner, E. R.)—27
—— (see McLean, W. B.)—796(L)
Fox, Gerald W. and Dean W. Stebbins. Effect of quartz filters on the distribution of energy in Laue patterns—405
Fox, J. G., E. C. Creutz, M. G. White and L. A. Delsasso. Difference in Coulomb energy of light, isobaric nuclei—1106
Frenkel, J. On the splitting of heavy nuclei by slow neutrons—987(L)
Fricke, Hugo. Dielectric properties of dielectrics dispersed in water and anomalous dispersion in bound, (oriented) water—1141(A)
Friedman, H. (see Beeman, W. W.)—1115(A)
—— **and W. W. Beeman.** X-ray K absorption limits of iron, nickel, copper and zinc—1115(A)
Friend, A. W. (see Colwell, R. C.)—595(A)
Fuller, H. Q. (see Almy, G. M.)—238(A)
Furry, W. H. Double β-disintegration and the theory of the neutrino—602(A)
——, **R. Clark Jones and L. Onsager.** On the theory of isotope separation by thermal diffusion—1083, 1137(A)
Fuson, N., H. M. Randall and D. M. Dennison. Far infrared, pure rotation spectrum and the molecular structure of heavy water vapor—590(A)
Gaerttner, E. R., W. A. Fowler and C. C. Lauritsen. Gamma-radiation from boron bombarded by deuterons—27
Gamertsfelder, Carl. Diffraction of x-rays by liquid tin and liquid chlorine—1116(A)
Gamertsfelder, G. R. (see Shoupp, W. E.)—1118(A)
Gamow, G. Evolution of red giants—796(L)
——. Physical possibilities of stellar evolution—718
—— **and E. Teller.** Energy production in red giants—791(L)
—— **and E. Teller.** On the origin of great nebulae—654
Garth, Robert C. (see Moore, George E.)—677(A)
——, **George E. Moore and Harold W. Webb.** Effect of pressure on the intensity of the recombination spectrum of mercury—677(A)
Gehman, S. D. and J. E. Field. X-ray investigation of crystallinity in rubber—594(A)
Gentner, W. and E. Segrè. Appendix on the calibration of the ionization chamber—814
Germer, L. H. Arrangement of atoms and molecules in extremely thin films—605(A)
—— **and K. H. Storks.** Rubbed films of barium stearate and stearic acid—648
Germeshausen, Kenneth J. New form of band igniter for mercury-pool tubes—228(L)
Gill, Piara S. Further study of cosmic rays on the Pacific Ocean—1111(A), 1151
—— Long period variations of cosmic rays—429
—— (see Compton, A. H.)—233(A)
—— (see Jesse, William P.)—414(L)
—— (see Schein, Marcel)—1111(A)
Gingrich, Newell S. Diffraction of x-rays of liquid sulphur at different temperatures—236(A)
—— **and C. N. Wall.** Structure of liquid potassium—1116(A)
Ginsburg, N. Intensities in the hydrogen secondary spectrum—1112(A)
Glasoe, G. N. (see Anderson, H. L.)—511(L)
—— (see Booth, E. T.)—982(L)
—— **and J. Steigman.** Fission products from uranium—982(L)
—— **and J. Steigman.** Radioactivity of the fission products from uranium bombarded with slow neutrons—1124(A)
Glathart, Justin L. Inner, initial, magnetic permeability of iron and nickel at ultra-high radiofrequencies—833
Glockler, George and J. H. Bachmann. Raman effect in difluorochloromethane—669(L)
—— **and J. H. Bachmann.** Raman effect in fluorochloromethane—1273(L)
Godart, O. On stability in the sense of Poisson for orbits of cosmic rays, and magnetic storms—875(L)
Goetz, Alexander. Possible use of superconductivity for radiometric purposes—1270(L)
Goldhaber, M. (see Collins, George B.)—507(L)
—— (see Waldman, B.)—1129(A)
——, **R. D. Hill, P. G. Kruger and F. W. Stallman.** Disintegration of boron by slow neutrons—1117(A)
——, **R. D. Hill and Leo Szilard.** Radioactivity induced by nuclear excitation. I. Excitation by neutrons—47
Goldsmith, H. H. (see Cohen, Victor W.)—106(L), 597(A)

—— (see Manley, J. H.)—39, 107(L), 1116(A)
—— (see Primakoff, H.)—1117(A)
——, **V. W. Cohen and J. R. Dunning.** Scattering of slow neutrons by uranium—1124(A)
Goodell, H. (see Hardy, J. D.)—1146(A)
Goodman, Clark (see Evans, R. D.)—931
Gorrill, Sterling. Cloud chamber studies of positive point-to-plane discharge in air at atmospheric pressure—1121(A)
Gottlieb, N. (see Hoag, J. Barton)—410(L)
Graaff, R. J. Van de. (see Trump, J. G.)—676(A)
Grabbe, E. M. (see McKeehan, L. W.)—505(L)
—— **and L. W. McKeehan.** Ferromagnetic anisotropy in nickel-iron alloys near Ni_3Fe—1142(A)
Graef, C. (see Vallarta, M. S.)—1
Graves, Alvin C. Packing fraction differences among the heavy elements—238(A), 863
Graves, Elizabeth R. (see Allison, Samuel K.)—107(L), 599(A)
Gray, J. A. γ-rays of radium E—586(L)
Green, Edward H. L_{III} absorption of iodine, barium and some compounds of barium—1072
Green, G. K. and Luis W. Alvarez. Heavily ionizing particles from uranium—417(L)
Green, J. B. and J. F. Eichelberger. Theory of the Paschen-back effect for intermediate coupling—1126(A)
—— **and J. A. Peoples, Jr.** Paschen-back effect in the spectrum of neon—1147(A)
Green, Louis C. New terms in Fe I, II, and III and additional far ultraviolet standards—1209
Grönblom, B. O. β-decay and spin of N^{18}—1130(A)
—— **and R. E. Marshak.** Binding energy of $4n$-nuclei on the α-particle model—229(L)
Gropper, Leon. Calculation of the second virial coefficient of helium gas for the lowest measured temperature—1095
Gross, B. Remark on the latitude effect of cosmic rays—112(L)
Grosse, Aristid V. Actinium series of radioactive elements and their influence on geological age measurements—584(L)
Gunn, Ross. Energy transformations in novae—591(A)
Guth, Eugene. On the statistical theory of rubber elasticity and related experiments—593(A)
—— Theory of electrodisintegration of beryllium—411(L)
—— (see Dart, F. E.)—1141(A)

Hafstad, L. R. (see Heydenburg, N. P.)—603(A)
—— (see Roberts, R. B.)—416(L), 664(L)
Haggstrom, E. (see Witcher, C.)—1135(A)
Hagstrum, Homer D. and John T. Tate. Heat of dissociation of carbon monoxide—1136(A)
Hale, Donald H. Townsend coefficients for ionization by collision in pure and contaminated hydrogen as a function of the cathode material—815, 1121(A)
Halford, R. S. (see Segrè, E.)—321(L)
Halpern, J. (see Crane, H. R.)—838
—— **and H. R. Crane.** Absorption coefficient of 5.8-Mev gamma-radiation in aluminum—258
—— **and H. R. Crane.** Experiments on the $F+H^1$ gamma-radiation and the Klein-Nishina absorption coefficient at 5.7 Mev—236(A)
—— **and H. R. Crane.** Further experiments on the recoil of the nucleus in beta-disintegration—1123(A)
—— **and H. R. Crane.** Gamma-rays from B+D—415(L)
—— **and H. R. Crane.** Fair internal conversion coefficient in the F+H reaction and measurements on the gamma-ray spectrum—260
Halpern, Otto. Remarks on the anomalous damping of ultrasonic waves—881(L)
—— (see Doermann, F. W.)—486
—— **and F. W. Doermann.** Determination of the nature of a light source from wide-angle interference experiments—681(A)
—— **and F. W. Doermann.** New proof of the H theorem—1077
——, **M. Hamermesh and M. H. Johnson.** On neutron scattering in crystals and alloys—1125(A)
—— **and Th. Holstein.** On depolarization of neutrons passing through ferromagnetic media—601(A)
—— **and M. H. Johnson.** On the magnetic scattering of neutrons—898
Ham, W. R. Diffusion of hydrogen through oxygen free copper—1137(A)
—— (see Simons, J. H.)—1137(A)
Hamermesh, Morton. (see Halpern, Otto)—1125(A)
—— **and Julian Schwinger.** Scattering of neutrons by hydrogen and deuterium molecules—679(A)
Hamilton, Donald R. and Nicholas A. Renzetti. Electric quadrupole moment of In^{115}—680(A)
Haney, Herschel H. (see Cleveland, Forrest F.)—1146(A)
Hanstein, H. B. (see Anderson, H. L.)—797(L)
Hardy, J. D. and A. I. Ryer. Recording infra-red spectrophotometer—1112(A)
——, **H. G. Wolff and H. Goodell.** Measurement of paid threshold and thermal radiation—1146(A)
Harkins, William D. (see Boyd, Edward)—1131(A)
—— (see Boyd, George)—237(A)
—— (see Florence, Robert T.)—237(A)
—— **and Richard W. Mattoon.** Effect of hydroxyl ion concentration (or of pH) on the film potentials of multilayers—320(L)
——, **H. W. Newson, R. J. Moon, A. H. Snell, L. A. Slotin, L. P. Borst, S. L. Simon, B. Carpenter and P. R. Bell.** University of Chicago cyclotron—1110(A)
Harrington, E. L. Viscosity of air—230(L)
Harris, W. T. Electron spectrograph—1135(A)
—— (see Barschall, H. H.)—989(L)
Harrison, G. R. (see Albertson, W. E.)—1119(A)
—— **and Francis Bitter.** Zeeman effect at fields of 100,000 gauss—1125(A)
Harrison, J. R. and I. P. Hooper. Striated luminous glow of the piezoelectric quartz resonator at flexural vibration frequencies—674(A)
Hartman, Paul L. (see Smith, Lloyd P.)—1145(A)
Harvey, G. G. X-ray diffraction by liquid ethyl alcohol—1115(A)
——. On alleged discontinuities in the diffuse scattering of x-rays from crystals at small angles—1147(A)
Harworth, K. (see Webster, D. L.)—682(A)
Haskins, C. P. (see Scott, G. W.)—1112(A)

Haworth, F. E. Apparatus for determining the orientation of crystals by x-rays—684(A)
Haxby, R. O. (see Hill, E. L.)—147
—— **and J. S. Allen.** Angular distribution of the α-particles from $B+H^1$—598(A)
——, **J. S. Allen and J. H. Williams.** Angular distribution of the disintegration products of light elements—140
Healea, Monica. Comparison of the secondary electron emission due to H_2^+ and D_2^+ ions—984(L)
Heaps, C. W. Magnetoresistance of nickel in large fields—1069
Hebb, M. H. Excitation of O^{++} by electron impact—1114(A)
—— (see Nordheim, L. W.)—1111(A)
Hector, L. G. and Mahlon F. Peck. Magnetic susceptibilities in weak fields—672(A)
Hegbar, H. R. (see Maxfield, F. A.)—592(A)
Hemmindinger, Arthur. Proton induced activity of manganese—604(A)
Hemmindinger, Henry. Lyman lines of hydrogen in solar emission—1119(A)
Henderson, Joseph E. and R. K. Dahlstrom. Energy distribution in field emission—473
Henderson, W. J. Energy of the β-rays from potassium—238(A)
—— (see King, L. D. P.)—1118(A)
——, **L. D. P. King and J. R. Risser.** Purdue cyclotron—1110(A)
Hennelly, E. F. (see Blewett, J. P.)—1138(A)
Herb, R. G. (see Plain, G. J.)—1135(A)
——, **D. W. Kerst, D. B. Parkinson and G. J. Plain.** Scattering of protons by protons—603(A), 998
Herman, R. C. (see Williams, V.)—684(A)
—— **and R. Hofstadter.** Further studies on the infra-red absorption spectra of the fatty acids—683(A)
Herring, Conyers. Compressibility of lithium—598(A)
—— (see Hill, A. G.)—1140(A)
—— **and A. G. Hill.** Theoretical constitution of metallic beryllium—673(A)
Herzog, G. Search for heavy cosmic-ray particles with a cloud chamber—1266(L)
Heydenburg, N. P., L. R. Hafstad and M. A. Tuve. Proton-proton scattering—603(A)
Hill, A. G. (see Herring, Conyers)—673(A)
—— **and Conyers Herring.** Excited electronic states and compressibility of metallic beryllium—1140(A)
——, **W. W. Buechner, J. S. Clark and J. B. Fisk.** Emission of secondary electrons under high energy positive ion bombardment—463
Hill, E. L. and R. O. Haxby. Note on the disintegration of boron by protons—147
Hill, J. E. Studies with the neutrons from p–n reactions in lithium and beryllium—1117(A)
—— **and G. E. Valley.** Study of radioactive Be^7—678(A)
Hill, R. D. (see Goldhaber, M.)—47, 1117(A)
Hippel, A. von. (see Buehl, R. C.)—1122(A)
—— (see Merrill, F. H.)—1122(A)
Hipple, John A., Jr. Spherical coil for a mass spectrometer—597(A)
Hirone, T. (see Okamura, T.)—102(L)
Hoag, J. Barton and N. Gottleib. Inner, initial permeability of iron and nickel from 98 to 410 megacycles—410(L)
Hofstadter, R. (see Herman, R. C.)—683(A)
—— (see Williams, V.)—684(A)
Hoisington, L. E. (see Breit, G.)—1103(L)
—— (see Share, S.)—1130(A)
Hollaender, Alexander (see Brackett, F. S.)—1120(A)
—— **and Peter A. Cole.** Absorption and fluorescence spectra in relation to the photolethal action of methylcholanthrene on yeast—597(A)
Holmes, R. M. and H. W. Allen. Effect of hydrostatic pressure on the resistance of single crystal of selenium—593(A)
Holstein, Th. (see Halpern, O.)—601(A)
—— (see Primakoff, H.)—1218
Holzer, R. E. (see Workman, E. J.)—598(A), 606(A)
Hooper, I. P. (see Harrison, J. R.)—674(A)
Hopkins, J. I., W. M. Nielsen and L. W. Nordheim. Cloud-chamber analysis of barytron secondaries—233(A)
Hornbostel, J. (see Manley, J. H.)—1116(A)
—— **and F. A. Valente.** On the resonance levels for neutron capture of iodine and indium—108(L)
Horvath, W. J. (see Salant, E. O.)—111(L)
Horvay, Gabriel. Iteration method—604(A)
—— On the iteration method and its application to the oxygen problem—70
Houston, W. V. Conservation of momentum in electrical conductivity—420(A), 1255
—— Momentum of electrons in a metal crystal—1140(A)
—— (see Davis, L.)—1143(A)
Howey, J. H. Noncubic growth of single crystals of silver by condensation from vapor—578
Hoyt, F. C. Determination of force fields from scattering in the classical theory—664(L)
Hudson, G. G. Offset and breakdown potentials in point-to-plane corona discharge in air as a function of pressure up to 30 atmospheres—1122(A)
Hudspeth, Emmett and Henry Dunlap. Low energy neutrons from the deuteron-deuteron reaction—587(L)
Hughes, A. L. Scattering of fast electrons in gases—350
—— **and Merle A. Starr.** Atomic electron velocities in nitrogen and methane—343
Hughes, J. M. and E. A. Coomes. Electrolytic " polishing " of tungsten—1138(A)
Hulburt, E. O. E region of the ionosphere—639
—— E region of the ionosphere during the total solar eclipse of October 1, 1940—646
—— (see Dawson, L. H.)—1128(A)
Hull, A. W. Dispenser cathode, a new type of thermionic cathode for gaseous discharge tubes—1145(A)
Humphreys, Richard F. Separation of bromine isotopes by centrifugation—674(A)
Hutner, R. Albagli. New periodic orbit in the field of a magnetic dipole—109(L)
—— On the penumbra of cosmic radiation—15
—— Penumbra at geomagnetic latitude 20° and the energy spectrum of primary cosmic radiation—614

Huxford, W. S. Townsend ionization coefficients in Cs-Ag-O photo-tubes filled with argon—754
——, **S. G. Eskin and R. W. Jones.** Autoelectronic emission in metal arcs—1146(A)

Ichimiya, T. (see Nichina, Y.)—585(L)
Ingersoll, L. R., Philip Rudnick and F. G. Slack. Optical and magneto-optical activity of nickel sulfate, α-hexahydrate, in the short infra-red spectrum—672(A)
Inglis, D. R. Angle dependence and range of nuclear forces—988(L)
—— On interpreting related magnetic moments of light nuclei—329
—— (see Brown, Harrison)—1182
Irvine, John W., Jr. Concentrating the uranium isotope of twenty-three-minute half-life—1105(L)

Jacobs, R. B. (see Starr, C.)—684(A)
James, Hubert M. and Albert Sprague Coolidge. Continuous spectra of H_2 and D_2—184, 234(A)
—— **and A. S. Coolidge.** Symmetry properties of variational functions—873
Jauch, J. M. Groups of quantum-mechanical contact-transformations and the degeneracy of energy-levels—1132(A)
Jauncey, G. E. M. Possibility of the internal scattering of the beta-rays from RaE—237(A)
—— (see McNatt, E. M.)—237(A)
—— **and E. M. McNatt.** Thermal vibrations and atomic structure of zinc crystals at 100° and 298°K—498
Jenkins, F. A. and E. Segrè. Quadratic Zeeman effect—52, 420(A)
—— **and E. Segrè.** Zeeman effect of the forbidden lines of potassium—545
Jesse, William P. and Piara S. Gill. Latitude effect for very large cosmic-ray bursts—414(L)
Johnson, M. H. (see Halpern, O.)—898, 1125(A)
Johnson, R. P. Decay of willemite and zinc sulphide phosphors—881(L)
—— (see Nelson, R. B.)—592(A)
Johnson, Thomas H. New Evidence on the nature of the primary cosmic radiation—1111(A)
—— (see Korff, S. A.)—600(A)
—— (see Pomerantz, Martin A.)—1111(A)
—— **and J. G. Barry.** East-west asymmetry of the cosmic radiation at very high elevations near the equator—503(L)
—— **and Martin A. Pomerantz.** Difference in the absorption of cosmic rays in air and water and the instability of the barytron—104(L)
—— **and M. A. Pomerantz.** Difference in the absorption of cosmic rays in air and water and the mean life of the barytron—600(A)
Jones, R. Clark (see Furry, W. H.)—1083, 1137(A)
Jones, R. W. (see Huxford, W. S.)—1146(A)

Kalbfell, D. C. Measurement of γ-ray energies—422(A)
Kane, Brother Gabriel. Equation of state of the frozen rare gases—1138(A)
Kanner, M. H. (see Barschall, H. H.)—989(L)
Kaplan, Joseph. Comment on a paper by W. E. Bowls, "Second Townsend Coefficient"—111(L)
—— Dellinger phenomenon—110(L)
—— Excitation of the new nitrogen line—598(A)
—— New nitrogen afterglow spectrum—606(A)
—— NH bands in the night sky spectrum—583(L)
Kaufmann, A. R. Approach to saturation of iron and nickel—1142(A)
—— (see Bitter, F.)—1142(A)
Kean, C. H. Pressure-temperature phase diagram of Na-K alloys and the effect of pressure on the resistance of the liquid phase—750
Keevil, N. B. (see Evans, R. D.)—931
Keller, J. M. Note on reduction for the rotation group—508(L)
Kellogg, J. M. B. (see Rabi, I. I.)—595(A)
——, **I. I. Rabi, N. F. Ramsey, Jr. and J. R. Zacharias.** Electrical quadrupole moment of the deuteron—318(L)
——, **I. I. Rabi, N. F. Ramsey, Jr. and J. R. Zacharias.** Magnetic moments of the proton and the deuteron—595(A)
Kemble, Edwin C. Thermal equilibrium and microscopic entropy—602(A)
Kennard, E. H. Shape of the domains in ferromagnetics—312
Kennedy, J. W. (see Seaborg, G. T.)—410(L), 794(L)
—— **and G. T. Seaborg.** Search for beta-particles emitted during uranium fission process—877(L)
Kent, R. H. Propagation of electric currents in terminated lines. Solutions of the telegraphic equation—762
Kerst, D. W. (see Herb, R. G.)—603(A), 998
Kikuchi, Seishi and Hiroo Aoki. Scattering of the D−D neutrons—108(L)
——, **Hiroo Aoki and Tetuo Wakatuki.** On the angular distribution of the fast neutrons scattered by atoms—1264(L)
King, G. W. and J. H. Van Vleck. Dipole-dipole resonance forces—1165
—— **and J. H. Van Vleck.** Relative intensities of singlet-singlet and singlet-triplet transitions—1120(A)
King, L. D. P. (see Henderson, W. J.)—1110(A)
——, **W. J. Henderson and J. R. Risser.** Production of artificial radioactivity by α-particles—1118(A)
King, Ronold. Variable oscillator for ultra-high frequency measurements—1127(A)
Kinzer, G. D. (see Almy, G. M.)—238(A)
Kip, Arthur F. Negative point-to-plane corona studies—1122(A)
—— Onset studies of positive point-to-plane corona in air atmospheric pressure—549
—— Positive point-to-plane corona onset studies—422(A)
Kirby-Smith, J. S. and L. G. Bonner. Raman spectra of gaseous amines—1114(A)
Kirkpatrick, Paul. (see Webster. D. L.)—682(A)
Kittel, Charles. Radioactivity of Li^8—515
Knipp, Julian K. On the calculation of polarizabilities and Van der Waals forces for atoms in S-states—1244
—— Van der Waals forces in the boron molecule—601(A)
Konopinsky, E. J. On the excitation functions of intermediate elements—235(A)

Koppius, O. G. (see Duffendack, O. S.)—1199
Korff, S. A. and W. E. Danforth. Comparison of counter and electroscope measurements in the stratosphere—675(A)
—— **and W. E. Danforth.** Neutron measurements with boron-trifluoride counters—980(L)
—— **and T. H. Johnson.** Absence of solar component of cosmic radiation at high elevations—600(A)
Krause, Ernst H. Sensitized fluorescence of potassium—164
Kruger, P. Gerald. (see Goldhaber, M.)—1117(A)
—— (see Shoupp, W. E.)—1118(A)
—— **and L. W. Phillips.** Sodium-like spectra of potassium, calcium and scandium—352
——, **F. W. Stallmann and W. E. Shoupp.** Nuclear energy levels in B^{10}—1129(A)
Kuerti, G. (see Wilkins, T. R.)—1134(A)
Kuper, J. B. H. and F. S. Brackett. Integrating meters for ultraviolet radiation—1128(A)
Kurie, Franz N. D. Technique of high intensity bombardment with fast particles—241(A)
Kusaka, S. (see Christy, R. F.)—665(L)
—— (see Vallarta, M. S.)—1
Kusch, P. (see Millman, S.)—596(A)
—— (see Rabi, I. I.)—526
—— **and F. W. Loomis.** Magnetic rotation spectra of SO_2 and CS_2 in the ultraviolet—850
—— **and S. Millman.** Determination of the nuclear magnetic moment of caesium by the molecular beam magnetic resonance method—596(A)
—— **and S. Millman.** On the nuclear moments of the rubidium and chlorine isotopes—680(A)
——, **S. Millman and I. I. Rabi.** On the nuclear magnetic moment of beryllium—666(L)
——, **S. Millman and I. I. Rabi.** Nuclear magnetic moments of N^{14}, Na^{23}, K^{39} and Cs^{133}—1176

Lagemann, R. T. (see Whitcomb, S. E.)—181
Lamar, Edward S. (see Stone, Albert M.)—1145(A)
——, **Albert M. Stone and Karl T. Compton.** The positive column of the nitrogen arc at atmospheric pressure—1235
Lamb, Willis E., Jr. Capture of neutrons by atoms in a crystal—190, 234(A)
—— (see Wheeler, John A.)—858
Lanczos, C. and G. C. Danielson. Application of trigonometric interpolation to x-ray analysis—242(A)
Landé, Alfred. Born's reciprocity and Mie's theory of field and matter—1132(A)
Landshoff, Rolf. Influence of chemical binding and crystal structure on x-ray absorption edges—631
—— Kinetic energy of the electrons in the Wigner-Seitz theory—603(A)
Lane, A. C. (see Evans, R. D.)—931
Langer, Lawrence M., Allan C. G. Mitchell and P. W. McDaniel. Coincidences between beta-rays and gamma-rays in indium and manganese—1123(A)
Langer, R. M. Abundance of interstellar atoms and ions—423(A)
Langmuir, D. B. (see Malter, L.)—743
—— **and L. Malter.** Rate of evaporation of tantalum—748
—— **and L. Malter.** Specific heat, heat of sublimation, and vapor pressure constant of tantalum—1138(A)
Langsdorf, Alexander, Jr. Continuously sensitive diffusion cloud chamber—421(A)
Lark-Horovitz, K. and C. H. Ehrhardt. X-ray atom factors for the Zn in ZnO—605(A)
——, **J. R. Risser and R. N. Smith.** Nuclear excitation of indium with alpha-particles—878(L)
Lauritsen, C. C. (see Gaerttner, E. R.)—27
—— (see McLean, W. B.)—796(L)
Lawson, A. W. and Richard Scheib. Variation of the adiabatic elastic constants of polycrystalline ammonium chloride with temperature between 200°K and 273°K—1268(L)
Lawson, J. L. Beta-ray spectra of radioactive phosphorus sodium and cobalt—1136(A)
—— (see Cork, J. M.)—1136(A)
—— **and A. W. Tyler.** Precision current control device—238(A)
Lee, D. D. (see Libby, W. F.)—245
—— **and W. F. Libby.** Beta-rays of mesothorium 1 and radium D—252
Leitzke, Victor A. (see Winans, J. Gibson)—242(A), 1126(A)
Lewis, Margaret N. and John U. White. Band spectrum of HS—894
Libby, W. F. Stability of uranium and thorium for natural fission—1269(L)
—— (see DeVault, Don C.)—322(L)
—— (see Lee, D. D.)—252
—— **and D. D. Lee.** Energies of the soft beta-radiations of rubidium and other bodies. Method for their determination—245
—— **and Earl A. Long.** Scattering of slow neutrons by gaseous ortho- and parahydrogen: spin dependence of the neutron-proton force—339
Liebhafsky, H. A. (see Blewett, J. P.)—1138(A)
Lifschutz, Harold and O. S. Duffendack. Advantages of scaling circuits in recording random counts—412(L)
—— **and O. S. Duffendack.** Experimental test of the statistical theory of scaling circuits—1133(A)
Linke, F. W. (see Masket, A. Victor)—674(A)
Livingood, J. J. (see Seaborg, G. T.)—794(L)
—— **and G. T. Seaborg.** Long-lived radioactive Fe^{55}—1268(L)
—— **and G. T. Seaborg.** New periods of radioactive tin—667(L)
—— **and G. T. Seaborg.** Radioactive antimony from I+n and Sn+D—414(L)
—— **and G. T. Seaborg.** Radioactive isotopes of zinc—457
Livingston, Stanley M., John H. Buck and Robley D. Evans. Massachusetts Institute of Technology cyclotron—1110(A)
Locher, Gordon L. Design and construction of reliable Geiger-Müller counters—675(A)
Loeb, Leonard B. Definition of the sparking potential—1121(A)
Logan, Hugh L. Determination of quenching rates in an aluminum alloy of the duralumin type—1139(A)

London, F. State of liquid helium below the λ point and the Bose-Einstein condensation—235(A)
Long, Earl A. (see Libby, W. F.)—339
Long, L. E. (see Ramsey, R. R.)—239(A)
Loomis, F. W. (see Kusch, P.)—850
Lowen, Irving S. Retarded interaction between electrons 601(A)
Ludeke, Carl A. On the interchange energy of two free electrons—315(L)
Ludloff, H. On thermal and stress dependence of elasticity in solids—681(A)
—— Ultrasonic method for the determination of elastic properties of solids—593(A)
Luyet, Basile J. Devitrification temperatures of aqueous solutions—1132(A)
Lyman, Ernest M. β-Ray spectrum of N^{13} and the mass of the neutrino—234(A)
—— Evidence for the composite character of the N^{13} β-ray spectrum—1123(A)
Lyman, Elisabeth Reed. Energy distribution of OH molecules in sensitized fluorescence—1126(A)

Mack, J. E. (see Roberson, J. H.)—1126(A)
MacNair, D. (see Nix, Foster C.)—605(A)
Malter, L. (see Langmuir, D. B.)—748, 1138(A)
—— **and D. B. Langmuir.** Resistance, emissivities and melting point of tantalum—743
Manley, J. H., H. H. Goldsmith and Julian Schwinger. Resonance absorption of slow neutrons in indium—107(L)
——, **H. H. Goldsmith, and Julian Schwinger.** Widths of nuclear energy levels—39
——, **J. Hornbostel and H. H. Goldsmith.** Mutual absorption of the Rh and In levels—1116(A)
Manning, Millard F. Electronic structure of alloys—682(A)
Margenau, Henry. Binding energy of He^4 and nuclear forces—678(A), 1173
—— Van der Waals forces in helium—1137(A)
—— (see Tyrell, W. A.)—790(L)
Marinelli, L. Portable gamma-ray detector—677(A)
—— (see White, T. N.)—676(A)
Marshak, R. E. (see Grönblom, B. O.)—229(L)
—— **and H. A. Bethe.** Temperature in white dwarf stars—681(A)
Marton, L. Field measurements and possible correction of aberrations for magnetic electron lenses—672(A)
Martyn, D. F. Concerning the nature of radio fade-out—983(L)
Masket, A. Victor, F. W. Linke and J. W. Beams. Ultracentrifuge for liquids—674(A)
Mason, W. P. Dynamic measurement of the elastic, electric and piezoelectric constants of rochelle salt—775, 1141(A)
Mattoon, Richard W. (see Harkins, William D.)—320(L)
Maxfield, F. A., H. R. Hegbar and J. R. Eaton. Possible cause of the glow to arc transition—592(A)
Maxwell, Louis R. Device for compounding sine functions—1135(A)
—— **and Vernon M. Mosley.** Internuclear distances in the gas molecules Se_2, $HgCl$, Cu_2Cl_2, Cu_2Br_2 and Cu_2I_2 by electron diffraction—238(A)
McCreary, Ralph (see Ewing, Douglas)—1136(A)
McCreary, R. L. (see Valley, G. E.)—666(L)
McDaniel, P. W. (see Langer, Lawrence M.)—1123(A)
McFadden, T. Ionization of mercury—797(L)
McKeehan, L. W. (see Grabbe, E. M.)—1142(A)
—— **and E. M. Grabbe.** Ferromagnetic anisotropy in nickel-iron crystals. Evidence for super-structure near Ni_3Fe—505(L)
McLean, W. B., R. A. Becker, W. A. Fowler and C. C. Lauritsen. Short range alpha-particles from $F^{19}+H^1$—796(L)
McMillen, Edwin. Radioactive recoils from uranium activated by neutrons—510(L)
McNatt, E. M. (see Baltzer, O. J.)—237(A)
—— (see Jauncey, G. E. M.)—498
—— **and G. E. M. Jauncey.** Atomic structure factors for zinc crystals at large scattering angles—237(A)
Meek, J. M. Mechanism of the lightning discharge—972, 1122(A)
Melvin, Eugene H. (see Wulf, Oliver R.)—600(A), 687
Merideth, George T. (see Broxon, James W.)—883
Merrill, F. H. and A. von Hippel. Atomphysical interpretation of " lichtenberg figures " and their application for studying electric discharge phenomena—1122(A)
Merrill, Harrison J. and Harold W. Webb. Electron scattering and plasma oscillations—1191
—— **and Harold W. Webb.** Plasma oscillations and scattering in low pressure discharges—597(A)
Metropolis, Nicholas. New ultraviolet band system of silver iodide—239(A), 636
—— **and H. Beutler.** Additional band systems of silver halide vapors and a new thermodynamical calculation of their dissociation energies—1113(A)
Meyer, R. C. (see Roberts, R. B.)—416(L), 510(L), 664(L)
Millikan, Robert A. Mesotron as the name of a new particle—105(L)
—— **and H. V. Neher.** Incoming cosmic-ray energies as function of latitude more accurately determined—599(A)
Millman, S. On the determination of the signs of nuclear magnetic moments by the molecular beam method of magnetic resonance—628
—— (see Kusch, P.)—596(A), 666(L), 680(A), 1176
—— (see Rabi, I. I.)—526
—— **and P. Kusch.** Nuclear magnetic moments of Na^{23} and K^{39}—596(A)
Mimno, H. R. (see Pierce, J. A.)—1128(A)
Mitchell, Allan C. G. (see Langer, Lawrence M.)—1123(A)
Miyahara, Syohei. Ferromagnetism of semi-conductors—105(L)
Montgomery, C. G. and D. D. Montgomery. Origin of the rays which produce the bursts of cosmic-ray ionization—676(A)
——, **W. E. Ramsey, D. B. Cowie and D. D. Montgomery.** Occurrence of slow mesotrons—1117(A)
Montgomery, D. D. (see Montgomery, C. G.)—676(A), 1117(A)
Moon, R. J. (see Harkins, W. D.)—1110(A)
Mooney, Robert L. Self-consistent field for doubly ionized chromium—557, 598(A)

Moore, Charlotte E. Arc spectrum of vanadium in the violet—710
Moore, George E. (see Garth, Robert C.)—677(A)
——, **Robert C. Garth and Harold W. Webb.** Spectral distribution of energy in the recombination spectrum of mercury—677(A)
Moore, William H. (see Brady, James J.)—308, 424(A)
Morgan, J. E. (see Nielsen, W. M.)—995
Morgan, K. Z. (see Nielsen, W. M.)—995
Morrison, P. (see Dancoff, S. M.)—122, 423(A)
Morton, G. A. (see Ramberg, E. G.)—409(L)
Mosley, Vernon M. (see Maxwell, Louis R.)—238(A)
Mouzon, J. C., R. D. Park and J. A. Richards, Jr. Gamma-rays from uranium activated by neutrons—668(L)
Mrozowski, S. Structure of the Be I line λ 4573A—798(L)
Mueller, Hans. Electro-optical effects in colloids—508(L)
—— Electro-optical effects in bentonite colloids—792(L)
Mulliken, Robert S. Absolute intensities in halide spectra—239(A)
Munier, J. H. High vacuum x-ray spectrometer—1116(A)
Murphy, Edgar J. (see Whitaker, Martin D.)—793(L)
Murray, M. J. (see Cleveland, Forrest F.)—600(A), 1113(A), 1146(A)
Murray, R. T. K. (see Alter, B. E. K.)—672(A)
Murrell, T. A. (see Roebuck, J. R.)—240(A)

Nadig, Francis H. (see Bohn, J. Lloyd)—685(A)
Neher, H. V. (see Millikan, R. A.)—599(A)
Nelson, Herbert. Phenomenon of secondary-electron emission—985(L)
Nelson, R. B. and R. P. Johnson. Decay of phosphorescence after electron bombardment—592(A)
Newson, H. W. (see Harkins, W. D.)—1110(A)
Nichols, Myron H. Thermionic constants of tungsten for various crystallographic directions—1144(A)
Nielsen, Harald H. Interaction between rotation and oscillation in deutero-formaldehyde—289
—— (see Shaffer, W. H.)—878(L), 1130(A)
Nielsen, W. M. Rossi transition curve for small angle showers—675(A)
—— (see Hopkins, J. I.)—233(A)
——, **J. E. Morgan and K. Z. Morgan.** Rossi transition curve for small angle showers—995
Nier, Alfred O. Isotopic constitution of uranium and the half-lives of the uranium isotopes, I—150
—— Isotopic constitution of radiogenic leads and the measurement of geological time, II—153
—— Isotopic constitution of iron and chromium—1143(A)
Nishina, Y., M. Takeuchi and T. Ichimiya. On the mass of the mesotron—585(L)
Nix, Foster C. Vacuum interferometric dilatometer with photographic recording for measuring thermal expansion of metals and alloys at elevated temperatures—606(A)
—— (see Steigman, J.)—605(A)
—— **and D. MacNair.** Elatometric study of the order-disorder process in single crystals of copper-gold alloys—605(A)
Nordheim, L. W. Lifetime of the Yukawa particle—506(L)
—— (see Hopkins, J. I.)—233(A)
—— **and M. H. Hebb.** On the production of hard component of the cosmic radiation within the atmosphere—1111(A)
Northrup, D. L. (see Van Atta, L. C.)—681(A)
Norton, Francis J. Influence of frequency on the electro-optical effect in colloids—668(L)
Nottingham, W. B. Ionization and excitation in mercury vapor produced by electron bombardment—203
—— New circuit for accurate control of current-intensity and time used in spot-welding—1144(A)
Nusbaum, C. Particle size determination with side-reflection x-ray cassette—1115(A)

O'Brien, Brian. Formation and properties of unsupported flowing liquid films—674(A)
—— Refinements in atmospheric transmission measurement for solar constant determination—1142(A)
—— (see Stewart, Harold S., Jr.)—1121(A)
O'Bryan, H. M. (see Skinner, H. W. B.)—604(A)
O'Callahan, Joseph T., S.J. Difference in scope of theoretical physics and pure mathematics—683(A)
O'Connor, J. S. (see Witcher, C.)—1135(A)
Okamura, T. and T. Hirone. On the change of magnetic properties of the single crystal of nickel due to temperature—102(L)
Oleson, N. L. (see Crane, H. R.)—1110(A)
Olsen, Leonard O. Quenching and depolarization of mercury resonance radiation by foreign gases—1126(A)
Onsager, L. Separation of gas (isotope) mixtures by irreversible processes—1136(A)
—— (see Furry, W. H.)—1083, 1137(A)
Oppenheimer, J. R. and G. M. Volkoff. On massive neutron cores—374
Overbeck, C. J. and E. Wiler. Effect of temperature on supersonic velocity in CO_2—1127(A)
Owens, Ralph G. and E. F. Barker. Infra-red absorption spectrum of methylamine—1119(A)

Packer, Donald M. Optical and photoelectric properties of potassium at liquid-air temperatures—1121(A)
Page, Chester H. Modification of special relativity—1131(A)
Park, R. D. (see Mouzon, J. C.)—668(L)
Parkinson, D. B. (see Herb, R. G.)—603(A), 998
Parratt, L. G. and C. A. Randall. *Lα* satellites for elements $41 < Z < 57$—1114(A)
Pasternack, Simon. Fine structure of Hα and Dα—421(A)
Patterson, A. L. Uniqueness of an x-ray crystal analysis—682(A)
Peck, Edson R. (see Fisher, Russell A.)—270
Peck, Mahlon F. (see Hector, L. G.)—672(A)
Peoples, J. A. (see Green, J. B.)—1147(A)
Pepinsky, Raymond. Crystal struction of $LiOH \cdot H_2O$—1115(A)
Perry, Tom (see Ewing, Douglas)—1136(A)
Phillips, L. W. Supplementary identifications in the spectra of K, Ca, Sc and Ti—708
—— (see Kruger, P. Gerald)—352
Pielemeier, W. H. and D. Telfair. Supersonics and the effect of water vapor on molecular vibrations in CO_2—1127(A)

Pierce, J. A. and H. R. Mimno. Apparent motion of clouds of abnormal *E* region ionization—1128(A)
Pietenpol, W. B. (see Westerfield, Everett C.)—306
Pigg, E. G. (see Fountain, C. R.)—592(A)
Pitzer, Kenneth S. (see Alvarez, Luis W.)—596(A)
Placzek, G. Slowing down of neutrons by heavy nuclei—1130(A)
Plain, G. J. (see Herb, R. G.)—603(A), 998
——, **R. G. Herb and R. E. Warren.** Gamma-rays from aluminum due to proton bombardment—1135(A)
Plyler, E. K. (see Cleaves, A. P.)—1113(A)
Pockman, L. T. (see Webster, D. L.)—682(A)
Pollard, W. G. Repulsive forces in van der Waals adsorption—1137(A)
—— Use of surface states in solids to explain activated adsorption—1147(A)
Pollock, H. C. and F. S. Cooper. Effect of gas pressure on the point-to-plane discharge in several gases—593(A)
Polye, William R. (see Collins, George B.)—412(L), 1123(A)
Pomerantz, Martin A. (see Johnson, Thomas H.)—104(L), 600(A)
—— **and Thomas H. Johnson.** Contribution to the soft compónent of cosmic radiation by the disintegration of mesotrons—1111(A)
Poritsky, H. (see Suits, C. G.)—1184
Preston, William M. Adsorption coefficient of gases for light of wave-length 1215.7A—1125(A)
Primakoff, H. and H. H. Goldsmith. On the relation between neutron-alpha and alpha-proton scattering—1117(A)
—— **and T. Holstein.** Many-body interactions in atomic and nuclear systems—1218

Quinn, Robert B. Sparking potentials at low pressure—240(A)
—— Sparking potentials at low pressures—482

Rabi, I. I. (see Kellogg, J. M. B.)—318(L), 595(A)
—— (see Kusch, P.)—666(L), 1176
——, **S. Millman, P. Kusch and J. R. Zacharias.** Molecular beam resonance method for measuring nuclear magnetic moments. Magnetic moments of $_3Li^6$, $_3Li^7$ and $_9F^{19}$—526
——, **J. R. Zacharias, N. F. Ramsey, Jr. and J. M. B. Kellogg.** Magnetic resonance experiments on H_2 and D_2 molecules—595(A)
Radle, W. F. (see Beck, C. A.)—1120(A)
Raines, Barbara G. Accommodation coefficient of helium *vs.* nickel—684(A)
Ramberg, E. G. and G. A. Morton. Variation of light output with current density and classification of willemite phosphors—409(L)
Ramsey, N. F., Jr. Rotational magnetic moment measurements on H_2 and D_2—595(A)
—— (see Kellogg, J. M. B.)—318(L), 595(A)
—— (see Rabi, I. I.)—595(A)
Ramsey, R. R., W. L. Chenault and L. E. Long. Oscillation of close-coupled circuits—239(A)
Ramsey, W. E. (see Montgomery, C. G.)—1117(A)
—— (see Swann, W. F. G.)—599(A)
Randall, C. A. (see Parratt, L. G.)—1114(A)
Randall, H. M. (see Fuson, N.)—590(A)
Randall, R. H., F. C. Rose and C. Zener. Dependence of internal friction in metals on grain size—1140(A)
Renzetti, Nicholas A. (see Hamilton, Donald R.)—680(A)
Ribner, H. S. Anomalies in the directional intensity distribution of cosmic rays—1271(L)
Richards, J. A., Jr. (see Mouzon, J. C.)—668(L)
Richardson, J. Reginald. *K*-electron capture in Ag^{106}—236(A)
—— Radiations from radioactive substances Au^{196}, Eu^{152}, Ag^{106}, Cu^{64} and N^{13}—609
—— Search for excited state of C^{13}—1129(A)
Richtmyer, F. K. (see Shrader, R. E.)—605(A)
Ridenour, L. N. (see Delsasso, L. A.)—113
Risser, J. R. (see Henderson, W. J.)—1110(A)
—— (see King, L. D. P.)—1118(A)
—— (see Lark-Horovitz, K.)—878(L)
Roberson, J. H. and J. E. Mack. Analysis of a queer Zeeman effect pattern in tungsten—1126(A)
Roberts, R. B. (see Salant, E. O.)—984(L)
—— **and P. Wang.** Transmission of medium fast neutrons—596(A)
——, **L. R. Hafstad, R. C. Meyer and P. Wang.** Delayed neutron emission which accompanies fission of uranium and thorium—664(L)
——, **R. C. Meyer and L. R. Hafstad.** Droplet fission of uranium and thorium nuclei—416(L)
——, **R. C. Meyer and P. Wang.** Further observations on the splitting of uranium and thorium—510(L)
Robinson, C. F. Fine structure of hydrogen isotopes—423(A)
Roebuck, J. R. and T. A. Murrell. Joule-Thomson effect in carbon dioxide—240(A)
Rogers, F. T., Jr. Note on the stopping power of hydrogen at very low energies—588(L)
—— **and Marguerite M. Rogers.** Independent determination of the binding energy of the deuteron—263
—— **and Marguerite M. Rogers.** New determination of the binding energy of the deuteron—106(L)
Rogers, Marguerite M. (see Rogers, F. T., Jr.)—106(L), 263
Rollin, B. V. Self-diffusion in copper—231(L)
Rose, Albert. Mechanical model for electron motion in a uniform magnetic field—1144(A)
Rose, F. C. (see Randall, R. H.)—1140(A)
Rose, M. E. and H. A. Bethe. Depolarization effects in the double scattering of electrons—601(A)
—— **and H. A. Bethe.** On the absence of polarization in electron scattering—277
Rosen, N. Field theory of elementary particles—94
—— General relativity theory and flat space—681(A)
Rosenberg, Paul. Collision cross sections of K atoms and K_2 molecules in gases—1267(L)
Roussinow, L. I. and A. A. Yusephovich. X-ray emission from the isomers of radioactive bromine—979(L)
Rudnick, Philip (see Ingersoll, L. R.)—672(A)
Rydbeck, Olof. Recording of critical frequencies of the ionosphere—1127(A)
Ryer, A. I. (see Hardy, J. D.)—1112(A)

Sabato, E. R. On Alfvén's hypothesis of a " cosmic cyclotron "—1272(L)
Sabine, George B. Reflectivities of evaporated metal films in the near and far ultraviolet—1064
Sachs, R. G. Nuclear spins and magnetic moments by the α-particle model—825, 1131(A)
Sagane, R. Radioactive isotopes of Cu, Zn, Ga and Ge—31
Salant, E. O., W. J. Horvath and H. I. Zagor. Absorption of slow neutrons of different energies by B, Co and Mn—111(L)
——, **R. B. Roberts and P. Wang**—Interaction of fast neutrons with protons—984(L)
Sanders, F. H. Transmission of sound through plates at oblique incidence—1127(A)
Saxton, Harold L. Theory of secondary peak for sound absorption in CO_2—1127(A)
Scheib, Richard (see Lawson, A. W.)—1268(L)
Schein, Marcel and Piara S. Gill. Cosmic-ray bursts in great thicknesses of lead—1111(A)
—— **and Volney C. Wilson.** Production of penetrating cosmic-ray particles by photons—233(A)
Schiff, L. I. On the paths of ions in the cyclotron—422(A)
—— (see Snyder, H.)—421(A)
—— **and H. Snyder.** Theory of the quadratic Zeeman effect—59
Schwinger, Julian. On the neutron-proton interaction—235(A)
—— (see Cohen, Victor W.)—106(L)
—— (see Hamermesh, Morton)—679(A)
—— (see Manley, J. H.)—39, 107(L)
Scott, G. W., Jr. Focused beam source of hydrogen and helium ions—954
—— (see Smith, Lloyd P.)—946
—— **and C. P. Haskins.** Homogeneous source of protons for use in biological investigations—1112(A)
Scott, R. B. (see Brickwedde, F. G.)—672(A)
Seaborg, G. T. (see Kennedy, J. W.)—877(L)
—— (see Livingood, J. J.)—414(L), 457, 667(L), 1268(L)
—— (see Segrè, E.)—321(L)
—— **and J. W. Kennedy.** Nuclear isomerism and chemical separation of isomers in tellurium—410(L)
—— **and E. Segrè.** Nuclear isomerism in element 43—808
——, **J. J. Livingood and J. W. Kennedy.** Radioactive tellurium: Further production and separation of isomers—794(L)
Seely, S., W. H. Zinn and V. W. Cohen. Scattering of D–D neutrons—679(A)
Segrè, Emilio. Unsuccessful search for transuranic elements—1104(L)
—— (see Gentner, W.)—814
—— (see Jenkins, F. A.)—52, 420(A), 545
—— (see Seaborg, G. T.)—808
——, **S. Halford and G. T. Seaborg.** Chemical separation of nuclear isomers—321(L)
Shackelford, Julia (see Cleveland, Forrest F.)—1146(A)
Shaffer, W. H., H. H. Nielsen and L. H. Thomas. Vibration-rotation energies in the tetrahedrally symmetric XY_4 type of molecule—878(L)
——, **H. H. Nielsen and L. H. Thomas.** Vibration-rotation energies of tetrahedrally symmetrical molecules—1130(A)
Share, S. S. (see Breit, G.)—1103(L)
—— **L. E. Hoisington and G. Breit.** Exponential and meson potentials—1130(A)
Sherr, R. (see Delsasso, L. A.)—113
Sherwin, C. W. and A. J. Dempster. Doppler effect and field distribution in the Hailer canal-ray tube—582(L)
Shih, J. W. and Tsu-Yen Chai. Powder patterns on permalloy crystals—1265(L)
Shive, J. N. High frequency modulation of Geiger counters—1133(A)
Shockley, W. (see Steigman, J.)—605(A)
Shonka, Francis R. New evidence for the existence of penetrating neutral particles—24, 234(A)
Shoupp, W. E. (see Kruger, P. Gerald)—1129(A)
——, **P. Gerald Kruger, F. W. Stallmann and G. R. Gamertsfelder.** Scattering of neutrons by helium nuclei—1118(A)
Shrader, R. E. and F. K. Richtmyer. Excitation potential of L satellites—605(A)
Simon, Ralph (see Watson, William W.)—358, 677(A)
Simon, S. L. (see Harkins, W. D.)—1110(A)
Simons, J. H. and W. R. Ham. Diffusion of gases through metals from a chemical point of view—1137(A)
Simons, Lennart. Neutron-proton scattering cross section—792(L)
Sinma, K. and F. Yamasaki. β-radioactivities of rhenium—320(L)
Skaggs, Lester S. (see Allison, Samuel K.)—107(L), 599(A)
Skarstrom, C., H. E. Carr and J. W. Beams. Concentration of the chlorine isotopes by centrifuging—591(A)
Skinner, H. W. B. and H. M. O'Bryan. Soft x-ray emission spectra of valence electrons—604(A)
Sklar, A. L. Ultraviolet absorption of substituted benzenes—1120(A)
Skolil, Lester L. Dispersion of water for electromagnetic waves—880(L)
Skramstad, Harold K. Experimental method for measurement of shearing stresses in turbulent air flow—1141(A)
Slack, Charles M. (see Ehrke, Louis F.)—684(A)
Slack, F. G. (see Anderson, H. L.)—511(L)
—— (see Booth, E. T.)—876(L), 981(L), 1124(A), 1273(L)
—— (see Ingersoll, L. R.)—672(A)
Slepian, Joseph and W. M. Brubaker. Experiments on the condensation rate of mercury vapor—1147(A)
Slotin, L. A. (see Harkins, W. D.)—1110(A)
Smith, A. E. (see Beeck, Otto)—601(A)
—— **and Otto Beeck.** Preparation and structure of oriented metal films—602(A)
Smith, C. G. Limiting currents in a ring discharge—1144(A)
Smith, Lloyd P. and G. W. Scott, Jr. Conditions for producing intense ionic beams—946
—— **and Paul L. Hartman.** Electron and potential distributions near the anode of a mercury discharge—1145(A)
Smith, Nicholas M., Jr. (see Allison, Samuel K.)—107(L), 599(A)
Smith, R. N. (see Lark-Horovitz, K.)—878(L)

Smythe, W. R. Cosmic rays and radioactive potassium—316(L)
Snell, A. H. (see Harkins, W. D.)—1110(A)
Snoddy, L. B. (see Beams, J. W.)—504(L)
—— (see Dietrich, J. R.)—591(A)
—— **and J. W. Beams.** Discharges between a stationary and a moving electrode—1145(A)
—— **and J. W. Beams.** Progressive breakdown in a conducting liquid—879(L)
—— **and J. W. Beams.** Spark discharge on surfaces—663(L)
Snyder, H. (see Schiff, L. I.)—59
—— **and L. I. Schiff.** On the theory of the quadratic Zeeman effect—421(A)
Spencer, Raymond G. X-ray study of the changes produced in metals by fatiguing—242(A)
—— X-ray study of the changes that occur in malleable iron during the process of fatiguing—991
Spencer, Roy C. Correction of experimental curves for the resolving power of the apparatus—239(A)
Spitzer, Lyman, Jr. General solution for the equations of natural line breadth—361
—— Stark-effect broadening of hydrogen lines. I. Single encounters—699
Sponer, H. Absorption spectrum of heavy benzene at 2730–2250A—683(A)
—— (see Bonner, L. G.)—1113(A)
Stair, R. (see Coblentz, W. W.)—590(A)
Stallmann, F. W. (see Goldhaber, M.)—1117(A)
—— (see Kruger, P. Gerald)—1129(A)
—— (see Shoupp, W. E.)—1118(A)
Starr, C. and R. B. Jacobs. Thermal conductance of metallic contacts—684(A)
Starr, Merle A. (see Hughes, A. L.)—343
Staub, H. (see Stephens, W. E.)—235(A)
—— **and W. E. Stephens.** Anomalous scattering of neutrons by helium—131
—— **and W. E. Stephens.** Neutrons from the breakup of He^4—845
Stebbins, Dean W. (see Fox, Gerald W.)—405
Steigman, J. (see Glasoe, G. N.)—982(L), 1124(A)
——, **W. Shockley and F. C. Nix.** Measurement of the self-diffusion of copper—605(A)
Stephens, W. E. (see Staub, H.)—131, 845
—— **and H. Staub.** Resonance scattering of neutrons in helium—235(A)
Stewart, David W. Nuclear isomers in radioactive strontium—674(A)
Stewart, G. W. Apparent ionic volumes in aqueous solutions of strong electrolytes—240(A)
Stewart, Harold S., Jr. and Brian O'Brien. Properties of type II photronic cells affecting photometric measurement—1121(A)
Stewart, J. K. (see Colwell, R. C.)—595(A)
Stewart, John Q. and Forrest C. Eggleston. Prediction of the remaining course of the present sunspot cycle—1102(L)
Stockmann, L. L. (see Curtiss, L. F.)—600(A)
Stone; Albert M. (see Lamar, Edward S.)—1235
—— **Karl T. Compton and Edward S. Lamar.** Positive column of the nitrogen arc—1145(A)
Storks, K. H. (see Germer, L. H.)—648
Strain, Charles V. Competition between p–n and p–γ reactions—679(A)
Strong, John. Observations with a new radiation pyrometer—1114(A)
Stubblefield, Edward M. (see Collins, George B.)—507(L)
—— (see Waldman, B.)—1129(A)
Suits, C. G. Convection currents in arcs in air—198
—— High pressure arcs in common gases in free convection—561
—— **and H. Poritsky.** Application of heat transfer data to arc characteristics—1184
Swann, W. F. G. and W. E. Ramsey. Automatic apparatus for recording the history of shower phenomena primarily in relation to showers produced by penetrating cosmic rays—599(A)
Szilard, Leo (see Goldhaber, M.)—47
—— **and Walter H. Zinn.** Instantaneous emission of fast neutrons in the interaction of slow neutrons with uranium—799(L)

Takeuchi, M. (see Nishina, Y.)—585(L)
Tape, Gerald F. Beta-spectra associated with iodine—1135(A)
Tate, John T. (see Baker, Richard F.)—236(A)
—— (see Hagstrum, Homer D.)—1136(A)
Telfair, D. (see Pielemeier, W. H.)—1127(A)
Teller, E. (see Gamow, G.)—654, 791(L)
Thaxton, H. M. (see Breit, G.)—603(A), 1018, 1103(L)
Thomas, L. H. Paths of ions in the cyclotron—1110(A)
—— (see Shaffer, W. H.)—878(L), 1130(A)
Thompson, Julian L. Critical analysis for sidereal time variations of cosmic rays on the Pacific—11
—— Diurnal variations of cosmic rays on the Pacific Ocean—233(A)
Thornton, R. L. (see Corson, D. R.)—509(L)
Timoféeff-Ressovsky, N. W. (see Zimmer, K. G.)—411(L)
Tolman, Richard C. Static solutions of Einstein's field equations for spheres of fluid—364
Tonks, L. Lack of "sucking" action by the cathode blast of mercury vapor in a pool rectifier—674(A)
Trichel, G. W. Mechanism of the positive point-to-plane corona in air at atmospheric pressure—382
Trump, J. G. and R. J. Van de Graaff. Compact pressure-insulated electrostatic x-ray generator for cancer therapy—676(A)
—— **and R. J. Van de Graaff.** Compact pressure-insulated electrostatic x-ray generator—1160
Turner, A. Francis (see Cartwright, C. Hawley)—595(A), 675(A), 1128(A)
Turner, Louis A. Simple circuit of short resolving time for coincidences—1134(A)
—— (see Barschall, H. H.)—989(L)
Tuve, M. A. (see Heydenburg, N. P.)—603(A)
Tyler, A. W. Beta- and gamma-ray spectra of Cu^{64} and Eu^{152}—1136(A)
—— (see J. L. Lawson)—238(A)

Tyrrell, Warren A., Jr. Theoretical binding energy of He^4—678(A)
——, **K. G. Carroll and H. Margenau.** Binding energies of light nuclei—790(L)

Urry, W. D. (see Evans, R. D.)—931

Valente, F. A. (see Hornbostel, J.)—108(L)
Vallarta, M. S. Are there multiple charged primary particles in cosmic radiation?—583(L)
—— **and R. P. Feynman.** Scattering of cosmic rays by the stars of a galaxy—506(L)
——, **C. Graef and S. Kusaka.** Galactic rotation and the intensity of cosmic radiation at the geomagnetic equator—1
Valley, G. E. (see Hill, J. E.—678(A)
—— **and R. L. McCreary.** Interval conversion electrons from Br^{80}—666(L)
Van Allen, J. A. (see Ellett, A.)—1129(A)
Van Atta, L. C. and D. L. Northrup. Measurement of x-ray production in the range 0.8 to 2.0 million volts—681(A)
Van de Graaff, R. J. (see Trump, John G.)—676(A), 1160
Van Vleck, J. H. On the theory of paramagnetic relaxation—673(A)
—— On the theory of the forward scattering of neutrons by paramagnetic media—924
—— (see King, G. W.)—1120(A), 1165
—— (see Weiss, P. R.)—673(A)
Vargus, Joseph A., Jr. Multiple scattering of cosmic-ray particles in 1 cm of platinum—422(A)
Vitter, A. L. and L. C. Brieger. Velocity of radio waves in air—416(L)
Volkoff, G. M. On the equilibrium of massive neutron cores—421(A)
—— On the equilibrium of massive spheres—413(L)
—— (see Oppenheimer, J. R.)—374

Wait, G. R. Radioactive content of the atmosphere as affected by the presence of condensation nuclei—591(A)
Wakatuki, Tetuo (see Seishi, Kikuchi)—1264(L)
Waldman, Bernard (see Collins, George B.)—412(L), 507(L), 1122(A)
——, **G. B. Collins, E. M. Stubblefield and M. Goldhaber.** Nuclear excitation of indium by x-rays—1129(A)
Wall, C. N. (see Gingrich, N. S.)—1116(A)
Wang, P. (see Roberts, R. B.)—510(L), 596(A), 664(L)
—— (see Salant, E. O.)—984(L)
Warren, R. E. (see Plain, G. J.)—1135(A)
Wasastjerna, J. A. On the structure of solid solutions—986(L)
Watson, R. E. (see Bartlett, J. H.)—235(A)
Watson, W. W. and R. Simon. Spectra of SnH and PbH at high pressure—677(A)
—— **and Ralph Simon.** Spectrum of tin hydride at high pressure—358
Way, Katharine. Energy levels of H^3, He^3 and He^4—678(A)
—— Liquid-drop model and nuclear moments—963
Webb, Harold W. (see Garth, Robert C.)—677(A)
—— (see Merrill, Harrison J.)—597(A), 1191
—— (see Moore, George E.)—677(A)
Webb, Wayne. Study of beta-brass in single crystal form—297
Webster, D. L., L. T. Pockman, K. Harworth and Paul Kirkpatrick. Probability of K ionization of nickel by cathode rays—682(A)
Weinberg, Alvin M. Nerve conduction with distributed capacitance—240(A)
Weiss, P. R. and J. H. Van Vleck. Theory of ferromagnetism—673(A)
Weisskopf, V. F. On the electromagnetic field produced by an electron—1131(A)
—— On the self-energy of the electron—678(A)
—— **and D. H. Ewing.** On the penetration probability of fast protons into nuclei—241(A)
Weisz, Paul. Zenith angle distribution of the hard component of cosmic rays and the mass of the mesotron—1266(L)
Wells, W. H. Design and construction features of the Westinghouse electrostatic generator—599(A)
Welo, Lars A. and Oskar Baudisch. Some evidence for the existence of higher hydrates of gamma- and alpha-ferric oxide—1143(A)
Westerfield, E. C. Thermal dilatation of superconductors—319(L)
—— **and W. B. Pietenpol.** Viscosity in an expanding bubble—306
Wheeler, A. (see Beeck, Otto)—601(A)
Wheeler, John A. (see Bohr, N.)—1124(A)
—— **and Willis E. Lamb, Jr.** Influence of atomic electrons on radiation and pair production—858
Whitaker, Martin D. and Harold G. Beyer. Transmission of slow neutrons through crystals—1101(L)
—— **and Harold G. Beyer.** Experimental study of the additivity of slow neutron cross sections—1124(A)
——, **Charles A. Barton, William C. Bright and Edgar J. Murphy.** Cross sections of metallic uranium for slow neutrons—793(L)
Whitcomb, S. E. and R. T. Lagemann. Infra-red spectrum and molecular constants of carbon monoxide—181
White, John U. (see Lewis, Margaret N.)—894
White, M. G. (see Delsasso, L. A.)—113
—— (see Fox, J. G.)—1106(L)
White, T. N., L. Marinelli, and G. Failla. Measurement of gamma-radiation in roentgens—676(A)
Whitmer, R. M. and H. J. Yearian. Intensity anomalies in electron scattering from ZnO—1114(A)
Wiler, E. (see Overbeck, C. J.)—1127(A)
Wilkins, T. R. and G. Kuerti. Camera for the study of nuclear scattering—1134(A)
Williams, Dudley. Absorption of thiocyanates in the 4.8μ region—1120(A)
Williams, H. J. and R. M. Bozorth. Magnetic anisotropy of iron-nickel and copper-nickel alloys—673(A)
Williams, J. H. (see Haxby, R. O.)—140
Williams, V., R. C. Herman and R. Hofstadter. Infra-red absorption spectrum of phenol vapor—684(A)
Wilson, Thomas C. Photoconductivity of metal films—316(L)
—— Effect of high pressure upon the order-disorder transformation in Cu-Zn and Cu-Au alloys—1140(A)

Wilson, Volney C. Nature of the penetrating cosmic rays —6
—— On the nature of the penetrating cosmic rays—234(A)
—— (see Schein, Marcel)—233(A)
Winans, J. Gibson, Francis J. Davis and Victor A. Leitzke. Fluorescence, absorption and discharge in a mercury-thallium mixture—242(A)
——, **Francis J. Davis and Victor A. Leitzke.** Sensitized fluorescence of lead—1126(A)
Witcher, C., E. Haggstrom, J. S. O'Conor and J. R. Dunning. Electron lens type of β-ray spectrometer—1135(A)
Witmer, Enos E. Parameters more fundamental than the space-time coordinates—1132(A)
Wolff, H. G. (see Hardy, J. D.)—1146(A)
Wood, R. W. and G. H. Dieke. Band spectra of heavy nitrogen and the spectra of $N^{15}H$ and $N^{15}D$—1120(A)
Workman, E. J. and R. E. Holzer. Quantities of charge transfers in lightning discharges—598(A)
—— **and R. E. Holzer.** Recording generating voltmeter for lightning studies—606(A)
Wulf, Oliver H. and Eugene H. Melvin. Band spectra in nitrogen at atmospheric pressure. A source of band spectra excitation—600(A), 687.
Wulff, J. (see Elliott, R. M.)—170
Yamasaki, F. (see Sinma, K.)—320(L)
Yearian, H. J. Proton diffraction by vapors—242(A)
—— (see Whitmer, R. M.)—1114(A)
Young, Gale. On the shape and stability of heavy nuclei—1102(L)
Yusephovich, A. A. (see Roussinow, L. L.)—979(L)

Zacharias, J. R. (see Kellogg, J. M. B.)—318(L), 595(A)
—— (see Rabi, I. I.)—526, 595(A)
Zachariasen, W. H. On the dynamical theory of x-ray diffraction in crystals—241(A)
Zagor, H. I. (see Salant, E. O.)—111(L)
Zavelsky, A. On the upper limit of the β-spectrum of ThC'' and ThB—317(L)
Zener, C. (see Randall, R. H.)—1140(A)
Zimmer, K. G. and N. W. Timoféeff-Ressovsky. Note on the biological effects of densely ionizing radiation—411(L)
Zinn, Walter H. (see Seely, S.)—679(A)
—— (see Szilard, Leo)—799(L)
Zwicky, F. On the theory and observation of highly collapsed stars—726
—— Cosmic rays from supernovae—986(L)

Tyrrell, Warren A., Jr. Theoretical binding energy of He^5—678(A)
——, **K. G. Carroll and H. Margenau.** Binding energies of light nuclei—790(L)

Urry, W. D. (see Evans, R. D.)—931

Valente, F. A. (see Hornbostel, J.)—108(L)
Vallarta, M. S. Are there multiple charged primary particles in cosmic radiation?—583(L)
—— **and R. P. Feynman.** Scattering of cosmic rays by the stars of a galaxy—506(L)
——, **C. Graef and S. Kusaka.** Galactic rotation and the intensity of cosmic radiation at the geomagnetic equator—1
Valley, G. E. (see Hill, J. E.—678(A)
—— **and R. L. McCreary.** Interval conversion electrons from Br^{80}—666(L)
Van Allen, J. A. (see Ellett, A.)—1129(A)
Van Atta, L. C. and D. L. Northrup. Measurement of x-ray production in the range 0.8 to 2.0 million volts—681(A)
Van de Graaff, R. J. (see Trump, John G.)—676(A), 1160
Van Vleck, J. H. On the theory of paramagnetic relaxation—673(A)
—— On the theory of the forward scattering of neutrons by paramagnetic media—924
—— (see King, G. W.)—1120(A), 1165
—— (see Weiss, P. R.)—673(A)
Vargus, Joseph A., Jr. Multiple scattering of cosmic-ray particles in 1 cm of platinum—422(A)
Vitter, A. L. and L. C. Brieger. Velocity of radio waves in air—416(L)
Volkoff, G. M. On the equilibrium of massive neutron cores—421(A)
—— On the equilibrium of massive spheres—413(L)
—— (see Oppenheimer, J. R.)—374

Wait, G. R. Radioactive content of the atmosphere as affected by the presence of condensation nuclei—591(A)
Wakatuki, Tetuo (see Seishi, Kikuchi)—1264(L)
Waldman, Bernard (see Collins, George B.)—412(L), 507(L), 1122(A)
——, **G. B. Collins, E. M. Stubblefield and M. Goldhaber.** Nuclear excitation of indium by x-rays—1129(A)
Wall, C. N. (see Gingrich, N. S.)—1116(A)
Wang, P. (see Roberts, R. B.)—510(L), 596(A), 664(L)
—— (see Salant, E. O.)—984(L)
Warren, R. E. (see Plain, G. J.)—1135(A)
Wasastjerna, J. A. On the structure of solid solutions—986(L)
Watson, R. E. (see Bartlett, J. H.)—235(A)
Watson, W. W. and R. Simon. Spectra of SnH and PbH at high pressure—677(A)
—— **and Ralph Simon.** Spectrum of tin hydride at high pressure—358
Way, Katharine. Energy levels of H^3, He^3 and He^5—678(A)
—— Liquid-drop model and nuclear moments—963
Webb, Harold W. (see Garth, Robert C.)—677(A)
—— (see Merrill, Harrison J.)—597(A), 1191
—— (see Moore, George E.)—677(A)
Webb, Wayne. Study of beta-brass in single crystal form—297
Webster, D. L., L. T. Pockman, K. Harworth and Paul Kirkpatrick. Probability of K ionization of nickel by cathode rays—682(A)
Weinberg, Alvin M. Nerve conduction with distributed capacitance—240(A)
Weiss, P. R. and J. H. Van Vleck. Theory of ferromagnetism—673(A)
Weisskopf, V. F. On the electromagnetic field produced by an electron—1131(A)
—— On the self-energy of the electron—678(A)
—— **and D. H. Ewing.** On the penetration probability of fast protons into nuclei—241(A)
Weisz, Paul. Zenith angle distribution of the hard component of cosmic rays and the mass of the mesotron—1266(L)
Wells, W. H. Design and construction features of the Westinghouse electrostatic generator—599(A)
Welo, Lars A. and Oskar Baudisch. Some evidence for the existence of higher hydrates of gamma- and alpha-ferric oxide—1143(A)
Westerfield, E. C. Thermal dilatation of superconductors—319(L)
—— **and W. B. Pietenpol.** Viscosity in an expanding bubble—306
Wheeler, A. (see Beeck, Otto)—601(A)
Wheeler, John A. (see Bohr, N.)—1124(A)
—— **and Willis E. Lamb, Jr.** Influence of atomic electrons on radiation and pair production—858
Whitaker, Martin D. and Harold G. Beyer. Transmission of slow neutrons through crystals—1101(L)
—— **and Harold G. Beyer.** Experimental study of the additivity of slow neutron cross sections—1124(A)
——, **Charles A. Barton, William C. Bright and Edgar J. Murphy.** Cross sections of metallic uranium for slow neutrons—793(L)
Whitcomb, S. E. and R. T. Lagemann. Infra-red spectrum and molecular constants of carbon monoxide—181
White, John U. (see Lewis, Margaret N.)—894
White, M. G. (see Delsasso, L. A.)—113
—— (see Fox, J. G.)—1106(L)
White, T. N., L. Marinelli, and G. Failla. Measurement of gamma-radiation in roentgens—676(A)
Whitmer, R. M. and H. J. Yearian. Intensity anomalies in electron scattering from ZnO—1114(A)
Wiler, E. (see Overbeck, C. J.)—1127(A)
Wilkins, T. R. and G. Kuerti. Camera for the study of nuclear scattering—1134(A)
Williams, Dudley. Absorption of thiocyanates in the 4.8μ region—1120(A)
Williams, H. J. and R. M. Bozorth. Magnetic anisotropy of iron-nickel and copper-nickel alloys—673(A)
Williams, J. H. (see Haxby, R. O.)—140
Williams, V., R. C. Herman and R. Hofstadter. Infra-red absorption spectrum of phenol vapor—684(A)
Wilson, Thomas C. Photoconductivity of metal films—316(L)
—— Effect of high pressure upon the order-disorder transformation in Cu-Zn and Cu-Au alloys—1140(A)

Wilson, Volney C. Nature of the penetrating cosmic rays —6
—— On the nature of the penetrating cosmic rays—234(A)
—— (see Schein, Marcel)—233(A)
Winans, J. Gibson, Francis J. Davis and Victor A. Leitzke. Fluorescence, absorption and discharge in a mercury-thallium mixture—242(A)
——, **Francis J. Davis and Victor A. Leitzke.** Sensitized fluorescence of lead—1126(A)
Witcher, C., E. Haggstrom, J. S. O'Conor and J. R. Dunning. Electron lens type of β-ray spectrometer—1135(A)
Witmer, Enos E. Parameters more fundamental than the space-time coordinates—1132(A)
Wolff, H. G. (see Hardy, J. D.)—1146(A)
Wood, R. W. and G. H. Dieke. Band spectra of heavy nitrogen and the spectra of $N^{15}H$ and $N^{15}D$—1120(A)
Workman, E. J. and R. E. Holzer. Quantities of charge transfers in lightning discharges—598(A)
—— **and R. E. Holzer.** Recording generating voltmeter for lightning studies—606(A)
Wulf, Oliver H. and Eugene H. Melvin. Band spectra in nitrogen at atmospheric pressure. A source of band spectra excitation—600(A), 687.
Wulff, J. (see Elliott, R. M.)—170
Yamasaki, F. (see Sinma, K.)—320(L)
Yearian, H. J. Proton diffraction by vapors—242(A)
—— (see Whitmer, R. M.)—1114(A)
Young, Gale. On the shape and stability of heavy nuclei—1102(L)
Yusephovich, A. A. (see Roussinow, L. L.)—979(L)

Zacharias, J. R. (see Kellogg, J. M. B.)—318(L), 595(A)
—— (see Rabi, I. I.)—526, 595(A)
Zachariasen, W. H. On the dynamical theory of x-ray diffraction in crystals—241(A)
Zagor, H. I. (see Salant, E. O.)—111(L)
Zavelsky, A. On the upper limit of the β-spectrum of ThC″ and ThB—317(L)
Zener, C. (see Randall, R. H.)—1140(A)
Zimmer, K. G. and N. W. Timoféeff-Ressovsky. Note on the biological effects of densely ionizing radiation—411(L)
Zinn, Walter H. (see Seely, S.)—679(A)
—— (see Szilard, Leo)—799(L)
Zwicky, F. On the theory and observation of highly collapsed stars—726
—— Cosmic rays from supernovae—986(L)

Analytic Subject Index to Volume 55

References with (A) are to abstracts of papers presented at meetings of the American Physical Society.
References with (L) are to Letters to the Editor.

Absorption coefficient (see also **Scattering of electrons, neutrons, and ions; X-ray, absorption; Collision diameter**)
- Internal conversion of γ-rays, S. M. Dancoff, P. Morrison—122; 423(A); J. Halpern, H. R. Crane—260
- Klein-Nishina absorption, J. Halpern, H. R. Crane—236(A); 258
- Of Rh and In for neutrons, J. H. Manley, J. Hornbostel, H. H. Goldsmith—1116(A)

Accommodation coefficient
- Of gases for 1215.7A, W. M. Preston—1125(A)
- Of He *vs.* Ni, B. G. Raines—684(A)

Acoustics
- Absorption in CO_2; supersonic, H. L. Saxton—1127(A)
- Anomalous damping of ultrasonic waves, O. Halpern—881(L)
- Chladni patterns on circular plates, R. C. Colwell, J. K. Stewart, A. W. Friend—595(A)
- Dissipative acoustic reflection in gases, R. S. Alleman—87
- Eigentones at low frequencies, R. H. Bolt—420(A)
- Molecular vibrations in CO_2, W. H. Pielemeier, D. Telfair—1127(A)
- Supersonic velocity in CO_2, C. J. Overbeck, E. Wiler—1127(A)
- Transmission through plates, F. H. Sanders—1127(A)

Adsorption
- Energies of adhesion, G. Boyd, W. D. Harkins—237(A)
- Surface states in solids, W. G. Pollard—1147(A)

Aerodynamics (see also **Hydrodynamics**)
- Stresses in turbulent air flow, H. K. Skramstad—1141(A)

Afterglow
- In N_2, J. Kaplan—583(L); 606(A)
- Nitrogen forbidden line, R. Bernard—511(L); J. Kaplan—598(A)

Alloys (see **Crystalline state**)

Astrophysics
- Einstein's field equations for spheres of fluid, R. C. Tolman—364
- Energy production in red giants, G. Gamow, E. Teller—791(L)
- Energy production in stars, H. A. Bethe—103(L); 434
- Energy transformations in novae, R. Gunn—591(A)
- Excitation of O^{++}, M. H. Hebb—1114(A)
- Great nebulae, origin of, G. Gamow, E. Teller—654
- Highly collapsed stars, F. Zwicky—726
- Interstellar atoms and ions, R. M. Langer—423(A)
- Lyman lines in solar emission, H. Hemmendinger—1119(A)
- Massive neutron cores, equilibrium of spheres, J. R. Oppenheimer, G. M. Volkoff—374; R. C. Tolman—364; G. M. Volkoff—413(L); 421(A)
- Prediction of sunspot cycle, J. Q. Stewart, F. C. Eggleston—1102(L)
- Stellar evolution, G. Gamow—718; 796(L)
- Temperature in white dwarfs, R. E. Marshak, H. A. Bethe—681(A)

Atomic and molecular beams
- Of K and K_2 in gases, P. Rosenberg—1267(L)
- Proton diffraction by vapors, H. J. Yearian—242(A)

Atomic form factors
- For Zn in ZnO, K. Lark-Horovitz, C. H. Ehrhardt—605(A)

Atomic structure (see also **Energy states of atoms; Spectra**)
- Electron velocities in nitrogen and methane, A. L. Hughes, M. A. Starr—343
- Self-consistent field for Cr II, R. L. Mooney—557; 598(A)

Biophysics
- Biological action of radiation, F. S. Brackett, A. Hollaender—1120(A)
- Cell division, G. Young—1102(L)
- Effects of densely ionizing radiation, K. G. Zimmer, N. W. Timoféeff-Ressovsky—411(L)
- Integrating meters for ultraviolet, J. B. H. Kuper, F. S. Brackett—1128(A)
- Introduction of drugs into the skin, H. A. Abramson—676(A)
- Nerve conduction, A. M. Weinberg—240(A)
- Pain threshold with thermal radiation, J. D. Hardy, H. G. Wolff, H. Goodell—1146(A)
- Photolethal action of methylcholanthrene on yeast, A. Hollaender, P. A. Cole—597(A)
- Proton beam for biological investigations, G. W. Scott, Jr., C. P. Haskins—1112(A)
- Ultraviolet microscopy, chemical structure in cell, P. A. Cole—597(A)

Broadening of spectral lines
- General solution for equations, L. Spitzer, Jr.—361
- Stark-effect of hydrogen lines, L. Spitzer, Jr.—699

Conductivity, electrical (see **Electrical conductivity; Discharge of electricity in gases**)

Conductivity, thermal (see **Thermal conductivity**)

Constants, physical, standards
- Fine structure constant, R. T. Birge—1119(A)
- Re-evaluation of atomic constants, F. G. Dunnington—683(A)

Cosmic radiation
- Absorption in air and water, instability of barytron, T. H. Johnson, M. A. Pomerantz—104(L); 600(A)
- Alfvén's "cosmic cyclotron," E. R. Sabato—1272(L)
- Angular distribution of hard rays, P. Weisz—1266(L)
- Anomalies in directional intensity, H. S. Ribner—1271(L)
- Asymptotic orbits, A. Baños, Jr.—621

Barytron secondaries, J. I. Hopkins, W. M. Nielsen, L. W. Nordheim—233(A)
Bursts in lead, M. Schein, P. S. Gill—1111(A)
Diurnal variations, J. L. Thompson—233(A)
East-west asymmetry, T. H. Johnson, J. G. Barry—503(L)
Effect on radioactive K, W. R. Smythe—316(L)
Energies as function of latitude, R. A. Millikan, H. V. Neher—599(A)
Fine structure in angle distribution, D. M. Cooper—1272(L)
Galactic rotation and intensity, M. S. Vallarta, C. Graef, S. Kusaka—1
γ-ray ion currents, J. W. Broxon, G. T. Merideth—883
G-M counters in stratosphere, L. F. Curtiss, A. V. Astin, L. L. Stockmann, B. W. Brown—600(A)
Hard component, L. W. Nordheim, M. H. Hebb—1111(A)
Heavy particles in cloud chamber, G. Herzog—1266(L)
Latitude effect, B. Gross—112(L)
Latitude effect, large bursts, W. P. Jesse, P. S. Gill—414(L)
Long period variations, P. S. Gill—429
Mass of mesotron, Y. Nishina, M. Takeuchi, T. Ichimiya—585(L)
Measurements in stratosphere, S. A. Korff, W. E. Danforth—675(A)
Mesotron, mass of, Y. Nishina, M. Takeuchi, T. Ichimiya—585(L)
Mesotron as name, R. A. Millikan—105(L)
Mesotrons, lifetime of, L. W. Nordheim—506(L)
Mesotrons, occurrence of slow, C. G. Montgomery, W. E. Ramsey, D. B. Cowie, D. D. Montgomery—1117(A)
Motion in interstellar space, H. Alfvén—425
Multiple charged primary particles, M. S. Vallarta—583(L)
Multiple scattering in Pt, J. A. Vargus, Jr.—422(A)
Nature of primary rays, T. H. Johnson—1111(A)
Orbit in field of a magnetic dipole, R. Albagli Hutner—109(L)
On the Pacific Ocean, P. S. Gill—1111(A); 1151
Particles at great depth, J. Barnóthy, M. Forró—870
Penetrating neutral particles, F. R. Shonka—24; 234(A)
Penetrating rays, V. C. Wilson—6; 234(A)
Penumbra at latitude 20°, energy spectrum, R. Albagli Hutner—15; 614
Production of penetrating particles, M. Schein, V. C. Wilson—233(A)
Rays which produce bursts, C. G. Montgomery, D. D. Montgomery—676(A)
Rossi transition curve, W. M. Nielsen—675(A); W. M. Nielsen, J. E. Morgan and K. Z. Morgan—995
Scattering by stars, M. S. Vallarta, R. P. Feynman—506(L)
Shower and vertical intensity, J. Barnóthy, M. Forró—868
Shower phenomena, penetrating rays, W. F. G. Swann, W. E. Ramsey—599(A)
Sidereal time variations, A. H. Compton, P. S. Gill—233(A); J. L. Thompson—11
Soft component, M. A. Pomerantz, T. H. Johnson—1111(A)
Solar component, S. A. Korff, T. H. Johnson—600(A)
Stability of orbits, O. Godart—875(L)
Stopping power of Hg and N_2, J. H. Bartlett, Jr.—803
From supernovae, F. Zwicky—986(L)
World-wide changes, S. E. Forbush—233(A)

Crystal structure

Crystal structure and x-ray, R. Landshoff—631
Of $LiOH \cdot H_2O$, R. Pepinsky—1115(A)
Orientation of crystals by x-rays, F. E. Haworth—684(A)
Solid solutions, J. A. Wasastjerna—986(L)
Super-structure in Ni-Fe crystals, L. W. McKeehan, E. M. Grabbe—505(L); 1142(A)
Uniqueness of x-ray analysis, A. L. Patterson—682(A)
Of Zn at 100° and 298°K, G. E. M. Jauncey, E. M. McNatt—498

Crystalline state

Actinoelectric effects in tartaric acid crystals, J. J. Brady, W. H. Moore—308
Band in Cu crystals, M. Chodorow—675(A)
Band structure of Cu and Ni, W. W. Beeman, H. Friedman—1115(A)
Beta-brass in single crystals, W. Webb—297
Binding energy of Be crystals, C. Herring, A. G. Hill—673(A)
Crystal energy levels, C. B. Ellis—1114(A)
Crystallinity in rubber, S. D. Gehman, J. E. Field—594(A)
Crystallization and melting of rubber, R. B. Dow—1141(A)
Devitrification temperatures, B. J. Luyet—1132(A)
Electronic states and compressibility of Be, A. G. Hill, C. Herring—1140(A)
Electronic structure of alloys, M. F. Manning—682(A)
Energy of electrons in Wigner-Seitz theory, R. Landshoff—603(A)
Internal friction in metals; grain size, R. H. Randall, F. C. Rose, C. Zener—1140(A)
Momentum of electrons in metal crystal, W. V. Houston—1140(A)
Noncubic growth of single Ag crystals, J. H. Howey—578
Order-disorder process in crystals of Cu-Au, F. C. Nix, D. MacNair—605(A)
Order-disorder transformation in Cu-Zn and Cu-Au alloys, T. C. Wilson—1140(A)
Pressure-temperature phase diagram of Na-K alloys, C. H. Kean—750
Properties of liquid and solid HD, F. G. Brickwedde R. B. Scott—672(A)
Ag films on mica, S. E. Essig—229(L)
Specific heat, vapor pressure of Ta, D. B. Langmuir, L. Malter—1138(A)
Thermal and stress dependence, H. Ludloff—681(A)

Dielectrics and dielectric properties
Of dielectrics dispersed in water, H. Fricke—1141(A)
Diffraction of atoms (see **Atomic and molecular beams**)
Diffusion
Of gases through metals, J. H. Simons, W. R. Ham—1137(A)
Of H_2 through Cu, W. R. Ham—1137(A)
Self-diffusion of copper, B. V. Rollin—231(L); J. Steigman, W. Shockley, F. C. Nix—605(A); W. H. Furry, R. C. Jones, L. Onsager—1083, 1137(A)
Thermal-gravitational separation of isotopes, A. K. Brewer, A. Bramley—590(A); L. Onsager—1136(A)
Discharge of electricity in gases
Anode effect and temperature, P. L. Copeland—1145(A)
Autoelectronic emission in metal arcs, W. S. Huxford, S. G. Eskin, R. W. Jones—1146(A)
Band igniter for Hg-pool tubes, K. J. Germeshausen—228(L)
Breakdown in long tubes, J. R. Dietrich, L. B. Snoddy—591(A)
Cathode blast of Hg rectifier, L. Tonks—674(A)
Charge transfers in lightning, E. J. Workman, R. E. Holzer—598(A)
Convection currents in arcs, C. G. Suits—198
Currents in ring discharge, C. G. Smith—1144(A)
Definition of sparking potential, L. B. Loeb—1121(A)
Discharge between stationary and rotating electrode, J. W. Beams, L. B. Snoddy—504(L); 1145(A)
Discharge on surfaces of solution, L. B. Snoddy, J. W. Beams—663(L)
Electron and potential distributions in Hg arc, L. P. Smith, P. L. Hartman—1145(A)
Electron scattering and plasma oscillations, H. J. Merrill, H. W. Webb—597(A); 1191
Glow to arc transition, F. A. Maxfield, H. R. Hegbar, J. R. Eaton—592(A)
Heat transfer in arcs, C. G. Suits, H. Poritsky—1184
High pressure arcs, C. G. Suits—561
Ionization of Hg, J. Kaplan—111(L)
Lichtenberg figures, F. H. Merrill, A. v. Hippel—1122(A)
Lightning discharge, J. M. Meek—972; 1122(A)
Point-to-plane discharge, S. Gorrill—1121(A); G. G. Hudson—1122(A); A. F. Kip—422(A); 549; 1122(A); H. C. Pollock, F. S. Cooper—593(A); G. W. Trichel—382
Positive column of N_2 arc, E. S. Lamar, A. M. Stone, K. T. Compton—1145(A); 1235
Spark breakdown potentials, F. Ehrenkranz—219
Sparking potentials, R. B. Quinn—240(A)
Sparking potentials at low pressures, R. B. Quinn—482
Spectral lines from Hg arc, O. S. Duffendack, O. G. Koppius—1199
Temperature distribution in Hg arc, W. Elenbaas—294
Townsend coefficients; glow potentials in argon, R. W. Engstrom—239(A)
Townsend coefficients in H_2, D. H. Hale—815; 1121(A)
Townsend coefficients in photo-tubes filled with A, W. S. Huxford—754
Transition from glow to arc, Hsu Yun Fan—769
Wall charge in long discharge tubes, J. R. Dietrich—1145(A)
Disintegration of nucleus (see also **Radioactivity**)
α-particles from $F^{19}+H^1$, W. B. McLean, R. A. Becker, W. A. Fowler, C. C. Lauritsen—796(L)
Angular distribution of disintegration products, R. O. Haxby, J. S. Allen—598(A); R. O. Haxby, J. S. Allen, J. H. Williams—140
Of Be by electrons, G. B. Collins, B. Waldman, W. R. Polye—1123(A)
Of B by $_1H^1$, E. L. Hill, R. O. Haxby—147
Of B by slow neutrons, J. B. Fisk—1117(A); M. Goldhaber, R. D. Hill, P. G. Kruger, F. W. Stallmann—1117(A)
Cross sections of metallic U, M. D. Whitaker, C. A. Barton, W. C. Bright, E. J. Murphy—793(L)
Detonation by fission, E. Feenberg—980(L)
Distribution in angle of H^1 from H^2-H^2 reaction, A. Ellett, J. A. Van Allen, D. S. Bayley—1129(A)
Electrodisintegration of Be, theory of, G. B. Collins, B. Waldman, W. R. Polye—412(L); 1123(A); E. Guth—411(L)
Energy production in stars, H. A. Bethe—103(L); 434
Excitation functions of Li and B, R. B. Bowersox—240(A)
Excitation for He, J. M. Cork, B. R. Curtis—1264(L)
Excitation of In with α-particles, K. Lark-Horovitz, J. R. Risser, R. N. Smith—878(L)
Excitation of intermediate elements, E. J. Konopinski—235(A)
Fission of U, P. Abelson—418(L); H. L. Anderson, E. T. Booth, J. R. Dunning, E. Fermi, G. N. Glasoe, F. G. Slack—511(L); in cloud chamber, D. R. Corson, R. L. Thornton—509(L); delayed neutron emission, E. T. Booth, J. R. Dunning, F. G. Slack—876(L); 1124(A); droplet fission, R. B. Roberts, R. C. Meyer, L. R. Hafstad—416(L); energy of fragments, E. T. Booth, J. R. Dunning, F. G. Slack—981(L); 1273(L); heavily ionizing particles, G. K. Green, L. W. Alvarez—417(L); mechanism of fission, N. Bohr, J. A. Wheeler—1124(A); J. Frenkel—987(L); neutrons produced, H. L. Anderson, E. Fermi, H. B. Hanstein—797(L); L. Szilard, W. H. Zinn—799(L); by neutrons, γ-rays, J. C. Mouzon, R. D. Park, J. A. Richards, Jr.—668(L); products of cleavage, P. Abelson—670(L); 876(L); G. N. Glasoe, J. Steigman—982(L); radioactive recoils, E. McMillan—510(L); radioactivity of products, G. N. Glasoe, J. Steigman—1124(A); range of fragments, E. T. Booth, J. R. Dunning, G. N. Glasoe—982(L); E. T. Booth, J. R. Dunning, F. G. Slack—981(L); search for β-particles, J. W. Kennedy, G. T. Seaborg—877(L); H. H. Barschall, W. T. Harris, M. H. Kanner, L. A. Turner—989(L)
Fission of U and Th, R. B. Roberts, R. C. Meyer, P. Wang—510(L); delayed neutron emission, R. B. Roberts, L. R. Hafstad, R. C. Meyer, P. Wang—664(L); intensity ionizing particles, R. D. Fowler, R. W. Dodson—417(L); radioactive halogens, R. W. Dodson, R. D. Fowler—880(L); resonance, N. Bohr—418(L)

γ-rays from Al, G. J. Plain, R. G. Herb, R. E. Warren—1135(A)
γ-rays from B+D, E. R. Gaerttner, W. A. Fowler, C. C. Lauritsen—27; J. Halpern, H. R. Crane—415(L)
Identification of x-rays, radioactive elements, P. Abelson—424(A)
Internal conversion coefficients, S. M. Dancoff, P. Morrison—122; 423(A)
Mesotron disintegration, C. C. Montgomery, W. E. Ramsey, D. B. Cowie, D. D. Montgomery—1117(A)
Neutrons from He^5, H. Staub, W. E. Stephens—845
Neutrons from H^2-H^2, low energy, E. Hudspeth, H. Dunlap—587(L)
Penetration of fast protons into nuclei, V. F. Weisskopf, D. H. Ewing—241(A)
Short range particles from Li and α-particles from B, R. B. Bowersox—323
By 6.5 Mev protons, L. A. DuBridge—603(A)
Of U, simple capture of neutrons, H. L. Anderson, E. Fermi—1106(L)
Of U, transuranic elements, E. Segrè—1104(L)

Doppler effect
In canal-ray tube, C. W. Sherwin, A. J. Dempster—582(L)

Dynamics
Inertial mass, P. Fireman—683(A)

Elasticity
Compressibility of Li, C. Herring—598(A)
Constants of NH_4Cl, A. W. Lawson, R. Scheib—1268(L)
Elastic, electric and piezoelectric constants of Rochelle salt, W. P. Mason—775; 1141(A)
Electronic states and compressibility of Be, A. G. Hill, C. Herring—1140(A)
Process of fatiguing, x-ray study, R. G. Spencer—242(A); 991
Stress-strain relationship for rubber, F. E. Dart, E. Guth—1141(A)
Theory of rubber elasticity, E. Guth—593(A)
Thermal dependence in solids, L. Brillouin—1139(A)
Thermal and stress dependence, H. Ludloff—681(A)
Ultrasonic determination of elastic properties, H. Ludloff—593(A)

Electrical conductivity and resistance
Anisotropy of metals, E. M. Baroody—1140(A)
Anomalies of zincblende crystals, M. Distad—1147(A)
β-brass in single crystals, W. Webb—297
Breakdown in single crystals, R. C. Buehl, A. v. Hippel—1122(A)
Change in magnetic field, L. Davis, W. V. Houston—1143(A)
Effect of electron bombardment on zincblende, M. Distad—1146(A)
Effect of pressure on single crystals, R. M. Holmes, H. W. Allen—593(A)
Of liquid Na-K alloys, C. H. Kean—750
Magnetoresistance of Ni, C. W. Heaps—1069
Momentum in electrical conductivity, W. V. Houston—420(A); 1255
Progressive breakdown in a liquid, L. B. Snoddy, J. W. Beams—879(L)
Of tantalum, L. Malter, D. B. Langmuir—743
Thermal dilatation of superconductors, E. C. Westerfield—319(L)

Electrolytes
Ionic volumes in aqueous solutions, G. W. Stewart—240(A)

Electromagnetic theory
Electric currents in terminated lines, R. H. Kent—762
Velocity of radio waves, G. H. Brown—1100(L); A. L. Vitter, L. C. Brieger—416(L)

Electron diffraction (see also **Electrons, scattering of**)
Compounding sine functions, L. R. Maxwell—1135(A)

Electrons (see also **Positrons** and ***e/m***)
Atomic electrons, radiation and pair production, J. A. Wheeler, W. E. Lamb, Jr.—858
Creation of pairs by fast electrons, H. R. Crane, J. Halpern—838
Electron velocities in nitrogen and methane, A. L. Hughes, M. A. Starr—343
Field and self-energy, V. F. Weisskopf—678(A); 1131(A)
Field theory, N. Rosen—94
Interactions of heavy electrons, J. F. Carlson—599(A)
Interchange energy of two free electrons, C. A. Ludeke—315(L)
Retarded interaction, I. S. Lowen—601(A)
Self-energy of electron, H. A. Bethe—681(A)

Electrons, scattering of
Of fast electrons in gases, J. H. Bartlett, R. E. Watson—235(A); A. L. Hughes—350
From ZnO, R. M. Whitmer, H. J. Yearian—1114(A)

Electrons, secondary
Contaminated surfaces, H. Nelson—985(L)
Electron multiplier, J. S. Allen—966; 1133(A)
By H_2^+ and D_2^+ ions on Ni, M. Healea—984(L)
From metals bombarded with protons, J. S. Allen—236(A); 336
Under positive ion bombardment, A. G. Hill, W. W. Buechner, J. S. Clark, J. B. Fisk—463
From Na films, P. L. Copeland—1270(L)
From tungsten and thorium-coated tungsten, E. A. Coomes—519

Electrons, thermionic (see **Thermionic emission**)

Electro-optical effects (see also **Photoelectric effect and properties**)
In colloids, H. Mueller—508(L); 792(L)
Influence of frequency, F. J. Norton—668(L)

E/m
Spectroscopic and free electron values, J. A. Bearden—584(L)

Equations of state
For ammonia and steam, J. L. Finck—682(A)
Of frozen rare gases, G. Kane—1138(A)
Virial coefficient of He, L. Gropper—1095

Errata
Range distribution of the uranium fission fragments, E. T. Booth, J. R. Dunning, F. G. Slack—1273(L)
The scattering of α-particles by argon, oxygen, and neon—G. Brubaker—877(L)

Evaporation
Of tantalum, D. B. Langmuir, L. Malter—748

Field currents
Energy distribution, J. E. Henderson, R. K. Dahlstrom—473
At high and low pressures, B. E. K. Alter, R. T. K. Murray—672(A)

Films, properties of
Activity and orientation of metal films, O. Beeck, A. Wheeler, A. E. Smith—601(A)
Atoms and molecules in extremely thin films, L. H. Germer—605(A)
Potentials of multilayers, W. D. Harkins, R. W. Mattoon—320(L)
Preparation of oriented metal films, A. E. Smith, O. Beeck—602(A)
Reflection from glass, multilayer films, C. H. Cartwright, A. F. Turner—595(A); 675(A)
Reflection of light from glass, K. B. Blodgett—391
Reflectivities of evaporated metal films, G. B. Sabine—1064
Rubbed films of barium stearate, electron diffraction patterns, L. H. Germer, K. H. Storks—648

Fluorescence
And absorption of diacetyl, G. M. Almy, H. Q. Fuller, G. D. Kinzer—238(A)
Of Pb vapor, J. G. Winans, F. J. Davis, V. A. Leitzke—1126(A)
In Hg-Tl mixtures, J. G. Winans, F. J. Davis, V. A. Leitzke—242(A)
Of OH molecules, E. R. Lyman—1126(A)
Sensitized fluorescence of K, E. H. Krause—164
By ultraviolet radiations, N. C. Beese—1126(A)

Geophysics
Intercalibration and comparison of measurements, ages of rocks, R. D. Evans, C. Goodman, N. B. Keevil, A. C. Lane, W. D. Urry—931
Natural fission of Th and U, W. F. Libby—1269(L)
Origin of earth's magnetic field, W. M. Elsasser—489
K^{40}/Ca^{40} and age of earth, A. K. Brewer—669(L)
Radiogenic leads, geological time, A. V. Grosse—584(L); A. O. Nier—153

Hall effect
Calculation of, L. Davis, W. V. Houston—1143(A)

Heat of dissociation
Of CO, H. D. Hagstrum, J. T. Tate—1136(A)

High voltage tubes and machines
Compact high voltage generator, J. G. Trump, R. J. Van de Graaff—676(A); 1160
Cyclotron at Chicago, W. D. Harkins, H. W. Newson, R. J. Moon, A. H. Snell, L. A. Slotin, L. P. Borst, S. L. Simon, B. Carpenter, P. R. Bell—1110(A)
Cyclotron at M. I. T., M. S. Livingston, J. H. Buck, R. D. Evans—1110(A)
Cyclotron at Purdue, W. J. Henderson, L. D. P. King, J. R. Risser—1110(A)
Ion paths in cyclotron, L. H. Thomas—1110(A)
Westinghouse electrostatic generator, W. H. Wells—599(A)

Hyperfine structure (see also **Nuclear moments and spin**)
Of Be I line λ4573A, S. Mrozowski—798(L)
Of Au, R. M. Elliott, J. Wulff—170
Of In III, J. S. Campbell, J. R. Davis—1125(A)
Of λ4686 of He, Djen-Yuen Chu—175; 423(A)
Of Mn I, R. A. Fisher, E. R. Peck—270

Instruments (see **Methods and instruments**)

Ionization by collision (see also **Ionization potentials**)
Of $CHBrF_2$, R. F. Baker, J. T. Tate—236(A)
Excitation in Hg vapor, T. McFadden—797(L); W. B. Nottingham—203
By neutrons in gases, P. C. Aebersold, G. A. Anslow—680(A); 1134(A)
K ionization of Ni by cathode rays, D. L. Webster, L. T. Pockman, K. Harworth, P. Kirkpatrick—682(A)
Probability; Hg atoms by electrons, M. E. Bell—201

Ionization potentials
Of Ca VII and Sc VIII, L. W. Phillips—708
Of Hg, T. McFadden—797(L); W. B. Nottingham—203

Ionization by radiation (see **Photoionization**)

Ionosphere
Changes, radiation from N_2, J. Kaplan—110(L)
Critical frequencies, recording of, O. Rydbeck—1127(A)
E region, E. O. Hulburt—639; during eclipse—646
Motion of clouds of abnormal ionization, J. A. Pierce, H. R. Mimno—1128(A)
Nature of radio fade-out, L. V. Berkner—536; D. F. Martyn—983(L)
Nocturnal *E*-layer, N. E. Bradbury—423(A)

Isomers, nuclear (see **Radioactivity**)

Isotopes
Of Br, separation by centrifuge, R. F. Humphreys—674(A)
Concentration of Cl isotopes, C. Skarstrom, H. E. Carr, J. W. Beams—591(A)
Concentration of U (23 min.), J. W. Irvine, Jr.—1105(L)
Of Hf, Yt, Lu and Ta, A. J. Dempster—794(L)
Of Fe and Cr, A. O. Nier—1143(A)
Mass difference $_4Be^9 - _4Be^8$, S. K. Allison, E. R. Graves, L. S. Skaggs, N. M. Smith, Jr.—107(L); 599(A)
Masses of light elements, S. K. Allison—624
Packing fraction differences, A. C. Graves—238(A); 863
Separation by thermal diffusion, W. H. Furry, R. C. Jones, L. Onsager—1083; 1137(A)
Thermal-gravitational separation, A. K. Brewer, A. Bramley—590(A); L. Onsager—1136(A)
Of U, half-lives of U isotopes, A. O. Nier—150

Joule-Thomson effect
In CO_2, J. R. Roebuck, T. A. Murrell—240(A)

Kinetic theory of gases
Condensation of Hg vapor, J. Slepian, W. M. Brubaker—1147(A)

Liquids (see also **Hydrodynamics**)
Liquid He below λ-point, F. London—235(A)
Properties of liquid and solid HD, F. G. Brickwedde, R. B. Scott—672(A)

Structure of liquid K, N. S. Gingrich, C. N. Wall—1116(A)
Structure of liquid Sn and Cl, C. Gamertsfelder—1116(A)
Unsupported flowing liquid films, B. O'Brien—674(A)

Magnetic properties
Anisotropy of Fe-Ni and Cu-Ni alloys, H. J. Williams, R. M. Bozorth—673(A)
Anisotropy in Ni-Fe alloys, superstructure, E. M. Grabbe, L. W. McKeehan—1142(A); 505(L)
Ferromagnetic impurities in metals, F. W. Constant, J. M. Formwalt—1143(A)
Ferromagnetism of semi-conductors, Syôhei Miyahara—105(L)
Ferromagnetism, theory of, P. R. Weiss, J. H. Van Vleck—673(A)
Higher hydrates of γ- and α-ferric oxide, L. A. Welo, O. Baudisch—1143(A)
Of Fe and Ni at ultra-high radiofrequencies, J. L. Glathart—833
Magnetoresistance of Ni, C. W. Heaps—1069
Of Ni crystals; temperature effects, T. Okamura, T. Hirone—102(L)
Origin of earth's magnetic field, W. M. Elsasser—489
Paramagnetic relaxation, theory of, J. H. Van Vleck—673(A)
Permeability of Fe and Ni from 98 to 410 megacycles, J. B. Hoag, N. Gottleib—410(L)
Powder patterns on crystals, J. W. Shih, Tsu-Yen Chai—1265(L)
Reversible magnetization, theory of, W. F. Brown, Jr.—568
Saturation of Fe and Ni, A. R. Kaufmann—1142(A)
Shape of domains in ferromagnetics, E. H. Kennard—312
Susceptibilities in weak fields, L. G. Hector, M. F. Peck—672(A)
Susceptibility of Cu-Fe alloys in high fields, F. Bitter, A. R. Kaufmann—1142(A)

Magneto-optical effects
Of nickel sulfate, α-hexahydrate, L. R. Ingersoll, P. Rudnick, F. G. Slack—672(A)

Mass defects (see **Isotopes**)

Mechanics, quantum—general
Born's reciprocity and Mie's theory, A. Landé—1132(A)
Contact-transformations, J. M. Jauch—1132(A)
Iteration method, G. Horvay—70; 604(A)
Symmetry properties of variational functions, H. M. James, A. S. Coolidge—873

Mechanics, statistical
Proof of *H* theorem, O. Halpern, F. W. Doermann—1077

Melting point
Of tantalum, L. Malter, D. B. Langmuir—743

Mesotrons
Lifetime, L. W. Nordheim—506(L)
Mass of, Y. Nishina, M. Takeuchi, T. Ichimiya—585(L)
Name, R. A. Millikan—105(L)
Occurrence of slow, C. G. Montgomery, W. E. Ramsey, D. B. Cowie, D. D. Montgomery—1117(A)

Metals (see **Crystalline state**)

Meteorology
Distribution of ozone in stratosphere, W. W. Coblentz, R. Stair—590(A)
Solar constant determinations, B. O'Brien—1142(A)

Methods and instruments
Ages of rocks, R. D. Evans, C. Goodman, N. B. Keevil, A. C. Lane, W. D. Urry—931
Air-blast atomization, R. A. Castleman, Jr.—592(A)
Band igniter for Hg-pool tubes, K. J. Germeshausen—228(L)
β-ray spectrometer, C. Witcher, E. Haggstrom, J. S. O'Conor, J. R. Dunning—1135(A)
Calibration of ionization chamber, W. Gentner, E. Segrè—814; G. T. Seaborg, E. Segrè—808
Camera for study of nuclear scattering, T. R. Wilkins, G. Kuerti—1134(A)
Circuit of short resolving time, L. A. Turner—1134(A)
Compact high voltage generator, J. G. Trump, R. J. Van de Graaff—676(A); 1160
Compounding sine functions, L. R. Maxwell—1135(A)
Continuously sensitive cloud chamber, A. Langsdorf, Jr.—421(A)
Control of current-intensity in spot-welding, W. B. Nottingham—1144(A)
Counters, design and construction, G. L. Locher—675(A)
Counters of unconventional geometry, S. C. Brown, R. D. Evans—1133(A)
Counting rate meter, R. D. Evans, R. L. Alder—1134(A)
Current control device, J. L. Lawson, A. W. Tyler—238(A)
Cyclotron at Chicago, W. D. Harkins, H. W. Newson, R. J. Moon, A. H. Snell, L. A. Slotin, L. P. Borst, S. L. Simon, B. Carpenter, P. R. Bell—1110(A)
Cyclotron at M. I. T., M. S. Livingston, J. H. Buck, R. D. Evans—1110(A)
Cyclotron at Purdue, W. J. Henderson, L. D. P. King, J. R. Risser—1110(A)
Detection of single ions, electrons and photons, J. S. Allen—966; 1133(A)
Dilatometer, elevated temperatures, F. C. Nix—606(A)
Dispenser cathode, thermionic cathode for gaseous discharge tubes, A. W. Hull—1145(A)
Electrolytic "polishing" of W, J. M. Hughes, E. A. Coomes—1138(A)
Electron spectrograph, W. T. Harris—1135(A)
Energies of soft β-radiations, W. F. Libby, D. D. Lee—245
Field distribution in Hailer canal-ray tube, C. W. Sherwin, A. J. Dempster—582(L)
Flowing liquid films, B. O'Brien—674(A)
Focused source of ions, G. W. Scott, Jr.—954
Fundamental space-time coordinates, E. E. Witmer—1132(A)
γ-radiation in roentgens, T. N. White, L. Marinelli, G. Failla—676(A)
γ-ray detector, L. Marinelli—677(A)
γ-ray energies, measurement of, D. C. Kalbfell—422(A)
Gettering powers of metals for gases, L. F. Ehrke, C. M. Slack—684(A)

Methods and instruments (continued)
High current ion tube, H. R. Crane, N. L. Oleson—1110(A)
High intensity bombardment, F. N. D. Kurie—241(A)
Integrating meters for ultraviolet, J. B. H. Kuper, F. S. Brackett—1128(A)
Intense ionic beams, L. P. Smith, G. W. Scott, Jr.—946
Ionization in chambers by fast neutrons, P. C. Aebersold, G. A. Anslow—1134(A)
Ions in cyclotron, L. I. Schiff—422(A)
LiF achromats for large spectral ranges, C. H. Cartwright—606(A)
Magnetic electron lenses, L. Marton—672(A)
Model for electron motion in a magnetic field, A. Rose—1144(A)
Modulation of G-M counters, J. N. Shive—1133(A)
Molecular beam resonance method for measuring nuclear magnetic moments, P. Kusch, S. Millman—596(A); S. Millman—628; I. I. Rabi, S. Millman, P. Kusch, J. R. Zacharias—526
Negative power factors in air capacitors, A. V. Astin—594(A); explanation, H. L. Curtis, A. V. Astin—594(A)
Neutron measurements with counters, S. A. Korff, W. E. Danforth—980(L)
Orientation of crystals by x-rays, F. E. Haworth—684(A)
Oriented metal films, A. E. Smith, O. Beeck—602(A)
Oscillator for ultra-high frequency, R. King—1127(A)
Particle size determination; x-ray reflection, C. Nusbaum—1115(A)
Photronic cells and photometric measurement, H. S. Stewart, Jr., B. O'Brien—1121(A)
Proton beam for biological investigations, G. W. Scott, Jr., C. P. Haskins—1112(A)
Quenching rates in alloys, H. L. Logan—1139(A)
Quiet boiling, N. E. Dorsey—594(A)
Radiation pyrometer, J. Strong—1114(A)
Recording G-M counter, L. J. Brady—1133(A)
Recording voltmeter for lightning studies, E. J. Workman, R. E. Holzer—606(A)
Reduction for rotation group, J. M. Keller—508(L)
Reflection from glass, reduction, C. H. Cartwright, A. F. Turner—595(A); 675(A)
Reflection of light from glass; interference, K. B. Blodgett—391
Resolving power of apparatus, R. C. Spencer—239(A)
Roots of polynomials, mechanical synthesizer, S. L. Brown—604(A)
Scaling circuits in random counts, H. Lifschutz, O. S. Duffendack—412(L); 1133(A)
Separation of gas isotopes, A. K. Brewer, A. Bramley—590(A); L. Onsager—1136(A); theory, W. H. Furry, R. C. Jones, L. Onsager—1083, 1137(A)
Separation of gases by centrifuging, J. W. Beams—591(A)
Separation of nuclear isomers, E. Segrè, R. S. Halford, G. T. Seaborg—321(L)
Single crystals of Fe, Co, Ni and their alloys, P. P. Cioffi, O. L. Boothby—673(A)
Source of band spectra excitation, O. H. Wulf, E. H. Melvin—600(A); 687
Spectrophotometer, infra-red, J. D. Hardy, A. I. Ryer—1112(A)
Spherical coil for uniform field, J. A. Hipple, Jr.—597(A)
Stopping power of hydrogen for H^1, F. T. Rogers, Jr.—588(L)
Superconductivity for radiometric purposes, A. Goetz—1270(L)
Temperature gradient in arc welding of cylindrical tubing, W. A. Bruce—594(A)
Theoretical physics and pure mathematics, J. T. O'Callahan, S.J.—683(A)
Theory of scaling circuits, H. Lifschutz, O. S. Duffendack—1133(A)
Thermal conductivity of solid or molten metals, C. C. Bidwell—1139(A)
Ultracentrifuge for liquids, A. V. Masket, F. W. Linke, J. W. Beams—674(A)
Ultrasonic determination of elastic properties, H. Ludloff—593(A)
Velocity of light apparatus, W. C. Anderson—1128(A)
Westinghouse electrostatic generator, W. H. Wells—599(A)
X-ray spectrometer, high vacuum, J. H. Munier—1116(A)

Molecular structure and constants (see also **Spectra, molecular** and **Raman spectra**)
Of CO, S. E. Whitcomb, R. T. Lagemann—181
Distances in gas molecules Se_2, HgCl, Cu_2, Cl_2, $CuBr_2$ and Cu_2I_2, L. R. Maxwell, V. M. Mosley—238(A)
Effect of shape on attraction in monolayers, R. T. Florence, W. D. Harkins—237(A)
Exchange forces in H_2, H. Beutler—1118(A)
Molecular vibrations in CO_2, W. H. Pielemeier, D. Telfair—1127(A)
Tetrahedrally symmetrical molecules, W. H. Shaffer, H. H. Nielsen, L. H. Thomas—1130(A)

Neutrino (see also **Radioactivity**)
Absorption, H. R. Crane—501
Recoil nucleus in β-disintegration, J. Halpern, H. R. Crane—1123(A)
Theory of, W. H. Furry—602(A)

Neutrons
Absorption by B, Co and Mn, E. O. Salant, W. J. Horvath, H. I. Zagor—111(L)
From breakup of He^4, H. Staub, W. E. Stephens—845
Capture by atoms in a crystal, W. E. Lamb, Jr.—190; 234(A)
Collimation of fast neutrons, P. C. Aebersold—596(A)
Cross sections, M. D. Whitaker, H. G. Beyer—1124(A)
Depolarization in ferromagnetic media, O. Halpern, Th. Holstein—601(A)
Dipole-dipole resonance forces, G. W. King, J. H. Van Vleck—1165
Forward scattering by paramagnetic media, J. H. Van Vleck—924
Highly collapsed stars or neutron stars, equilibrium of spheres, J. R. Oppenheimer, G. M. Volkoff—374; R. C. Tolman—364; G. M. Volkoff—413(L); 421(A); F. Zwicky—726

Magnetic scattering, O. Halpern, M. H. Johnson—898
Measurements with counters, S. A. Korff, W. E. Danforth—980(L)
Neutron-proton interaction, J. Schwinger—235(A)
Resonance absorption in In, J. H. Manley, H. H. Goldsmith, J. Schwinger—107(L)
Scattering cross section, V. W. Cohen, H. H. Goldsmith, J. Schwinger—106(L)
Scattering of D-D neutrons, Seishi Kikuchi, Hiroo Aoki—108(L)
Scattering by He, H. Staub, W. E. Stephens—131; 235(A)
Scattering in ortho- and parahydrogen, L. W. Alvarez, K. S. Pitzer—596(A)
Slowing down by heavy nuclei, G. Placzek—1138(A)
Transmission of medium fast neutrons, R. B. Roberts, P. Wang—596(A)
Transmission through crystals, M. D. Whitaker, H. G. Beyer—1101(L)
Yields from p–n reactions in Li and Be, J. E. Hill—1117(A)

Nuclear moments and spin (see also **Hyperfine structure**)
Basis of α-particle model, R. G. Sachs—825; 1131(A)
Of Be^9, P. Kusch, S. Millman, I. I. Rabi—666(L)
Of Cs, P. Kusch, S. Millman—596(A)
And liquid-drop model, K. Way—963
Of Mn, R. A. Fisher, E. R. Peck—270
From multiplets, R. A. Fisher—1112(A)
Of N^{14}, Na^{23}, K^{39} and Cs^{133}, P. Kusch, S. Miliman, I. I. Rabi—1176
Of H^1 and H^2, J. M. B. Kellogg, I. I. Rabi, N. F. Ramsey, Jr., J. R. Zacharias—318(L); 595(A)
Quadrupole moment of In^{115}, D. R. Hamilton, N. A. Renzetti—680(A)
Resonance experiments on H_2 and D_2, I. I. Rabi, J. R. Zacharias, N. F. Ramsey, Jr., J. M. B. Kellogg—595(A)
Rotational magnetic moment of H_2 and D_2, N. F. Ramsey, Jr.—595(A)
Of Rb and Cl, P. Kusch, S. Millman—680(A)
Signs of nuclear magnetic moments by molecular beam, S. Millman—628
Of Na^{23} and K^{39}, S. Millman, P. Kusch—596(A)
Of $_3Li^6$, $_3Li^7$ and $_9F^{19}$, I. I. Rabi, S. Millman, P. Kusch, J. R. Zacharias—526

Nuclear structure (see also **Disintegration of nucleus**)
Analysis of binding energies, W. H. Barkas—691
Binding energy of H^2, F. T. Rogers, Jr., M. M. Rogers—106(L); 263
Binding energy of He^5, W. A. Tyrrell, Jr.—678(A)
Binding energy of He^6, H. Margenau—678(A); 1173
Energy of isobaric nuclei, J. G. Fox, E. C. Creutz, M. G. White, L. A. Delsasso—1106
Binding energy of Li^7, K. G. Carroll—1128(A)
Energies of light nuclei, W. A. Tyrrell, Jr., K. G. Carroll, H. Margenau—790(L)
Energy of $4n$-nuclei, B. O. Grönblom, R. E. Marshak—229(L)
Energy levels in B^{10}, P. G. Kruger, F. W. Stallmann, W. E. Shoupp—1129(A)
Energy levels of H^3, He^3 and He^5, K. Way—678(A)
Excited state of C^{13}, J. R. Richardson—1129(A)
γ-radiation from B, E. R. Gaerttner, W. A. Fowler, C. C. Lauritsen—27; J. Halpern, H. R. Crane—415(L)
γ-rays from Al, G. J. Plain, R. G. Herb, R. E. Warren—1135(A)
Internal conversion of γ-rays, S. M. Dancoff, P. Morrison—122
Iteration method, oxygen problem, G. Horvay—70; 604(A)
Liquid-drop model, K. Way—963
Many-body interactions in nuclear systems, H. Primakoff, T. Holstein—1218
Meson potentials, G. Breit, L. E. Hoisington, S. S. Share, H. M. Thaxton—1103(L); S. Share, L. E. Hoisington, G. Breit—1130(A)
Meson theory of nuclear forces, H. A. Bethe—1130(A); 1261
Nuclear forces from field theories, E. Feenberg—602(A)
Nuclear models, H. Brown, D. R. Inglis—1182
Quadrupole moment of H^2, R. F. Christy, S. Kusaka—665(L)
Range of forces, D. R. Inglis—988(L)
Related magnetic moments, D. R. Inglis—329
Resonance levels of I and In, J. Hornbostel, F. A. Valente—108(L)
Shape and stability of heavy nuclei, E. Feenberg—504(L); G. Young—1102(L)
Stability of $_4Be^8$, S. K. Allison, E. R. Graves, L. S. Skaggs, N. M. Smith, Jr.—107(L)
Widths of energy levels, J. H. Manley, H. H. Goldsmith, J. Schwinger—39

Optical constants and properties
Dispersion of water, L. L. Skolil—880(L)
Infra-red pleochroism, CH_2 groups, J. W. Ellis, J. Bath—1098
Of K at low temperatures, D. M. Packer—1121(A)
Reflecting power of multilayer films, C. H. Cartwright, A. F. Turner—1128(A)
Reflection from glass, multilayer films, C. H. Cartwright, A. F. Turner—675(A)
Reflectivities of evaporated metal films, G. B. Sabine—1064
Scattering of light by water, L. H. Dawson, E. O. Hulburt—1128(A)

Optical theory
Wide-angle interference experiments, F. W. Doermann, O. Halpern—486; 681(A)

Packing fraction (see also **Isotopes**)
Of heavy elements, A. C. Graves—863

Paschen-Back effect
Of Ne, J. B. Green, J. A. Peoples, Jr.—1147(A)

Phosphorescence
Decay after electron bombardment, R. B. Nelson, R. P. Johnson—592(A)
Decay of willemite, R. P. Johnson—881(L)
Light output and current density, E. G. Ramberg, G. A. Morton—409(L)

Photoconductivity
Of crocoite crystals, J. J. Brady, W. H. Moore—424(A)
Of metal films, T. C. Wilson—316(L)
Photoelectric effect and properties; cells
Of the deuteron, L. Eisenbud—1129(A)
Surface and volume emission from Ba, R. J. Cashman, E. Bassoe—63
Photoionization
γ-ray ion currents in air, J. W. Broxon, G. T. Merideth—883
Photovoltaic effect
Actinoelectric effects in tartaric acid crystals, J. J. Brady, W. H. Moore—308
Piezoelectric effect
Constants of Rochelle salt, W. P. Mason—775; 1141(A)
Striated luminous glow on quartz, J. R. Harrison, I. P. Hooper—674(A)
Positrons
Creation by fast electrons, H. R. Crane, J. Halpern—838
Proceedings of the American Physical Society
Chicago Meeting, November 25–26, 1938—232
Los Angeles Meeting, December 19, 1938—420
New York State Section, November 5, 1938—513
Washington, D. C., Meeting, December 27–29, 1938—589
New York Meeting, February 23–25, 1939—671
Metropolitan Section, March 24, 1939—801
Washington, D. C., Meeting, April 27–29, 1939—1109

Quantum mechanics (see **Mechanics, quantum**)
Quenching of radiation
Of Hg resonance radiation, L. O. Olsen—1126(A)

Radiation
Emissivity of tantalum, L. Malter, D. B. Langmuir—743
Radio
Absorption and reradiation by resonators, C. R. Fountain, E. G. Pigg—592(A)
Nature of fade-out, L. V. Berkner—536; D. F. Martyn—983(L)
Oscillation of close-coupled circuits, R. R. Ramsey, W. L. Chenault, L. E. Long—239(A)
Velocity of waves, G. H. Brown—1100(L); A. L. Vitter, L. C. Brieger—416(L)
Radioactivity (see also **Disintegration of nucleus**)
Activity of Mn by H^1, A. Hemmendinger—604(A)
Of Sb, J. J. Livingood, G. T. Seaborg—414(L)
Of Be^7, J. E. Hill, G. E. Valley—678(A)
β- and γ-ray spectra of Cu^{64} and Eu^{152}, A. W. Tyler—1136(A)
β-decay of N^{13}, B. O. Grönblom—1130(A)
β-radiations of Rb, W. F. Libby, D. D. Lee—245
β-ray spectra of P, Na and Co, J. L. Lawson—1136(A)
β-ray spectrum of N^{13}, E. M. Lyman—234(A); 1123(A)
β-ray theory, A. I. Alichanian, V. Berestezky—978(L)
β-rays of mesothorium and RaD, D. D. Lee, W. F. Libby—252
β-rays from K, W. J. Henderson—238(A)
β-spectra of I, G. F. Tape—1135(A)
β-spectrum of ThC'' and ThB, A. Zavelsky—317(L)
Of Br^{80}, D. C. DeVault, W. F. Libby—322(L)
Of Cd and In, J. M. Cork, J. L. Lawson—1136(A)
Coincidences between β-rays and γ-rays, L. M. Langer, A. C. G. Mitchell, P. W. McDaniel—1123(A)
Constancy of activity of K^{40}, A. K. Brewer—669(L)
Double β-disintegration, theory of neutrino, W. H. Furry—602(A)
Effect of cosmic rays, W. R. Smythe—316(L)
Einstein's field equations for spheres of fluid, R. C. Tolman—364
Equilibrium of spheres, G. M. Volkoff—413(L)
Excitation of In by x-rays, G. B. Collins, B. Waldman, E. M. Stubblefield, M. Goldhaber—507(L); 1129(A)
Excitation by neutrons, M. Goldhaber, R. D. Hill, L. Szilard—47
Excitation by protons, S. W. Barnes, P. W. Aradine—50
Of fission products from U, P. Abelson—670(L); G. N. Glasoe, J. Steigman—982(L); E. McMillan—510(L)
γ-radiation from Co, B. R. Curtis—1136(A)
γ-rays from Au^{198}, Eu^{152}, Ag^{106}, Cu^{64} and N^{13}, J. R. Richardson—609
γ-rays from RaE, J. A. Gray—586(L)
Geological age measurements, A. V. Grosse—584(L); A. O. Nier—153
Induced by $_1H^1$ in Cu, Ni, Ag, A and Mo, L. A. Delsasso, L. N. Ridenour, R. Sherr, M. G. White—113
Induced in Cd and In by H^1, S. W. Barnes—241(A)
Interval conversion electrons from Br^{80}, G. E. Valley, R. L. McCreary—666(L)
Of Fe^{55}, J. J. Livingood, G. T. Seaborg—1268(L)
Isomerism and chemical separation in Te, G. T. Seaborg, J. W. Kennedy—410(L)
Isomerism in $_{43}$Ma, G. T. Seaborg, E. Segrè—808
Isomers of Br, L. I. Roussinov, A. A. Yusephovich—979(L)
Of isomers of Ag^{106}, T. Enns—1118(A)
Isomers of Sr, D. W. Stewart—674(A)
Isotopes of Cu, Zn, Ga and Ge, R. Sagane—31
Isotopes of element 43, B. N. Cacciapuoti—110(L)
Isotopes of Zn, J. J. Livingood, G. T. Seaborg—457
Of Li^8, C. Kittel—515
Of Mo, D. Ewing, T. Perry, R. McCreary—1136(A)
Natural fission of Th and U, W. F. Libby—1269(L)
Periods of Sn, J. J. Livingood, G. T. Seaborg—667(L)
K-electron capture in Ag^{106}, J. R. Richardson—236(A)
Probability of p–n and p–γ reactions, C. V. Strain—679(A)
Production by α-particles, L. D. P. King, W. J. Henderson, J. R. Risser—1118(A)
Radioactive content of atmosphere, G. R. Wait—591(A)
Radon content of spring waters, J. L. Bohn, F. H. Nadig—685(A)
Recoil of nucleus in β-disintegration, J. Halpern, H. R. Crane—1123(A)
Of Re, K. Sinma, F. Yamasaki—320(L)
Of Te; isomers, G. T. Seaborg, J. J. Livingood, J. W. Kennedy—794(L)
Raman spectra
Depolarization factors, F. F. Cleveland, M. J. Murray, J. Shackelford, H. H. Haney—1146(A)

Depolarization measurements, F. F. Cleveland, M. J. Murray—1113(A)
In difluorochloromethane, G. Glockler, J. H. Bachmann —669(L)
Of fluorochloromethane, G. Glockler, J. H. Bachmann— 1273(L)
Of gaseous amines, J. S. Kirby-Smith, L. G. Bonner— 1114(A)
Of phenyl-1-propyne-1 and chloro-2-phenyl-1-acetylene, F. F. Cleveland, M. J. Murray—600(A)

Relativity
Equilibrium of spheres, J. R. Oppenheimer, G. M. Volkoff—374; R. C. Tolman—364; G. M. Volkoff— 413(L); 421(A)
General theory and flat space, N. Rosen—681(A)
Modification of special relativity, C. H. Page—1131(A)

Resistance, electrical (see **Electrical conductivity and resistance**)

Resonance radiation
Of Hg, quenching, L. O. Olsen—1126(A)

Scattering of atoms and molecules (see also **Atomic and molecular beams**)
Of K and K_2 in gases, P. Rosenberg—1267(L)

Scattering of electrons, neutrons and ions (see also **Electrons, scattering of; Electron diffraction**)
Analysis of scattering of H^1 by H^1, G. Breit, H. M. Thaxton, L. Eisenbud—603(A); 1018
Angular distribution of neutrons, Seishi Kikuchi, Hiroo Aoki, Tetuo Wakatuki—1264(L)
Cross sections of metallic U for neutrons, M. D. Whitaker, C. A. Barton, W. C. Bright, E. J. Murphy— 793(L)
Cross sections for slow neutrons, M. D. Whitaker, H. G. Beyer—1124(A)
Depolarization effects for electrons, M. E. Rose, H. A. Bethe—601(A)
Determination of force fields, F. C. Hoyt—664(L)
Of D–D neutrons, S. Seely, W. H. Zinn, V. W. Cohen— 679(A)
Electron scattering, radiative corrections, S. M. Dancoff —959
Erratum: The scattering of α-particles by argon, oxygen, and neon, G. Brubaker—877(L)
Of fast β-particles by nuclei, F. C. Champion, A. Barber —111(L)
Of fast electrons in gases, J. H. Bartlett, R. E. Watson— 235(A); A. L. Hughes—350
Of fast neutrons, Hiroo Aoki—795(L)
Of fast neutrons by Pb, R. F. Bacher—679(A)
Internal scattering of β-rays, G. E. M. Jauncey—237(A)
Neutron-alpha and alpha-proton scattering, H. Primakoff, H. H. Goldsmith—1117(A)
Neutron-proton cross section, L. Simons—792(L)
Of neutrons in crystals, O. Halpern, M. Hamermesh, M. H. Johnson—1125(A)
Of neutrons in ferromagnetics, temperature dependence, F. Bloch—1118(A)
Of neutrons in He, W. E. Shoupp, P. G. Kruger, F. W. Stallmann, G. H. Gamertsfelder—1118(A); H. Staub, W. E. Stephens—131; 235(A)
Of neutrons by H_2 and D_2, M. Hamermesh, J. Schwinger —679(A)
Of neutrons by protons, V. W. Cohen, H. H. Goldsmith —597(A); E. O. Salant, R. B. Roberts, P. Wang— 984(L)
Of neutrons by ortho- and parahydrogen, L. W. Alvarez, K. S. Pitzer—596(A); W. F. Libby, E. A. Long—339
Polarization, absence of, M. E. Rose, H. A. Bethe—277
Proton-proton scattering, N. P. Heydenburg, L. R. Hafstad, M. A. Tuve—603(A)
Proton-proton scattering, experimental, R. G. Herb, D. W. Kerst, D. B. Parkinson, G. J. Plain—603(A); 998
Of H^1 by Li, E. C. Creutz—679(A); 819
Of slow neutrons by U, H. H. Goldsmith, V. W. Cohen, J. R. Dunning—1124(A)

Secondary electrons (see **Electrons, secondary**)

Solid state (see **Crystalline state**)

Spark discharge (see **Discharge of electricity, etc.**)

Specific heat
Of monatomic liquids, W. J. Archibald—1139(A)
Of Ta, D. B. Langmuir, L. Malter—1138(A)

Spectra, absorption
Of NH_3 perpendicular vibrations, E. F. Barker—657
Of fatty acids, infra-red, R. C. Herman, R. Hofstadter— 683(A)
Of heavy benzene at 2730–2250A, H. Sponer—683(A)
Of heavy water vapor, N. Fuson, H. M. Randall, D. M. Dennison—590(A)
Of HS, M. N. Lewis, J. U. White—894
Of hydroxyl groups, infra-red, J. W. Ellis—597(A)
Intensities in benzene vapor, C. A. Beck, W. F. Radle— 1120(A)
Of liquid water at 2.52μ, J. R. Collins—470
Of methylamine, infra-red, L. G. Bonner, A. P. Cleaves, H. Sponer—1113(A); A. P. Cleaves, E. K. Plyler— 1113(A); R. G. Owens, E. F. Barker—1119(A)
Of phenol vapor, infra-red, V. Williams, R. C. Herman, R. Hofstadter—684(A)
Of silver halides, N. Metropolis, H. Beutler—1113(A)
Of Ag I, ultraviolet, N. Metropolis—239(A); 636
Of substituted benzenes, A. L. Sklar—1120(A)
Of thiocyanates, D. Williams—1120(A)

Spectra, atomic
Of Ce II, W. E. Albertson, G. R. Harrison—1119(A)
Excitation of O^{++}, M. H. Hebb—1114(A)
Fine structure of Hα and Dα, S. Pasternack—421(A); C. F. Robinson—423(A)
Fine structure of λ4686 of He II, Djen-Yuen Chu— 423(A)
Intensities of singlet-singlet and singlet-triplet transitions, G. W. King, J. H. Van Vleck—1120(A)
Lines and terms in ionized K, Cu, Sc and Ti, L. W. Phillips—708
New terms in Fe, L. C. Green—1209
Nitrogen forbidden line, R. Bernard—511(L); J. Kaplan —598(A)
Of K, Ca and Sc, P. G. Kruger, L. W. Phillips—352
Recombination spectrum of Hg, R. C. Garth, G. E. Moore, H. W. Webb—677(A); energy distribution —677(A)

Spectra, atomic (continued)
Self-consistent field for Cr II, R. L. Mooney—557; 598(A)
Of V I in violet, C. E. Moore—710
Spectra, general
Intensity of lines in Hg arc, O. S. Duffendack, O. G. Koppius—1199
Spectra, molecular (see also **Molecular structure and constants**)
Of H_2 and D_2, H. M. James, A. S. Coolidge—184; 234(A)
Intensities in halide spectra, R. S. Mulliken—239(A)
Intensities in H_2 spectrum, N. Ginsburg—1112(A)
Interaction between rotation and oscillation, H. H. Nielsen—289
Magnetic rotation spectra of SO_2 and CS_2, P. Kusch, F. W. Loomis—850
Of $N^{14}H$, $N^{15}D$ and N^{15}, R. W. Wood, G. H. Dieke—1120(A)
In N_2, O. R. Wulf, E. H. Melvin—600(A); 687
NH bands in night sky, J. Kaplan—583(L)
Of SnH, W. W. Watson, R. Simon—358
Vibration-rotation energies in XY_4, W. H. Shaffer, H. H. Nielsen, L. H. Thomas—878(L)
Of SnH and PbH, W. W. Watson, R. Simon—677(A)
Spectroscopy, technique
Spectrophotometer, infra-red, J. D. Hardy, A. I. Ryer—1112(A)
Spinor analysis
Fundamental space-time coordinates, E. E. Witmer—1132(A)
Structure factor
For zinc crystals, E. M. McNatt, G. E. M. Jauncey—237(A)
Superconductivity (see **Electrical conductivity**)

Thermal conductivity
Of metallic contacts, C. Starr, R. B. Jacobs—684(A)
Of solid or molten metals, C. C. Bidwell—1139(A)
Thermionic emission of electrons; Emitting surfaces
Thermionic cathode for gaseous discharge tubes, A. W. Hull—1145(A)
Time changes in oxide-coated cathodes, J. P. Blewett—713
Of W for various crystallographic directions, M. H. Nichols—1144(A)
Thermodynamics
Equilibrium and microscopic entropy, E. C. Kemble—602(A)

Van der Waals forces
In B molecule, J. K. Knipp—601(A)
And calculation of polarizabilities, J. K. Knipp—1244
In He, H. Margenau—1137(A)
Repulsive forces in adsorption, W. G. Pollard—1137(A)
Vapor pressure
Of BaO, J. P. Blewett, H. A. Liebhafsky, E. F. Hennelly—1138(A)
Virial coefficient
Of He gas for the lowest measured temperature, L. Gropper—1095
Viscosity
Of air, E. L. Harrington—230(L)
In an expanding bubble, E. C. Westerfield, W. B. Pietenpol—306
In two-dimensional systems, E. Boyd, W. D. Harkins—1131(A)

X-rays, absorption
Chemical binding and absorption edges, R. Landshoff—631
Of Fe, Ni, Cu and Zn, H. Friedman, W. W. Beeman—1115(A)
L_{III} absorption of I, Ba, and Ba compounds, E. H. Green—1072
X-rays, diffraction, scattering, reflection, refraction and polarization
Diffraction by liquid ethyl alcohol, G. G. Harvey—1115(A)
Diffraction by liquid K, N. S. Gingrich, C. N. Wall—1116(A)
Diffraction by liquid sulphur, N. S. Gingrich—236(A)
Diffraction by liquid Sn and liquid Cl, C. Gamertsfelder—1116(A)
Diffuse scattering from single crystals, O. J. Baltzer, E. M. McNatt—237(A)
Diffuse scattering from Zn, G. E. M. Jauncey, E. M. McNatt—498
Discontinuities in diffuse scattering, G. G. Harvey—1147(A)
Dynamical theory, W. H. Zachariasen—241(A)
Laue patterns, effect of quartz filters, G. W. Fox, D. W. Stebbins—405
Particle size determination, C. Nusbaum—1115(A)
Trigonometric interpolation, C. Lanczos, G. C. Danielson—242(A)
X-rays, emission (see also **X-rays, spectra and spectroscopy**, etc.)
$L\alpha$ satellites, R. E. Shrader, F. K. Richtmyer—605(A)
$L\alpha$ satellites, L. G. Parratt, C. A. Randall—1114(A)
K ionization of Ni, D. L. Webster, L. T. Pockman, K. Harworth, P. Kirkpatrick—682(A)
Ag L-series lines from K Auger transitions, C. J. Burbank—421(A)
Spectra of valence electrons, H. W. B. Skinner, H. M. O'Bryan—604(A)
X-rays, tubes, apparatus
High vacuum spectrometer, J. H. Munier—1116(A)
Measurement of x-ray production, M. I. T. generator, L. C. Van Atta, D. L. Northrup—681(A)
Memorial Hospital installation, G. Failla—677(A)
Pressure-insulated electrostatic x-ray generator, J. G. Trump, R. J. Van de Graaff—676(A)

Zeeman effect
At fields of 100,000 gauss, G. R. Harrison, F. Bitter—1125(A)
Forbidden lines of K, F. A. Jenkins, E. Segrè—545
Quadratic effect, F. A. Jenkins, E. Segrè—52; 420(A); theory, L. I. Schiff, H. Snyder—59; 421(A)
Theory of Paschen-Back, J. B. Green, J. F. Eichelberger—1126(A)
In W; line λ4659, J. H. Roberson, J. E. Mack—1126(A)

VOLUME 55 SECOND SERIES

CONTENTS

JANUARY 1, 1939

Galactic Rotation and the Intensity of Cosmic Radiation at the Geomagnetic Equator . . . M. S. VALLARTA, C. GRAEF AND S. KUSAKA 1

Nature of the Penetrating Cosmic Rays . . . VOLNEY C. WILSON 6

Critical Analysis for Sidereal Time Variations of Cosmic Rays on the Pacific . . . JULIAN L. THOMPSON 11

On the Penumbra of Cosmic Radiation . . . R. ALBAGLI HUTNER 15

New Evidence for the Existence of Penetrating Neutral Particles . . . FRANCIS R. SHONKA 24

Gamma-Radiation from Boron Bombarded by Deuterons . . . E. R. GAERTTNER, W. A. FOWLER AND C. C. LAURITSEN 27

Radioactive Isotopes of Cu, Zn, Ga and Ge . . . R. SAGANE 31

Widths of Nuclear Energy Levels . . . J. H. MANLEY, H. H. GOLDSMITH AND JULIAN SCHWINGER 39

Radioactivity Induced by Nuclear Excitation. I. Excitation by Neutrons . . . M. GOLDHABER, R. D. HILL AND LEO SZILARD 47

Radioactivity Induced by Nuclear Excitation. II. Excitation by Protons . . . S. W. BARNES AND P. W. ARADINE 50

Quadratic Zeeman Effect . . . F. A. JENKINS AND E. SEGRÈ 52

Theory of the Quadratic Zeeman Effect . . . L. I. SCHIFF AND H. SNYDER 59

Surface and Volume Photoelectric Emission from Barium . R. J. CASHMAN AND ELSE BASSOE 63

On the Iteration Method and Its Application to the Oxygen Problem . . GABRIEL HORVAY 70

Dissipative Acoustic Reflection Coefficients in Gases by Ultrasonic Interferometry . . . R. S. ALLEMAN 87

Field Theory of Elementary Particles . . . N. ROSEN 94

Letters to the Editor:

On the Change of Magnetic Properties of the Single Crystal of Nickel Due to Temperature . . . T. OKAMURA AND T. HIRONE 102

Energy Production in Stars . . . H. A. BETHE 103

Difference in the Absorption of Cosmic Rays in Air and Water and the Instability of the Barytron . . . THOMAS H. JOHNSON AND MARTIN A. POMERANTZ 104

Ferromagnetism of Semi-Conductors . . . SYÔHEI MIYAHARA 105

Mesotron as the Name of a New Particle . . . ROBERT A. MILLIKAN 105

New Determination of the Binding Energy of the Deuteron . . . F. T. ROGERS, JR. AND MARGUERITE M. ROGERS 106

Neutron-Proton Scattering Cross Section . . . VICTOR W. COHEN, H. H. GOLDSMITH AND JULIAN SCHWINGER 106

Resonance Absorption of Slow Neutrons in Indium . . . J. H. MANLEY, H. H. GOLDSMITH AND JULIAN SCHWINGER 107

Precise Measurement of the Mass Difference $_4Be^9$—$_4Be^8$; The Stability of $_4Be^8$ . . . SAMUEL K. ALLISON, ELIZABETH R. GRAVES, LESTER S. SKAGGS AND NICHOLAS M. SMITH, JR. 107

On the Resonance Levels for Neutron Capture of Iodine and Indium . . . J. HORNBOSTEL AND F. A. VALENTE 108

Scattering of the D—D Neutrons . . . SEISHI KIKUCHI AND HIROO AOKI 108

New Periodic Orbit in the Field of a Magnetic Dipole . . . R. ALBAGLI HUTNER 109

Dellinger Phenomenon . . . JOSEPH KAPLAN 110

Radioactive Isotopes of Element 43 . . . B. N. CACCIAPUOTI 110

Comment on a Paper by W. E. Bowls, "Second Townsend Coefficient" . . . JOSEPH KAPLAN 111

Elastic Scattering of Fast β-Particles by Atomic Nuclei . . . F. C. CHAMPION AND A. BARBER 111

Absorption of Slow Neutrons of Different Energies by B, Co and Mn . . . E. O. SALANT, W. J. HORVATH AND H. I. ZAGOR 111

Remark on the Latitude Effect of Cosmic Rays . . . B. GROSS 112

JANUARY 15, 1939

Artificial Radioactivity Produced by Protons . . . L. A. DELSASSO, L. N. RIDENOUR, R. SHERR AND M. G. WHITE 113

Calculation of Internal Conversion Coefficients . . . S. M. DANCOFF AND P. MORRISON 122

Anomalous Scattering of Neutrons by Helium . . . H. STAUB AND W. E. STEPHENS 131

Angular Distribution of the Disintegration Products of Light Elements . . . R. O. HAXBY, J. S. ALLEN AND J. H. WILLIAMS 140

Note on the Disintegration of Boron by Protons . . . . . E. L. Hill and R. O. Haxby 147
Isotopic Constitution of Uranium and the Half-Lives of the Uranium Isotopes. I . . . . . Alfred O. Nier 150
Isotopic Constitution of Radiogenic Leads and the Measurement of Geological Time. II . . . . . Alfred O. Nier 153
Sensitized Fluorescence of Potassium . . . . . Ernst H. Krause 164
Hyperfine Structure of Gold . . . . . R. M. Elliott and J. Wulff 170
Fine Structure of the Line λ4686 of Ionized Helium . . . . . Djen-Yuen Chu 175
Infra-Red Spectrum and Molecular Constants of Carbon Monoxide . . . . . S. E. Whitcomb and R. T. Lagemann 181
Continuous Spectra of H_2 and D_2 . . Hubert M. James and Albert Sprague Coolidge 184
Capture of Neutrons by Atoms in a Crystal . . . . . Willis E. Lamb, Jr. 190
Convection Currents in Arcs in Air . . . . . C. G. Suits 198
Probability of Ionization of Mercury Atoms by Collision with Low Velocity Electrons . . . . . Maurice E. Bell 201
Ionization and Excitation in Mercury Vapor Produced by Electron Bombardment . . . . . W. B. Nottingham 203
Spark Breakdown Potentials as a Function of the Product of the Pressure by the Plate Separation in A, N_2 and H_2 for Pt and Na Cathodes . . . . . Florence Ehrenkranz 219

Letters to the Editor:

New Form of Band Igniter for Mercury-Pool Tubes . . . . . Kenneth J. Germeshausen 228
Silver Films on a Mica Crystal Face . . . . . Sanford Essig 229
Binding Energy of $4n$-Nuclei on the α-Particle Model . . B. O. Grönblom and R. E. Marshak 229
Viscosity of Air . . . . . E. L. Harrington 230
Self-Diffusion in Copper . . . . . B. V. Rollin 231

Proceedings of the American Physical Society

Chicago Meeting, November 25–26, 1938; Minutes and Abstracts 1–48; Author Index 232

February 1, 1939

Energies of the Soft Beta-Radiations of Rubidium and Other Bodies. Method for their Determination . . . . . W. F. Libby and D. D. Lee 245
Beta-Rays of Mesothorium 1 and Radium D . . . . . D. D. Lee and W. F. Libby 252
Absorption Coefficient of 5.8-Mev Gamma-Radiation in Aluminum . . . . . J. Halpern and H. R. Crane 258
Pair Internal Conversion Coefficient in the F+H′ Reaction and Measurements on the Gamma-Ray Spectrum . . . . . J. Halpern and H. R. Crane 260
Independent Determination of the Binding Energy of the Deuteron . . . . . F. T. Rogers, Jr. and Marguerite M. Rogers 263
Hyperfine Structure of Manganese I and Nuclear Magnetic Moment . . . . . Russell A. Fisher and Edson R. Peck 270
On the Absence of Polarization in Electron Scattering . . . M. E. Rose and H. A. Bethe 277
Interaction Between Rotation and Oscillation in Deutero-Formaldehyde . Harald H. Nielsen 289
Temperature Distribution in the High Pressure Mercury Discharge Tube . . W. Elenbaas 294
Study of Beta-Brass in Single Crystal Form . . . . . Wayne Webb 297
Viscosity in an Expanding Bubble . . . Everett C. Westerfield and W. B. Pietenpol 306
Actinoelectric Effects in Tartaric Acid Crystals . James J. Brady and William H. Moore 308
Shape of the Domains in Ferromagnetics . . . . . E. H. Kennard 312

Letters to the Editor:

On the Interchange Energy of Two Free Electrons . . . . . Carl A. Ludeke 315
Cosmic Rays and Radioactive Potassium . . . . . W. R. Smythe 316
Photoconductivity of Metal Films . . . . . Thomas C. Wilson 316
On the Upper Limit of the β-Spectrum of ThC″ and ThB . . . . . A. Zavelsky 317
Electrical Quadrupole Moment of the Deuteron . . . . . J. M. B. Kellogg, I. I. Rabi, N. F. Ramsey, Jr. and J. R. Zacharias 318
Thermal Dilatation of Superconductors . . . . . E. C. Westerfield 319
β-Radioactivities of Rhenium . . . . . K. Sinma and F. Yamasaki 320
Effect of Hydroxyl Ion Concentration (or of pH) on the Film Potentials of Multilayers . . . . . William D. Harkins and Richard W. Mattoon 320
Chemical Separation of Nuclear Isomers . . E. Segrè, R. S. Halford and G. T. Seaborg 321
Evidence for the Gamma-Radioactivity of a 4.5-hour Br^{80} from Radiobromate . . . . . Don C. DeVault and W. F. Libby 322

FEBRUARY 15, 1939

Efficiency of Production of Short Range Particles from Lithium and of 4.4-cm Alpha-Particles from Boron Under Proton Bombardment . . . . . RALPH B. BOWERSOX 323
On Interpreting Related Magnetic Moments of Light Nuclei . . . . . D. R. INGLIS 329
Emission of Secondary Electrons from Metals Bombarded with Protons . . JAMES S. ALLEN 336
Scattering of Slow Neutrons by Gaseous Ortho- and Parahydrogen: Spin Dependence of the Neutron-Proton Force . . . . . W. F. LIBBY AND EARL A. LONG 339
Atomic Electron Velocities in Nitrogen and Methane . A. L. HUGHES AND MERLE A. STARR 343
Scattering of Fast Electrons in Gases . . . . . A. L. HUGHES 350
Sodium-Like Spectra of Potassium, Calcium and Scandium . . . . . P. GERALD KRUGER AND L. W. PHILLIPS 352
Spectrum of Tin Hydride at High Pressure . . WILLIAM W. WATSON AND RALPH SIMON 358
General Solution for the Equations of Natural Line Breadth . . . . LYMAN SPITZER, JR. 361
Static Solutions of Einstein's Field Equations for Spheres of Fluid . . RICHARD C. TOLMAN 364
On Massive Neutron Cores . . . . . J. R. OPPENHEIMER AND G. M. VOLKOFF 374
Mechanism of the Positive Point-to-Plane Corona in Air at Atmospheric Pressure . . . . . G. W. TRICHEL 382
Use of Interference to Extinguish Reflection of Light from Glass . KATHARINE B. BLODGETT 391
Effect of Quartz Filters on the Distribution of Energy in Laue Patterns . . . . . GERALD W. FOX AND DEAN W. STEBBINS 405

Letters to the Editor:

Variation of Light Output with Current Density and Classification of Willemite Phosphors . . . . . E. G. RAMBERG AND G. A. MORTON 409
Inner, Initial Permeability of Iron and Nickel from 98 to 410 Megacycles . . . . . J. BARTON HOAG AND N. GOTTLIEB 410
Nuclear Isomerism and Chemical Separation of Isomers in Tellurium . . . . . G. T. SEABORG AND J. W. KENNEDY 410
Note on the Biological Effects of Densely Ionizing Radiation . . . . . K. G. ZIMMER AND N. W. TIMOFÉEFF-RESSOVSKY 411
Theory of Electrodisintegration of Beryllium . . . . . EUGENE GUTH 411
Electrodisintegration of Beryllium . . . . . GEORGE B. COLLINS, BERNARD WALDMAN AND WILLIAM R. POLYE 412
Advantages of Scaling Circuits in Recording Random Counts . . . . . HAROLD LIFSCHUTZ AND O. S. DUFFENDACK 412
On the Equilibrium of Massive Spheres . . . . . G. M. VOLKOFF 413
Latitude Effect for Very Large Cosmic-Ray Bursts . . WILLIAM P. JESSE AND PIARA S. GILL 414
Radioactive Antimony from I+n and Sn+D . . . . . J. J. LIVINGOOD AND G. T. SEABORG 414
Gamma-Rays from B+D . . . . . J. HALPERN AND H. R. CRANE 415
Velocity of Radio Waves in Air . . . . . A. L. VITTER AND L. C. BRIEGER 416
Droplet Fission of Uranium and Thorium Nuclei . . . . . R. B. ROBERTS, R. C. MEYER AND L. R. HAFSTAD 416
Heavily Ionizing Particles from Uranium . . . . . G. K. GREEN AND LUIS W. ALVAREZ 417
Intensely Ionizing Particles Produced by Neutron Bombardment of Uranium and Thorium . . . . . R. D. FOWLER AND R. W. DODSON 417
Cleavage of the Uranium Nucleus . . . . . PHILIP ABELSON 418
Resonance in Uranium and Thorium Disintegrations and the Phenomenon of Nuclear Fission . . . . . N. BOHR 418

Proceedings of the American Physical Society:

Los Angeles Meeting, December 10, 1938; Minutes and Abstracts 1–19; Author Index 420

MARCH 1, 1939

On the Motion of Cosmic Rays in Interstellar Space . . . . . HANNES ALFVÉN 425
Long Period Variations of Cosmic Rays . . . . . PIARA S. GILL 429
Energy Production in Stars . . . . . H. A. BETHE 434
Radioactive Isotopes of Zinc . . . . . J. J. LIVINGOOD AND G. T. SEABORG 457
Emission of Secondary Electrons Under High Energy Positive Ion Bombardment . . . . . A. G. HILL, W. W. BUECHNER, J. S. CLARK AND J. B. FISK 463
New Infra-Red Absorption Band of Liquid Water at 2.52μ . . . . . J. R. COLLINS 470
Energy Distribution in Field Emission . . JOSEPH E. HENDERSON AND R. K. DAHLSTROM 473
Sparking Potentials at Low Pressures . . . . . ROBERT B. QUINN 482

Theoretical Evaluation of a Wide-Angle Interference Experiment . . . F. W. DOERMANN AND O. HALPERN 486
On the Origin of the Earth's Magnetic Field . . . WALTER M. ELSASSER 489
Thermal Vibrations and Atomic Structure of Zinc Crystals at 100° and 298°K . . . G. E. M. JAUNCEY AND E. M. MCNATT 498
Attempt to Observe the Absorption of Neutrinos . . . H. R. CRANE 501

Letters to the Editor:

East-West Asymmetry of the Cosmic Radiation at Very High Elevations Near the Equator . . . T. H. JOHNSON AND J. G. BARRY 503
Electrical Discharge Between a Stationary and a Rotating Electrode . . . J. W. BEAMS AND L. B. SNODDY 504
On the Shape and Stability of Heavy Nuclei . . . EUGENE FEENBERG 504
Ferromagnetic Anisotropy in Nickel-Iron Crystals. Evidence for Super-Structure near Ni_3Fe . . . L. W. MCKEEHAN AND E. M. GRABBE 505
Lifetime of the Yukawa Particle . . . L. W. NORDHEIM 506
Scattering of Cosmic Rays by the Stars of a Galaxy . . . M. S. VALLARTA AND R. P. FEYNMAN 506
Nuclear Excitation of Indium by X-Rays . . . GEORGE B. COLLINS, BERNARD WALDMAN, EDWARD M. STUBBLEFIELD AND M. GOLDHABER 507
Electro-Optical Effects in Colloids . . . HANS MUELLER 508
Note on Reduction for the Rotation Group . . . J. M. KELLER 508
Disintegration of Uranium . . . D. R. CORSON AND R. L. THORNTON 509
Radioactive Recoils from Uranium Activated by Neutrons . . . EDWIN MCMILLAN 510
Further Observations on the Splitting of Uranium and Thorium . . . R. B. ROBERTS, R. C. MEYER AND P. WANG 510
Presence of the Nitrogen Forbidden Line $^2P \rightarrow {}^4S$ in the Auroral Spectrum . . . RENÉ BERNARD 511
Fission of Uranium . . . H. L. ANDERSON, E. T. BOOTH, J. R. DUNNING, E. FERMI, G. N. GLASOE AND F. G. SLACK 511

Proceedings of the New York State Section of the American Physical Society, November 5, 1938 513

MARCH 15, 1939

Radioactivity of Li^8 . . . CHARLES KITTEL 515
Total Secondary Electron Emission from Tungsten and Thorium-Coated Tungsten . . . EDWARD A. COOMES 519
Molecular Beam Resonance Method for Measuring Nuclear Magnetic Moments. The Magnetic Moments of $_3Li^6$, $_3Li^7$ and $_9F^{19}$ . . . I. I. RABI, S. MILLMAN, P. KUSCH AND J. R. ZACHARIAS 526
Concerning the Nature of Radio Fade-Out . . . L. V. BERKNER 536
Zeeman Effect of the Forbidden Lines of Potassium . . . F. A. JENKINS AND E. SEGRÈ 545
Onset Studies of Positive Point-to-Plane Corona in Air at Atmospheric Pressure . . . ARTHUR F. KIP 549
Self-Consistent Field for Doubly Ionized Chromium . . . ROBERT L. MOONEY 557
High Pressure Arcs in Common Gases in Free Convection . . . C. G. SUITS 561
Theory of Reversible Magnetization in Ferromagnetics . . . WILLIAM FULLER BROWN, JR. 568
Noncubic Growth of Single Crystals of Silver by Condensation from Vapor . . . J. H. HOWEY 578

Letters to the Editor:

Doppler Effect and Field Distribution in the Hailer Canal-Ray Tube . . . C. W. SHERWIN AND A. J. DEMPSTER 582
Are There Multiple Charged Primary Particles in Cosmic Radiation? . . . M. S. VALLARTA 583
NH Bands in the Night Sky Spectrum . . . JOSEPH KAPLAN 583
Spectroscopic and Free Electron Values of e/m . . . J. A. BEARDEN 584
Actinium Series of Radioactive Elements and Their Influence on Geological Age Measurements . . . ARISTID V. GROSSE 584
On the Mass of the Mesotron . . . Y. NISHINA, M. TAKEUCHI AND T. ICHIMIYA 585
γ-Rays of Radium E . . . J. A. GRAY 586
Low Energy Neutrons from the Deuteron-Deuteron Reaction . . . EMMETT HUDSPETH AND HENRY DUNLAP 587
Note on the Stopping Power of Hydrogen at Very Low Energies . . . F. T. ROGERS, JR. 588

Proceedings of the American Physical Society:

Washington, D. C., Meeting, December 27–29, 1938; Minutes and Abstracts 1–79; Author Index . 589

APRIL 1, 1939

Radiations from Radioactive Substances: Au^{198}, Eu^{152}, Ag^{106}, Cu^{64} and N^{13} . . . . . J. REGINALD RICHARDSON 609
Penumbra at Geomagnetic Latitude 20° and the Energy Spectrum of Primary Cosmic Radiation . . . . . R. ALBAGLI HUTNER 614
On Asymptotic Orbits of Primary Cosmic Rays . . . . . ALFREDO BAÑOS, JR. 621
Masses of Li^6, Li^7, Be^8, Be^9, B^{10} and B^{11} . . . . . SAMUEL K. ALLISON 624
On the Determination of the Signs of Nuclear Magnetic Moments by the Molecular Beam Method of Magnetic Resonance . . . . . S. MILLMAN 628
Influence of Chemical Binding and Crystal Structure on X-Ray Absorption Edges . . . . . ROLF LANDSHOFF 631
New Ultraviolet Band System of Silver Iodide . . . . . NICHOLAS METROPOLIS 636
E Region of the Ionosphere . . . . . E. O. HULBURT 639
E Region of the Ionosphere During the Total Solar Eclipse of October 1, 1940 . E. O. HULBURT 646
Rubbed Films of Barium Stearate and Stearic Acid . . . L. H. GERMER AND K. H. STORKS 648
On the Origin of Great Nebulae . . . . . G. GAMOW AND E. TELLER 654
Perpendicular Vibrations of the Ammonia Molecule . . . . . E. F. BARKER 657

Letters to the Editor:

Spark Discharge on Surfaces . . . . . L. B. SNODDY AND J. W. BEAMS 663
Delayed Neutron Emission which Accompanies Fission of Uranium and Thorium . . . . . R. B. ROBERTS, L. R. HAFSTAD, R. C. MEYER AND P. WANG 664
Determination of Force Fields from Scattering in the Classical Theory . . . . . F. C. HOYT 664
Electric Quadrupole Moment of the Deuteron . . . . . R. F. CHRISTY AND S. KUSAKA 665
Interval Conversion Electrons from Br^{80} . . . . . G. E. VALLEY AND R. L. MCCREARY 666
On the Nuclear Magnetic Moment of Beryllium . . . P. KUSCH, S. MILLMAN AND I. I. RABI 666
New Periods of Radioactive Tin . . . . . J. J. LIVINGOOD AND G. T. SEABORG 667
Gamma-Rays from Uranium Activated by Neutrons . . . . . J. C. MOUZON, R. D. PARK AND J. A. RICHARDS, JR. 668
Influence of Frequency on the Electro-Optical Effect in Colloids . . . . . FRANCIS J. NORTON 668
Raman Effect in Difluorochloromethane . . . . . GEORGE GLOCKLER AND J. H. BACHMANN 669
Constancy of K^{40} . . . . . A. KEITH BREWER 669
Further Products of Uranium Cleavage . . . . . PHILIP ABELSON 670

Proceedings of the American Physical Society:

New York Meeting, February 23–25, 1939; Minutes and Abstracts 1–64; Author Index 671

APRIL 15, 1939

Band Spectra in Nitrogen at Atmospheric Pressure. A Source of Band Spectra Excitation . . . . . OLIVER R. WULF AND EUGENE H. MELVIN 687
Analysis of Nuclear Binding Energies . . . . . WALTER H. BARKAS 691
Stark-Effect Broadening of Hydrogen Lines. I. Single Encounters . . LYMAN SPITZER, JR. 699
Supplementary Identifications in the Spectra of K, Ca, Sc and Ti . . . . L. W. PHILLIPS 708
Arc Spectrum of Vanadium in the Violet . . . . . CHARLOTTE E. MOORE 710
Time Changes in Emission from Oxide-Coated Cathodes . . . . . J. P. BLEWETT 713
Physical Possibilities of Stellar Evolution . . . . . G. GAMOW 718
On the Theory and Observation of Highly Collapsed Stars . . . . . F. ZWICKY 726
Resistance, Emissivities and Melting Point of Tantalum . L. MALTER AND D. B. LANGMUIR 743
Rate of Evaporation of Tantalum . . . . . D. B. LANGMUIR AND L. MALTER 748
Pressure-Temperature Phase Diagram of Na-K Alloys and the Effect of Pressure on the Resistance of the Liquid Phase . . . . . C. H. KEAN 750
Townsend Ionization Coefficients in Cs-Ag-O Photo-Tubes Filled with Argon . W. S. HUXFORD 754
Propagation of Electric Currents in Terminated Lines. Solutions of the Telegraphic Equation . . . . . R. H. KENT 762
Transition from Glow Discharge to Arc . . . . . HSU YUN FAN 769
Dynamic Measurement of the Elastic, Electric and Piezoelectric Constants of Rochelle Salt . . . . . W. P. MASON 775

Letters to the Editor:

Binding Energies of Light Nuclei . . . W. A. Tyrrell, Jr., K. G. Carroll and H. Margenau 790
Energy Production in Red Giants . . . . . G. Gamow and E. Teller 791
Electro-Optical Effects in Bentonite Colloids . . . . . Hans Mueller 792
Neutron-Proton Scattering Cross Section . . . . . Lennart Simons 792
Cross Sections of Metallic Uranium for Slow Neutrons . . . . . Martin D. Whitaker, Charles A. Barton, William C. Bright and Edgar J. Murphy 793
Radioactive Tellurium: Further Production and Separation of Isomers . . . . . G. T. Seaborg, J. J. Livingood and J. W. Kennedy 794
Isotopic Constitution of Hafnium, Yttrium, Lutetium and Tantalum . . . Arthur J. Dempster 794
On the Scattering of Fast Neutrons of Different Energy . . . . . Hiroo Aoki 795
Short Range Alpha-Particles from $F^{19}+H^1$ . . . . . W. B. McLean, R. A. Becker, W. A. Fowler and C. C. Lauritsen 796
Evolution of Red Giants . . . . . G. Gamow 796
Ionization of Mercury . . . . . T. McFadden 797
Production of Neutrons in Uranium Bombarded by Neutrons . . . . . H. L. Anderson, E. Fermi and H. B. Hanstein 797
Structure of the Be I Line λ4573A . . . . . S. Mrozowski 798
Instantaneous Emission of Fast Neutrons in the Interaction of Slow Neutrons with Uranium . . . . . Leo Szilard and Walter H. Zinn 799

Proceedings of the Metropolitan Section of the American Physical Society, March 24, 1939 . 801

May 1, 1939

Stopping Power of Mercury and of Nitrogen for Cosmic-Ray Electrons . . . . . James H. Bartlett, Jr. 803
Nuclear Isomerism in Element 43 . . . . . G. T. Seaborg and E. Segrè 808
Appendix on the Calibration of the Ionization Chamber . . . W. Gentner and E. Segrè 814
Townsend Coefficients for Ionization by Collision in Pure and Contaminated Hydrogen as a Function of the Cathode Material . . . . . Donald H. Hale 815
Resonance Scattering of Protons by Lithium . . . . . E. C. Creutz 819
Nuclear Spins and Magnetic Moments by the α-Particle Model . . . . . R. G. Sachs 825
Inner, Initial, Magnetic Permeability of Iron and Nickel at Ultra-High Radiofrequencies . . . . . Justin L. Glathart 833
On the Creation of Pairs or Positrons by Fast Electrons . . H. R. Crane and J. Halpern 838
Neutrons from the Breakup of He^5 . . . . . H. Staub and W. E. Stephens 845
Magnetic Rotation Spectra of SO_2 and CS_2 in the Ultraviolet . P. Kusch and F. W. Loomis 850
Influence of Atomic Electrons on Radiation and Pair Production . . . . . John A. Wheeler and Willis E. Lamb, Jr. 858
Packing Fraction Differences Among Heavy Elements . . . . . Alvin C. Graves 863
Diurnal and Sidereal Effects and the Meteorologic Influences on Shower and Vertical Intensity of Cosmic Rays . . . . . J. Barnóthy and M. Forró 868
Cosmic-Ray Particles at Great Depth . . . . . J. Barnóthy and M. Forró 870
Symmetry Properties of Variational Functions . . . . H. M. James and A. S. Coolidge 873

Letters to the Editor:

On Stability in the Sense of Poisson for Orbits of Cosmic Rays, and Magnetic Storms . O. Godart 875
Delayed Neutron Emission from Uranium . . E. T. Booth, J. R. Dunning and F. G. Slack 876
Identification of Some of the Products of Uranium Cleavage . . . . . Philip Abelson 876
Search for Beta-Particles Emitted During Uranium Fission Process . . . . . J. W. Kennedy and G. T. Seaborg 877
Erratum: The Scattering of Alpha-Particles by Argon, Oxygen, and Neon . Gordon Brubaker 877
Nuclear Excitation of Indium with Alpha-Particles . . . . . K. Lark-Horovitz, J. R. Risser and R. N. Smith 878
Vibration-Rotation Energies in the Tetrahedrally Symmetric XY_4 Type of Molecule . . . . . W. H. Shaffer, H. H. Nielsen and L. H. Thomas 878
Progressive Breakdown in a Conducting Liquid . . . . . L. B. Snoddy and J. W. Beams 879
Radioactive Halogens Produced by the Neutron Bombardment of Uranium and Thorium . . . . . R. W. Dodson and R. D. Fowler 880
Dispersion of Water for Electromagnetic Waves . . . . . Lester L. Skolil 880
Decay of Willemite and Zinc Sulphide Phosphors . . . . . R. P. Johnson 881
Remarks on the Anomalous Damping of Ultrasonic Waves . . . . . O. Halpern 881

MAY 15, 1939

Gamma-Ray Ion Currents in Air at High Pressures and High Gradients at High and Low Temperatures . . . . . JAMES W. BROXON AND GEORGE T. MERIDETH 883
Band Spectrum of HS . . . . . MARGARET N. LEWIS AND JOHN U. WHITE 894
On the Magnetic Scattering of Neutrons . . . . . O. HALPERN AND M. H. JOHNSON 898
On the Theory of the Forward Scattering of Neutrons by Paramagnetic Media . . . . . J. H. VAN VLECK 924
Intercalibration and Comparison in Two Laboratories of Measurements Incident to the Determination of the Geological Ages of Rocks . . . . . R. D. EVANS, CLARK GOODMAN, N. B. KEEVIL, A. C. LANE AND W. D. URRY 931
Conditions for Producing Intense Ionic Beams . . LLOYD P. SMITH AND G. W. SCOTT, JR. 946
Focused Beam Source of Hydrogen and Helium Ions . . . . . G. W. SCOTT, JR. 954
On Radiative Corrections for Electron Scattering . . . . . S. M. DANCOFF 959
Liquid-Drop Model and Nuclear Moments . . . . . KATHARINE WAY 963
Detection of Single Positive Ions, Electrons and Photons by a Secondary Electron Multiplier . . . . . JAMES S. ALLEN 966
Mechanism of the Lightning Discharge . . . . . J. M. MEEK 972

Letters to the Editor:

On the Interpretation of β-Disintegration Data . . . A. I. ALICHANIAN AND V. BERESTEZKY 978
X-Ray Emission from the Isomers of Radioactive Bromine . . . . . L. I. ROUSSINOW AND A. A. YUSEPHOVICH 979
Neutron Measurements with Boron-Trifluoride Counters . S. A. KORFF AND W. E. DANFORTH 980
Detonation of Nitrogen Iodide by Nuclear Fission . . . . . EUGENE FEENBERG 980
Energy Distribution of Uranium Fission Fragments . . . . . E. T. BOOTH, J. R. DUNNING AND F. G. SLACK 981
Range Distribution of the Uranium Fission Fragments . . . . . E. T. BOOTH, J. R. DUNNING AND G. N. GLASOE 982
Fission Products from Uranium . . . . . G. N. GLASOE AND J. STEIGMAN 982
Concerning the Nature of Radio Fade-Out . . . . . D. F. MARTYN 983
Comparison of the Secondary Electron Emission Due to H_2^+ and D_2^+ Ions . . MONICA HEALEA 984
Interaction of Fast Neutrons with Protons . . . E. O. SALANT, R. B. ROBERTS AND P. WANG 984
Phenomenon of Secondary-Electron Emission . . . . . HERBERT NELSON 985
Cosmic Rays from Supernovae . . . . . F. ZWICKY 986
On the Structure of Solid Solutions . . . . . J. A. WASASTJERNA 986
On the Splitting of Heavy Nuclei by Slow Neutrons . . . . . J. FRENKEL 987
Angle Dependence and Range of Nuclear Forces . . . . . D. R. INGLIS 988
Penetrating Beta-Particles from Uranium Activated by Neutrons . . . . . H. H. BARSCHALL, W. T. HARRIS, M. H. KANNER AND LOUIS A. TURNER 989

JUNE 1, 1939

X-Ray Study of the Changes that Occur in Malleable Iron During the Process of Fatiguing . . . . . RAYMOND G. SPENCER 991
Rossi Transition Curve for Small Angle Showers . . . . . W. M. NIELSEN, J. E. MORGAN AND K. Z. MORGAN 995
Scattering of Protons by Protons . . . . . R. G. HERB, D. W. KERST, D. B. PARKINSON AND G. J. PLAIN 998
Analysis of Experiments on the Scattering of Protons by Protons . . . . . G. BREIT, H. M. THAXTON AND L. EISENBUD 1018
Reflectivities of Evaporated Metal Films in the Near and Far Ultraviolet . . . . . GEORGE B. SABINE 1064
Magnetoresistance of Nickel in Large Fields . . . . . C. W. HEAPS 1069
L_{III} Absorption of Iodine, Barium and Some Compounds of Barium . . EDWARD H. GREEN 1072
New Proof of the H Theorem . . . . . O. HALPERN AND F. W. DOERMANN 1077
On the Theory of Isotope Separation by Thermal Diffusion . . . . . W. H. FURRY, R. CLARK JONES AND L. ONSAGER 1083
Calculation of the Second Virial Coefficient of Helium Gas for the Lowest Measured Temperature . . . . . LEON GROPPER 1095
Infra-Red Pleochroism and Fermi Resonance Associated with CH_2 Groups in Crystals . . . . . JOSEPH W. ELLIS AND JEAN BATH 1098

Letters to the Editor:

Velocity of Radio Waves in Air . . . . . GEORGE H. BROWN 1100
Transmission of Slow Neutrons through Crystals . MARTIN D. WHITAKER AND HAROLD G. BEYER 1101
Prediction of the Remaining Course of the Present Sunspot Cycle . . . . . JOHN Q. STEWART AND FORREST C. EGGLESTON 1102
On the Shape and Stability of Heavy Nuclei . . . . . GALE YOUNG 1102
Approximate Equality of the Proton-Proton and Proton-Neutron Interactions for the Meson Potential . . . . . G. BREIT, L. E. HOISINGTON, S. S. SHARE AND H. M. THAXTON 1103
Unsuccessful Search for Transuranic Elements . . . . . EMILIO SEGRÈ 1104
Concentrating the Uranium Isotope of Twenty-Three-Minute Half-Life . . JOHN W. IRVINE, JR. 1105
Difference in Coulomb Energy of Light, Isobaric Nuclei . . . . . J. G. FOX, E. C. CREUTZ, M. G. WHITE AND L. A. DELSASSO 1106
Simple Capture of Neutrons by Uranium . . . . . H. L. ANDERSON AND E. FERMI 1106

Proceedings of the American Physical Society:

New York State Section, Hamilton College Meeting, April 1, 1939; Minutes 1108
Washington Meeting, April 27–29, 1939; Minutes and Abstracts 1–183; Author Index 1109

JUNE 15, 1939

Further Study of Cosmic Rays on the Pacific Ocean . . . . . PIARA S. GILL 1151
Compact Pressure-Insulated Electrostatic X-Ray Generator . . . . . JOHN G. TRUMP AND R. J. VAN DE GRAAFF 1160
Dipole-Dipole Resonance Forces . . . . . G. W. KING AND J. H. VAN VLECK 1165
Binding Energy of He^6 and Nuclear Forces . . . . . H. MARGENAU 1173
Nuclear Magnetic Moments of N^{14}, Na^{23}, K^{39} and Cs^{133} . . . . . P. KUSCH, S. MILLMAN AND I. I. RABI 1176
Coulomb Energies and Nuclear Models . . . . . HARRISON BROWN AND D. R. INGLIS 1182
Application of Heat Transfer Data to Arc Characteristics . . C. G. SUITS AND H. PORITSKY 1184
Electron Scattering and Plasma Oscillations . HARRISON J. MERRILL AND HAROLD W. WEBB 1191
Variation with the Density of Mercury Vapor of the Intensity of the Spectral Lines of Mercury Excited by Electron Impact . . . . . O. S. DUFFENDACK AND O. G. KOPPIUS 1199
New Terms in Fe I, II, and III and Additional Far Ultraviolet Standards . LOUIS C. GREEN 1209
Many-Body Interactions in Atomic and Nuclear Systems . H. PRIMAKOFF AND T. HOLSTEIN 1218
Positive Column of the Nitrogen Arc at Atmospheric Pressure . . . . . EDWARD S. LAMAR, ALBERT M. STONE AND KARL T. COMPTON 1235
On the Calculation of Polarizabilities and Van der Waals Forces for Atoms in *S* States . . . . . JULIAN K. KNIPP 1244
Conservation of Momentum in Electrical Conductivity . . . . . W. V. HOUSTON 1255
Meson Theory of Nuclear Forces . . . . . H. A. BETHE 1261

Letters to the Editor:

Excitation Function for Iron by Energetic Deuterons . . . . . J. M. CORK AND B. R. CURTIS 1264
On the Angular Distribution of the Fast Neutrons Scattered by Atoms . . . . . SEISHI KIKUCHI, HIROO AOKI AND TETUO WAKATUKI 1264
Powder Patterns on Permalloy Crystals . . . . . J. W. SHIH AND TSU-YEN CHAI 1265
Search for Heavy Cosmic-Ray Particles with a Cloud Chamber . . . . . G. HERZOG 1266
Zenith Angle Distribution of the Hard Component of Cosmic Rays and the Mass of the Mesotron . . . . . PAUL WEISZ 1266
Collision Cross Sections of K Atoms and K_2 Molecules in Gases . . . . . PAUL ROSENBERG 1267
Variation of the Adiabatic Elastic Constants of Polycrystalline Ammonium Chloride with Temperature between 200°K and 273°K . . . . . A. W. LAWSON AND RICHARD SCHEIB 1268
Long-Lived Radioactive Fe^{55} . . . . . J. J. LIVINGOOD AND G. T. SEABORG 1268
Stability of Uranium and Thorium for Natural Fission . . . . . W. F. LIBBY 1269
Secondary Emission of Electrons from Sodium Films Contaminated by Gas . PAUL L. COPELAND 1270
Possible Use of Superconductivity for Radiometric Purposes . . . . . ALEXANDER GOETZ 1270
Anomalies in the Directional Intensity Distribution of Cosmic Rays . . . . . H. S. RIBNER 1271
Fine Structure in the Zenith Angle Distribution of Cosmic Rays . . . . . DENSIL M. COOPER 1272
On Alfven's Hypothesis of a "Cosmic Cyclotron" . . . . . E. R. SABATO 1272
Raman Effect of Fluorochloromethane . . . . . GEORGE GLOCKLER AND J. H. BACHMANN 1273
Erratum: Range Distribution of the Uranium Fission Fragments . . . . . E. T. BOOTH, J. R. DUNNING AND F. G. SLACK 1273

Author Index to Volume 55 1274
Analytic Subject Index to Volume 55 1290
Volume Table of Contents iii

THE PHYSICAL REVIEW

VOLUME 55 | Second Series | NUMBER 12

JUNE 15, 1939

Published for the
AMERICAN PHYSICAL SOCIETY
by the
AMERICAN INSTITUTE OF PHYSICS
Incorporated
LANCASTER, PA., AND NEW YORK, N. Y.

THE PHYSICAL REVIEW

A journal of experimental and theoretical physics established by E. L. Nichols in 1893

BOARD OF EDITORS

John T. Tate, *Editor* — **J. W. Buchta**, *Assistant Editor*

Associate Editors

K. T. Bainbridge — A. L. [illegible] — W. Bleakney

H. P. Robertson — T. H. [illegible] — G. Breit

H. B. Wahlin — P. A. [illegible] — D. M. Dennison

Manuscripts for publication should be submitted to John T. Tate, University of Minnesota, Minneapolis, Minnesota.

Proof and all correspondence concerning papers in the process of publication, should be addressed to the Publications Manager, American Institute of Physics, 175 Fifth Avenue, New York, New York.

Subscription Price

United States and Possessions and Canada $15.00

Foreign $16.50

Back Numbers

Complete set: Series 2,[1] Vol. 1, 1913–Vol. 34, 1938—$200.00

Yearly rate: $16.50

Single copies: $1.50 each prior to July, 1929; 1.75 each after July, 1929.

Subscriptions and orders for back numbers should be addressed to Prince and Lemon Streets, Lancaster, Pennsylvania, or to the American Institute of Physics, 175 Fifth Avenue, New York, New York.

Advertising is not accepted for the *Physical Review* but attention is called to the *Review of Scientific Instruments* and the *Journal of Applied Physics*, companion publications of the Institute, and media through which the field of physics can be reached most effectively. Rates and other information will be furnished on request to the Advertising Manager.

Changes of address and complaints of failure to receive the *Physical Review* in the case of members of the American Physical Society, should be addressed to the Treasurer; in the case of other subscribers, to the Publications Manager. New copies can be sent free in response to complaints of non-delivery only if notice of non-delivery is received within three months of date of issue.

[1] For Series 1 inquire of Physics Department, Cornell University, Ithaca, N. Y.

The Physical Review is published semi-monthly at Prince and Lemon Streets, Lancaster, Pennsylvania.

Entered at the Post Office at Lancaster, Pennsylvania, as second class matter.

Entered for mailing at special rate of postage provided for in section 1103, Act of October 3, 1917, authorized September 6, 1926.

THE AMERICAN INSTITUTE OF PHYSICS

INCORPORATED

ADMINISTRATIVE STAFF

HENRY A. BARTON, *Director*

MADELINE M. MITCHELL, *Publications Manager*

Office: 175 Fifth Avenue, New York, New York

JOURNALS

THE PHYSICAL REVIEW
REVIEWS OF MODERN PHYSICS
JOHN T. TATE, *Editor*
J. W. BUCHTA, *Assistant Editor*

JOURNAL OF APPLIED PHYSICS
ELMER HUTCHISSON, *Editor*

THE JOURNAL OF THE OPTICAL SOCIETY OF AMERICA
THE REVIEW OF SCIENTIFIC INSTRUMENTS
F. K. RICHTMYER, *Editor*

JOURNAL OF THE ACOUSTICAL SOCIETY OF AMERICA
F. R. WATSON, *Editor*

THE JOURNAL OF CHEMICAL PHYSICS
HAROLD C. UREY, *Editor*

THE AMERICAN PHYSICS TEACHER
DUANE ROLLER, *Editor*

GOVERNING BOARD

For The American Physical Society:

JOHN T. TATE, *Chairman*
University of Minnesota

GEORGE B. PEGRAM, *Secretary*
Columbia University

KARL T. COMPTON
Massachusetts Institute of Technology

For The Optical Society of America:

E. C. CRITTENDEN
National Bureau of Standards

A. C. HARDY
Massachusetts Institute of Technology

W. B. RAYTON
Bausch & Lomb Optical Company

For The Acoustical Society of America:

FLOYD A. FIRESTONE
University of Michigan

HARVEY FLETCHER
Bell Telephone Laboratories

WALLACE WATERFALL
The Celotex Corporation

For The Society of Rheology:

WHEELER P. DAVEY
Pennsylvania State College

MELVIN MOONEY
United States Rubber Products, Inc.

R. L. PEEK, JR.
Bell Telephone Laboratories

For The American Association of Physics Teachers:

PAUL E. KLOPSTEG
Central Scientific Company

FREDERIC PALMER, JR.
Haverford College

F. K. RICHTMYER
Cornell University

The American Institute of Physics is a membership corporation of which five societies are the founding members. These five societies are the principal national societies devoted to pure and applied physics in America. Their names, and those of their representatives who form the Governing Board of the Institute, are given above. The principal work of the Institute is the publication of journals sponsored by the societies or by itself. The names and the editors of the journals are also listed above.

The broad purpose of the Institute is to represent in all matters of wide or common interest, the five thousand or more members and subscribers associated with the Founder Societies and the Journals. It aims to advance the science and profession of physics, and to promote cooperation between pure research, the applied sciences and the industries. To achieve these aims, it is greatly in need of an endowment and is empowered by law to administer grants and funds of any kind.

CONTENTS

Vol. 55, No. 12 (1949) JUNE 15

...ity of Cosmic Rays on the Pacific Ocean . . . . . PIERRE S. GILL 1151

...Recoil Ionization Differentials X-Ray Spectrometer . . . . . JOHN G. TRUMP AND R. J. VAN DE GRAAFF 1160

...ic Resonance Powder . . . . . G. W. KING AND J. H. VAN VLECK 1165

...ergy of Hg¹ and Nuclear Forces . . . . . H. MARGENAU 1173

...Magnetic Moments of Rb⁸⁵, Rb⁸⁷, K⁴⁰ and Cs ¹³³. P. KUSCH, S. MILLMAN AND I. I. RABI 1176

...Nuclear Models . . . . . HARRISON BROWN AND D. R. INGLIS 1182

...of Weak Tritium Beta in Ane Chromosulphate . . . C. S. SMITH AND H. FORTESCU 1184

...Scattering and Electron Oscillations . HARRISON J. HUMMEL AND HAROLD W. WEBB 1191

...ith the Intensity of Minority Vapor of the Intensity of the Spectral Lines of Mercury ...ted by Electron Impact . . . . . O. S. DUFFENDACK AND O. G. KOPTIUG 1199

...Values in Fe I, II, and III and Additional Fine Ultraviolet Standards . . LOUIS C. GREEN 1209

...ty Interactions in Atomic and Nuclear Systems . . H. FESHBACH AND T. HOLSTEIN 1218

...Spectrum of the Nitrogen Arc at Atmospheric Pressure . . . . . EDWARD S. LAMAR, ALBERT M. STONE AND KARL T. COMPTON 1233

...Distribution of Polyelectrolytes and Van der Waals Forces for Atoms in a Gas . . . . . JULIAN E. KNIPP 1244

...Correction of Momentum in Electrical Conductivity . . . . . W. V. HOUSTON 1255

...Theory of Nuclear Forces . . . . . H. A. BETHE 1261

...to the Editor:

...Wave Function for Iron by Hartree's Method . . . . . J. M. CASE AND R. R. CHIEN 1264

...Angular Distribution of the Hard Neutrons Scattered by Atoms . . . . . SHIRO HAYAKAWA, HIDEO AOKI AND TSUYO WADAYAMA 1264

...Polarity on Piezoelectric Crystals . . . . . J. W. SHIH AND TSO-YEE CHAI 1265

...for Heavy Cosmic-Ray Particles with a Cloud Chamber . . . . . G. HARRIS 1266

...Angle Distribution of the Shock Component of Cosmic Rays and the Mass of the Mesotron . . . . . PAUL WEISS 1266

...Cross Sections of H Atoms and H_2 Molecules in Gases . . . . . PAUL ROSENBERG 1267

...Origin of the Ultraviolet Bands Constituent of Polyoxymethine Association Colorants with Temperature Intervals 300°K and 350°K . . . . . A. W. LAWSON AND RICHARD SCHEER 1268

...Short Chain Radioactivity Re^{187} . . . . . J. J. LIVINGOOD AND G. T. SEABORG 1268

...Stability of Uranium and Thorium for Natural Fission . . . . . W. F. LIBBY 1269

...Secondary Radiation of Electrons from Sodium Films Contaminated by Gas . . PAUL L. COPELAND 1270

...Possible Use of Superconductivity for Radiometric Purposes . . . . . ALEXANDER GOETZ 1270

...Irregularities in the Directional Intensity Distribution of Cosmic Rays . . . . . H. S. RINGER 1271

...Anomalies in the Fourth Angle Distribution of Cosmic Rays . . . . . DONALD M. COOPER 1272

...Dirac's Hypothesis of a "Cosmic Cyclotron" . . . . . H. R. CROANE 1272

...Isotope Effect of Fluorodichloropentane . . . . . GEO. GLOCKLER AND J. H. SAMPSON 1273

...Isotope Distribution of the Uranium Fission Fragments . . . . . E. T. BOOTH, J. R. DUNNING AND F. G. SLACK 1273

Author Index to Volume 55 1276

Subject Index to Volume 55 1280

Table of Contents iii

LANCASTER PRESS, INC., LANCASTER, PA.